UNIVERSITÀ DEGLI STUDI DI TRIESTE

XXXI CICLO DEL DOTTORATO DI RICERCA IN

AMBIENTE E VITA

TITOLO DELLA TESI
Phylogenetic relationships among extremotolerant rock-inhabiting fungi and their associations with algae

Settore scientifico-disciplinare: BIO/01

DOTTORANDO
Claudio Gennaro Ametrano

COORDINATORE
Prof. Giorgio Alberti

SUPERVISORE DI TESI
Dr.ssa Lucia Muggia, PhD

ANNO ACCADEMICO 2017/2018

Summary

Thesis abstract

Fungi with dark-coloured mycelia - also known as black fungi - form a ubiquitous fraction of microbial communities on rock surfaces all over the world. These organisms show a high capacity to adapt to a wide range of ecological conditions, including those peculiar of extreme environments. Their high tolerance to multiple abiotic stresses, such as solar radiation and osmotic stress is assured by the production of melanin pigments and osmoprotective compounds. The cosmopolitan genera *Lichenothelia* and *Saxomyces* were taken as iconic representatives of polyextremotolerant rock-inhabiting black fungi. I investigated their phylogenetic relationships with an extended taxon sampling within the class Dothideomycetes, the most diverse and life-style rich fungal class in Ascomycota. The three loci phylogenetic inference I set up, considering both environmental samples and culture isolates, highlighted the paraphyly of the two genera. The integrative taxonomy approach based on morphological as well as phylogenetic evidences allowed the taxonomical revision of the genera and the description of three new taxa.

Rock inhabiting fungi often share substrata with green algae and cyanobacteria and some of them are associated with lichen thalli. *Lichenothelia* is of a particular interest because it includes lichen parasites and species which are loosely associated with algae or which grow independently on rock. Given their life style plasticity, we chose it for an *in vitro* culture experiment, studying the development of three *Lichenothelia* species when co-cultured with two different subaerial algae isolated from lichens (i.e., lichen photobionts). The results showed that the presence of algae neither influence the growth rate of fungi nor the formation of any lichen-like structure. However, this standardized approach proved suitable for future investigations on fungal-algal interactions in other systems.

Previous multi-locus phylogenies of Dothideomycetes have investigated evolutionary relationships at order and family level within the class but they often failed to resolve the early diverging nodes, which were generating inconsistent placements of some clades. Here, I applied a phylogenomic approach to resolve relationships in Dothideomycetes, adding the newly sequenced *Lichenothelia* and *Saxomyces* genomes, to a wide dataset comprised of 238 individuals. I explored the influence of tree inference methods, supermatrix vs. coalescent-based species tree, and the impact of varying amounts of genomic data. The phylogenomic reconstructions, based on up to three thousand genes, provide well-supported topologies for Dothideomycetes, recovering *Lichenothelia* and *Saxomyces* among the earliest diverging lineages in the class together with other rock inhabiting fungi and lichens and thus, suggesting the rock-inhabiting life style as ancestral in the class. Further studies will be necessary to shed light on the molecular bases of stress tolerance and latent capacity of establishing symbiosis of these fungi.

Riassunto della tesi

I funghi con il micelio di colore scuro, anche noti come funghi neri, formano una parte ubiquitaria delle comunità microbiche delle superfici rocciose in tutto il mondo. Questi organismi mostrano una grande capacità di adattamento ad un'ampia gamma di condizioni ecologiche, incluse quelle peculiari degli ambienti estremi. La loro grande tolleranza a stress abiotici multipli, come quello determinato dalla radiazione solare o lo stress osmotico è assicurata dalla produzione di melanine e composti osmoprotettivi. I generi cosmopoliti *Lichenothelia* e *Saxomyces* sono stati selezionati in quanto rappresentanti iconici dei funghi neri poliestremotolleranti che vivono sulle rocce. Ho investigato i loro rapporti filogenetici mediante un'ampia selezione di campioni appartenenti alla classe Dothideomycetes, la più ricca di diversità e stili di vita in Ascomycota. L'inferenza filogenetica basata su tre geni che è stata impostata, utilizzando sia campioni ambientali che colture, ha evidenziato la parafilia dei due generi. L'approccio di tassonomia integrata basato sia su evidenze morfologiche che filogenetiche ha permesso la revisione tassonomica dei generi e la descrizione di tre nuovi taxa.

I funghi neri che vivono sulle rocce spesso dividono il substrato con alghe verdi e cianobatteri mentre alcuni di essi sono associati ai talli lichenici. *Lichenothelia* è di particolare interesse perché include sia specie parassite di licheni sia associate in modo non specifico con alghe o che crescono in maniera indipendente su roccia. Data la loro plasticità, abbiamo selezionato tre specie di *Lichenothelia* per un esperimento *in vitro* che prevedeva la loro co-coltura con due specie di alghe isolate da licheni (i.e. fotobionti lichenici). I risultati hanno mostrato come la presenza dell'alga non stimoli né il tasso di crescita del fungo né la formazione di alcuna struttura assimiliabile a un tallo lichenico. Tuttavia, questo approccio standardizzato si è rivelato adeguato al fine di indagare interazioni alga-fungo in sistemi diversi.

Le precedenti analisi filogenetiche di Dothideomycetes basate sul loci multipli, hanno investigato relazioni evolutive a livello di ordine e di famiglia all'interno della classe, ma spesso non sono state in grado di risolvere i nodi basali, generando un posizionamento non congruente di alcuni cladi. In questo studio ho quindi applicato un approccio filogenomico al fine di risolvere le relazioni evolutive in Dothideomycetes; I genomi di *Lichenothelia* e *Saxomyces*, sequenziati per la prima volta, sono entrati in un dataset composto da altri 238 campioni. Inoltre ho esplorato l'influenza del metodo di ricostruzione della filogenesi, adottando sia un approccio basato sulla concatenzione che uno basato sulla coalescenza, e l'impatto della quantità di dati genomici utilizzati, sull'inferenza filogenetica. La ricostruzione filogenomica, basata su un massimo di tremila geni, fornisce una topologia con alti valori di supporto per Dothideomycetes, individuando *Lichenothelia* e *Saxomyces* tra i gruppi il cui evento di speciazione è avvenuto precocemente, assieme ad altri fughi che che vivono su roccia e licheni; questo ha suggerito che lo stile di vita di questi funghi possa essere considerato come ancestrale per l'intera classe.

Ulteriori studi saranno necessari per far luce sulle basi molecolari della loro tolleranza agli stress e la loro ipotizzata capacità di instaurare una simbiosi.

General introduction

The present work aims at resolving the phylogenetic relationships among two genera of rock-inhabiting black fungi, namely *Lichenothelia* and *Saxomyces*, and at bringing further insights into their lifestyles and genomic diversity. Black fungi have been of particular interest in the past decade as they have been recognized to be among the most extremotolerant end extremophilic eukaryotic organisms on Earth. They can thrive in both natural and artificial environments characterized by a multiplicity of different stress factors.

I have organized the work of my thesis into four main parts which here correspond to the four chapters, and each either published, or submitted and accepted, or in preparation papers. The research overarches cultures-based and molecular approaches, including phylogenetic and phylogenomic analyses. The general structure and the topic dealt with in each chapter are outlined here below.

The first chapter represents the introductive section on extremotolerant black fungi, it is entitled "Extremotolerant black fungi from rocks and lichens". It corresponds to a book chapter prepared for the book "Fungi in Extreme Environments: Ecological Role and Biotechnological Significance" and submitted in September 2018. Here I overview the general characteristics and ecological traits of extremotolerant black fungi, i.e. their ability to colonize extreme and oligotrophic environment, to use unusual carbon source and the possible biotechnological application, and their wide, still mainly uncovered, cryptic biodiversity. All together the genetic and the phenotypic traits of these group of fungi make them perfectly suitable to be considered as model/reference organisms for investigations based on culture-based and molecular approaches.

The second chapter is entitled "Phylogenetic relationships of rock-inhabiting black fungi belonging to the widespread genera *Lichenothelia* and *Saxomyces*", it is now in press at the journal *Mycologia*. Here I aimed at resolving and improving the phylogenetic support for the order Lichenotheliales within the ascomycetous class Dothideomycetes by expanding the taxon sampling of previous works, and at testing its relationship with the genus *Saxomyces*. In particular, both aims were achieved by applying an integrative taxonomy approach and succeeded in describing new species for science of both *Lichenothelia* and *Saxomyces*.

The third chapter is entitled "A standardized approach for co-culturing Dothidealean rock-inhabiting fungi and lichen photobionts in vitro". It corresponds to a paper published in March 2017 in the journal *Symbiosis*. In this work I aimed at *i)* verifying the potential lifestyle plasticity of selected strains of *Lichenothelia* and *Saxomyces*, and *ii)* testing their ability to establish trophic and/or structure-driven relationships with common lichen photobionts of the genera *Trebouxia* and *Coccomyxa* using *in vitro* experiments of mixed cultures.

The fourth chapter is entitled "Genome-scale data suggest an ancestral rock-inhabiting life-style of Dothideomycetes (Ascomycota)". It represents a manuscript in its almost final form which will be submitted by the end of the year (2018) or in the early days of 2019 to a still to be defined journal. In this contribution I reconsidered the big class Dothideomycetes and reassessed the phylogenetic placement of the genera *Lichenothelia* and *Saxomyces* using a genome scale approach. In doing this, I also focused on evolutionary and methodological issues which may arise in the reconstruction of phylogenomic inferences. Here, the improved support of the most basal node and the relationships among family- and genus-level monophyletic lineages has been pursued including the largest possible number of markers retrieved from published genomes. Further, the stability of phylogenetic inference was assessed when the data amount varied, different phylogenetic reconstruction methods and different amount of missing data were applied, and different alignment filtering methods were implemented.

During the doctoral period I have been involved also in the project entitled "Development of NGS metabarcoding for the characterization of airborne pollen samples", assigned to my supervisor by the Finanziamento per la Ricerca di Ateneo (FRA2016) of the University of Trieste. Because the whole work results from the participation of several colleagues, and I have been responsible for the molecular and bioinformatic parts, I report here in the Appendix the abstracts of the first published paper (e.g. "DNA metabarcoding uncovers fungal diversity of mixed airborne samples in Italy" by Banchi et al. 2018; PLoS One) and of the second paper now in preparation. The first, published contribution describes a pilot study carried

out in four localities in Italy to uncover the diversity of airborne fungi using the DNA metabarcoding approach. The second, ongoing research instead aims at analysing both plant and fungal airborne diversity using DNA metabarcoding analyses; it also has augmented the number of sampling localities and the type of data to be integrated (e.g. climatic/abiotic, morphological data, and data on land use).

Chapter 1

Extremotolerant black fungi from rocks and lichens

Claudio Gennaro AMETRANO[1], Lucia MUGGIA[1], Martin GRUBE[2*]

[1] University of Trieste, Department of Life Science, via Giorgieri 10, 34127 Trieste, Italy; E-mail: claudiogennaro.ametrano@phd.units.it; lmuggia@units.it
[2] University of Graz, Institute of Biology, Holteigasse 6, 8010 Graz, Austria; martin.grube@uni-graz.at

* Corresponding author: Martin Grube; martin.grube@uni-graz.at; orcid.org/0000-0001-6940-5282; tel. 0043316 380 5655

Abstract

Fungi with dark-colored cells and mycelia - also known as black fungi - form a ubiquitous fraction of microbial communities of rock surfaces all over the world. The diversity and life styles of these stress- and pollution-tolerant fungi are still insufficiently known. Most of these fungi demonstrate a high degree of phenotypic plasticity, which we regard as important to adapt and thrive in a wide range of ecological conditions, including extreme environments. The production of melanin pigments in cell walls shields black fungi effectively against radiation stress and the high osmotic tolerance, a key factor to withstand a wide range of environmental challenges, such as drought, temperature and pH extremes, is mediated by osmoprotective small compounds (osmolytes). In their natural habitats, black fungi are frequently associated with lichens, either growing in their vicinity or on the symbiotic structures. As co-culture experiments show, some of the black fungi have a transient capacity to develop primitive, lichen-like associations with algae (or cyanobacteria). First genomic data from black fungi do not suggest a specific set of genes or gene family enrichments that would correlate with tolerance to stress factors.

Kew words: Life-styles, melanins, oligotrophy, phylogenetics, symbioses, thallus.

Introduction

While a large number of fungi is specialized to spread comfortably in the shelter of substrates or hosts, some other languish on exposed surfaces. With little competition on nutrient-deprived conditions, such a stressful life-style also requires adaptations to fluctuations in water accessibility and to other challenges. Such fungi also need to shield their cell content from excessive radiation using various kinds of pigments in their cell walls. With their colorful symbiotic thalli, lichen-forming fungi offer good examples for evolutionary success on substrate surfaces. Lichen-forming fungi establish diverse forms of characteristically compacted mycelial morphologies, which use pigments to filter light to internally grown photosynthetic algae. The other large group of fungi does not develop such complex symbiotic structures and is characterized by dark pigments. These fungi, also known as “black fungi”, are the focus of the present chapter. In contrast to lichen-forming fungi, black fungi do not depend on a symbiotic metabolic interplay with partners, and are therefore found also on surfaces, where lichens would not survive, e.g. at dark, indoor or polluted places. In this chapter we provide an overview of the current understanding of diversity and taxonomy of black fungi, as well as their ecological and evolutionary links with the lichen symbiosis.

The phenotypes of black fungi have evolved in different lineages of ascomycetes. Under the extremes of abiotic conditions the typical morphology is usually restricted to vegetative mycelia with insufficient diagnostic characters. In this stage it is impossible to identify the species directly in the environment.

Diagnostic characters are expressed under controlled laboratory conditions. Otherwise, DNA sequence data serve to classify these fungi in a phylogenetic framework. Since many lineages have so far not been named as species or belonging to genera which turn out to be polyphyletic (e.g. Ertz et al. 2014), DNA data are still of limited use to recognize species.

Phylogenetic relationships of black fungi within Dothideomycetes and Eurotiomycetes

The major lineages of black fungi belong to early diverging clades of Dothideomycetes and Eurotiomycetes in Ascomycota (Fig. 1). With more than 19.000 species, Dothideomycetes is the lineage with the largest number of species in Ascomycota (Kirk et al. 2008; Schoch et al. 2009a, b). Representatives of this class generally pursue a wide diversity of life styles, and this diversity is scattered across many different clades (Egidi et al. 2014, Muggia et al. 2016). Within Dothideomycetes, the order Capnodiales is particularly rich in extremotolerant species. They comprise fungi isolated from rocks of Antarctic dry valleys (Onofri et al. 2007a, b; Selbmann et al. 2005; Egidi et al. 2014), from high-altitude rocks of the Alps (Selbmann et al. 2014) from hot deserts (Muggia et al. 2015), and black yeasts from marine salters (Gunde-Cimerman et al. 2000). Even within genera of this lineage different lifestyles can be found. For example, the genus *Rachicladosporium* (Capnodiales) includes both rock inhabitants and plant pathogens (Egidi et al. 2014). The environmental versatility of closely related fungi suggests that they keep a shared set of traits, which facilitates adaption to new habitats. Ruibal et al. (2009) and Egidi et al. (2014) show that many of the rock-inhabiting fungi, isolated from both mild and extreme climates, are found in the family Teratosphaeriaceae (Capnodiales), such as *Friedmanniomyces endolithicus*, *Elasticomyces elasticus* and *Recurvomyces mirabilis*. While many of these fungi seem to be widespread, *Cryomyces antarcticus* seems so far to be an endemic extremophile confined to Antarctica (Ruibal et al. 2009).

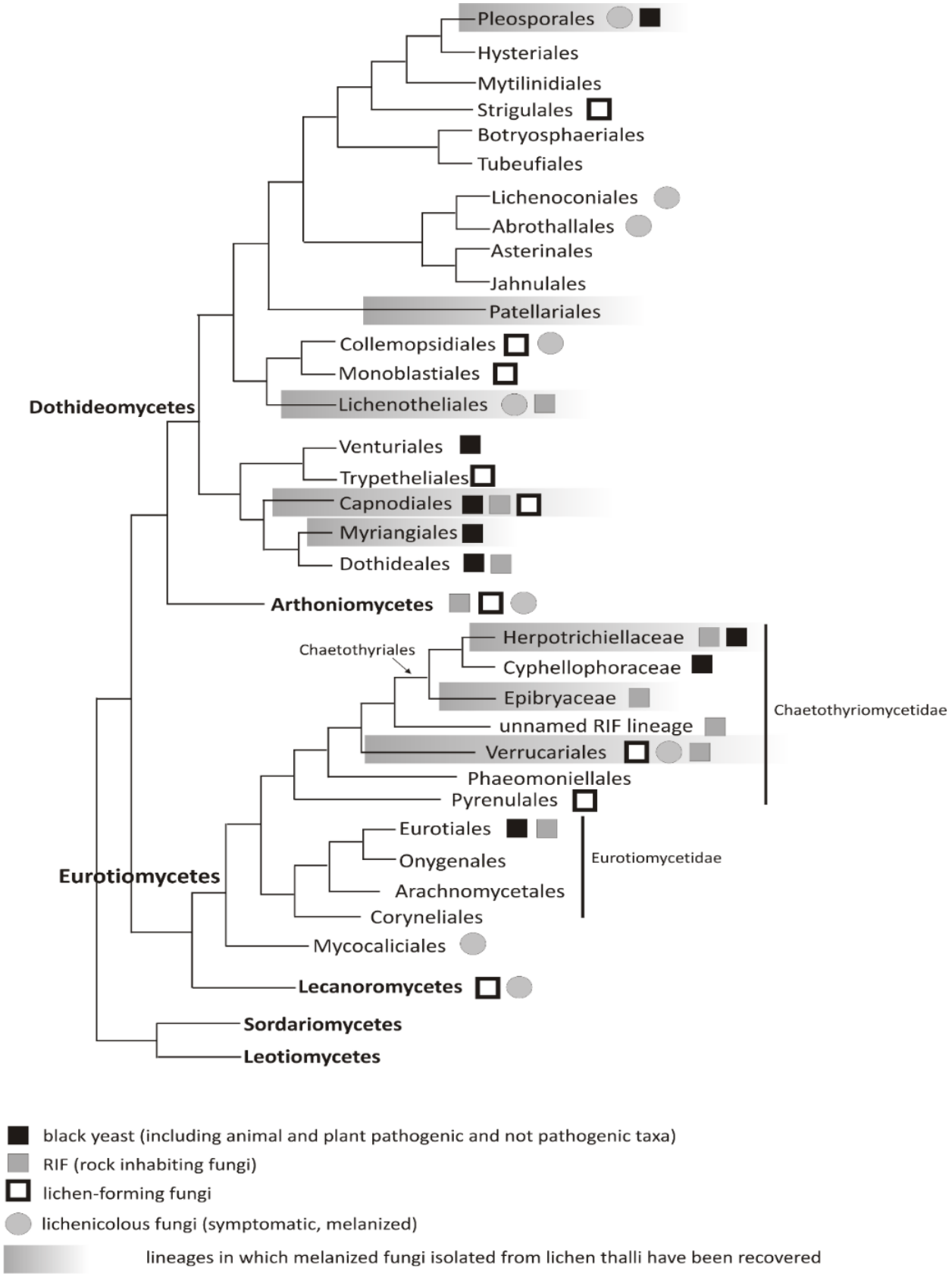

Figure 1. Schematic representation of the major lineages in Dothideomycetes and Eurotiomycetes (Ascomycota) in which black fungi with different life styles are found. Lineages in which black fungi have been isolated from lichen thalli are shaded in grey. The phylogeny was graphically reconstructed merging information from most recent phylogenetic studies of Hyde et al. (2013, Gueidan et al. (2014), Chen et al. (2015), Liu et al. (2017), Teixeira et al. (2017).

Black fungi in Eurotiomycetes are mainly found in the order Chaetothyriales (Gueidan et al. 2011). Chaetothyriales are mostly known as saprophytic and pathogenic fungi - with a wide variety of hosts (Geiser et al. 2006; Teixeira et al. 2017) -, but they also comprise a relevant number of species living on rocks (Sterflinger et al 1999; Ruibal et al. 2005), for instance species from the genera *Knufia, Bradymyces, Cladophialophora, Capronia* and *Sterlitziana* (Ruibal et al. 2008; Réblová et al. 2016). It has been suggested that rock-inhabiting species in Eurotiomycetes are ancestral to present lineages of pathogenic and lichenized fungi in Chaetothyriales and Verrucariales (Gueidan et al. 2008), because they appear particularly diverse in early diverging lineages of these orders.

The circumscription of many black fungi has been hampered by ambiguous diagnostic characters and lack of sexual reproductive forms (e.g. Crous et al. 2004; Muggia et al. 2008; Taylor 2011). Molecular phylogenetic studies alone may not always resolve species delimitation problems of black fungi, thus authors considered the species as complexes containing (so far) cryptic species (Hyde et al. 2013; Egidi et al. 2014; Muggia et al. 2015). An integrative, or polyphasic, taxonomic approach is required to circumscribe closely related lineages. This has been demonstrated with the species complex of *Aureobasidium pullulans*, where a redefinition of its varieties by Zalar et al. (2008) initiated more detailed analyses that resulted in species descriptions for the former varieties (Gostinčar et al. 2014).

Important features of extremotolerant fungi

Plastic growth strategies – The typical growth forms of polyextremotolerant black and the ability to switch among them, is also a key adaptation to cope with stressful environmental conditions. Filamentous mycelia are able to explore the surrounding environment for nutrients. Substantially different mycelial organisations can be formed by the same strain on rock surfaces and on culture media. The hyphae of rock-inhabiting mycelia are often short celled, and mycelia may become compact to form so called microcolonies. Many species of black fungi, especially in Dothideales, can also switch between filamentous and yeasts growth forms (pleomorphism) depending on the circumstances of the habitat. Transitions exist to completely budding forms, which are often called black yeasts. This ability is termed phenotypic plasticity, which has been recently studied in *Aureobsidium pullulans* by Slepecky and Starmer (2009). In addition, variation exists between individual cells within genetically-uniform mycelia. For example, when single cells of black fungi become detached from the surface, they tend to develop budding forms (Staley et al. 1982; Gorbushina et al. 1993). The phenotypic heterogeneity results from differences in gene expression, which occur either stochastically or as result from the relative position of cells in a mycelium (Hewitt et al. 2016).

Melanization – A characteristic phenotypic trait of all black fungi is the presence of melanins in the cell walls. Melanins are a group of polymeric secondary compounds that have been interpreted as a “fungal armour” (Gómez and Nosanchuk 2003; Keller 2015), as they act as protective agents against a wide range of environmental stresses (Sterflinger 2006). The term melanins gives little information about the chemical structure of the polymeric molecules, it only denotes a black pigment of biological origin. Melanins are produced by a wide range of organisms including plants, animals and certain species of bacteria (Swan 1974). The polymer structures are still partially known as there is no simple structure of the polymeric nature and the composition varies among different species. Therefore, melanins are classified according to their precursors and synthetic pathway (Eisenman and Casadevall 2012). Eumelanins, the most common type of melanins, are produced during the oxidation of tyrosine (and/or phenylalanine) to 3,4-dihydroxyphenylalanine (DOPA) or dopaquinone which further undergoes cyclization to 5,6-dihydroxyindole or 5,6-dihy-droxyindole-2-carboxylic acid (Butler and Day 1998). Pheomelanins are initially synthesized like eumelanins, but DOPA undergoes cysteinylation into cysteinyl-dopa, which further polymerizes into various derivatives of benzothiazines (Plonka and Grabaca, 2006). Allomelanins, the least studied group of polymers, are produced through polymerization of 1,8-dihydroxynaphthalene (DHN). In this pathway, the precursor molecule is acetyl-coenzymeA (acetyl-CoA) or malonyl-CoA. The first step, formation of 1,3,6,8-

tetrahydroxynaphthalene, is catalyzed by a polyketide synthase (PKS). Subsequently, a sequence of reactions produces the intermediary compounds scytalone, 1,3,8-trihydroxynaphthalene, vermelone, and DHN, which is then polymerized to yield melanin (Butler and Day 1998; Langfelder et al. 2003; Plonka and Grabaca 2006). Most melanins characterized from ascomycetes are DHN-melanins (allomelanins) but DOPA-melanins (eumelanins) occur as well (Eisenman and Casadevall 2012), however the latter are more typical for basidiomycetes (Butler and Day 1998).

The best-known function of melanins is to protect against UV radiation, which is of particularly importance for the rock-inhabiting fungi thriving on bare rock surfaces in open environments. The melanins accumulated in the cell walls of spores and hyphae. Singaravelan et al. (2008) showed by *in vitro* experiments how physiological stress caused by UV radiation enhanced the synthesis of melanin as adaptive response in *Aspergillus niger*. A significantly higher concentration of melanin was measured in the conidia which positively correlated with their germination capacity. Further, in the phytopathogenic fungus *Bipolaris oryzae* the expression of 1,3,8-trihydroxynaphthalene reductase (THR1) gene - essential for DHN-melanin production - is transcriptionally enhanced by increased doses of UV radiation (Kihara et al. 2004). Melanins accomplish the same function also in basidiomycetes: the pathogenic black yeast *Cryptococcus neoformans* shows a lower susceptibility to UV light damages when the cells are protected by melanins (Wang and Casadevall 1994). Both DOPA and DHN-melanins are efficient protectors also against ionizing radiation (Pacelli et al. 2017). The radioprotective properties of fungal melanins derive from a combination of physical shielding and free radical quenching (Dadachova et al. 2008). Ionizing radiation alters the oxidative-reduction potential of melanins and is correlated with a faster growth rate in melanised fungi, suggesting that melanins might also function as energy traps (Dadachova et al. 2007; Dadachova and Casadevall 2008).

Melanins accumulate within the cell wall of black fungi as electron dense granules, which contain various functional groups as carboxyl, phenolic, hydroxyl and amine. These functional groups provide multiple binding sites for metal ions. The maximum binding capacity of fungal melanins has been reported for copper, calcium, magnesium and zinc in the following order: Cu > Ca > Mg > Zn (Fogarty and Tobin 1996). Binding mechanisms of fungal melanins have been studied mostly for Cu, which binds mainly at a phenolic hydroxyl group and at a carboxyl group, as in humic acids (Fogarty and Tobin 1996). Though fungal melanins can bind Cu, they show a higher affinity for Fe, if both ions are co-present in a solution: Fe is in this case able to partially substitute Cu (Senesi et al. 1987). The high affinity of fungal melanins to Fe and Cu has also been demonstrated in the lower, melanized cortex of parmelioids lichens and in the melanized apothecia of the lichen *Trapelia involuta*, respectively (Fortuna et al. 2017; McLean et al. 1998). The capacity of melanins to bind ions becomes biologically relevant especially when toxic metal ions are abundant in the environment around the fungal cells: when bound, their decreased concentration allow the fungi to grow also in contaminated environments. Moreover, binding and exposition of cations on the hyphal surface can protect fungi from antagonistic microbes, either reducing the availability of microelements or interfering with the activity of hydrolytic enzymes (Fogarty and Tobin 1996).

Though essential to aerobic life, high electronegativity renders oxygen (O_2) one of the most reactive element on Earth. During its reduction to water, Reactive Oxygen Species (ROS) are generated as by-products and cause oxidative stress (Turrens 2003). Also abiotic stresses, such as desiccation, freezing, heavy metals and other xenobiotic compounds are likely to induce oxidative stress in fungi. A great overlap was found in cellular stress response between oxidative stress and many other abiotic stresses (Jamieson 1998; Lushchak 2011). ROS (e.g. superoxide radical, hydrogen peroxide and hydroxyl radical) cause severe cell damage and living organisms have developed both enzymatic and not-enzymatic defence mechanisms. In fungi (both basidiomycetes and ascomycetes), melanins have a relevant redox buffer function and act as non-enzymatic defences against oxidative stress, as known for example in *Inonotus obliquus, Phellinus robustus, Aspergillus carbonarius, Paecilomyces variotii* (Shcherba et al. 2000), *Cryptococcus neoformans* (Jacobson and Tinnell 1993), *Exophiala dermatitidis, Alternaria alternata* (Jacobson et al. 1995) and *Aspergillus nidulans* (Goncalves and Pombeiro-Sponchiado 2005). The redox buffering capacity of melanins has been studied mostly in pathogenic fungi identifying melanin as a virulence factor, as one of the most common reaction to pathogens is the production of ROS by leukocytes. Moreover, in pathogenic black fungi melanins have also

been claimed to generate appressorium turgor which is essential to penetrate animal/plant tissues (Sterflinger 2006).
Melanins seems also to confer resistance to osmotic stresses as fungi isolated on saline media are almost exclusively melanized (Gunde-Cimerman et al. 2000). In this context, the action mechanism of melanins has not been fully elucidated, though Plemenitaš et al. (2008) hypothesized that the dense, shield-like layer of melanin granules accumulated in the cell wall reduces glycerol loss during salt stress. Glycerol, indeed, is the most abundant compatible solute produced by halotolerant black yeasts, such as *Hortaea wernekii*, to compensate the loss of water from the cells in high concentrated salt solutions. Therefore, the reduction of cell permeability carried out by melanins would results in an increased efficiency of the cells to counteract the osmotic stress (Plemenitaš et al. 2008).

Oligotrophy, unusual carbon sources, desiccation and temperature tolerance – On bare rock surfaces with limited nutrient resources and discontinuous presence of liquid water, fungi must be able to exploit a wide range of carbon sources deposited by dust, water or in form of volatile organic compounds (VOC; Prenafeta-Boldu et al. 2001, 2006). These carbon sources can also derive from algae. There have also been studies using C^{14} labelled CO_2 and HCO_3^-(Mirocha and DeVay 1971; Palmer and Friedman 1988), which suggest the capacity of some fungi and black fungi to directly fix carbon dioxide. As they lack the Calvin cycle metabolism, they might incorporate carbon via any of the potential alternative pathways (Bar-Even et al. 2012). Yet, these studies still need confirmation and additional work to find out the possible pathways of CO_2 incorporation. So far studies mostly focused on the spectrum of organic compounds efficiently usable by these fungi. For example, aerobic metabolism of a large spectrum of L and D forms of monosaccharides, disaccharides and alcohols has been investigated (Sterflinger 2006). Ethanol can be usually degraded, whereas the oxidation of methanol is rare; the use of meso-erythrol is also often reported and several rock-inhabiting fungi are even able to degrade simple and polycyclic aromatic hydrocarbons (Prenafeta-Boldu et al. 2006; Sterflinger 2006; Nai et al. 2013). *Knufia petricola* (Chaetothyriales, Eurotiomycetes) in particular, was proposed as model organism for further analysis of the physiology of rock inhabiting black fungi (Nai et al. 2013). This fungus indeed tolerates and grows on media containing monoaromatic compounds, confirming its capacity to utilize recalcitrant carbon sources eventually spurned by other microorganisms (Nai et al. 2013). Further, one of the most striking evidence that fungi are capable of exploiting unusual carbon source is the black mould *Racodium cellare* (Dothideomycetes, Capnodiales). Its metabolism seems to benefit volatiles released by wine barrels as carbon source and it is able also to grow using other VOCs (Tribe et al. 2006). Another black fungus associated with alcoholic vapours is *Baudoinia compniacensis*, which is frequently found near distilleries (Scott et al. 2007).

The ability to degrade aromatic compounds appears more typical for black fungi in Chaetothyriales, and in particular to the members of the family Herpotrichiellaceae. This family has been mainly studied for its role in human pathogenesis, but many species have been isolated from hydrocarbon-rich environments as well, such as soil contaminated by hydrocarbon, fuel tanks, washing machines, soap dispensers, indoor moist environments or rotten wood (Prenafeta-Boldù et al. 2006, Badali et al. 2011, Zalar et al. 2011, Isola et al. 2013). These and other recent works highlighted a possible connection between neurotropism (affinity of a pathogen for brain tissues) and the metabolization of aromatic hydrocarbons in the environment (Moreno et al. 2018a).

In this context, hydrocarbon assimilation may represent an additional virulence factor, as brain contains monoaromatic catecholamine neurotransmitters (e.g. dopamine). Moreover, neurotransmitters catabolism compounds and other substances detected in the human brain are also found as product of lignin degradation (Prenafeta-Boldù et al. 2006). Even though some pathogenic fungi have been isolated from environmental sources too, the source of many of them is unknown yet. Therefore it has been hypothesized that hydrocarbon-rich environments could represent a possible pathogen reservoir. Badali et al. (2011) for instance, investigated the potential pathogenicity of *Cladophialophora psammophila*, as its congeneric *C. bantiana* is a notorious human pathogen, but with negative results. *Exophiala* species isolated by Isola et al.

(2013) confirm this finding: indeed, severe pathogens and hydrocarbon associated black fungi have been found mostly in ecologically divergent lineages of *E. xenobiotica*. With the shared adaptive traits of pathogens and extremotolerant or hydrocarbon-growing black fungi, opportunistic pathogens probably still have the ability to grow outside the host, while some environmental strains may occassionally become pathogenic. *E. mesophila*, indeed, is the first reported clinical strain able to grow on alkylbenzenes (Blasi et al. 2016) and environmental *Fonsecaea erecta* is able to infect and survive in animal host tissue (Vicente et al. 2017). The ability to thrive in polluted environment and to use aliphatic and aromatic hydrocarbon as energy and carbon source in otherwise extremely oligotrophic environment is of particular interest for application in bioremediation of polluted environmental matrices and gas effluent biofilters (Kennes & Veiga, 2004; Blasi et al. 2016).

Beside the microcolonial growth, microcolonial black fungi also share few other characteristics which make them survive in extreme environments, including the capacity to suspend their metabolism for long periods until favourable conditions return, and the ability to build “skins” and “shells” made of extracellular matrix and minerals on the surface of the cell wall (Gorbushina, 2007). The compact shape of fungal microcolonies efficiently protect them against heat and desiccation, by optimizing the volume/surface ratio (Gorbushina, 2007). Moreover, by their colonial growth black fungi can form extensive biofilms, which are highly resistant to antifungals (Kirchhoff et al. 2017). The desiccation tolerance is further highly enhanced by the accumulation of the disaccharide trehalose which stabilizes enzymes and cell membranes, avoiding degradation and breakage during dehydration phases (Sterflinger 2006). The desiccation tolerance is highly correlated with temperature tolerance, dried fungal colonies are metabolically inactive and can survive at temperatures of 80° and 90°C for 60 min (Onofri et al. 2008). Alternatively, temperatures between 35 and 75 °C are lethal for hydrated colonies (Sterflinger 1998). As further adaptation to temperature extremes and dehydration, rock fungi from Mediterranean regions synthesize heat-shock protenins (HSP) whereas Antarctic rock-inhabiting fungi down-regulate their metabolism (Selbmann et al. 2015). Rock fungi from cold environments usually produce also a high amount of extracellular polymeric substances (EPS) to increase their resistance against freeze-thaw damage (Selbmann et al. 2015). The best example of psychrophilic black fungi is *Cryomyces antarcticus*, isolated from rocks from Antarctic dry deserts, which shows a growth optimum below 15 °C and still has a detectable growth near 0 °C (Onofri et al. 2007a). Moreover, this fungus, and other black fungi isolated from cryptoendolithic antarctic communities, are able to survive repeated freeze/thaw cycles, outstandingly frequent in antarctic summer season.

Figure 2 Natural environments where black rock-inhabiting fungi cooccur with lichens: **A.** Alpine habitat at high elevation (Mt. Rosa, Western Alps, 4500 m a.s.l.); **B.** rock scree richly colonized by lichens; **C.** outcrops and walls at low elevation (Taya Tal, Czech Republic). Photos were taken by LM.

Life styles of black fungi

The above-outlined traits of black fungi facilitate their adaptation in a wide range of niches. Many of them seem to be widespread environmental species, whereas certain lineages comprise important clinical strains of medical interest (de Hoog et al. 2013). Many strains are also recurrent endophytic components in plants (known as dark-septate endophytes; e.g., Rodriguez et al. 2008). Furthermore, their thermal tolerance can facilitate their occurrence as opportunists and pathogens in warm blooded animals (de Hoog et al. 2000). In the case of many species of human black yeast pathogens, the pathogenicity seems to be mostly coincidental and suggests that the original niche lies outside the human host. These pathogenic black yeasts lack a specific mechanism to enter the host tissue if no accidental trauma occurs, suggesting a low specialization as pathogens. Their pathogenic potential in the animal tissues is attributed to thermal tolerance, pleomorphic growth, melanisation of cells walls, and the ability to degrade complex carbohydrates. The ability to tolerate and degrade a range of toxic aromates may also explain why many black fungi are able to associate with ants (Vasse et al. 2017). Voglmayr et al. (2011) suggested that adaptation to the lichen-habitat might be the basis for the tolerance factors of ant-associated black fungi.

However, the highest diversity of black fungi has been detected in rocky environments and it has been speculated that these fungi represent the ancestors of those lineages of black fungi, which later evolved other life styles (Gueidan et al. 2011; de Hoog et al. 2013). Black rock-inhabiting fungi are found in every climatic zone on a wide range of surfaces, they tolerate also at high latitudes and altitudes or other extremes (Onofri *et*

al. 2007a, Gostinčar et al. 2012; Fig. 2). They also colonize diverse artificial building materials, and with their enormous extent concrete surfaces are of particular importance. Fungi on concrete have earlier been studied in the context of biodeterioration and pollution (e.g., Krumbein 2012 and references therein). Most striking is the presence of dark fungi with potential clinical relevance (e.g., strains of *Alternaria* and *Epicoccum* are frequently found among our isolates from concrete, unpublished data). A prevalence of clinically relevant fungi on concrete may be significant for refined health risk assessment. Indeed, black fungi can be involved in allergic disorders, and at least *Alternaria* causes asthma or chronic rhinosinusitis in people with sensitivity. Spores and hyphal fragments of *Alternaria*, in particular, are among the most abundant allergens spread in airborne samples (Banchi et al. 2018), and the genus is always reported in the pollen bulletins of air monitoring.

Links to lichen symbiosis

Gorbushina and Broughton (2009) interpreted the rock surface as a kind of "symbiotic playground," where they considered antibiosis (detrimental interactions between species) to be rare and counterproductive. The authors also mentioned that co-cultivation of the cynobacterium *Nostoc* with a rock-inhabiting fungus (*Sarcinomyces*) resulted in a specific association, without presenting this association in greater detail. Such associations have been observed previously, e.g. by Turian (1977), who described *Coniosporium aeroalgicola*. This species, a dematious hyphomycete, seems to be a ubiquitous component of aereo-algal communities and able to form some sort of symbiotic structures with algae. Other rock-inhabiting microcolonial fungi develop into lichenoid structures within months when co-cultured with lichen algae (Gorbushina et al. 2005). Brunauer et al. (2007) reported a black fungus that was isolated from a rock-inhabiting lichen. Surprisingly, this fungus formed layered lichen-like associations with algae from the host algae in experimental settings.

The study of lichen-infecting fungi has a long history, as symptoms of fungal infections have been observed already before the symbiotic nature of lichens was discovered. Their propagative structures were used to characterize the c. 2000 so far described species of lichenicolous fungi. Microscopic analyses show that there are often additional and dark colored fungal hyphae in lichens, which cannot clearly be assigned to known species. Culturing and sequencing approaches have shown more recently that many more fungi have a so far unrecognized association with lichens (e.g. Fernandez-Mendoza et al. 2017). Their precise activities in lichen symbiosis and phylogenetic relationships still need to be explored, yet a fair fraction of cultivable fungi from lichens belong to groups which are also known as rock-inhabiting black fungi (Harutyunyan et al. 2008).

The shared occurrence on rocks and on lichens of black fungi, and the transient ability of certain isolates to form associations with algae, could indicate an implicit link between the extremotolerant and the lichen life styles. Ancestral proximities of certain lichenized fungal lineages and different lineages of black fungi have been outlined: rock-inhabitants are phylogenetically basal to the mainly lichenized lineages of Arthoniomycetes and Verrucariales (Gueidan et al. 2008; Ruibal et al. 2009). In these groups we also find, both complex morphologies with stratified lichen thalli and to less extent loss of thallus-formation and sporadic evolution towards the lichen-infecting life style. The lichen representatives in Dothideomycetes are scattered among different clades within this huge class (Muggia et al. 2008; Nelsen et al. 2009). They generally do not form complicate thallus structures and are more closely related to fungi adapted to other life styles, in particular to oligotrophic rock environments.

Gostinčar et al. (2012) suggested that small protective molecules that are known to accumulate in black fungi as stress-responsive osmolytes could also be linked with potential transition from rock-inhabiting to the lichen life style. In particular, the polyol metabolism could be involved in both extremotolerance and lichenization. Ribitol, sorbitol, and erythritol (as well as glucose by cyanobacteria) are provided by photoautotropic symbionts to the fungal partners as food molecules, where they are transformed to mannitol (Friedl and Büdel, 2008). Efficient osmolyte metabolism, as found in oligotrophic black fungi, could therefore be a pre-adaptation to facilitate the transition to a lichen symbiotic life style.

As an example, Muggia et al. (2013, 2015) explored *Lichenothelia* as a link between rock-colonizing and algal-associated life-styles. *Lichenothelia* comprises both rock-inhabiting and lichenicolous fungi and has therefore been considered a link between lichenized and non-lichenized fungi (Hawksworth 1981, Muggia et al. 2013). The genus was introduced by Hawksworth (1981), who considered the morphological and anatomical characters of the ascomata and their type of development in his classification of fungi with typically dothidealean ascus ontogeny. He separated *Lichenothelia* from similar fungi, such *Microthelia* and others. *Lichenothelia scopularia* (Hawksworth 1981) was assigned as the type species of the genus; since then 28 species (MycoBank, February 2018) have been recognized by both morphological and phylogenetic analyses (Hessen 1987; Øvstedal and Smith 2001; Atienza and Hawksworth 2008; Zhurbenko 2008; Etayo 2010; Muggia et al. 2013, 2015; Valadbeigi et al. 2016). The family Lichenotheliaceae and the order Lichenotheliales (Hyde et al. 2013) are recognized a monophyletic lineage within Dothideomycetes, but this result is still based on only five sequenced species (e.g. *Lichenothelia arida*, *L. calcarea*, *L. convexa*, *L. rugosa* and *L. umbrophila*, and by a yet undescribed *Lichenothelia* sp. (Hyde et al. 2013; Muggia et al. 2013, 2015). These recent studies partially clarified the phylogenetic placement of the genus and the order within Dothideomycetes, whereas many *Lichenothelia* species have been initially described as *Lichenostigma* (Lichenostigmatales, Arthoniomycetes) on a morphological basis. However, the most recent phylogeny of *Lichenostigma* places this genus at the basis of Arthoniomycetes (Ertz et al. 2014). Phylogenies which include *Lichenothelia* place the order Lichenotheliales as related to *Cryomyces* and *Saxomyces*.

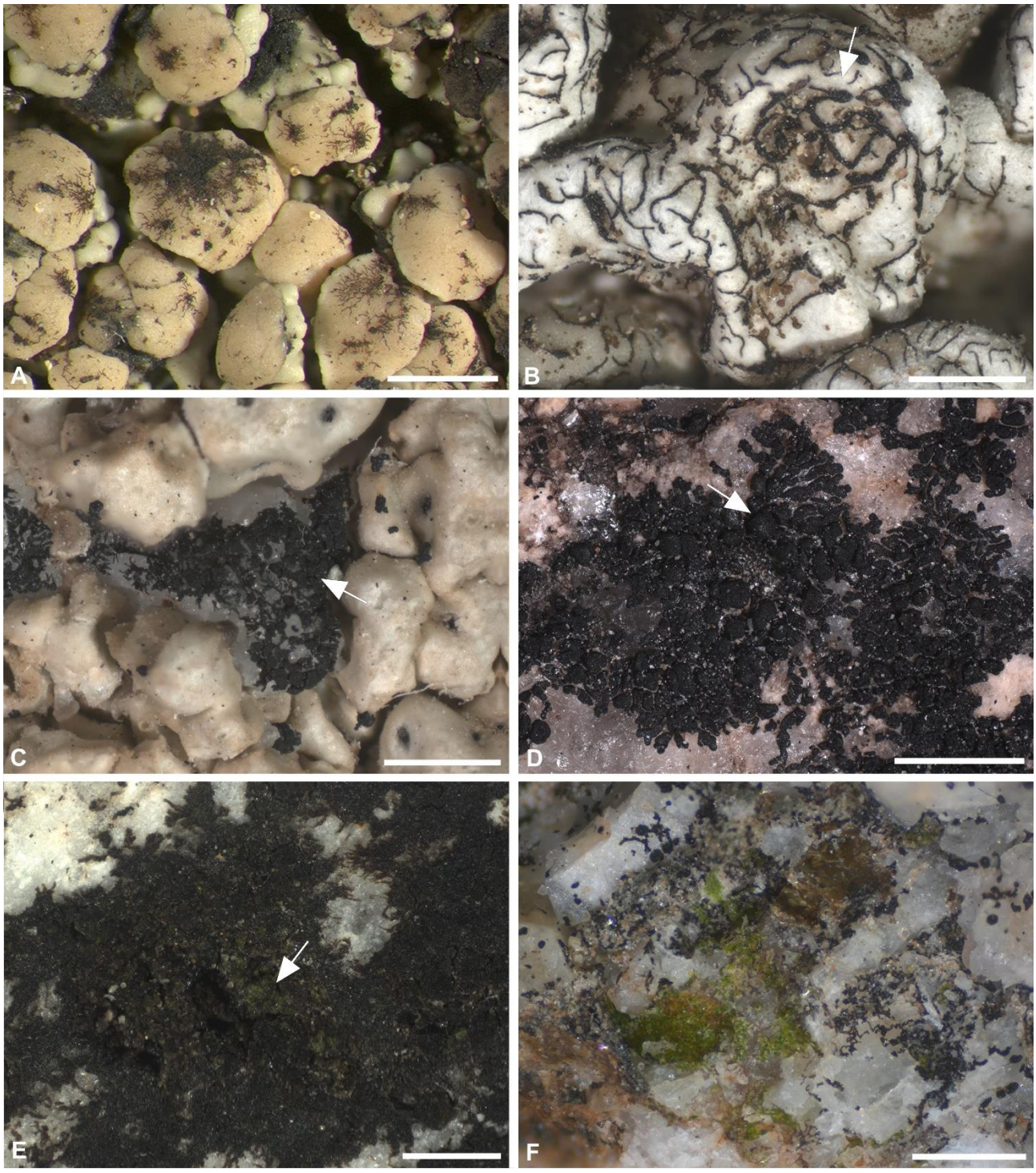

Figure 3. Habit and life styles of black fungi in nature (in parenthesis fungal order and or class are reported): **A.** lichenicolous black fungus (Dothideomycetes) spreading hyphae on the apothecium of the lichen *Lecanora polytropa*; **B.** lichen parasitic fungus *Lichenostigma rouxii* (Arthoniomycetes) developing hyphae and ascomata (arrow) on the thallus areolas of *Pertusaria* sp., sample n. SPO1428; **C.** *Lichenostigma epirupestre* (Arthoniomycetes) on rock in between of thallus areolas of *Pertusaria* sp., sample n. SPO1433; **D.** Lichenicolus and rock inhabiting *Lichenothelia arida* (Lichenotheliales, Dothideomycetes) on rocks developing abundant ascomata (arrow) at thallus center, sample n. L2162; **E.** Lichenicolus and rock inhabiting *Lichenothelia scopularia* (Lichenotheliales, Dothideomycetes), thallus in which algae (arrow) are visible and wrapped by the melanized hyphae, sample n. L2181; **F.** Rock inhabiting *Lichenothelia* sp. growing in proximity of algal colonies in rock crevices, sample n. L1298. Scale bars: A, D = 1 mm; B, C, E, F = 0,5 mm.

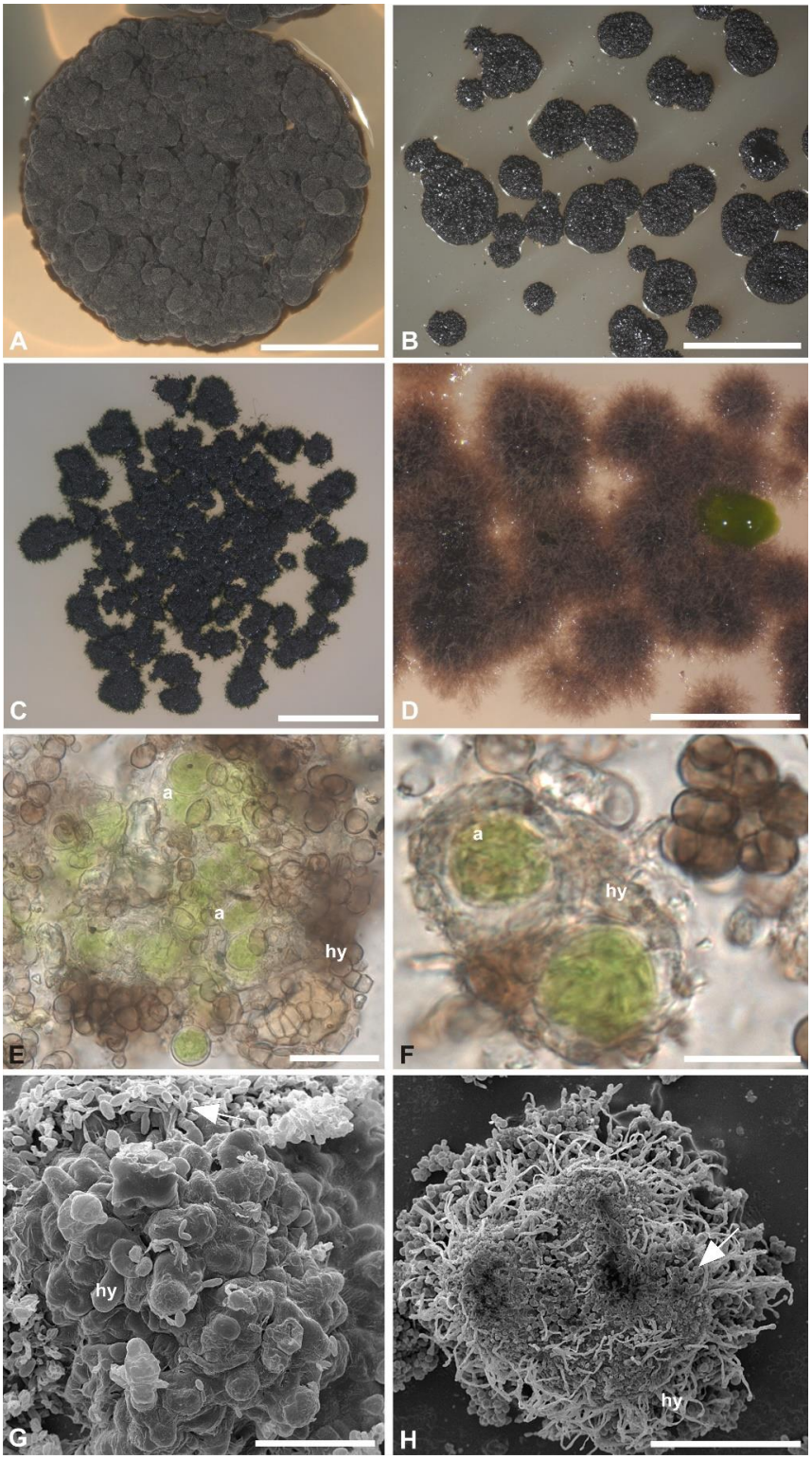

Figure 4 Habit of black fungi in culture and their co-growth with algae. **A.** Culture isolate of chaetothyrealean black fungus strain A564; **B.** Culture isolate of *Saxomyces americanus* (strain L1853); **C.** Culture isolate of *Lichenothelia convexa* (strain L1844); **D.** *Lichenothelia calcarea* co-cultured with *Coccomyxa* sp. (strain PL2-1); **E, F.** Thallus of environmental sample of *Lichenothelia* sp. (sample L2181) in which fungal hyphae wrap algal cells of *Trebouxia* sp.; **G.** Scanning electron microscopy (SEM) microphotograph of *Saxomyces alpinus* (CCFEE 5470) co-cultured with *Coccomyxa* sp. strain PL2-1; **H.** SEM microphotograph of *Lichenothelia convexa* (strain L1844) co-cultured with *Trebouxia* sp. Scale bars: A = 4 mm; B, C = 2 mm; D = 1 mm; E = 25 micon; F = 10 micron; G, H = 100 micron.

Although the mycelium of *Lichenothelia* never builds a typical "thallus" with an internal algal layer, rather, algae are often found in close contact with the fungal hyphae (Fig. 3e, f). So far, *in vitro* experiments by which both growth rate and structure of mixed culture of *Lichenothelia* with algae were tested (Fig. 4 b-d, g, h) did not provide experimental evidence of symbiosis establishment (Ametrano et al. 2017). Certain black fungi might better suit as experimental models to study lichen-like associations (Gorbushina et al. 2005; Brunauer et al. 2007). Few black fungal species indeed form lichen associations with a characteristic thallus morphology, as shown by the microfilamentous cushions formed by the genera *Cystocoleus* and *Racodium* (Muggia et al. 2008), and several (small) lichenized lineages in the Dothideales show that there is a inherent capacity for exhibiting this life style (Nelsen et al. 2009).

Why black fungi can only form very primitive types of associations with algae? We argue that a major step to lichen thalli is associated with the down-regulation of melanin production. Lichenized fungi shelter their algal partners beneath a protective peripheral fungal layer, which develops by the conglutination of the outer cell walls of the fungi. This dense fungal layer needs to keep the thallus structure tight and functional even when mechanic stress occurs by shrinking and swelling with changing water conditions. We argue that the required flexibility is impeded when cell walls are made rigid by highly crosslinked melanin polymers. Most lichens have found other ways to screen against high doses of light, e.g. by forming crystals that are deposited outside of the cell walls.

Omics approaches for the study of black fungi

'Omics' approaches, genomics, transcriptomics, proteomics, etc., speeded up the view on the organization of life in 21th century biology. Large amount of data is generated by these approaches that require substantial statistical and computational analyses (Zhang et al. 2010), as well as easy access to information for comparative analyses. Fungal comparative genomics has become an affordable and popular endeavour, as exemplified by project to sequence and analyse 1000 fungal genomes (http://1000.fungalgenomes.org). We are only beginning to interpret the details of the biology of black fungi within an omics framework.

More than 37 genomes of chaetothyrealean black yeasts are now available in different databases (Moreno et al. 2018b). Black yeast genomes of Chaetothyriomycetidae are similar in size, ranging from 25.8 Mb in *Capronia coronata* CBS617.96 to 43 Mb in *Cladophialophora immunda* CBS 834.96. These sizes are in the lower average of filamentous ascomycetes, and the length of genomes is not correlated with adaptations to the ecological extremes. However, several protein families in black fungal genomes have undergone extensive gene duplication events (Teixeira et al. 2017). Among the expanded families, cytochromes p450 (CYP), drug efflux pumps, alcohol dehydrogenase (ADH), and aldehyde dehydrogenase (ALDHs) seem to be widely distributed across black yeasts. Retention of duplicated genes suggests that the broadening of corresponding metabolic processes and promiscuity for substrates played a role to adapt to their habitats. Based on these findings, Teixeira et al. (2017) suggested that detoxification by black fungi occurs by catabolism of phenolic compounds via phenylacetic acid and homogentisate.

Since its beginning, genome sequencing of Dothideomycetes has advanced much further and as of March 2018, the Joint Genome Institute site listed 123 sequenced genomes. The great interest in Dothideomycetes is certainly associated with the large number of plant pathogens in that class (Ohm et al. 2012). The number of sequenced extremotolerant fungi is, though, still fairly low. Sterflinger et al. (2014) used comparative genomics to study the differences between *Cryomyces antarcticus* and the mesophilic fungi *Neurospora crassa*, *Coniosporium apollinis* (a species highly tolerant to UV radiation, desiccation and high temperature), the halotolerant *Hortaea werneckii*, the human pathogens *Exophiala dermatitidis* and *Cladosporium sphaerospermum*. However, as Sterflinger and coauthors (2014) concluded, the analysis of draft genomes did not reveal any significant deviations of *Cryomyces* genomes and those of mesophilic hyphomycetes. Subsequent analyses revealed duplications of genes potentially associated with stress tolerance. The genome of *Hortaea werneckii* revealed enrichment of metal cation transporters, beside other duplications

(Lenassi et al. 2013). In four varieties of *Aureobasidium pullulans*, genome and proteome analyses recovered genes possibly associated with degradation of plastic and aromatic compounds, in addition to most of the enzyme families involved in degradation of plant material and many sugar transporters (Gostinčar et al. 2014). All of the components of the high-osmolarity glycerol pathway were present, and the genomes were enriched in putative stress-tolerance genes, e.g. aquaporins and aquaglyceroporins, alkali-metal cation transporters, genes for the synthesis of compatible solutes and melanin, and bacteriorhodopsin-like proteins. The differences in the genomes among the four *Aureobasidium* varieties prompted Gostinčar et al. (2014) to distinguish them into different species, and this raises the question about the amount of variation that has to be expected when further ecologically different strains would be investigated. Additional genome sequences, with limited effort of comparative analysis, have been provided from antarctic extremotolerant black fungi of the genus *Rachicladosporium* (Coleine et al. 2017). Even though the results show that extremotolerance in fungi is not reflected in genome size, genes potentially conferring certain metabolic adaptations to stress tolerance seem to be enriched.

Genome sequencing provides important new insights, but it is still not possible to directly infer the involvement of genes in particular functions by merely using the common annotation classifiers. The genome sequences also give no information about their regulation, nor whether there is a homogenous response over the analysed sample. Further work is therefore needed to relate the information of genome sequencing and annotation to their actual biological relevance. In order to do that, information obtained from genome sequencing should be complemented with transcriptomics and proteomics. As gene expression can be quickly modulated by environmental stressors, transcriptomics may suit better than genomics in testing specific hypotheses. Within chaetothyrealean black yeasts, most experiments have been conducted on *Exophiala (Wangiella) dermatitidis*, which may be considered a model among pathogenic black fungi. *E. dermatitidis* has been sampled from diverse environments, ranging from glaciers to saunas and dishwashers (Zalar et al. 2011, Zupančič et al. 2016). Therefore, its transcriptomic responses to a wide range of temperatures (1-45 °C) could be analyzed (Blasi et al. 2015). The data showed that *E. dermatitidis* usually responds to low temperatures by upregulating genes which modify lipidome composition towards membrane fluidity, whereas there is almost no stress signal in the transcriptome when the fungus is at 45 °C. Adaptation to ionizing radiations and the role of melanin (claimed by Dadachova et al. 2008) have been investigated from a transcriptomic perspective exposing both wild and melanin-deficient mutants of *E. dermatitidis*. According to these results, a high number of genes (3000) are differentially expressed, and an increased growth rate has been observed in both strains (in comparison to the corresponding not irradiated samples), when they are exposed to low dose of ionizing radiations. However, the majority of regulated genes overlap between wild strain and melanin-deficient mutant, therefore, transcriptional response to the radiation is mainly determined by cellular components other than melanin. The expression of ribosomal biogenesis genes is significantly up-regulated only in the wild-type strain (Robertson et al. 2012). However, wether melanin production might directly help to contribute energy for protein translation is doubtful, we rather assume that transcription regulators contribute to both pigment production and general transcriptional response. Comparative genomic and transcriptomic approaches have complemented in the study of Chen et al. (2014), who investigated the *E. dermatitidis* genome and the transcriptional response to low pH. The genome encodes three independent pathways for the melanin synthesis; these were active during pH stress, likely acting as a defense against oxidative damages occurring under stress conditions. The most recent transcriptomics applied to *E. dermatitidis* was an artificial infection of an *ex-vivo* skin model experiment which aimed at identifying changes in gene expression during infection and potential virulence factors among coding and noncoding RNAs. Even though the yeast-like growth is prevalent during infection, there are evidences of upregulation of genes related to hyphal growth as well. Melanins (often considered as virulence factor) and genes associated to its production are only upregulated in the L-tyrosine pathway which produces pyomelanin (these melanins are hypothesized to be involved in iron uptake as an indirect factor of pathogenicity). The other melanin pathways are instead not modulated during skin infection. Moreover, *E. dermatitidis* switches to gluconeogenesis pathway in order

to respond to decreasing level of glucose when growing on skin instead of growing in a glucose-rich medium. Genes related to metal cation (Fe, Mg) transporters are also upregulated (Poyntner et al. 2016).

Within Dothideomycetes most scientific attention focused on economically important crop pathogens, while still little is known about transcriptomics of extremotolerant fungi in this group. Nevertheless, due to its halotolerance and its biotechnological potential, *Hortaea wernekii* is among the better investigated dothidealean fungi to date. Its genome assembly has been recently improved via PacBio sequencing and combined with gene expression analyses to complement the genome annotation (Sinha et al. 2017). These analyses confirmed the previous hypothesis of a recent whole genome duplication (Lenassi et al. 2013) and identified the presence of some novel high osmolarity glycerol (HOG) pathway components. These are similar in other fungi, such as *Saccharomyces cerevisiae* and *Wallemia ichthyophaga*, but some relevant differences seem to account for the advanced salt tolerance of *Hortaea* (Plemenitaš et al. 2014).

Proteomics has been suggested as a valid instrument to investigate peculiar features of extremophilic black fungi (Marzban et al. 2013), but few proteomic analyses have been carried out within this group. The proteome of *Cryomyces antarcticus*, a fungal model for astrobiology, has been analyzed by Zakharova and co-authors (2014b). Conserved protein families involved in the house-keeping metabolism were found, but a protein pool that differs significantly from other fungal species might confer adaptation to extreme conditions. The overall number of proteins detected was low, suggesting that only a limited part of the genome, which has an average size among fungi (Sterflinger et al. 2014), is actually transcribed. This is in accordance with the findings for the proteome of *Friedmanniomyces*. *C. antarcticus* differed by expression of high levels of heat shock proteins (HSP), even when it is cultured under optimal temperature condition. This "lazy" attitude in regulation processes, which was also seen during dehydration (Zakharova et al. 2013), makes *C. antarcticus* perfectly adapted to its rather constant, extreme environment, but less competitive than other mesophilic stress-tolerant fungi.

The alteration of protein expression patterns in rock-inhabiting fungi has been analysed also under temperature variation (Tesei et al. 2012) and Mars-like simulated conditions, being the latter a combination of temperature extremes, dryness, low O_2 pressure and high radiations (Zakharova et al. 2014b). In these almost anaerobic conditions *Cryomyces antarcticus* together with *Knufia perforans* and *Exophiala jeanselmei* still proved to be metabolically active, exhibiting a significant decrease of expressed proteins during the first 24 h. Although both the extremotolerant (e.g. *Knufia*) and extremophilic (e.g. *Cryomyces*) microcolonial fungi are active under stressful abiotic condition a main difference has been found: extremophiles are always equipped with a proteome withstanding harsh conditions and just slightly tend to downregulate their activity, extremotolerants are flexible to change their proteomic profile according to the environmental conditions.

Acknowledgments

We thank Theodora Gössler for assistance in the lab. Financial support was granted by the Austrian Science Foundation (FWF P to LM).

References

Ametrano CG, Selbmann L, Muggia L (2017) A standardized approach for co-culturing dothidealean rock-inhabiting fungi and lichen photobionts *in vitro*. *Symbiosis* 73: 1–10.

Atienza V, Hawksworth DL (2008) *Lichenothelia renobalesiana* sp. nov. (Lichenotheliaceae), for a lichenicolous ascomycete confused with *Polycoccum opulentum* (Dacampiaceae). *Lichenologist* 40: 87–96.

Badali H, Prenafeta-Boldu FX, Guarro J, Klaassen CH, Meis JF, De Hoog GS (2011) *Cladophialophora psammophila*, a novel species of Chaetothyriales with a potential use in the bioremediation of volatile aromatic hydrocarbons. *Fung. Biol.* 115: 1019–1029.

Banchi E, Ametrano CG, Stanković et al. (12 authors) (2018) DNA metabarcoding uncovers fungal diversity of mixed airborne samples in Italy. *PLoS One* 13: 0194489.

Bar-Even A, Noor E, Milo R (2012) A survey of carbon fixation pathways through a quantitative lens. *J. Exp. Bot.* 63: 2325–2342.

Blasi B, Tafer H, Tesei D, Sterflinger K (2015) From glacier to sauna: RNA-seq of the human pathogen black fungus *Exophiala dermatitidis* under varying temperature conditions exhibits common and novel fungal response. *PLoS One 10*: e0127103.

Blasi B, Poyntner C, Rudavsky T, Prenafeta-Boldú FX, De Hoog S, Tafer H, Sterflinger K (2016) Pathogenic yet environmentally friendly? Black fungal candidates for bioremediation of pollutants. *Geomicrobiol. J.* 33: 308–317.

Brunauer G, Blaha J, Hager A, Türk R, Stocker-Wörgötter E, Grube M (2007) An isolated lichenicolous fungus forms lichenoid structures when co-cultured with various coccoid algae. *Symbiosis* 44: 127–136.

Butler MJ, Day AW (1998) Fungal melanins: a review. *Can. J. Microbiol.* 44: 1115–1136.

Chen Z, Martinez DA, Gujja S, Sykes SM, Zeng Q, Szaniszlo PJ, Wang Z, Cuomo CA (2014) Comparative genomic and transcriptomic analysis of *Wangiella dermatitidis*, a major cause of phaeohyphomycosis and a model black yeast human pathogen. *G3*: 113.

Chen KH, Miadlikowska J, Molnár K et al. (8 authors) (2015) Phylogenetic analyses of eurotiomycetous endophytes reveal their close affinities to Chaetothyriales, Eurotiales, and a new order - Phaeomoniellales. *Mol. Phylogenet. Evol.* 85: 117–130.

Coleine C, Masonjones S, Selbmann L, Zucconi L, Onofri S, Pacelli C, Stajich JE (2017) Draft genome sequences of the antarctic endolithic fungi *Rachicladosporium antarcticum* CCFEE 5527 and *Rachicladosporium* sp. CCFEE 5018. *Genome Announcements* 5: e00397-17.

Crous PW, Groenewald JZ, Mansilla JP, Hunter GC, Wingfield MJ (2004) Phylogenetic reassessment of *Mycosphaerella* spp. and their anamorphs occurring on Eucalyptus. *Stud. Mycol.* 50: 195–214.

Dadachova E, Casadevall A (2008). Ionizing radiation: how fungi cope, adapt, and exploit with the help of melanin. *Curr. Op. Microbiol.* 11: 525–531.

Dadachova E, Bryan RA, Huang X, et al. (8 authors) (2007) Ionizing radiation changes the electronic properties of melanin and enhances the growth of melanized fungi. *PLoS One* 2: e457.

Dadachova E, Bryan RA, Howell RC, Schweitzer AD, Aisen P, Nosanchuk JD, Casadevall A (2008) The radioprotective properties of fungal melanin are a function of its chemical composition, stable radical presence and spatial arrangement. *Pigment Cell. Melanoma Res.* 21: 192–199.

de Hoog GD, Queiroz-Telles F, Haase G et al. (13 authors) (2000) Black fungi: clinical and pathogenic approaches. *Medical Mycology* 38, suppl.1: 243–250.

de Hoog GS, Vicente VA, Gorbushina AA (2013) The bright future of darkness—the rising power of black fungi: black yeasts, microcolonial fungi, and their relatives. *Mycopathologia 175*: 365–368.

Egidi E, de Hoog GS, Isola D et al. (8 authors) (2014) Phylogeny and taxonomy of meristematic rock-inhabiting black fungi in the Dothideomycetes based on multi-locus phylogenies. *Fung. Div.* 65: 127–165.

Eisenman HC, Casadevall A (2012) Synthesis and assembly of fungal melanin. *Appl. Microbiol. Biotechnol.* 93: 931–940.

Ertz D, Lawrey JD, Common RS, Diederich P (2014) Molecular data resolve a new order of Arthoniomycetes sister to the primarily lichenized Arthoniales and composed of black yeasts, lichenicolous and rock-inhabiting species. *Fung. Div.* 66: 113–137.

Etayo J (2010) Líquenes y hongos liquenícolas de Aragón. *Guineana* 16: 1–501.

Fogarty RV, Tobin JM (1996) Fungal melanins and their interactions with metals. *Enzyme Microb. Technol.* 19: 311–317.

Fernández-Mendoza F, Fleischhacker A, Kopun T, Grube M, Muggia L (2017) ITS 1 metabarcoding highlights low specificity of lichen mycobiomes at a local scale. *Mol. Ecol.* 26: 4811–4830.

Fortuna L, Baracchini E, Adami G, Tretiach M (2017) Melanization Affects the Content of Selected Elements in Parmelioid Lichens. *J. Chem. Ecol.* 43: 1–11.

Friedl T, Büdel B (2008) Photobionts. In: Nash T III (ed.) Lichen biology 2ed. Cambridge Univ. Press, pp. 9–26.

Geiser DM, Gueidan C, Miadlikowska J et al. (11 authors) (2006). Eurotiomycetes: Eurotiomycetidae and Chaetothyriomycetidae. *Mycologia* 98: 1053–1064.

Gómez BL, Nosanchuk JD (2003) Melanin and fungi. *Curr. Op. Infect. Dis.* 16: 91–96.

Goncalves RDCR, Pombeiro-Sponchiado SR (2005) Antioxidant activity of the melanin pigment extracted from *Aspergillus nidulans*. *Biol. Pharm. Bull.* 28: 1129–1131.

Gorbushina AA (2007) Life on the rocks. *Environ. Microbiol.* 9: 1613–1631.

Gorbushina AA, Beck A, Schulte A (2005) Microcolonial rock inhabiting fungi and lichen photobionts: evidence for mutualistic interactions. *Mycol. Res.* 109: 1288–1296.

Gorbushina AA, Broughton WJ (2009) Microbiology of the atmosphere-rock interface: how biological interactions and physical stresses modulate a sophisticated microbial ecosystem. *Ann. Rev. Microbiol.* 63: 431–450.

Gorbushina AA, Krumbein WE, Hamman CH, Panina L, Soukharjevski S, Wollenzien U (1993) Role of black fungi in color change and biodeterioration of antique marbles. *Geomicrobiol. J.* 11: 205–221.

Gostinčar C, Muggia L, Grube M (2012) Polyextremotolerant black fungi: oligotrophism, adaptive potential, and a link to lichen symbioses. *Front. Microbiol.* 3: 390.
Gostinčar C, Ohm RA, Kogej T et al. (17 authors) (2014) Genome sequencing of four *Aureobasidium pullulans* varieties: biotechnological potential, stress tolerance, and description of new species. *BMC Genomics* 15: 549.
Gueidan C, Aptroot A, da Silva Cáceres ME, Badali H, Stenroos S (2014) A reappraisal of orders and families within the subclass Chaetothyriomycetidae (Eurotiomycetes, Ascomycota). *Mycol Prog* 13: 1027–1039.
Gueidan C, Ruibal C, de Hoog GS, Schneider H (2011) Rock-inhabiting fungi originated during periods of dry climate in the late Devonian and middle Triassic. *Fung. Biol.* 115: 987–996.
Gueidan C, Villaseñor CR, De Hoog GS, Gorbushina AA, Untereiner WA, Lutzoni F (2008) A rock-inhabiting ancestor for mutualistic and pathogen-rich fungal lineages. *Stud. Mycol.* 61: 111–119.
Gunde-Cimerman N, Zalar P, de Hoog S, & Plemenitaš A (2000). Hypersaline waters in salterns–natural ecological niches for halophilic black yeasts. *FEMS Microbiol. Ecol.32*: 235-240.
Hawksworth DL (1981) *Lichenothelia*, a new genus for the *Microthelia aterrima* group. *Lichenologist* 13: 141–153
Harutyunyan S, Muggia L, Grube M (2008) Black fungi in lichens from seasonally arid habitats. *Stud. Mycol.* 61: 83–90.
Henssen A (1987) *Lichenothelia*, a genus of microfungi on rocks. *Biblioth. Lichenol.* 25: 257–293.
Hewitt SK, Foster DS, Dyer PS, Avery SV (2016) Phenotypic heterogeneity in fungi: importance and methodology. *Fung. Biol. Rev.* 30: 176–184.
Hyde KD, Jones EG, Liu JK, et al. (68 authors) (2013) Families of Dothideomycetes. *Fung. Div.* 63: 1–313.
Jacobson ES, Hove E, Emery HS (1995) Antioxidant function of melanin in black fungi. *Infection Immun*. 63: 4944–4945.
Jacobson ES, Tinnell SB (1993) Antioxidant function of fungal melanin. .*J Bacteriol.* 175: 7102–7104.
Jamieson DJ (1998) Oxidative stress responses of the yeast *Saccharomyces cerevisiae*. *Yeast 14*: 1511–1527.
Keller NP (2015) Translating biosynthetic gene clusters into fungal armor and weaponry. *Nat. Chem. Biol.* 11: 671–677.
Kennes C, Veiga MC (2004) Fungal biocatalysts in the biofiltration of VOC-polluted air. *J. Biotechnol.* 113: 305–319.
Kihara J, Moriwaki A, Ito M, Arase S, Honda Y (2004) Expression of THR1, a 1, 3, 8-Trihydroxynaphthalene reductase gene involved in melanin biosynthesis in the phytopathogenic fungus *Bipolaris oryzae*, is enhanced by near-ultraviolet radiation. *Pigment Cell. Melanoma Res.* 17: 15–23.
Kirchhoff L, Olsowski M, Zilmans J et al. (10 authors) (2017) Biofilm formation of the black yeast-like fungus *Exophiala dermatitidis* and its susceptibility to antiinfective agents. *Sci. Rep.* 7: 42886.
Kirk PM, Cannon PF, Minter DW, Stalpers JA (2008) *Dictionary of the Fungi*. CABI, Wallingford, UK.
Krumbein WE (2012) Microbial interactions with mineral materials. In: Houghton DR, Smith RN, Eggins HO (eds) Biodeterioration 7. Springer Science & Business Media, pp. 78–100.
Isola D, Selbmann L, de Hoog GS, Fenice M, Onofri S, Prenafeta-Boldú FX, Zucconi L (2013) Isolation and screening of black fungi as degraders of volatile aromatic hydrocarbons. *Mycopathol.* 175: 369–379.
Langfelder K, Streibl M, Jahn B, Haase G, Brakhage AA (2003) Biosynthesis of fungal melanins and their importance for human pathogenic fungi. *Fun. Gen. Biol.* 38: 143–158.
Lenassi M, Gostinčar C, Jackman S et al. (10 authors) (2013) Whole genome duplication and enrichment of metal cation transporters revealed by de novo genome sequencing of extremely halotolerant black yeast *Hortaea werneckii*. *PLoS One* 8: e71328.
Liu JK, Hyde KD, Jeewon R, Phillips AJL et al. (8 authors) (2017) Ranking higher taxa using divergence times: a case study in Dothideomycetes. *Fung. Div.* 84: 75–99.
Lushchak VI (2011) Adaptive response to oxidative stress: bacteria, fungi, plants and animals. *Comp. Biochem. Physiol. C: Toxicol. Pharmacol. 153*: 175–190.
Marzban G, Tesei D, Sterflinger K (2013) A review beyond the borders: Proteomics of microclonial black fungi and black yeasts. *Natural Sci.* 5: 640.
McLean J, Purvis OW, Williamson BJ, Bailey EH (1998) Role for lichen melanins in uranium remediation. *Nature* 391: 649.
Mirocha CJ, DeVay JE (1971) Growth of fungi on an inorganic medium. *Can. J. Microbiol.* 17: 1373–1378.
Moreno LF, Ahmed AA, Brankovics B et al. (2018a) Genomic understanding of an infectious brain disease from the desert. *G3:* g3-300421.
Moreno LF, Vicente VA, de Hoog S (2018b) Black yeasts in the omics era: Achievements and challenges. *Medical Mycol.* 56: S32–S41.
Muggia L, Fleischhacker A, Kopun T, Grube M (2016) Extremotolerant fungi from alpine rock lichens and their phylogenetic relationships. *Fung. Div. 76*: 119–142.
Muggia L, Gueidan C, Knudsen K, Perlmutter G, Grube M (2013) The lichen connections of black fungi. *Mycopathol.* 175: 523–535.
Muggia L, Hafellner J, Wirtz N, Hawksworth DL, Grube M (2008) The sterile microfilamentous lichenized fungi *Cystocoleus ebeneus* and *Racodium rupestre* are relatives of plant pathogens and clinically important dothidealean fungi. *Mycol. Res.* 112: 50–56.

Muggia L, Kocourková J, Knudsen K (2015) Disentangling the complex of *Lichenothelia* species from rock communities in the desert. *Mycologia* 107: 1233–1253.

Nai C, Wong HY, Pannenbecker A et al. (2013) Nutritional physiology of a rock-inhabiting, model microcolonial fungus from an ancestral lineage of the Chaetothyriales (Ascomycetes). *Fung. Gen. Biol.* 56: 54–66.

Nelsen MP, Lücking R, Grube M, Mbatchou JS, Muggia L, Plata ER, Lumbsch HT (2009) Unravelling the phylogenetic relationships of lichenised fungi in Dothideomyceta. *Stud. Mycol.* 64: 135–144.

Ohm RA, Feau N, Henrissat B et al. (28 authors) (2012) Diverse Lifestyles and Strategies of Plant Pathogenesis Encoded in the Genomes of Eighteen *Dothideomycetes* Fungi. *PLoS Pathog.* 8: e1003037.

Onofri S, Selbmann L, De Hoog GS, Grube M, Barreca D, Ruisi S, Zucconi L (2007a) Evolution and adaptation of fungi at boundaries of life. *Adv. Space Res.* 40: 1657–1664.

Onofri S, Zucconi L, Selbmann L, de Hoog S, de los Ríos A, Ruisi S, Grube M (2007b). Fungal associations at the cold edge of life. In Seckbach J (ed.) *Algae and Cyanobacteria in Extreme environments*. Springer, Dordrecht, pp. 735–757.

Øvstedal DO, Smith RL (2001) *Lichens of Antarctica and South Georgia: a guide to their identification and ecology*. Cambridge University Press.

Pacelli C, Bryan RA, Onofri S, Selbmann L, Shuryak I, Dadachova E (2017) Melanin is effective in protecting fast and slow growing fungi from various types of ionizing radiation. *Environ. Microbiol.* 19: 1612–1624.

Palmer RJ, Friedmann EI (1988) Incorporation of inorganic carbon by antarctic cryptoendolithic fungi. *Polarforschung* 58: 189–191.

Plonka PM, Grabacka M (2006) Melanin synthesis in microorganisms-biotechnological and medical aspects. *Acta Biochim. Polonica* 53: 429–443.

Plemenitaš A, Lenassi M, Konte T, Kejžar A, Zajc J, Gostinčar C, Gunde-Cimerman N (2014) Adaptation to high salt concentrations in halotolerant/halophilic fungi: a molecular perspective. *Front. Microbiol. 5*: 199.

Plemenitaš A, Vaupotič T, Lenassi M, Kogej T, Gunde-Cimerman N (2008) Adaptation of extremely halotolerant black yeast *Hortaea werneckii* to increased osmolarity: a molecular perspective at a glance. *Stud. Mycol.* 61: 67–75.

Poyntner C, Blasi B, Arcalis E, Mirastschijski U, Sterflinger K, Tafer H (2016) The transcriptome of *Exophiala dermatitidis* during *ex-vivo* skin model infection. *Front. Cell. Infect. Microbiol.* 6: 136.

Prenafeta-Boldu FX, Summerbell R, de Hoog SG (2006) Fungi growing on aromatic hydrocarbons: biotechnology's unexpected encounter with biohazard? *FEMS Microbiol. Rev.* 30: 109–130.

Prenafeta-Boldú FX, Kuhn A, Luykx D, Anke H, van Groenestijn JW, de Bont JAM (2001) Isolation and characterisation of fungi growing on volatile aromatic hydrocarbons as their sole carbon and energy source. *Mycol. Res.* 105: 477–484.

Réblová M, Hubka V, Thureborn O, Lundberg J, Sallstedt T, Wedin M, Ivarsson M (2016). From the tunnels into the treetops: new lineages of black yeasts from biofilm in the Stockholm metro system and their relatives among ant-associated fungi in the Chaetothyriales. *PLoS One* 11: e0163396.

Robertson KL, Mostaghim A, Cuomo CA, Soto CM, Lebedev N, Bailey RF, Wang Z (2012) Adaptation of the black yeast *Wangiella dermatitidis* to ionizing radiation: molecular and cellular mechanisms. *PLoS One 7*: e48674.

Rodriguez RJ, Henson J, Van Volkenburgh E et al. (2008) Stress tolerance in plants via habitat-adapted symbiosis. *ISME J. 2*: 404–416.

Ruibal C, Gueidan C, Selbmann L et al. (2009) Phylogeny of rock-inhabiting fungi related to Dothideomycetes. *Stud. Mycol. 64*: 123–133.

Ruibal C, Platas G, Bills GF (2005). Isolation and characterization of melanized fungi from limestone formations in Mallorca. *Mycol. Prog*. 4: 23–38.

Ruibal C, Platas G, Bills GF (2008). High diversity and morphological convergence among melanised fungi from rock formations in the Central Mountain System of Spain. *Persoonia* 21: 93–110.

Schoch CL, Crous PW, Groenewald JZ, et al. (2009a). A class-wide phylogenetic assessment of Dothideomycetes. *Stud. Mycol.* 64: 1–15.

Schoch CL, Sung GH, López-Giráldez F et al. (64 authors) (2009b). The Ascomycota tree of life: a phylum-wide phylogeny clarifies the origin and evolution of fundamental reproductive and ecological traits. *Syst. Biol.* 58: 224–239.

Scott JA, Untereiner WA, Ewaze JO, Wong B, Doyle D (2007) *Baudoinia*, a new genus to accommodate *Torula compniacensis*. *Mycologia* 99: 592–601.

Selbmann L, de Hoog GS, Mazzaglia A, Friedmann EI, Onofri S (2005) Fungi at the edge of life: cryptoendolithic black fungi from Antarctic deserts. *Stud. Mycol.* 51: 1–32

Selbmann L, Isola D, Egidi E, Zucconi L, Gueidan C, de Hoog GS, Onofri S (2014) Mountain tips as reservoirs for new rock-fungal entities: *Saxomyces* gen. nov. and four new species from the Alps. *Fung. Div.* 65: 167–182.

Selbmann L, Zucconi L, Isola D, Onofri S (2015) Rock black fungi: excellence in the extremes, from the Antarctic to space. *Curr. Gen.* 61: 335–345.

Senesi N, Sposito G, Martin JP (1987) Copper (II) and iron (III) complexation by humic acid-like polymers (melanins) from soil fungi. *Sci. Tot. Env.* 62: 241–252.

Shcherba VV, Babitskaya VG, Kurchenko VP, Ikonnikova NV, Kukulyanskaya TA (2000) Antioxidant properties of fungal melanin pigments. *Appl. Biochem. Microbiol.* 36: 491–495.
Singaravelan N, Grishkan I, Beharav A, Wakamatsu K, Ito S, Nevo E (2008) Adaptive melanin response of the soil fungus *Aspergillus niger* to UV radiation stress at "Evolution Canyon", Mount Carmel, Israel. *PLoS One* 3: e2993.
Sinha S, Flibotte S, Neira M et al. (10 authors) (2017). Insight into the recent genome duplication of the halophilic yeast *Hortaea werneckii*: Combining an improved genome with gene expression and chromatin structure. *G3*: 117.
Slepecky RA, Starmer WT (2009) Phenotypic plasticity in fungi: a review with observations on *Aureobasidium pullulans*. *Mycologia* 101: 823–32
Staley JT, Palmer F, Adams JB (1982) Microcolonial fungi: common inhabitants on desert rocks? *Science* 215: 1093–1095.
Sterflinger K (1998) Ecophysiology of rock inhabiting black yeasts with special reference to temperature and osmotic stress. *Antonie van Leeuwenhoek* 74: 271–281.
Sterflinger K (2006) Black yeasts and meristematic fungi: ecology, diversity and identification. In. Rosa CA, Peter G (eds) *Biodiversity and ecophysiology of yeasts.* Springer Berlin Heidelberg, pp. 501–514.
Sterflinger K, de Hoog GS, Haase G (1999) Phylogeny and ecology of meristematic ascomycetes. *Stud. Mycol.* 43: 5–22.
Sterflinger K, Lopandic K, Pandey RV, Blasi B, Kriegner A (2014) Nothing special in the specialist? Draft genome sequence of *Cryomyces antarcticus*, the most extremophilic fungus from Antarctica. *PLoS One* 9: e109908.
Swan G (1974) Structure, chemistry, and biosynthesis of the melanins. In Herz W, Grisebach H, Kirby GW (eds) *Progress in the Chemistry of Organic Natural Products.* Springer, Vienna, pp. 521–582.
Taylor JW (2011) One fungus = one name: DNA and fungal nomenclature twenty years after PCR. *IMA Fungus* 2: 113–120.
Teixeira MM, Moreno LF, Stielow BJ et al. (28 authors) (2017) Exploring the genomic diversity of black yeasts and relatives (Chaetothyriales, Ascomycota). *Stud. Mycol.* 86: 1–28.
Tesei D, Marzban G, Zakharova K, Isola D, Selbmann L, Sterflinger K (2012) Alteration of protein patterns in black rock inhabiting fungi as a response to different temperatures. *Fung. Biol.* 116: 932–940.
Tribe HT, Thines E, Weber RW (2006) Moulds that should be better known: the wine cellar mould, *Racodium cellare* Persoon. *Mycologist* 20: 171–175.
Turian G (1977) *Coniosporium aeroalgicolum* sp. hov., moissisure dèmatièe semi-lichenisante. *Ber. Schweiz. Bot. Ges.* 87: 19–24.
Turrens JF (2003) Mitochondrial formation of reactive oxygen species. *J. Physiol.* 552: 335–344.
Valadbeigi T, Schultz M, Von Brackel W (2016) Two new species of *Lichenothelia* (Lichenotheliaceae) from Iran. *Lichenologist* 48: 191–199.
Vasse M, Voglmayr H, Mayer V et al. (10 authors) (2017) A phylogenetic perspective on the association between ants (Hymenoptera: Formicidae) and black yeasts (Ascomycota: Chaetothyriales). *Proc. R. Soc. B* 284: 20162519.
Vicente VA, Weiss VA, Bombassaro A et al. (28 authors) (2017). Comparative genomics of sibling species of *Fonsecaea* associated with human chromoblastomycosis. *Front. Microbiol.* 8: 1924.
Voglmayr H, Mayer V, Maschwitz U, Moog J, Djieto-Lordon C, Blatrix R (2011) The diversity of ant-associated black yeasts: insights into a newly discovered world of symbiotic interactions. *Fungal Biol.* 115: 1077–1091.
Wang Y, Casadevall A (1994) Decreased susceptibility of melanized *Cryptococcus neoformans* to UV light. *Appl. Environ. Microbiol.* 60: 3864–3866.
Zakharova K, Sterflinger K, Razzazi-Fazeli E, Noebauer K, Marzban G (2014) Global proteomics of the extremophile black fungus *Cryomyces antarcticus* using 2D-Electrophoresis. *Natural Sci.* 6: 978.
Zakharova K, Tesei D, Marzban G, Dijksterhuis J, Wyatt T (2013) Microcolonial fungi on rocks: A life in constant drought? *Mycopathologia* 175: 537–547
Zalar P, Gostinčar C, de Hoog GS, Uršič V, Sudhadham M, Gunde-Cimerman N (2008) Redefinition of Aureobasidium pullulans and its varieties. *Stud. Mycol.* 61: 21–38.
Zalar P, Novak M, de Hoog GS, Gunde-Cimerman N (2011) Dishwashers a man-made ecological niche accommodating human opportunistic fungal pathogens. *Fung. Biol.* 115: 997–1007.
Zhang W, Li F, Nie L (2010) Integrating multiple 'omics' analysis for microbial biology: application and methodologies. *Microbiology* 156: 287–301.
Zhurbenko MP (2008) A new species from the genus *Lichenothelia* (Ascomycota) from the Northern Ural. *Mikologia i Fitopatologia* 42*:* 240–243.
Zupančič J, Novak Babič M, Zalar P, Gunde-Cimerman N (2016) The black yeast *Exophiala dermatitidis* and other selected opportunistic human fungal pathogens spread from dishwashers to kitchens. *PLoS One* 11: e0148166.

Chapter 2

Phylogenetic relationships of rock-inhabiting black fungi belonging to the widespread genera *Lichenothelia* and *Saxomyces*

Claudio G. AMETRANO[a], Kerry KNUDSEN[b], Jana KOCOURKOVÁ[b], Martin GRUBE[c], Laura SELBMANN[d, e], Lucia MUGGIA[a*]

[a] University of Trieste, Department of Life Sciences, via Giorgieri 10, 34127 Trieste, Italy; [b] Czech University of Life Sciences Prague, Faculty of Environmental Sciences, Department of Ecology, Czech Republic, Kamýcká 129, 16500 Praha 6, Czech Republic; [c] Karl-Franzens University of Graz, Institute of Plant Science, Holteigasse 6, 8010 Graz, Austria; [d] University of Tuscia, Largo dell' Università, Department of Ecological and Biological Sciences, 01100 Viterbo, Italy; [e] Italian Antarctic National Museum (MNA), Mycological Section, Genova, Italy.

Abstract

Rock-inhabiting fungi (RIF) are adapted to thrive in oligotrophic environments and to survive under conditions of abiotic stress. Under these circumstances they form biocoenoses with other tolerant organisms, such as lichens, or with less specific phototrophic consortia of aerial algae or cyanobacteria. RIF are phylogenetically diverse, and their plastic morphological characters hamper the straightforward species delimitation of many taxa. Here we present a phylogenetic study of two RIF genera, *Lichenothelia* and *Saxomyces*. Representatives of both genera inhabit rather similar niches on rocks, but their phylogenetic relationships are unknown so far. The cosmopolitan genus *Lichenothelia* is recognized by characters of fertile ascomata and includes species with different life strategies. In contrast, *Saxomyces* species were described exclusively by mycelial characters found in cultured isolates from rock samples collected at high alpine elevations. Here we use an extended taxon sampling of Dothideomycetes to study the phylogenetic relationships of both *Lichenothelia* and *Saxomyces*. We consider environmental samples, type species and cultured isolates of both genera and demonstrate their paraphyly, as well as the occurrence of teleomorphs in *Saxomyces*. We applied three species delimitation methods to improve species recognition based on molecular data. We show the distinctiveness of the two main lineages of *Lichenothelia* (Lichenotheliales s.str.) and *Saxomyces* and discuss differences in species delimitation depending on molecular markers or methods. We revise the taxonomy of the two genera and describe three new taxa, *Lichenothelia papilliformis*, *L. muriformis* and *Saxomyces americanus,* and the teleomorph of *S. penninicus*.

Key words: Ascomycota, Dothideomycetes, evolution, integrative taxonomy, molecular systematics, morphology, ribosomal DNA, species delimitation, teleomorph.

Introduction

Natural and anthropogenic lithic substrates are colonized frequently by black, rock inhabiting fungi (RIF; Sterflinger 2006). RIF are cosmopolitan and known from a wide range of habitats that are hardly colonized by any other eukaryotic life forms, including both hot and cold deserts (Staley et al. 1982; Friedmann 1982; Onofri et al. 1999). Oligotrophic RIF seem to outcompete other fungi in part via their survival capacities, including a pronounced desiccation tolerance and resistance to diverse environmental stresses (Staley et al. 1982; Sterflinger 2006; Gorbushina 2007; Onofri et al. 2008; Gostincar et al. 2012; Selbmann et al. 2015).

Rock-inhabiting fungi represent a complex of polyphyletic taxa that evolved early and independently in the Dothideomycetes and Eurotiomycetes (Gueidan et al. 2008, 2011). Close relatives of RIF are taxa that share similar polyextremotolerant features but have different lifestyles (Gostincar et al. 2011, 2012). They include plant and human pathogens, lichenicolous fungi, or fungi that form lichen-like structures with algae (Ruibal et al. 2005, 2009; Brunauer et al. 2007; Harutyunyan et al. 2008; Muggia et al. 2008, 2013, 2016; Selbmann et al. 2005, 2013). Even if RIF occurring directly on exposed rocks do not necessarily form associations with algae, they may be able to do so in culture (Gorbushina et al. 2005; Gorbushina & Broughton 2009; Ametrano et al. 2017). These findings prompted the authors to speculate about phylogenetic links between RIF and lichenized fungi (Gostincar et al. 2012).

Notwithstanding the overall similarities in morphological characters, RIF present subtle variation in mycelial or microcolonial forms that are consistent with their genetic diversity (Ruibal et al. 2005, 2009; Muggia et al. 2015). This variation may be induced by spatial isolation or local environmental pressures that contribute to adaptive radiation (Selbmann et al. 2014), which complicates species delimitation (a cryptic species phenomenon). This also renders it difficult to assess the variation of species described in the past, especially in lineages represented by only few specimens, e.g. in the genus *Lichenothelia* (Henssen 1987). More recent descriptions of RIF species are based on cultured strains (e.g. *Vermiconia*, Egidi et al. 2014; *Saxomyces*, Selbmann et al. 2014). Nucleic sequence data help to identify them as species and to place them in larger phylogenetic frameworks. Such studies, using a broad taxon sampling (e.g. in Dothideomycetes) may also uncover lineages of RIF at higher taxonomic levels (e.g., orders) (Selbmann et al. 2008; Ruibal et al. 2009; Schoch et al. 2009; Muggia et al. 2013, 2015).

Here, we focused on two genera of RIF, i.e. *Lichenothelia* and *Saxomyces*, which have originally been described according two different approaches. Since their description, isolates obtained in culture and genetic sequence data have enabled further comparisons of their morphological traits and genetic diversity. *Lichenothelia* comprises 28 taxa (according to Mycobank, January 2018) and represents a group of usually fertile and globally distributed fungi. *Lichenothelia* species generally have been described by morphological characters studied in environmental samples (Hawksworth 1981; Henssen 1987; Atienza & Hawksworth 2008; Zhurbenko 2008; Etayo 2010; Muggia et al. 2015; Valadbeigi et al. 2016). These studies revealed *Lichenothelia* as a genus with diverse life strategies. Species may inhabit rocks or lichens, or grow loosely associated with algae as borderline lichens (Henssen 1987; Muggia et al. 2015). For this reason, the genus was hypothesized to represent a link between rock-inhabiting and lichenized fungi (Hawksworth 1981; Muggia et al. 2013). Because of its versatile life style, *Lichenothelia* also has been included in lichen surveys either as lichenized fungi (Etayo 2010) or as lichen parasites (Kocourková & Knudsen 2009). Muggia et al. (2015) recently focused on *Lichenothelia* species distributed in desert regions in California (USA) and characterized five species, revising the *Lichenothelia* species concept introduced by Henssen (1987) in the first survey of the genus. *Saxomyces*, on the other hand, has been isolated from rock samples from high altitudes in the Alps and was described exclusively from cultured isolates as anamorphic hyphomycetes for which only conidiophores and conidiospores were observed (Selbmann et al. 2014).

We present a broad taxon sampling of Dothideomycetes in which we consider environmental samples and culture isolates of *Lichenothelia* and *Saxomyces* collected in multiple localities and including the types of *Saxomyces* and of some *Lichenothelia* species. We discuss their phylogenetic relationships, their identity, and their taxonomic treatment, aiming at: *i)* resolving in more detail (at species level) and improving phylogenetic support for the monophyletic lineage Lichenotheliaceae/Lichenotheliales as identified previously in Hyde et al. (2013) and Muggia et al. (2013, 2015); *ii)* testing how a morphologically based approach of species recognition reconciles with a phylogenetic species concept and species delimitations in *Lichenothelia* and *Saxomyces*; *iii)* evaluating the relationships of *Saxomyces* and *Lichenothelia* and revising their taxonomy in accordance to their anamorphic and teleomorphic states.

Matherials and methods

Sampling. — Samples of *Lichenothelia* and *Saxomyces* were collected in seven localities across Europe (Italy and Czech Republic) and U.S.A. (California) in the period 2009–2016 (Table 1). The samples include thalli growing on different substrates and under different ecological conditions. Specimens were stored at room temperature until processing. A total of 49 samples were considered for morphological analyses. Of these, 47 were selected for molecular analyses, and of these 47 ten were further selected for culture isolations. The samples are stored in GZU, UCR and the private Herbarium Mycologicum Kocourková & Knudsen (Hb. K & K) collections, with some duplicates distributed to other herbaria (B, H, KRAM, NY, PRM, UPS).

Morphological analyses. — We analysed the morphology of all samples and segregated species also based on the monophyly that the samples showed in the phylogenetic analyses. The descriptions of the two genera is here not reported as they correspond to the original descriptions of *Lichenothelia* (and Lichenotheliaceae) by Hennsen (1986) and Hyde et al. (2013), and of *Saxomyces* by Selbmann et al. (2014), respectively. The following morpho-anatomical traits were analyzed in the environmental samples and used for species delimitation as in Muggia et al. (2015): fertile stromata stipitate or not; presence or absence of slender interascal filaments; ascospore size and septation; and morphology of the thallus, especially of superficial hyphae. Structures of samples were studied in water and 10% KOH (K). Amyloid reactions were tested in fresh and undiluted Lugol's iodine without pre-treatment with K, and ascus stains were studied with I with or without pre-treatment with K. Ascospore measurements were made in water with an accuracy of 0.5 µm and given as (min.–) X1–X2–X3 (–max.), where min. / max. are the extremes from all measurements, X1 is the lowest arithmetic mean observed for a specimen, X2 is the arithmetic mean of all observations, X3 is the highest arithmetic mean observed for a specimen. They are followed by the number of measurements (n). The length/breadth ratio of ascospore is indicated as l/b and given in the same form.

Macrophotographs of environmental samples were taken with digital cameras (Nikon D810, Keyence VHX 6000, Olympus DP72 and DP74) mounted on Olympus SZX 7 and SZX16 stereomicroscopes equipped with PRO-SZM1-Focus Drive Motorization for stacking pictures. The images were stacked with the Olympus DeepFocus 3.4 module. Microphotographs were taken with a digital camera Olympus DP72 and DP74, mounted on an Olympus BX51 Light Microscope fitted with Nomarski interference contrast and using Promicra QuickPhoto Camera 3.1 software. Figure plates were processed with QuickPhoto Camera 3.1 software fitted with Promicra Publisher Module.

Morphological analyses of the cultured strains were performed on six to ten-month-old cultures. We considered the following characters as in Egidi et al (2014), Selbmann et al. (2014) and Muggia et al. (2015): form of growth, filamentous vs. yeast-like; branching of the hyphae; hyphal maturation and degree of melanization; and conidiogenesis. Small fragments of the mycelium were taken and squashed sections were mounted in water. Images were acquired with a ZeissAxioCam MRc5 digital camera fitted to the microscopes. Images of growth habit and hyphaal structure were digitally optimized using the CombineZM software (open source image processing software available at www.hadleyweb.pwp.blueyonder.co.uk/). The figures were prepared with CorelDRAW X4.

Culture isolation. —Fungal strains were isolated from environmental samples under a sterile hood. Several washing steps with a 1:10 dilution of Tween80 solution and sterile deionized water were performed on a magnetic stirrer to decrease possible external contamination by bacteria and yeast (Bubrick & Galun 1986; 15 min washing in deionized sterile water, 15 min washing in 1:10 Tween80 solution, 5 min rinse in deionized sterile water). A final washing step was performed by pipetting the 1:10 Tween80 solution directly on the selected area of the thallus and finally washing by pipetting with deionized sterile water. Up to 15 inocula were prepared for each sample on Bold Basal medium (BBM, Bold 1949) amended with ampicillin. When specimens were fertile, the ascomata were dissected and the hymenial parts were used to inoculate the medium. For sterile specimens, pieces as tiny as possible of vegetative black hyphae were picked. Agar plates were

incubated in a growth chamber at 20 °C with a dark-light regime of 12:12 h. After 3 months inocula were sub–cultured on malt yeast medium (MY, Ahmadjian 1967). After 1–2 month a fragment of the subculture was taken for genetic identification, morphological analyses, and cryostock preparations. The cultured strains are maintained at the University of Graz in the culture collection Cultures of Lichens and Extremotolerant Organisms (CLEO) established by LM, at the public culture collections of Culture Collection of Fungi from Extreme Environments (CCFEE) at the University of Viterbo, and at the Mycotheca Universitatis Taurinensis (MUT) at the University of Turin (Italy). Cultured strains are referenced as their DNA extraction number (culture identification numbers (LMCCxxxx) are reported in Table 1). The identity of the cultures was checked by sequencing the nuclear and mitochondrial loci (nuclear 28S and 18S rDNA, mitochondrial 12S rDNA) selected for the environmental samples.

Table 1. Environmental samples and cultured strains of *Lichenothelia* spp. and *Saxomyces* spp. included in the phylogenetic analyses of FIG. 1, FIGs S1–S3 and S5.

species name	DNA extr. N.	congruency	substrate and ecology	geographic origin	voucher information	altitude m (a.s.l.)	nucLSU	nucSSU	mtSSU
Saxomyces alpinus	-		-	Stolenberg, Monte Rosa (I), in Selbmann et al. (2014)	CCFEE 5462	3200	KC315870	KC315859	KC315881
S. alpinus	-		granite	Stolenberg, Monte Rosa (I), in Selbmann et al. (2014)	CCFEE 5466	3200	GU250392	GU250350	GU250433
S. alpinus	-		-	Stolenberg, Monte Rosa (I), in Selbmann et al. (2014)	CCFEE 5469	3200	KC315871	KC315860	KC315882
S. alpinus	-		-	Italy, Val de La Mare, Passo Stelvio (I), in Selbmann et al. (2014)	CCFEE 5470	2570	KC315872	KC315861	KC315883
S. alpinus	-		-	Italy, Colle delle Pisse, Monte Rosa (I), in Selbmann et al. (2014)	CCFEE 5477	3112	KC315873	KC315862	KC315884
S. alpinus	-		sandstone	Stolenberg, Monte Rosa (I), in Selbmann et al. (2014)	CCFEE 5491	3200	KC315874	KC315863	KC315885
S. penninicus	-		-	Italy, Punta Indren, Monte Rosa (I), in Selbmann et al. (2014)	CCFEE 5495	3300	KC315875	KC315864	KC315886
Lichenotheliaceae sp.	-		-	in Ertz *et al.* (2014)	Ertz D. 15255 (BR)	-	KF176950	-	-
Lichenotheliaceae sp.	-		-	in Ertz *et al.* (2014)	Ertz D. 16122 (BR)	-	KF176956	-	KF176982
Lichenotheliaceae sp.	-		-	in Ertz *et al.* (2014)	Ertz D. 16340 (BR)	-	KF176957	-	KF176983
Lichenotheliaceae sp.	-		-	in Ertz *et al.* (2014)	Ertz D. 16455 (BR)	-	KF176958	-	KF176984
Lichenotheliaceae sp.	-		-	in Ertz *et al.* (2014)	Ertz D. 17457 (BR)	-	KF176959	-	KF176985
L. convexa	-		-	in Ertz *et al.* (2014)	Diederich P. 17491	-	KF176962	-	KF176988
L. rugosa	-		lichenicolous on *Diploschistes scruposus*	in Ertz *et al.* (2014)	Ertz D. 16065 (BR)	-	KF176964	-	-
L. rugosa	-		lichenicolous on *Diploschistes scruposus*	in Ertz *et al.* (2014)	Diederich P. 17310	-	KF176963	-	KF176989
Lichenothelia sp.	L984		granitic boulder; shady	U.S.A., North Carolina, WakeCounty, Mark´s Creek, 35°44´48" N/ 78°25´27" W.	Perlmutter G. 2617	64	KC015074	KC015087	-
Lichenothelia sp.	L985		granitic boulder; shady	U.S.A., North Carolina, WakeCounty, Mark´s Creek, 35°44´48" N/ 78°25´27" W.	Perlmutter G. 2621	64	KC015075	KC015088	-
Lichenothelia sp.	L986		granitic boulder; shady	U.S.A., North Carolina, WakeCounty, Mark´s Creek, 35°44´48" N/ 78°25´27" W.	Perlmutter G. 2620	64	KC015076	KC015089	KR045782

L. umbrophila	L1323		conglomerate siliceous-calcareous rocks	Europe, Czech Republic, South Moravia, Moravsky Krumlov.	Muggia L. & Kocourkova J.	300	KC015061	KC015081	-
L. umbrophila	L1324		conglomerate siliceous-calcareous rocks	Europe, Czech Republic, South Moravia, Moravsky Krumlov.	Muggia L. & Kocourkova J.	300	KC015062	KC015082	-
L. convexa	L1606		granite; also on lichen thalli	U.S.A., California, Mojave Desert, Joshua Tree NP, Malapai Hill, 33°56´20" N/ 116°04´58"W	Knudsen K. 12564 (UCR, 67675)	1163	KC015068	KC015083	KR045778
L. convexa	L1609	5	shale	Europe, Czech Republic, Pitkovice, Pitkovicka stran, 50°01´26" N/ 14°34´21" E.	Knudsen K. 12452 (UCR, 1304KK64)	276	KC015071	KC015086	-
L. arida	L1703		granite	U.S.A., California, San Bernardino County, Mojava Desert, Joshua Tree NP, Covington Flats, 34°00´51" N/ 116°18´08" W.	Knudsen K. 14037 (UCR, 773KK64)	1426	-	KR045799	KR045772
S. americanus	L1705		granite boulders (seasonally flushed by water)	U.S.A., California, San Bernardino County, Mojava Desert, Joshua Tree NP, Smith Water Canyon, 34°01´46" N/ 116°16´44" W.	Knudsen K. 13041 (UCR, 1816KK64)	1279	MH258986	-	-
L. umbrophila	L1706		monzogranite	U.S.A., California, Riverside County, Mojava Desert, Joshua Tree NP, Indian Cove, 34°01´14" N/ 116°10´29" W.	Knudsen K. 13079.2 (UCR, 1782KK64)	1244	KC015063	KR045807	-
L. arida	L1707		gneiss and granite	U.S.A., California, Riverside County, Mojava Desert, Joshua Tree NP, Malapai Hill, 33°55´21" N/ 116°02´35" W.	Knudsen K. 12670 (UCR, 1576KK64)	995	KC015064	KR045795	KR045770
L. arida	L1708		granite and pinto gneiss	U.S.A., California, Riverside County, Mojava Desert, Joshua Tree NP, Malapai Hill, 33°55´21" N/ 116°02´35" W.	Knudsen K. 12672 (UCR, 1503KK64)	995	KC015065	KR045800	KR045773
L. umbrophila	L1715		monogranite	U.S.A., California, Riverside County, Mojava Desert, Joshua Tree NP, Indian Cove, 34°01´14" N/ 116°10´29" W.	Knudsen K. 13079.2 (UCR, 1782KK64)	1244	KC015066	KR045808	-
L. arida	L1717		monzogranite	U.S.A., California, Riverside County, Mojava Desert, Joshua Tree NP, Malapai Hill, 33°57´22.3" N/ 116°00´55" W.	Knudsen K. 13482 (UCR, 1778KK64)	1040	KC015067	KR045798	-

L. calcarea	L1799	3	limestone	U.S.A., California, San Bernardino Couty, Mojave Desert, Clark Mountain, 53°30´37"N/ 115°36´39"W.	Knudsen K. 11741 (UCR, 62126)	1768	KR045746	KR045804	KR045775
L. convexa	L1835	5*	-	culture from *Lichenothelia convexa* L1609	LMCC0499		KR045749	-	KR045779
L. calcarea	L1840	3*	-	culture from *Lichenothelia calcarea* L1799 (LICAL2)	LMCC0065		KR045747	KR045802	KR045776
L. convexa	L1844	5*	-	culture from *Lichenothelia convexa* L1609	LMCC0061		KR045750	KR045805	KR045780
Lichenothelia sp.	L1851		-	culture from *Lichenostigma epirupestre* L1709	LMCC0511		MH258987	MH259040	-
L. convexa	L1852	5*	-	culture from *Lichenothelia convexa* L1609	LMCC0484		KR045751	KR045806	KR045781
S. americanus	L1853	1*	-	culture from *Lichenothelia tenuissima* L1798	LMCC0060		-	MH259041	-
Lichenoconiales sp.	L2023		granite	U.S.A., California, Riverside County, Peninsular Range, San Jacinto Mts, San jacinto peak, 33°47´59.9" N/ 116°29´ W.	Knudsen K. 15807 (UCR, 338KK12)		KR045759	-	-
L. arida	L2024		granite	U.S.A., California, Riverside County, Peninsular Range, San Jacinto Mts, San jacinto peak, 33°47´59.9" N/ 116°29´ W.	Knudsen K. 15807 (UCR, 338KK12), duplicate	2971	-	KR045796	KR045771
L. arida	L2126		acid rock; shady, along shallow wash	U.S.A., California, Riverside County, Colorado Desert, Joshua Tree NP, 30°49´30" N/ 115°16´23.6" W.	Knudsen K. 14427 (UCR, 437KK64)	159	-	-	MH259115
L. arida	L2127		hard gneiss boulder; partly shady	U.S.A., California, San Bernardino County, Mojave Desert, Joshua Tree NP, 34°00´51.7" N/ 116°18´05" W.	Knudsen K. 14029 (UCR, 823KK64)	1435	-	-	MH259116
S. americanus	L2155		metamorphosed; shale	U.S.A, California, Mono County, Sierra Nevada, Tioga Pass, 37°56´17.5" N/ 119°14´46.2" W.	Knudsen K. 14765.1 (UCR, 224760)	2893	-	MH259042	MH259117
S. americanus	L2156	2	metamorphosed; shale	U.S.A, California, Mono County, Sierra Nevada, Tioga Pass, Inyo National Forest, 37°56´17.5" N/ 119°14´46.2" W.	Knudsen K. 14765.2 (UCR, 236492)	2893	-	MH259043	MH259118
Lichenostigmatales sp.	L2159		decaying monzogranite boulder; shady	U.S.A, California, Riverside County, Mojave Desert, Joshua Tree NP, Indian Cove, 34°01´14.8" N/ 116°10´29.4" W.	Knudsen K. 16330 (UCR, 947KK12)	1244	-	MH259044	-
L. arida	L2162		granite	U.S.A, California, San Bernardino County, Mojave Desert, San Bernardino Mts, 34°18´57.8" N/ 116°48´37.5" W.	Knudsen K. 16389 (UCR, 1005KK12)	1834	-	KR045797	-

L. arida	L2165		granite	U.S.A, California, San Bernardino County, Mojave Desert, Joshua Tree NP, Queen Mts, 34°06´22.7" N/ 116°06´18.1" W.	Knudsen K. 13471 (UCR, 220429)	844	-	KR045793	-
L. intermixta	L2166		granite boulders; shady	U.S.A, California, San Bernardino County, Mojave Desert, Joshua Tree NP, Queen Mts, 34°06´22.7" N/ 116°06´18.1" W.	Knudsen K. 13472.1 (UCR, 2200508)	844	-	MH259113	-
L. arida	L2167		granite	U.S.A, California, San Bernardino County, Mojave Desert, Joshua Tree NP, Queen Mts, 34°06´22.7" N/ 116°06´18.1" W.	Knudsen K. 13472.1 (UCR, 2200508)	844	-	KR045794	-
L. arida	L2172		gneiss and quartz	U.S.A, California, Riverside County, Mojave Desert, Joshua Tree NP, Malapai Hill, 33°55´21.3" N/ 116°02´35.2" W.	Knudsen K. 16329 (UCR, 946KK12)	995	-	KR045801	KR045774
Saxomyces-group	L2173		granite boulder; shady	U.S.A, California, Riverside County, Peninsula Range, Santa Ana Mts, Wildomar, 33°31´40" N/ 117°16´53.3" W.	Knudsen K. 16386 (UCR, 1002KK12)	572	-	MH259045	MH259119
Saxomyces-group	L2174		granite boulder; shady	U.S.A, California, Riverside County, Peninsula Range, Santa Ana Mts, Wildomar, 33°31´40" N/ 117°16´53.3" W.	Knudsen K. 16386 (UCR, 1002KK12)	572	MH258988	MH259046	MH259120
Saxomyces-group	L2175		granite boulder; shady	U.S.A, California, Riverside County, Peninsula Range, Santa Ana Mts, Wildomar, 33°31´40" N/ 117°16´53.3" W.	Knudsen K. 16386 (UCR, 1002KK12)	572	-	MH259047	MH259121
Capnodiales sp.	L2176	2*	-	culture from *Saxomyces americanus* L2156	-		-	MH259048	-
Capnodiales sp.	L2177	2*	-	culture from *Saxomyces americanus* L2155	-		MH258989	MH259049	MH259122
Saxomyces sp.	L2178		granite boulder; along perennial stream	U.S.A, California, San Bernardino County, San Bernardino Mts, 34°13´36.7" N/ 117°17´41.8" W.	Knudsen K. 16381 (UCR, 986KK12)	1083	MH258990	MH259050	MH259123
Saxomyces sp.	L2179		granite boulder; along perennial stream	U.S.A, California, San Bernardino County, San Bernardino Mts, 34°13´36.7" N/ 117°17´41.8" W.	Knudsen K. 16381 (UCR, 986KK12)	1083	MH258991	-	-

Saxomyces sp.	L2180	4	granite boulder; along perennial stream	U.S.A, California, San Bernardino County, San Bernardino Mts, 34°13´36.7" N/ 117°17´41.8" W.	Knudsen K. 16381 (UCR, 986KK12)	1083	MH258992	MH259051	-
Saxomyces sp.	L2181		granite boulder; along perennial stream	U.S.A, California, San Bernardino County, San Bernardino Mts, 34°13´36.7" N/ 117°17´41.8" W.	Knudsen K. 16381 (UCR, 986KK12)	1083	MH258993	MH259052	-
Saxomyces sp.	L2182		granite boulder; along perennial stream	U.S.A, California, San Bernardino County, San Bernardino Mts, 34°13´36.7" N/ 117°17´41.8" W.	Knudsen K. 16381 (UCR, 986KK12)	1083	MH258994	MH259053	-
Saxomyces sp.	L2183		granite boulder; along perennial stream	U.S.A, California, San Bernardino County, San Bernardino Mts, 34°13´36.7" N/ 117°17´41.8" W.	Knudsen K. 16381 (UCR, 986KK12)	1083	MH258995	MH259054	-
L. dimelaenae	L2184		lichenicolous on *Dimelaena oreina*	culture of *Lichenothelia* on *Dimelaena oreina* (JK8234)	LMCC0504		MH258996	MH259055	MH259124
L. arida	L2195		-	culture from *Lichenothelia arida* L2170 (inoculum A)	LMCC0496		KR045754	KR045809	KR045783
L. arida	L2196		-	culture from *Lichenothelia arida* L2170 (inoculum B)	LMCC0497		KR045753	KR045810	KR045786
L. arida	L2197		-	culture from *Lichenothelia arida* L2168	-		KR045752	KR045811	KR045784
Capnodiales sp.	L2198		-	culture from *L. arida* L2161 (inoculum 1)	LMCC0063		KR045755	KR045812	KR045785
L. arida	L2199		-	culture from *Lichenothelia arida* L2161 (inoculum 4)	-		-	MH259114	MH259165
Lichenothelia arida	L2200		-	culture from *Lichenothelia arida* L2168 (inoculum x)	-		MH258997	MH259056	MH259125
S. americanus	L2212	8	HCl-metamorphosed shale	U.S.A., California, Inyo County, White Mts, 37°21´18 "N/ 118°10´51" W.	Knudsen K. 16933 (UCR, 200KKhp)	2779	MH258998	MH259057	MH259126
S. americanus	L2214	9	hard limestone in shade; shady	U.S.A., California, Inyo County, White Mts, 37°18´46.2" N/ 118°10´54 W.	Knudsen K. 16946 (UCR, 203KKhp)	2550	MH258999	MH259058	MH259127
S. americanus	L2215	9	hard limestone; shady	U.S.A., California, Inyo County, White Mts, 37°18´46.2" N/ 118°10´54 W.	Knudsen K. 16946 (UCR, 203KKhp)	2550	MH259000	MH259059	-

L. intermixta	L2216	9	hard limestone; shady	U.S.A., California, Inyo County, White Mts, 37°18´46.2" N/ 118°10´54 W.	Knudsen K. 16946 (UCR, 203KKhp)	2550	-	MH259060	MH259128
L. arida	L2217	9	hard limestone; shady	U.S.A., California, Inyo County, White Mts, 37°18´46.2" N/ 118°10´54 W.	Knudsen K. 16946 (UCR, 203KKhp)	2550	MH259001	MH259061	MH259129
S. americanus	L2218	7	metamorphosed shale; light shady	U.S.A., California, Inyo County, White Mts, 37°18´28.6" N/ 118°10´29.7" W.	Knudsen K. 16947 (UCR, 201KKhp)	2380	MH259002	MH259062	MH259130
S. americanus	L2219	7	metamorphosed shale; light shady	U.S.A., California, Inyo County, White Mts, 37°18´28.6" N/ 118°10´29.7" W.	Knudsen K. 16947 (UCR, 201KKhp)	2380	MH259003	MH259063	MH259131
L. intermixta	L2220	6	hard limestone	U.S.A., California, Inyo County, White Mts, 37°18´46.2" N/ 118°10´54 W.	Knudsen K. 16949 (UCR, 204KKhp)	2550	-	MH259064	-
L. intermixta	L2221	6	hard limestone	U.S.A., California, Inyo County, White Mts, 37°18´46.2" N/ 118°10´54 W.	Knudsen K. 16949 (UCR, 204KKhp)	2550	MH259004	MH259065	-
L. arida	L2258		quartzite; shady	U.S.A., California, San Bernardino County, Transverse range, San Bernardino Mts, 34°17´27" N/ 116°48´05.3" W.	Knudsen K. 16138.1 (UCR, 1107KKn)	2094	-	MH259066	MH259132
L. arida	L2259		quartzite; shady	U.S.A., California, San Bernardino County, Transverse range, San Bernardino Mts, 34°17´27" N/ 116°48´05.3" W.	Knudsen K. 16138.1 (UCR, 1107KKn)	2094	-	MH259067	MH259133
L. arida	L2260		quartzite; shady	U.S.A., California, San Bernardino County, Transverse range, San Bernardino Mts, 34°17´27" N/ 116°48´05.3" W.	Knudsen K. 16138.1 (UCR, 1107KKn)	2094	-	MH259068	MH259134
L. intermixta	L2282	6*	-	culture from L2220; L2221	LMCC0543		-	-	MH259135
L. intermixta	L2283	6*	-	culture from L2220; L2221	LMCC0544		-	MH259069	MH259136
L. intermixta	L2284	6*	-	culture from L2220; L2221	LMCC0525		-	MH259070	MH259137
Lichenostigmatales sp.	L2285	7*	-	culture from L2218; L2219	LMCC0526		MH259005	MH259071	MH259138
Capnodiales sp.	L2286	8*	-	culture from L2212	LMCC0527		MH259006	MH259072	MH259139
Lichenostigmatales sp.	L2287	7*	-	culture from L2218; L2219	LMCC0528		MH259007	MH259073	-
Lichenostigmatales sp.	L2288	7*	-	culture from L2218; L2219	LMCC0529		MH259008	MH259074	-
Lichenostigmatales sp.	L2289	7*	-	culture from L2218; L2219 (inoculum 1)	LMCC0530		MH259009	MH259075	-
S. americanus	L2291	7*	-	culture from L2218; L2219 (inoculum 3)	LMCC0531		MH259010	MH259076	MH259140
S. americanus	L2292	7*	-	culture from L2218; L2219 (inoculum 4)	LMCC0532		MH259011	MH259077	MH259141
S. americanus	L2293	9*	-	culture from L2214; L2215; L2216; L2217 (inoculum 1)	LMCC0533		MH259012	MH259078	MH259142

S. americanus	L2294	9*	-	culture from L2214; L2215; L2216; L2217 (inoculum 2)	LMCC0534		MH259013	MH259079	MH259143
S. americanus	L2295	9*	-	culture from L2214; L2215; L2216; L2217 (inoculum 3)	LMCC0535		MH259014	MH259080	MH259144
S. americanus	L2296	9*	-	culture from L2214; L2215; L2216; L2217 (inoculum 4)	LMCC0536		MH259015	MH259081	MH259145
S. americanus	L2297	4*	-	culture from L2180	LMCC0537		MH259016	MH259082	MH259146
Saxomyces sp.	L2298		-	culture from L2129 (later contaminated)	-		-	MH259083	-
L. dimelaenae	L2299		-	culture of *Lichenothelia* on *Dimelaena oreina* (JK8234)	LMCC0504		-	MH259084	MH259147
L. muriformis	L2302		granite; shady	U.S.A., California, San Bernardino County, San Bernardino Mts, 34°15'53.6" N/ 116°43'54.1" W.	Knudsen K. 17476 (UCR, 1029KK13)	1867	MH259017	MH259085	-
L. muriformis	L2303		granite; shady	U.S.A., California, San Bernardino County, San Bernardino Mts, 34°15'53.6" N/ 116°43'54.1" W.	Knudsen K. 17476.2 (UCR, 1029KK13)	1867	MH259018	MH259086	MH259148
S. penninicus	L2304		granite boulder; shady	U.S.A., California, San Bernardino County, San Bernardino Mts, 34°10'12.6" N/ 116°49'51.1" W.	Knudsen K. 17509 (UCR, 1006KK13)	1913	MH259019	MH259087	-
S. penninicus	L2305		granite boulder; shady	U.S.A., California, San Bernardino County, San Bernardino Mts, 34°10'12.6" N/ 116°49'51.1" W.	Knudsen K. 17509.1 (UCR, 1006KK13)	1913	MH259020	MH259088	-
S. americanus	L2306		granite; open understorey	U.S.A., California, San Bernardino County, San Bernardino Mts, 34°10'29.9" N/ 116°44'48.1" W.	Knudsen K. 17521.1 (UCR, 1031KK13)	2294	MH259021	MH259089	MH259149
Dothideomycetes sp.	L2307		embedded granite rock; shady	U.S.A., California, San Bernardino County, San Bernardino Mts, 34°10'23" N/ 116°53'31.4" W.	Knudsen K. 17538 (UCR, 989KK13)	1845	MH259022	MH259090	-
L. muriformis	L2308		granite boulder	U.S.A., California, San Bernardino County, San Bernardino Mts, 34°10'58.8" N/ 116°52'56.7" W.	Knudsen K. 17538 (UCR, 1032KK13)	1729	MH259023	MH259091	-
S. americanus	L2309		metamorphosed shale; in full sun	U.S.A., California, San Bernardino County, San Bernardino Mts, 37°18'20.4" N/ 118°11'26.4" W.	Knudsen K. 17855 (UCR, 1392KK13)	2391	MH259024	MH259092	MH259150
S. americanus	L2310		metamorphosed shale; shady	U.S.A., California, Inyo County, White Mts, 37°20'18.1" N/ 118°10'40.1" W.	Knudsen K. 17872 (UCR, 1388KK13)	2612	MH259025	MH259093	-
Dothideomycetes sp.	L2311		dolomite; shady	U.S.A., California, San Bernardino County, San Bernardino Mts, 34°18'19.6" N/ 116°47'55.5" W.	Knudsen K. 17930 (UCR, 1526KK13)	1865	MH259026	MH259094	MH259151
L. papilliformis	L2312		dolomite	U.S.A., California, San Bernardino County, San Bernardino Mts, 34°18'19.6" N/ 116°47'55.5" W.	Knudsen K. 17935 (UCR, 1524KK13)	1865	MH259027	MH259095	-

L. intermixta	L2313	dolomites; shady	U.S.A., California, San Bernardino County, San Bernardino Mts, 34°18'19.6" N/ 116°47'55.5" W.	Knudsen K. 17936 (UCR, 1517KK13)	1865	MH259028	MH259096	MH259152
L. intermixta	L2314	dolomite; partly shady	U.S.A., California, San Bernardino County, San Bernardino Mts, 34°18'19.6" N/ 116°47'55.5" W.	Knudsen K. 17937 (UCR, 1531KK13)	1865	MH259029	MH259097	MH259153
L. papilliformis	L2316	dolomite; partly shady	U.S.A., California, San Bernardino County, San Bernardino Mts, 34°18'19.6" N/ 116°47'55.5" W.	Knudsen K. 17939 (UCR, 1521KK13)	1865	MH259030	MH259098	MH259154
L. papilliformis	L2317	dolomite; partly shady	U.S.A., California, San Bernardino County, San Bernardino Mts, 34°18'19.6" N/ 116°47'55.5" W.	Knudsen K. 17940 (UCR, 1516KK13)	1865	-	MH259099	-
L. intermixta	L2318	dolomite; partly shady	U.S.A., California, San Bernardino County, San Bernardino Mts, 34°18'18.6" N/ 116°47'54.7" W.	Knudsen K. 17941 (UCR, 1516KK13)	1849	MH259031	MH259100	MH259155
L. papilliformis	L2319	dolomite; partly shady	U.S.A., California, San Bernardino County, San Bernardino Mts, 34°18'18.6" N/ 116°47'54.7" W.	Knudsen K. 17943 (UCR, 1520KK13)	1849	MH259032	MH259101	MH259156
Dothideomycetes sp.	L2320	dolomite; partly shady	U.S.A., California, San Bernardino County, San Bernardino Mts, 34°18'18.6" N/ 116°47'54.7" W.	Knudsen K. 17944 (UCR, 1515KK13)	1849	-	MH259102	MH259157
L. papilliformis	L2321	dolomite; partly shady	U.S.A., California, San Bernardino County, San Bernardino Mts, 34°18'18.6" N/ 116°47'54.7" W.	Knudsen K. 17946 (UCR, 1529KK13)	1849	-	MH259103	MH259158
L. intermixta	L2322	dolomite; partly shady	U.S.A., California, San Bernardino County, San Bernardino Mts, 34°18'18.6" N/ 116°47'54.7" W.	Knudsen K. 17947 (UCR, 1527KK13)	1849	MH259033	MH259104	MH259159
Lichenothelia sp.	L2332	Vinschgauer mica schist; in full sun	Europe, Italy, South Tyrol, Vinschgau, Schlanders, 46°38'14" N/ 10°48'46" E.	Knudsen K. 18344	1415	MH259034	MH259105	MH259160
Lichenothelia sp.	L2333	Vinschgauer mica schist; partly shady	Europe, Italy, Trentino-Alto-Adige, Bolzano, NE of Schlanders, NW of Tappein farm, 46°38'37.18"N / 10°47'18.64" E.	Kocourkova J. 8999, (Knudsen, Ametrano & Muggia)	1585	MH259035	MH259106	-
Lichenothelia sp.	L2334	Vinschgauer mica schist; in full sun	Europe, Italy, Trentino-Alto-Adige, Bolzano, NE of Schlanders, NW of Tappein farm, 46°38'37.18"N / 10°47'18.64" E.	Kocourkova J. 8999-dupl. (Knudsen, Ametrano & Muggia)	1585	MH259036	MH259107	-
Lichenothelia sp.	L2335	Vinschgauer mica-schist; in full sun	Europe, Italy, South Tyrol, Vinschgau, Schlanders, 46°37'50" N/ 10°46'46" E.	Knudsen K. 18352 (Kocourkova, Ametrano & Muggia)	781	-	-	MH259161

Saxomyces sp.	L2336	Vinschgauer mica-schist; in full sun	Europe, Italy, South Tyrol, Vinschgau, Schlanders, 46°37'50" N/ 10°46'46" E.	Knudsen K. 18354 (Kocourkova, Ametrano & Muggia)	781	MH259037	MH259108	-
S. penninicus	L2337	Vinschgauer mica-schist	Europe, Italy, Trentino Alto-Adige, Bolzano, Vezzano, 46°38'13.14" N/ 10°48'13.37" E.	Kocourkova J. 8993 (Knudsen, Ametrano & Muggia)	1391	-	MH259109	-
Saxomyces sp.	L2338	Vinschgauer mica-schist; in full sun	Europe, Italy, South Tyrol, Vinschgau, Schlanders, 46°37'50" N/ 10°46'46" E.	Knudsen K. 18356 (Kocourkova, Ametrano & Muggia)	781	MH259038	MH259110	-
Lichenothelia sp.	L2339	Vinschgauer mica-schist; in full sun	Europe, Italy, South Tyrol, Vinschgau, Schlanders, 46°37'50" N/ 10°46'46" E.	Knudsen K. 18334 (Kocourkova, Ametrano & Muggia)	781	-	MH259111	MH259162
Lichenothelia sp.	L2340	Vinschgauer mica-schist; in full sun	Europe, Italy, South Tyrol, Vinschgau, Schlanders, 46°37'50" N/ 10°46'46" E.	Knudsen K. 18334-dupl. (Kocourkova, Ametrano & Muggia)	781	-	-	MH259163
Lichenothelia sp.	L2343	Vinschgauer mica-schist; in full sun	Europe, Italy, South Tyrol, Vinschgau, Schlanders, 46°37'50" N/ 10°46'46" E.	Knudsen K. 18357 (Kocourkova, Ametrano & Muggia)	831	MH259039	MH259112	MH259164

DNA extraction, amplification and sequencing. — The fungal material used for DNA extraction and culture isolation was taken from a single area of the mycelium and transferred into a 1.5 ml tube. DNA extractions were performed using either a small group of ascomata or, if these were rare or absent, about 0.5 cm^2 of the dry crustose, melanized thallus. The DNA of pure cultures and environmental samples was extracted according to the CTAB method (Maniatis et al. 1982) with some minor modifications. Fungal material from the axenic cultures was dried overnight in silica before grinding in liquid nitrogen. Quality and amount of the extracted DNA were checked by Nanodrop™. PCR amplifications were carried out following a touch-down protocol as in Muggia et al. (2013, 2015). The nuclear ribosomal 28S (nucLSU) locus was amplified with primers LR3R and LR7 (Vilgalys & Hester 1990). The nuclear 18S (nucSSU) was amplified with primers NS1 (White et al. 1990) and nuSSU0852 (Gargas & Taylor 1992). The mitochondrial 12S (mtSSU) locus was amplified with primers mtSSU1KL (Lohtander et al. 2002) and MSU7 (Zhou & Stanosz 2001). PCR products were cleaned using Ezna Cycle Pure Kit (Omega) and sequencing was performed by Microsynth (Austria). Amplification of the nuclear internal transcribed spacers and 5.8S gene (ITS), as the standard fungal DNA barcode (Schoch et al. 2012), was performed with primers ITF1F (Gardens & Bruns 1993) and ITS4 (White et al. 1990). However, most samples yielded multiple PCR products and were not sequenced successfully. Therefore, we exluded the ITS locus from the analyses.

Alignment and phylogenetic analyses. — Newly obtained sequences of *Lichenothelia* and *Saxomyces* sequences were added to a broad dataset including representatives of most of the orders of Dothideomycetes (available up to August 2017) and previous data from Muggia et al. (2013, 2015). As Arthoniomycetes are considered the sister group of Dothideomycetes according to recent phylogenetic inferences (Schoch et al. 2009; Egidi et al. 2014; Ertz et al. 2014), four species belonging to Arthoniales (*Dendrographa leucophaea*, *Lecanactis abietina*, *Schismatomma decolorans* and *Roccella fuciformis*) were used as outgroups. Single locus alignments were prepared in Bioedit 7.2.5 (Hall 1999). The multilocus alignment was prepared using Sequence Matrix 1.7.8. and partitioned by locus. JModelTest 2.1.10 (Darriba et al. 2012) was used to assess the best model of nucleotide substitution for each gene via the corrected Akaike Information Criterion (cAIC, Akaike, 1974).

Both Bayesian and Maximum likelihood (ML) approaches were used to reconstruct phylogenetic inferences. Bayesian phylogenies (single and multi-locus) were generated in MrBayes 3.2.6 on the Cipres Science gateway 3.3 (Miller et al. 2010). The B/MCMC analyses run with six chains simultaneously in two runs for 2 $x10^7$ generations and trees were sampled every 100 generations. Log-likelihood scores against generation time were plotted with Tracer 1.6 (Rambaut & Drummond 2007) and ESS (effective sample size) belonging to all parameters of the substitution models were checked. Burn-in was set at 2.5 x 10^6 generation to ensure that likelihood stationarity was reached. The consensus tree was calculated from the sampled trees. Convergence of the analyses was confirmed by the potential scale reduction factor (PSRF) approaching 1. Three independent runs of the same analysis were conducted. The ML phylogenies were generated on a local machine in RAxML 7.0.3 (Stamatakis et al. 2005, Stamatakis 2006). The analysis was performed using the GTRMIX model combined with 1000 bootstrap replicates.

ViPhy 1.3.1 (Bremm et al. 2011) was used to compare tree topologies and highlight differences in sample composition of clusters. Tree topologies were compared via both the leaf–based and the element–based algorithms, which assign a similarity score (0–1) to tree nodes depending on the consistency of the trees relative to a user defined reference tree. The leaf-based method only considers consistency of tips below a certain node, while the element-based method considers both tips and inner nodes to calculate the similarity score. The 'best match' selection option was then used to highlight samples that were always within a certain clade (either Lichenotheliales s.str. or *Saxomyces*) in every phylogeny compared to the multi-locus tree.

Species delimitation analyses. — In order to cluster samples into Evolutionarily Significant Units (ESU; Simpson 1951; Tang et al. 2014), three species delimitation approaches were tested: Automatic Barcode Gap

Discovery (ABGD; Puillandre et al. 2012), Poisson Tree Process (PTP; Zhang et al. 2013) and Generalized Mixed Yule coalescent (GMYC; Pons et al. 2006). The input data were the subsets of samples belonging to the clades Lichenotheliales s.str. (59 samples) and *Saxomyces* (44 samples), treated individually, as identified in the main phylogeny of Dothideomycetes (FIG. 1; Table 1, Supplementary material Table S1). Each approach was performed on the three single locus datasets mtSSU, nucLSU, nucSSU, which contained a variable number of sequences (31–49) due to the different number of successfully sequenced loci for each sample. Further, to test whether outgroups influence species delimitation, the analyses were performed with two different outgroups. First, representatives of Arthoniales were selected (as reported above); second, the most basal lineages of the Lichenotheliales s.str. and *Saxomyces* clades were chosen. The latter two, as reported below, corresponded to the clade *Cryomyces* for Lichenotheliales s.str. and representatives of Myriangiales (*Myriangium duriaei*, Myriangiales sp. A554 and Myriangiales sp. A578) for the *Saxomyces* clade. Each distance matrix or phylogeny used for species delimitation analyses was generated also with a reduced dataset, which only includes samples with three loci in order to avoid the different amount of missing data which could affect the number of delimited ESU.

ABGD (http://wwwabi.snv.jussieu.fr/public/abgd/abgdweb.html) was applied to the distance matrix obtained from the dataset alignments. This matrix was generated in MEGA7 with the following setting: Tamura-Nei distance, gamma distributed rates among site, gamma shape parameter according to JModelTest 2.1.10, and pairwise deletion of missing data to retain the maximum amount of information (due to different length of the sequences).

PTP and GMYC were tested as single and multi-rate PTP and single and multi-threshold GMYC. The analyses are identified as sPTP, mPTP, sGMYC and mGMYC, respectively. The Bayesian GMYC (bGMYC) was further implemented as it uses a random subset of posterior trees (after burn-in) generated by BEAST (*Bayesian* Evolutionary Analysis Sampling Trees; Rambaut & Drummond 2007). PTP analyses were performed on the corresponding web server (http://species.h-its.org/; http://mptp.h-its.org/), whereas GMYC analyses were performed in R (splits and bGMYC packages). The input data were phylogenies generated using BEAST and MrBayes. Phylogenetic trees inferred by MrBayes were not ultrametric and therefore used only in PTP. These phylogenies have been additionally smoothed using the R package ape 4.0 with the function *chronos* (Paradis et al. 2004) with λ=0, model =" relaxed", to use them also in GYMC as well (asChronos smoothed phylogenies were used as a third input dataset for both PTP and GMYC analyses). Substitution models were set according to cAIC criterion. Maximum clade credibility trees were obtained by three to four runs of 10^7 generations in BEAST and two runs of 5×10^6 generations in MrBayes.

Results

Morphological analyses of environmental samples. — According to morphological analyses we recognize three new taxa, which are formally described as *Lichenothelia muriformis, L. papilliformis,* and *Saxomyces americanus*. We revise the circumscription of the species *Lichenothelia intermixa* Henssen, provide the new combination of *Lichenothelia dimelaenae* (Calat. & Hafellner) Kocourk., K. Knudsen & Muggia for *Lichenostigma dimelaenae* Calat. & Hafellner and describe the teleomorph of *Saxomyces penninicus.* The detailed species descriptions are reported in the Taxonomy section below.

Morphological analyses of culture isolates. — Fewer than 10% of inocula remained uncontaminated during cultivation, reflecting the biological complexity and diversity present in environmental samples. Those that were subcultured successfully were used for molecular and morphological analyses. We recovered culture isolates in four clades (FIG. 1): Lichenostigmatales, Lichenotheliales s.str., Capnodiales and *Saxomyces* group. The strains L2282–L2284 within Lichenotheliales; L2291, L2293 and L2296 within *Saxomyces*-group; and L2285 and L2289 within Lichenostigmatales were chosen for morphological inspection, as they developed a sufficient amount of mycelium. Strains L2282–L2284 represent *Lichenothelia intermixta* (FIG. 2a–k); they are

characterized by a dense mycelium which abundantly secretes oil drops and by hyphae majorly constituted by isodiametric cells (FIG. 2c–h, j, k). Abundant branching was observed in younger parts of the colonies where hyphae are still rather hyaline (FIG. 2c–f). Mature parts of the colonies are highly melanized (FIG. 2g, j, k) and mainly composed by dense agglomerates of isodiametric cells. Strains L2291 (FIG. 2l–o) and L2293 (FIG. 2p–s) represent *Saxomyces americanus* and form hyphae that are highly melanized overall (FIG. 2m–o, q–s), branching, and composed by both elongated (FIG. 2m–o, r, s) and isodiametric cells, which densely agglomerate in older parts of the colony (FIG. 2q).

Strains L2184 and L2299 are two isolates obtained from *Lichenothelia dimelaenae* infecting the lichen *Dimelaena oreina* JK8234. These cultures were checked for their genetic identity at the time the two inocula have grown. However, the inocula were preserved as cryostocks and not subcultured any longer. Due to the extremely slow growth of the re–plated cryostocks, these strains were not available for the morphological analyses to be included here.

The strains L2285 (FIG. 2t, u) and L2289 (FIG. 2v, w) of Lichenostigmatales develop both filamentous hyphae and yeast morphs (FIG. 5t–v). Filamentous hyphae with slightly elongated cells were observed between the dense agglomerates of isodiametric, highly melanized yeast–like cells (FIG. 2w).

Phylogenetic analyses. — A total of 113 new sequences were obtained. Four samples were represented only by a single locus, 21 samples by two loci, and 22 samples by all three markers.

JModeltest analyses set the best models for the gene partitions as follows: GTR+I+G for nucLSU, SYM+I +G for nucSSU and HKY+I+G for mtSSU. All criteria gave the same result except the cAIC, which assigned the GTR+I+G model as the most suitable for each molecular marker. As AIC tends to over-parameterize by picking models with more parameters than those strictly necessary (Davidson & MacKinnon 2004), models suggested by the other three decision criteria were set for the phylogenetic analyses.

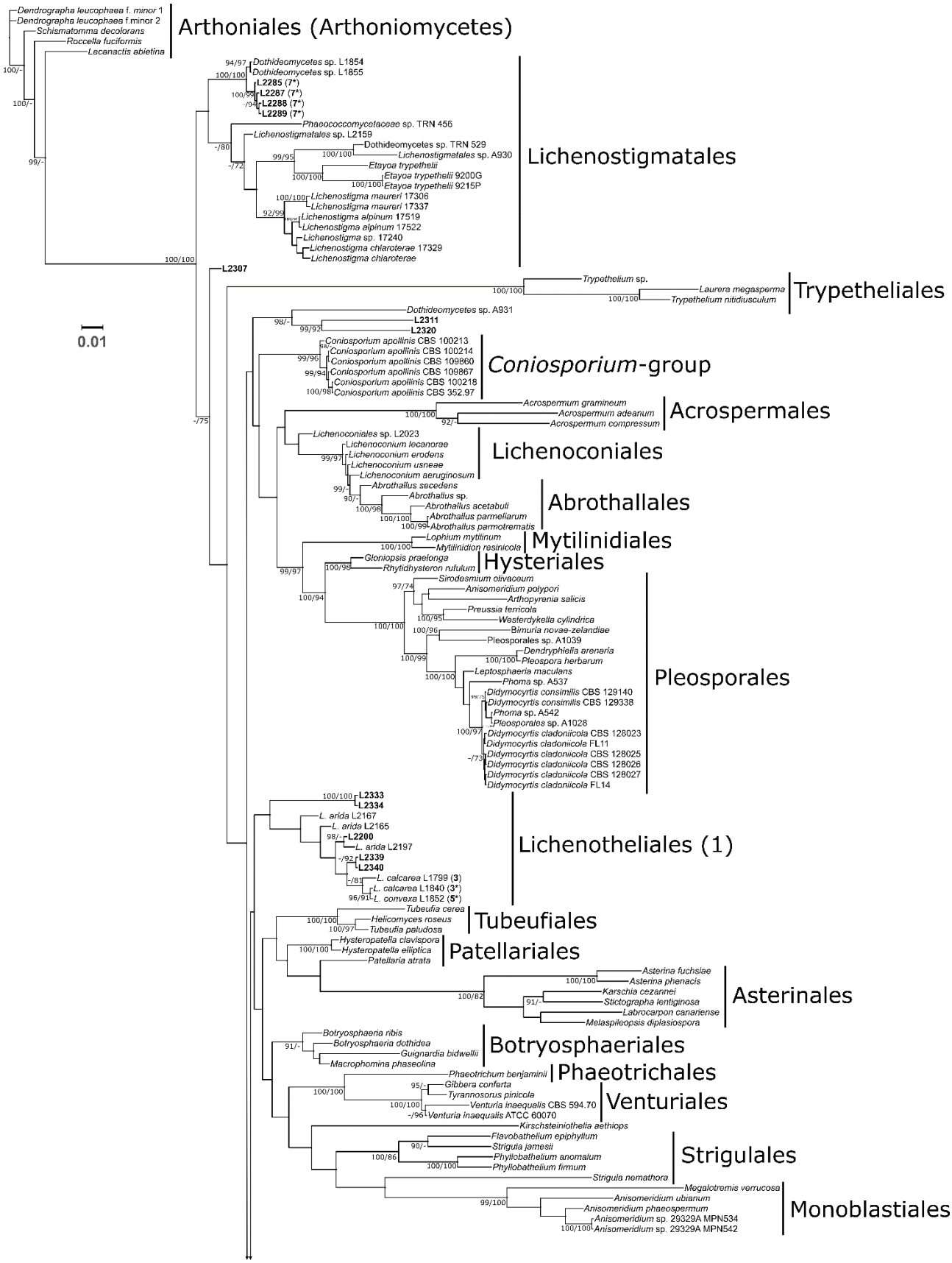
Arthoniales (Arthoniomycetes)
Dendrographa leucophaea f. minor 1
Dendrographa leucophaea f.minor 2
Schismatomma decolorans
Roccella fuciformis
Lecanactis abietina
Lichenostigmatales
Dothideomycetes sp. L1854
Dothideomycetes sp. L1855
L2285 (7*)
L2287 (7*)
L2288 (7*)
L2289 (7*)
Phaeococcomycetaceae sp. TRN 456
Lichenostigmatales sp. L2159
Dothideomycetes sp. TRN 529
Lichenostigmatales sp. A930
Etayoa trypethelii
Etayoa trypethelii 9200G
Etayoa trypethelii 9215P
Lichenostigma maureri 17306
Lichenostigma maureri 17337
Lichenostigma alpinum 17519
Lichenostigma alpinum 17522
Lichenostigma sp. 17240
Lichenostigma chlaroterae 17329
Lichenostigma chlaroterae
L2307
Trypetheliales
Trypethelium sp.
Laurera megasperma
Trypethelium nitidiusculum
0.01
Dothideomycetes sp. A931
L2311
L2320
Coniosporium-group
Coniosporium apollinis CBS 100213
Coniosporium apollinis CBS 100214
Coniosporium apollinis CBS 109860
Coniosporium apollinis CBS 109867
Coniosporium apollinis CBS 100218
Coniosporium apollinis CBS 352.97
Acrospermales
Acrospermum gramineum
Acrospermum adeanum
Acrospermum compressum
Lichenoconiales
Lichenoconiales sp. L2023
Lichenoconium lecanorae
Lichenoconium erodens
Lichenoconium usneae
Lichenoconium aeruginosum
Abrothallales
Abrothallus secedens
Abrothallus sp.
Abrothallus acetabuli
Abrothallus parmeliarum
Abrothallus parmotrematis
Mytilinidiales
Lophium mytilinum
Mytilinidion resinicola
Hysteriales
Gloniopsis praelonga
Rhytidhysteron rufulum
Pleosporales
Sirodesmium olivaceum
Anisomeridium polypori
Arthopyrenia salicis
Preussia terricola
Westerdykella cylindrica
Bimuria novae-zelandiae
Pleosporales sp. A1039
Dendryphiella arenaria
Pleospora herbarum
Leptosphaeria maculans
Phoma sp. A537
Didymocyrtis consimilis CBS 129140
Didymocyrtis consimilis CBS 129338
Phoma sp. A542
Pleosporales sp. A1028
Didymocyrtis cladoniicola CBS 128023
Didymocyrtis cladoniicola FL11
Didymocyrtis cladoniicola CBS 128025
Didymocyrtis cladoniicola CBS 128026
Didymocyrtis cladoniicola CBS 128027
Didymocyrtis cladoniicola FL14
Lichenotheliales (1)
L2333
L2334
L. arida L2167
L. arida L2165
L2200
L. arida L2197
L2339
L2340
L. calcarea L1799 (3)
L. calcarea L1840 (3*)
L. convexa L1852 (5*)
Tubeufiales
Tubeufia cerea
Helicomyces roseus
Tubeufia paludosa
Patellariales
Hysteropatella clavispora
Hysteropatella elliptica
Patellaria atrata
Asterinales
Asterina fuchsiae
Asterina phenacis
Karschia cezannei
Stictographa lentiginosa
Labrocarpon canariense
Melaspileopsis diplasiospora
Botryosphaeriales
Botryosphaeria ribis
Botryosphaeria dothidea
Guignardia bidwellii
Macrophomina phaseolina
Phaeotrichales
Phaeotrichum benjaminii
Venturiales
Gibbera conferta
Tyrannosorus pinicola
Venturia inaequalis CBS 594.70
Venturia inaequalis ATCC 60070
Strigulales
Kirschsteiniothelia aethiops
Flavobathelium epiphyllum
Strigula jamesii
Phyllobathelium anomalum
Phyllobathelium firmum
Strigula nemathora
Monoblastiales
Megalotremis verrucosa
Anisomeridium ubianum
Anisomeridium phaeospermum
Anisomeridium sp. 29329A MPN534
Anisomeridium sp. 29329A MPN542

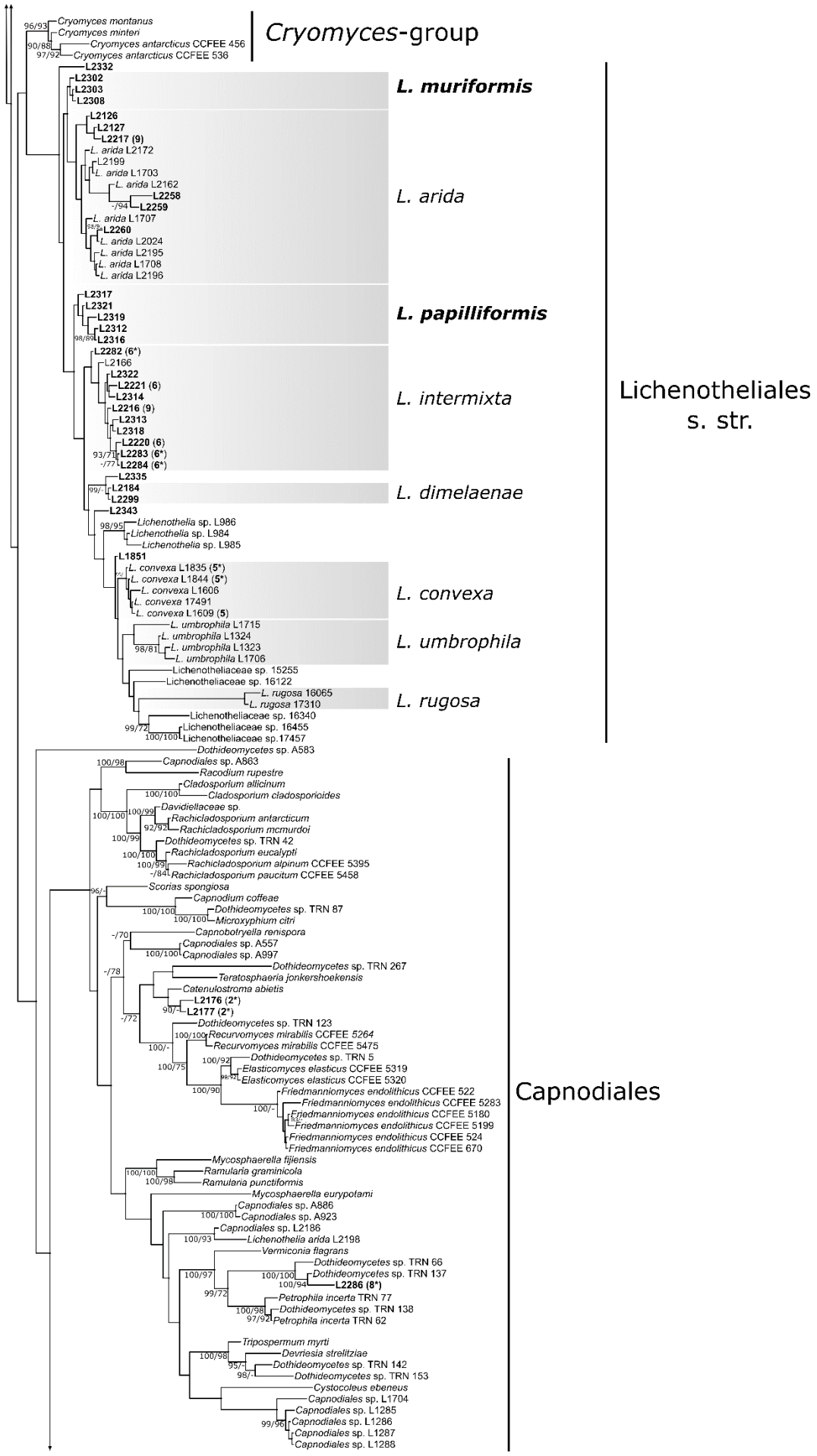
Cryomyces-group
Cryomyces montanus
Cryomyces minteri
Cryomyces antarcticus CCFEE 456
Cryomyces antarcticus CCFEE 536
L. muriformis
L. arida
L. papilliformis
L. intermixta
L. dimelaenae
L. convexa
L. umbrophila
L. rugosa
Lichenotheliales s. str.
Capnodiales

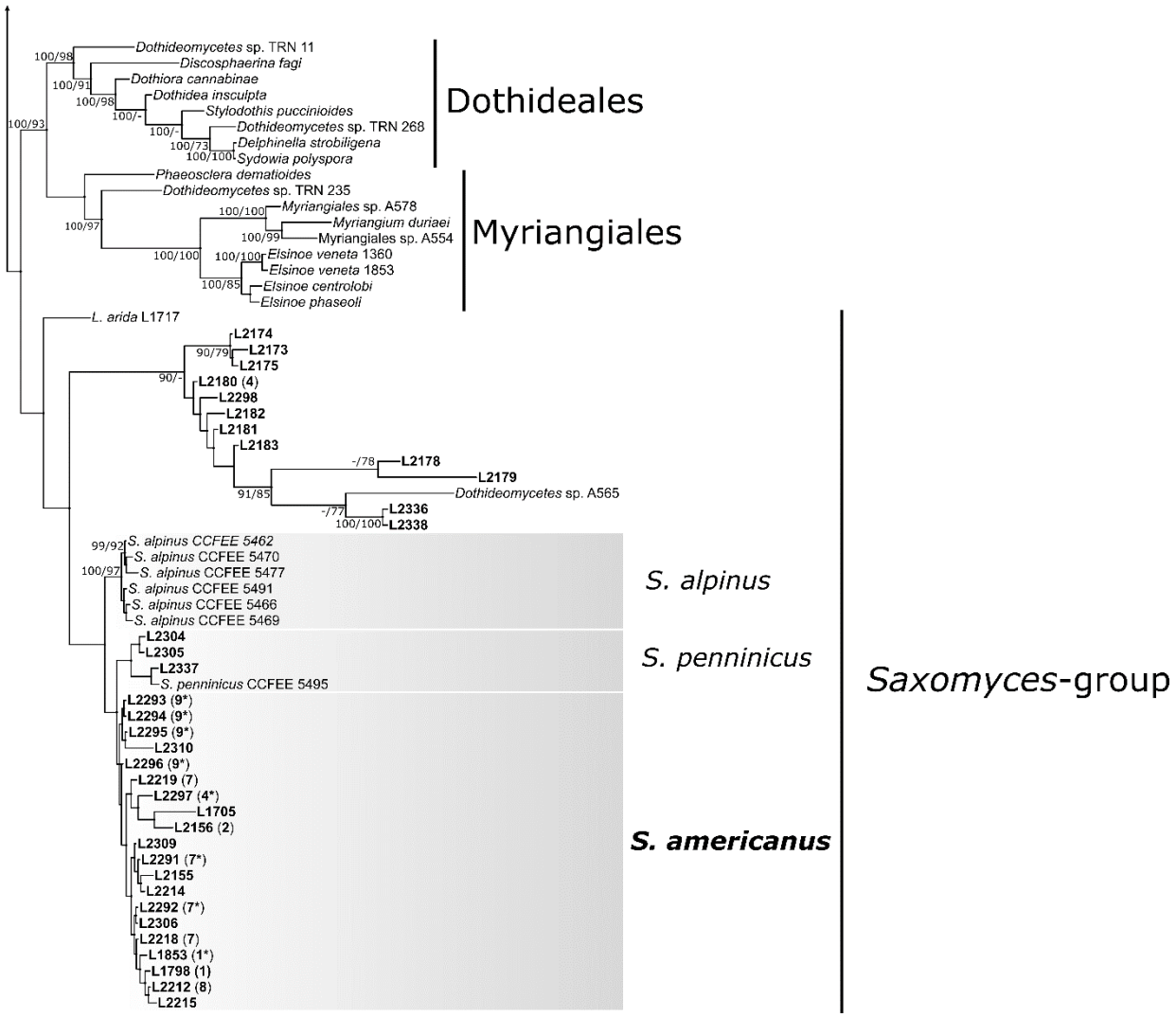

Figure 1. Phylogenetic inference of the class Dothideomycetes inferred via Bayesian analyses of the combined dataset comprising 28S (nucLSU), 18S (nucSSU) and 12S (mtSSU) loci. Bootstrap values ≥70 and Bayesian posterior probabilities ≥90 are shown above or next to the branches. Samples newly analysed in this study are in bold. Numbers next to sample names [e.g. (1) or (1*)] indicate correspondence between environmental samples and their culture isolates (marked by *). Species in bold are newly described.

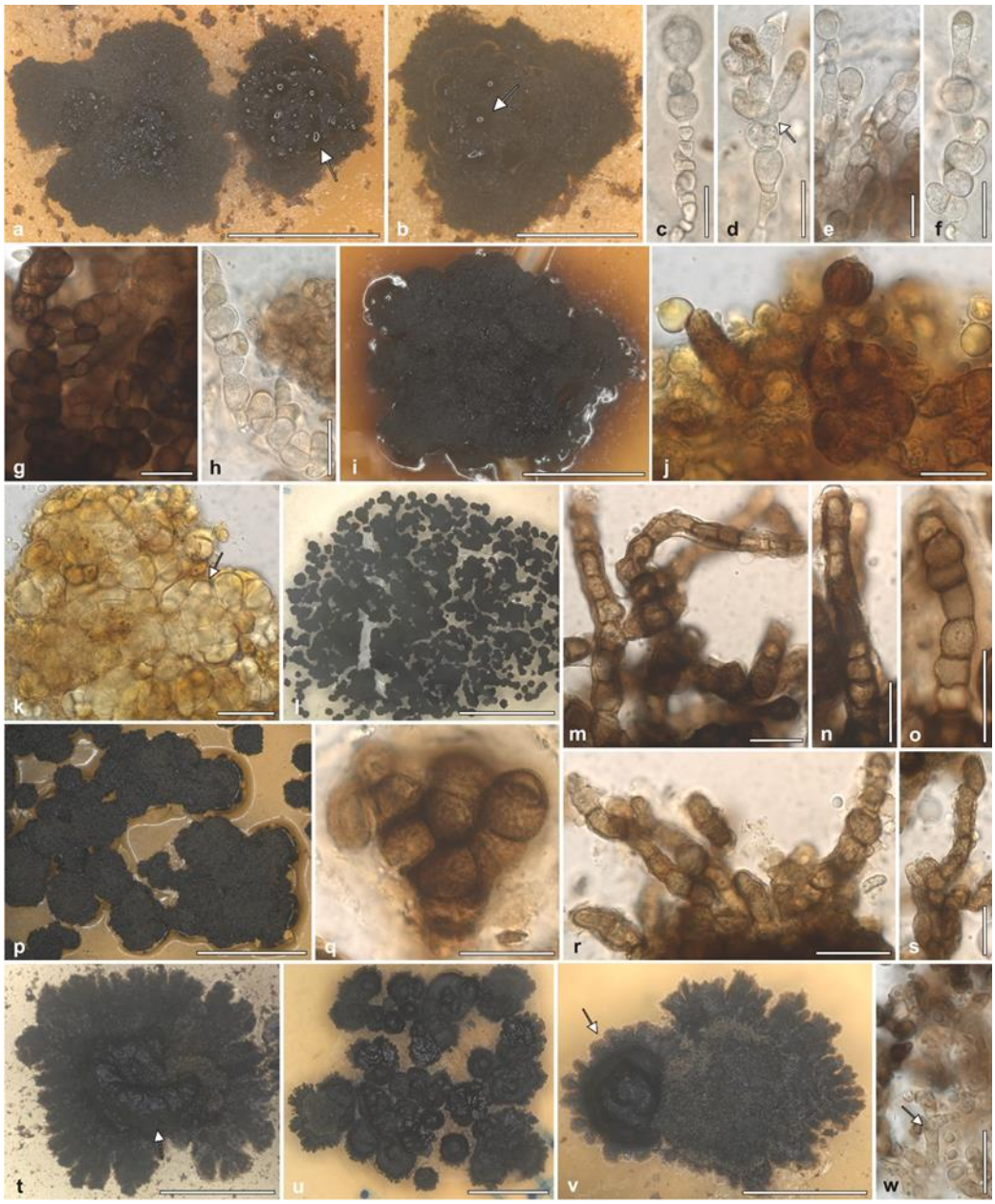

Figure 2. Habitus of cultured black fungi belonging to the lineages **a–j** Lichenotheliales s.str., **k–s** *Saxomyces*–group and **t–w** Lichenostigmatales as in the phylogeny of FIG. 1. Cultures were grown on MY medium. **a–j** strains of *Lichenothelia intermixta* (Lichenotheliales s.str.) **a–h** L2282, **j**, **k** L2283 and **i** L2284; habit of strains **a**, **b** L2282 and **i** L2284, arrows indicate abundant oil drops secreted by the fungus (a, b); **c–h**, **j**, **k** hyphae are majorly constituted by isodiametric cells, abundantly branching (arrow in d) are observed in younger parts of the colonies where hyphae are still rather hyaline(**c**–**f**), **g**, **j**, **k** mature parts of the colonies are highly melanized and mainly composed by dense agglomerates of isodiametric cells. **l–s** strains of *Saxomyces americanus* (*Saxomyces*–group) **l–o** L2291, **p–s** L2293; habitus of **l** L2291 and **p** L2293; **m–o**, **q–s** hyphae are overall highly melanized, composed by elongated (m–o, r, s) and also isodiametric cells, which form dense agglomerates (**q**) in older parts of the colony. **t–w** strains of Lichenostigmatales **t, u** L2285 and **v, w** L2289, fungi develop both filamentous hyphae and yeast morphs (arrow in t, v). **w** Filamentous hyphae with slightly elongated cells are observed in between of the dense agglomerates of isodiametric, highly melanized yeast–like cells. Scale bars: **l** = 8 mm, **i, u** = 4 mm, **a, p, v =** 2 mm, **b, t** = 1 mm, **c–h, j, k, m–o, q–s, w** = 20 µm.

Notwithstanding the low support obtained for the basal branches in Dothideomycetes, the phylogenetic inference (FIG. 1) is topologically congruent with previous analyses (Hyde et al. 2013; Wijayawardene et al. 2014; Liu et al. 2017). Orders and families are consistently monophyletic and highly supported. Samples representing both *Lichenothelia* and *Saxomyces* are recovered in distinct clades in both single-locus and multilocus analyses and are recognized as Lichenotheliales s.str., Lichenotheliales (1) and *Saxomyces*-group. These three lineages present low support, hinting at a potentially undefined position within Dothideomycetes.

The *Saxomyces* lineage is recovered with a consistent composition of samples across the different MrBayes phylogenies. It splits into two clades with low support (FIG. 1; Supplementary material FIG. S1). The Lichenotheliales s.str. always resolve as monophyletic, but with low support in both Bayesian and ML analyses. The third, smaller clade Lichenotheliales (1) contains 11 samples. It is always identified in the Bayesian multi-locus analyses (FIG. 1) but its monophyly is not supported by ML analyses.

Single-locus Bayesian phylogenies (Supplementary material FIG. S2) were compared with the multi-locus phylogeny (FIG. 1). Leaf-based phylogenetic inferences (FIG. S3) have a higher similarity score than element-based ones (Supplementary material FIG. S4), as clades are similar in sample composition but differ substantially in the internal topology of the subtrees. Both Lichenotheliales s.str. and *Saxomyces*-group lineages are recognizable. The nucSSU-based phylogeny (FIG. S3d) is the most consistent considering *Saxomyces* clade. Conversely, the nucLSU-based phylogeny (FIG. S3c) and, to a lesser extent the mtSSU-based phylogeny (FIG. S3b), have a slightly different taxa composition than the reference clade in the multi-locus phylogeny (FIG. S3a). The mtSSU phylogeny (FIG. S3f) is the most consistent for the Lichenotheliales clade and carries the greatest part of the phylogenetic information among the considered markers, likely influencing the final topology of the multi-locus phylogeny.

Correspondence between environmental samples and their culture isolates was confirmed for samples L2218 and L2219 (7), L1609 (5), L1798 (1), L1799 (3), L2180 (4), L2220 and L2221 (6) (FIG. 1, Table 1). Isolates obtained from the samples L2156 (2) and L2212 (8), did not correspond to the *Lichenothelia* fungus sequenced from the environmental samples but were recovered in Capnodiales (FIG. 1). Isolates from L2216 and L2217 (9) belong to *Saxomyces* clades but fungi corresponding to the environmental samples are recovered in Lichenotheliales s.str. The two cultured strains L2184 and L2299 isolated from a sample of *Lichenostigma dimelaenae* (parasitic on the lichen *Dimelaena oreina*) are within Lichenotheliales s.str. as well, but no molecular data were gained from the environmental specimen for comparison. The two samples L1717 and L2198 recognized as *L. arida* in Muggia et al. (2015) are placed in the present phylogeny at the base of *Saxomyces*-group and within Capnodiales, respectively (FIG. 1).

Species delimitation analyses. — A total of 18 analyses was carried out for each PTP method (single and multi-rate): 12 analyses using each GMYC method (single and multi–threshold) and six analyses using ABGD (Supplementary material Table S2 and Table S3). The distribution of the number of delimited ESU is shown by box and whisker plots (FIG. S5) both using the complete dataset (FIG. S5a, b) and the reduced dataset (FIG. S5c, d). The two datasets provided similar results when the delimitation methods are compared; however, the reduced dataset provided fewer ESU because 42% of the samples are devoid of missing data.

Delimitation of the Lichenotheliales s. str. and *Saxomyces* clade for every analysis, and their average values with SD, are reported in Supplementary material (Table S2 and S3). ABGD did not find an adequate barcode gap to identify any cluster in Lichenotheliales s.str. (FIG. S5a, c). The only exception is the clade *Saxomyces* based on the mtSSU locus (FIG. S5b, d). In both Lichenotheliales s.str. and the *Saxomyces* clades, sPTP and mGMYC tend to delimit more ESU than mPTP and sGMYC do (FIG. S5). Furthermore, mPTP and sGMYC show a narrower distribution of the number of delimited ESU than sPTP and mGMYC.

Most ABGD analyses and some mPTP and sGMYC analyses were not effective: they did not produce any valid species delimitation in our dataset. For the nuclear loci in *Saxomyces* (FIG. S6d, f) most of the methods (ABGD, mPTP, sGMYC) tend to lump the dataset whereas sPTP split them markedly (Dayrat 2005; Rittmayer & Austin, 2012). Analyses on Lichenotheliales s.str. clade (FIG. S6a, c, e) confirm the difficulties

to find any valid threshold useful to delimit ESU. In the case of nucLSU (FIG. S6c), three of the five methods did not find any cluster. As observed for the *Saxomyces* clade, sPTP always tends to delimit many ESU. The two GMYC methods are the most effective for Lichenotheliales s.str. mtSSU (FIG. S6a), with an almost identical ESU delimitation to each other and a conceivable number of delimited ESU. Among the applied methods, only GMYC provides also the statistically significance of delimitation results. The likelihood ratio test (LRT) highlighted a significantly higher value than the null model (one species) for both Lichenotheliales s. str. and *Saxomyces* mtSSU BEAST trees ($p<0.05$), when delimited with both the single and multi-threshold GMYC.

Bayesian GMYC was applied only on BEAST trees as they produce the least variable delimitations across genes and outgroups tested for Lichenotheliales s.str. clade (Supplementary material, Table S2). The heat-map output of bGMYC was added next to the bars for each BEAST generated phylogeny (FIG. S6). These square matrices show the posterior probability that the taxa belong to the same ESU. This representation allows for the visualization of uncertainty in species boundaries and for more lumping or splitting approaches to the delimitation of the same dataset depending on the selected probability.

Taxonomy

Lichenothelia dimelaenae (Calat. & Hafellner) Kocourk., K. Knudsen & Muggia, comb. nov. – MycoBank MB367253; FIG. 3.

Basionym: Lichenostigma dimelaenae Calat. & Hafellner, Lichen Flora of the Greater Sonoran Desert 2: 666 (2004).

Type: U.S.A., ARIZONA, Coconino Co., Grand Canyon National Park, north slope along Grand View trail below Grand View, 36°00'N, 111°59'W, ca. 2000 m, rocky slope with scattered trees of *Pinus edulis*, on cliffs of siliceous sandstone, 10 July 1994, *J. Hafellner 36909* (GZU, holotype, not seen).

Description: see Calatayud et al. (2004).

Ecology and distribution: Previously known from North America from Arizona (Calatayud et al. 2004) and California (Kocourková & Knudsen 2015), and from Turkey (Halici et al. 2010, Yazici & Etayo 2014). We report the species new for Central Europe from the Czech Republic, for Macaronesia from Canary Islands, and for several countries in Asia: Afghanistan, Armenia, Kazakhstan, and Kirgizia.

Specimens examined (all on *Dimelaena oreina*). U.S.A., CALIFORNIA, Riverside Co., between Hexie and Little San Bernardino Mts, north slope of Malapai Hill, 33°56'25.9"N, 116°5'14.5''W, 1247 m, small desert shrubs with basalt outcrops, on basalt outcrop, 16 Nov. 2012, *J. Kocourková 8234* and *K. Knudsen* (Hb. K & K). San Bernardino Co., San Bernardino Mountains, Burns Canyon, 34°15'20.4"N, 116°43′18.2"W, 2093 m, on granite, 5 Nov. 2014, J. *Kocourková et al. 8548* (Hb. K & K). COLORADO, Boulder Co., South slope of Flagstaff Mt. at west edge of Boulder. 5400–6000 ft, with Ponderosa pine, Douglas fir, juniper and cactum, 2 June 1967, *C.M. Wetmore 15757* (GZU). Yuma Co., at south edge of Wray on rock ledges. 3700 ft, mostly north facing cliffs with *Yucca, Opuntia* and *Selaginella*, 2 June 1967, *C.M. Wetmore 15720* (GZU). Weld Co., along Colorado Highway 52, 3.2 km N of Stoneham, 40°35ˈN, 103°45ˈW, 1372 m, rolling terrain with rock outcrops, on rock, 14 June 1961, *S. Shushan*. Anderson and Shushan: Lichens of Western North America no. 53 (GZU). IDAHO, Lemhi Co., Lemhi Vallea, Mollie Gulch S of Little Eightmile Creek, NW of Leadore, 44°45'N, 113°28'W, ca 1800 m, quarzitic boulders close to the ground, 30 July 1999, *H. Mayrhofer 13879*, & *R. Rosentreter, C.B. Davis* (GZU). Ibidem: *H. Mayrhofer 13878, & R. Rosentreter, C.B. Davis* (GZU) EUROPE, CZECH REPUBLIC, Central Bohemia, distr. Praha, Dolní Liboc, Divoká Šárka Nature Reserve, 50°5'39.95"N, 14°19'15.58"E, 335 m, on plateau of Šestákova rock, at SE edge of rock, on lydite, 18 May 2015, *J. Kocourková*, 1593 (Hb. K & K). SPAIN, Macaronesia, Canary Islands, Tenerife, flächendeckend an trockengetönten, lichtoffenen und windgefegten Stirnflächen feinkörnigen Ergussgesteins im Dimelaenetum oreinae Frey, 2200–2300 m, NO–NW, pH 6.9, Nordabfall of Montaña de Guajara in südlichen Cañadaszirkel. March 1980, *G. Follmann Lichenes Exssicati Selecti a Museo Historiae Naturalis Casselensi Editi. No. 330*

(GZU). ASIA, AFGANISTAN, Prov. Kabul, Paghman Gebirge, oberhalb des Ortes Paghman, an der Talgabelung Chap–Darrah und Rast–Farrah, 34°37'N, 68°56'E, 2550 m, on Silikatfelsenwände, ± S–SW exponiert, 30 May 1970, *M. Steiner* (GZU). Ibidem: Frontalflächen, z. T. überhangend nach N. 21 June 1970, *M. Steiner* (GZU). ARMENIA, Caucasus, distr. Sevan, in vicinitate pagi Covagjukh, 2100–2300 m, 1 July 1982, *V. Vašák* (GZU). Distr. Krasnoselsk, in declivibus montium Sevarskij chrebet, supra lacum Sevan dictum, 1950–2200 m, 29 June–6 July 1982, *A. Vězda* (GZU). KAZAKHSTAN, Vost. Kazakhstanskaja, N of the road SE of Karatogay, 18°15'N, 84°36'E, 610 m, dry sandy area close to a mountain ridge, on rocks, 11 June 1993, *R. Moberg & A. Nordin* (GZU, Lichenes Selecti Upsaliensis no. 170). KIRGHIZIA, Central Tian–Schan, Basin of Sazy–Dzaz River, Canyon of Molo River, 42°N, 79–80°E, 3200 m, alpine zone, rock outcrops, *N. Baibulatova* 242 (GZU).

The DNA extraction numbers of the cultured isolates correspond to L2184 and L2299 (FIG. 1, Table 1).

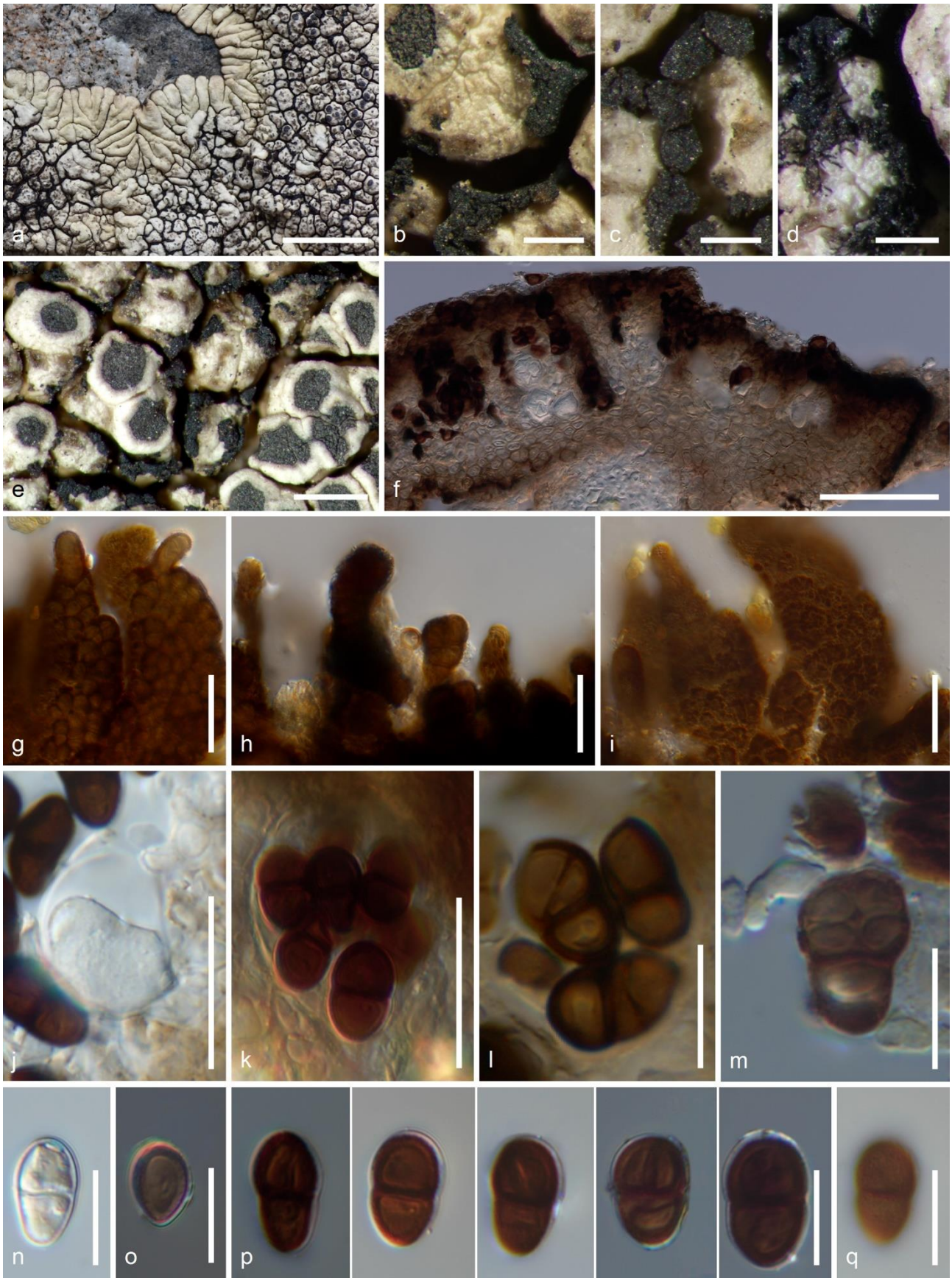
a
b
c
d
e
f
g
h
i
j
k
l
m
n
o
p
q

Figure 3. (Previous page) *Lichenothelia dimelaenae*, habitus and anatomical structures (sample *A. Vězda*, GZU). **a** Infected thallus of *Dimelaena oreina*, **b** fertile stromata lining edges of host areoles, **c** fertile stromata forming chains, **d** scarce superficial hyphae on host areoles, **e** infection slightly suppressing growth of areoles, **f** vertical section of part of ascoma, paraplectenchymatous tissue between asci, **g, h** stromatic hyphae, **i** verruculose surface of stromatic hyphae, **j** young subglobose ascus, **k** ascus with mature ascospores, **l** old thick–walled 1–2–septate ascospores, **m** germinating ascospore, **n** young aseptate hyaline ascospore, **o** brown young aseptate ascospore, **p** mature brown 1–septate spores with perispore, **q** verruculose surface of spore. Scale bars: **a** = 5 mm; **b–d** = 200 µm; **e** = 500 µm; **f** = 50 µm; **g–k** = 20 µm; **p–q** = 10 µm.

Lichenothelia intermixta Henssen, Bibliotheca Lichenologica 25:260 (1987) – MycoBank MB130681; FIG.4

Typification: U.S.A., CALIFORNIA, Inyo County, Darwin Wash, 1200 m, on limestone, 1981, C. Bratt 2140a (MB, holotype, n.v.; SBBG! H! Boise State University n.v., isotypes).

Description: Thallus black, saxicolous (FIG. 4a), rarely dendrite (FIG. 4b–d), never areolate, either solitary stromata or in groups immersed in pits in rock (FIG. 4 e, f) or epilithic with scattered sterile and fertile stromata (FIG. 4a). Thallus without hyphae observed penetrating rock, easily detached when wet. Young epilithic branches usually form new stromata at their terminals (FIG. 4b). Young fertile stromata still connected with epilithic branches (FIG. 4d, n), later breaking off and leaving independent mature stromata. Sterile or fertile stromata paraplectenchymatous (FIG. 4h, i, k, n), outer wall red brown and verruculose (FIG. 4l), cells round, 5–8 µm wide, internal cells hyaline to pale brown, 7–14 µm in diam. (FIG. 4m). Sterile stromata abundant, 30–40 µm high and 40–110 µm wide, with or without 1–3 epilithic septate branches, verruculose, brown, 6–8 µm wide, up to 60 µm long, forming new stromata usually at end of branches (FIG. 4d, n), rarely stromata growing directly from side of stromata and eventually dividing (wrongly described as macroconidia in Henssen 1987). Fertile stromata black, applanate, uniloculate, with ostiole round or as several more or less radiating cracks, 100–470 µm wide, 60–150 µm high, with distinct one or two stipes 40–60 µm wide, 60–250 µm high attaching them to the rock, later fertile stromata dividing by splitting from top (FIG. 4e, g), eventually forming independent fertile stromata (FIG. 4f), outer wall 10 to 20 µm thick. Asci arising from base of stroma, scarce interascal filaments 1 µm wide only around asci, eventually dissolving, interascal gel amyloid (FIG. 4o), asci saccate, 20–28 µm wide and 32–35 µm high, 4 to 8–spored, ascospores non–seriate (FIG. 4j), ascoplasm I– (dextrinoid) (FIG. 4o), outer wall I+ light blue, with or without short I– ocular chamber in tholus. Ascospores hyaline in ascus, becoming light brown, eventually becoming dark brown, often 1–septate, cells equal or sub–soleiform, occasionally becoming 2– to 4–septate, rarely becoming muriform with 8–cells in old ascospores (FIG. 4j), smooth–walled with halo (FIG. 4p), (10–)13.1–15.6–18(–20) × (6–)7.3–9.5–11.6(–13) µm (n=20), l/b (1.1–)1.3–1.7–2.1(–2.5). Pycnidia not seen.

Ecology and distribution: On both hard and soft calcareous rock, at elevations from 1200–2550 m. Not associated with trees and detritus, usually in full sun; not parasitic when in association with lichens. Source of nutrition unknown. Distributed in western North America, in southern and eastern California in the Mojave Desert and in the Basin and Range Province, in Inyo County (Darwin Wash and White Mountains) and San Bernardino County (Cactus Flats in San Bernardino Mountains).

Cultured strains: Cultured *Lichenothelia intermixta* strains L2282–L2284 (FIG. 1) on MY medium are characterized by a dense mycelium which secretes abundantly oil drops and by hyphae of predominately isodiametric cells (FIG. 2c–h, j, k) with abundant branching (FIG. 2c–f) observed in younger parts of the colonies, where hyphae are still rather hyaline (FIG. 2c–f). Mature parts of the colonies are highly melanized (FIG. 2g, j, k) and mainly composed by dense agglomerates of isodiametric cells. Oil inspersion was particularly abundant and prevented a proper analysis of the colony structure in the strain L2284.

Notes: The thallus of *Lichenothelia intermixta* varies in size depending on elevation, with stromata and ascospores being smaller in the type collection in Darwin Wash in Inyo County (stromata 40–80 µm; ascospores 10–15 × 7–9 µm). In the San Bernardino Mountains in southern California at elevations of 1200–1850 meters we observed a larger size of stromata and ascospores then in samples from the White Mountains in the Basin and Range Province at elevations of 2500–2600 m (stromata 50–110 µm wide; ascopores 14–20

× 7–10 µm). Henssen's protologue of *Lichenothelia intermixta* (Henssen 1987) describes a single collection, collected at its lowest recorded elevation (1200 meters) with most stromata growing solitary and immersed in the rock among dendrite *Lichenothelia calcarea* Henssen. From this single collection, Henssen (1987) described very small sterile stromata almost completely lacking septate epilithic branches and very small fertile stromata without stipes (80 µm). She did not describe the interior of infertile or fertile stromata or whether interascal gel was amyloid or not. Specimens were impossible to be positively identified before we completed our study. The inaccuracy of Henssen's descriptions from single specimens highlights the unreliability of morphological descriptions of new *Lichenothelia* species from single specimens. If a description is based on a comparison with a table of Henssen's species, the analysis should include the study of her types. She apparently conserved her types and probably did only one or two sections when she wrote the descriptions. In her description of *Lichenothelia calcarea* and *L. convexa*, further studies of type and topotype material revealed a wider ascospore variability then she described, which was later confirmed by phylogenetic studies of analyzed specimens (Kocourková & Knudsen 2009; Muggia et al. 2013).

Specimens examined. U.S.A, CALIFORNIA, San Bernardino Co., San Bernardino Mountains, Cactus Flats, north–facing slope, Pinyon-juniper woodland, 34°18'18.6"N, 116° 47'54.7"W, 1865 m, on limestone, 25 Sept. 2015, *K. Knudsen 17936 & 17937* (H, GZU, UCR); north–facing slope, Pinyon-juniper woodland, 34°18'18.6"N, 116°47'54.7"W, 1849 m, on limestone, 25 Sept. 2015, *K. Knudsen 17941 & 17947* (GZU, UCR, Hb. K & K). Inyo Co., White Mountains, Pinyon-juniper woodland, 37°18'46.2"N, 118°10'54.3"W, 2550 m, on scattered limestone boulders among metamorphosed shale, 14 Aug. 2014, *K. Knudsen 16949* (UCR, Hb. K & K); east of White Mountain Road, 37°20'12.7"N, 118°11'03.7"W, 2596 m, on hard dolomite, 15 Sept. 2015, *K. Knudsen 17871* (H, Hb. K &K).

The DNA extraction numbers of the analyzed samples correspond to L2220, L2221, L2313, L2314, L2318, L2322 (FIG. 1, Table 1).

Figure 4. (Following page) *Lichenothelia intermixta*, habitus and anatomical structures. **a, c, d, k, m–o** sample *K. Knudsen 17947* (hb. K & K), **b, e, f, h, j, l** sample *K. Knudsen 17949* (hb. K & K), **g, i, p–s** sample *K. Knudsen 16949*. **a** Thallus with dispersed stromata, **b** young thallus sterile stromata with epilithic hyphae, one young fertile stroma present, **c** mature stromata in group, hyphae still present (on the upper left), **d** young stromata in chains on hyphae, **e** group of mature fertile stromata immersed in pits, **f** two fertile stromata immersed in pits of soft limestone, **g** two fertile stromata side by side with mature asci with ascospores, **h** vertical section of old fertile stroma with two stipes, **i** section of fertile stroma with one stipe, paraplectenchymatous wall of stroma, **j** 6–spored cylindrical ascus, **k** smooth surface of young fertile stroma, **l** verruculose surface of older fertile stroma (h), **m** internal paraplectenchymatous tissue of stroma formed of globose cells, **n** 1–cell wide, septate hypha connecting sterile stroma and formation of new stroma (arrow), **o** iodine blue reaction of internal tissue of stroma, **p** young halonate ascospores, **q** variability of ascospores, young ascospore first on left, **r** verruculose surface of ascospore, **s** iodine blue reaction of ascospore perispore. Scale bars: **a** = 500 µm; **b, d–f** = 200 µm; **c, g, h** = 100 µm; **i, n** = 50 µm; **j, o, p** = 20 µm; **k–m, q–s** = 10 µm.

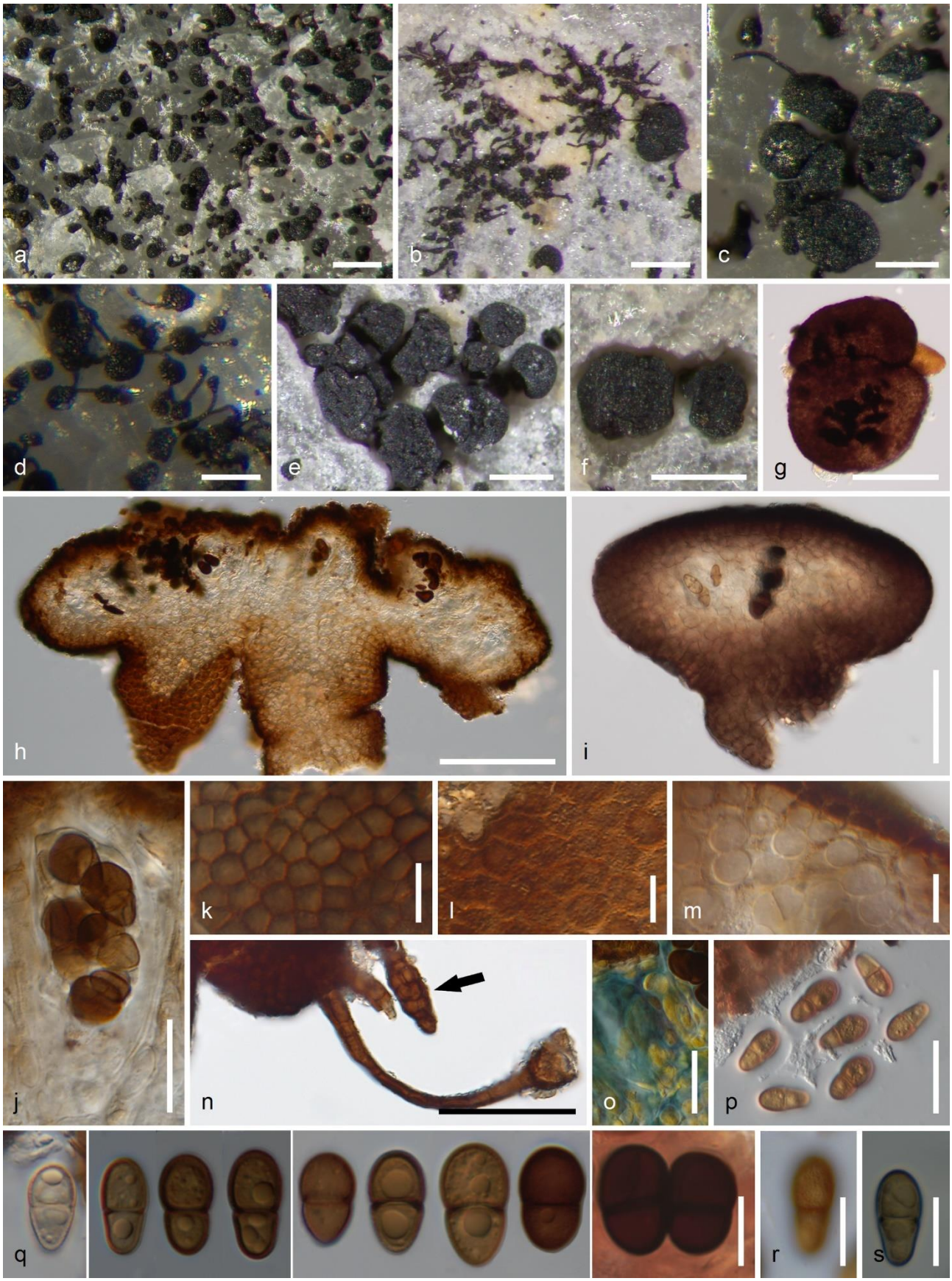
a
b
c
d
e
f
g
h
i
j
k
l
m
n
o
p
q
r
s

Lichenothelia muriformis Ametrano, K. Knudsen, Kocourk. & Muggia, sp. nov. – MycoBank MB 825180; FIG. 5

Holotype: U.S.A., California, San Bernardino Mountains: near Seven Oaks Road in flood plain of Santa Ana River, 34°10'58.8"N, 116°52'56.7"W, 1729 m, open conifer forest, on granite, 2 July 2015, *Knudsen 17561* (GZU, holotype; NY, UCR, isotypes).

Diagnosis: Similar to *Lichenothelia scopularia* but differing in having large muriform ascospores (19–)22.1–25.5–28.8(–30) × (9–)11–12.6–14.2(–15) µm.

Etymology: Producing large and muriform ascospores.

Description: Thallus black, saxicolous, orbicular (FIG. 5a) to irregularly dendrite, areolate, with epilithic branches (FIG. 5b), connected or independent, coalescent in center of thalli, 40–500 µm long, up to 50 µm tall and up to 40 µm wide, multiple layers of cells 8–12 µm wide, round to square, hyaline internally, outer surface reddish brown to black, scabrid, with increasing melanization finally eventually obscuring outer surface. In old populations epilithic branches merge and thalli are not dendrite in appearance but continuous with branches usually indistinct. Hyphae penetrating rock lacking, easily removed when wet. Fertile stromata round or irregular (FIG. 5c, d), stipitate (FIG. 5f, g), ostiolate (FIG. 5b, e), 1 to several locules with separate, often excentric ostioles, becoming applanate or convex, emerging from foundation of sterile tissue or dividing from side of fertile stromata, 250–350 µm wide and up to 250 µm high, with stipe 100–120 µm wide and 100–150 µm high of paraplectenchyma of vertical rows of short cylindrical to quadratic cells (FIG. 5j), outer wall smooth to verruculose (FIG. 5i), reddish brown to black, cells globose, 6–9 µm wide, internal cells same size, hyaline (FIG. 5h), locules with interascal filaments, cells 4 × 4–5 µm wide, dissolving as asci expand, interascal gel I+ amyloid (FIG. 5n). Asci clavate 50–70 × 20–30 µm, with tholus and short ocular chamber, outer wall I+ light blue (FIG. 5l), ascoplasm I– (dextrinoid) (FIG. 5m), ascospores hyaline in early development, distinctly halonate with halo up to 9 µm wide (FIG. 5o), becoming golden brown to dark brown in asci, often 1–septate, 16–18 µm long, ellipsoid to broadly ellipsoid, cells not equal in size, upper cell larger and round, lower cell narrower and shorter or becoming muriform or submuriform but below 20 µm long, growing after being released from asci, mature spores dark brown and muriform (FIG. 5r), 8–celled, constricted or not at center septa, sometimes irregularly and lumpy in shape (19–)22.1–25.5–28.8(–30) × (9–)11–12.6–14.2(–15) µm, (n=20), l/b (1.6–)1.8–2.0–2.3(–2.5), with (FIG. 5p, r) or without halo (FIG. 5q, s) (only mature muriform ascospores measured outside ascus, immature 1–septate ascospores or submuriform not measured). Internal hyaline conidigenous cells not distinguished from other cells, conidia hyaline 1.5–2 × 1 µm.

Notes: This is the first species described with multiple ostioles and locules in fertile stromata. As with *Lichenothelia scopularia* (Nyl.) D. Hawksw., *Saxomyces americanus* and *S. penninicus,* fertile stromata emerge from an areolate or non–areolate thallus, which forms a foundation of sterile paraplectenchymatous hyphae.

Specimens examined. U.S.A., CALIFORNIA, San Bernardino Co., San Gabriel Mountains, San Antonio Mountain region, along Gold Ridge Trail to Thunder mountain, *Pinus lambertiana–Abies concolor* forest, 34°16'10.4"N, 117°36'8.5'W, 2492 m, on granite boulder beneath *Abies concolor,* 3 Aug. 2016, *J. Kocourková 9055 & K. Knudsen* (Hb. K & K). San Bernardino Mountains, pinyon–Joshua tree woodland, 34°15'53.6"N, 116°43'54.1"W, 1867m, in understory of pinyon pines, on granite, 10 July 2015, *K. Knudsen 17476.1, 17476.2* (GZU, NY).

The DNA extraction numbers of the analyzed samples correspond to L2302, L2303 and L2308 (FIG. 1, Table 1).

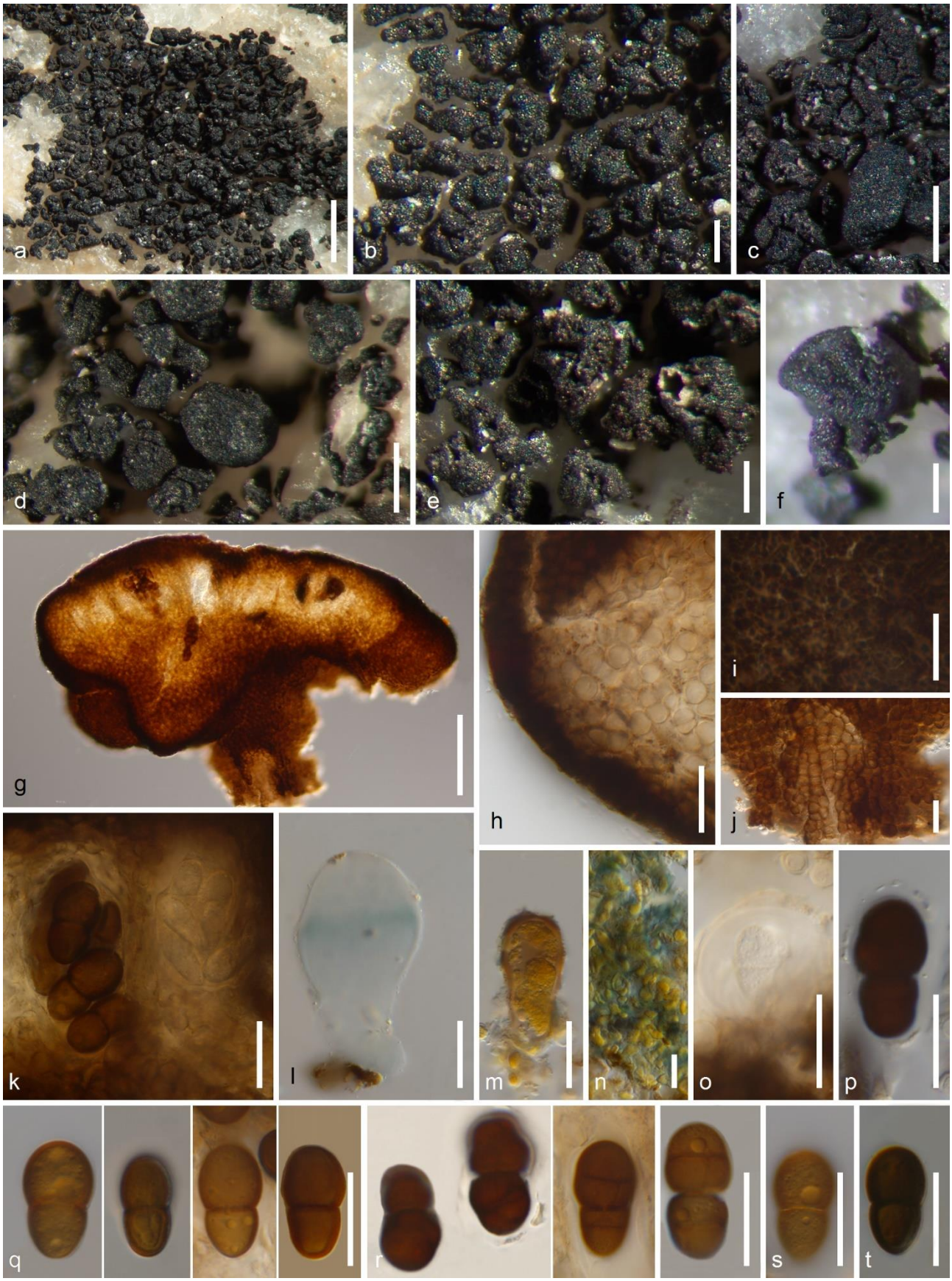
a
b
c
d
e
f
g
h
i
j
k
l
m
n
o
p
q
r
s
t

Figure 5. (Previous page) *Lichenothelia muriformis*, habitus and anatomical structures, sample *K. Knudsen 17651* (GZU - Holotype). **a** Orbicular dendrite thallus with marginal branches, **b** detail of thick marginal branches, **c** detail of the thallus with fertile stromata, several stromata splitting, **d** fertile stromata, **e** stromata with ostiola, **f** fertile stroma with long central stipe, **g** vertical section through fertile stroma with two stipes, **h** vertical section of stroma with dark reddish brown wall and subhyaline globose internal cells, **i** verruculose upper surface of fertile stroma, **j** stipe formed of parallel chains of subglobose to quadratic cells, **k** two 6-spored asci, with hyaline immature and nearly mature brown but still 1-septate ascospores, **l** empty ascus with amyloid (I+ blue) reaction of the wall, **m** I– (dextrinoid) reaction of the ascoplasm, **n** interascal gel I+ amyloid, **o** very young hyaline ascospore with wide halo, **p** old brown ascospore with dissolving halo, **q** nearly mature 1–septate ascospores, **r** muriform ascospores, some still halonate, **s** left ascospore in water showing lightly verruculose surface, **t** the same ascospore in Lugol´s solution with amyloid perispore. Scale bars: **a** = 500 µm; **b, e–g** = 100 µm; **c, d** = 200 µm; **h, j–m, o–t** = 20 µm; **i, n** = 10 µm.

Lichenothelia papilliformis Ametrano, K. Knudsen, Kocourk. & Muggia, sp. nov. – MycoBank MB 825181; FIG. 6, 7.

Holotype: U.S.A., CALIFORNIA, San Bernardino Co.: San Bernardino Mountains: Cactus Flats, north–facing slope, Pinyon-juniper woodland, 34°18'18.6"N 116°47'54.7"W, 1849 m, on limestone, 25 Sept. 2015, *K. Knudsen 17943* (Holotype, GZU; isotype, UCR, Hb. K & K).

Etymology: Referring to the thallus surface becoming papillate.

Diagnosis: Similar to *Lichenothelia scopularia* but differing in production short aerial hyphae with stromata at their terminus, papillate areoles, and fertile stromata with blue–brown paraplectenchymatous tissue of the wall.

Description: Thallus black, saxicolous, of dispersed areoles mixed with cupulate fertile stromata (FIG. 6a). Sterile areoles 30–100 µm wide, up to 120 µm high, irregular in shape, with verruculose surface or forming stipitate stromata bearing usually 10 to 20 sessile pyriform papillae around the top (FIG. 6e), 25–35 µm high, 20–25 µm wide, paraplectenchymatous throughout, cells mostly 5–8 µm, outer walls of sterile stromata dark red–brown, smooth to lightly ornamented, interior cells hyaline to a light charcoal hue. Young thallus dendrite (FIG. 6b, c) of aerial hyphae (FIG. 6f) one cell wide and 1–3 cells high, or epilithic hyphae up to 100 µm long (FIG. 6b, c), septate, cells 5–7 µm wide and 5–8 µm long, round to square to elongate (called stolons in Hennsen 1987), forming at the end new stromata (FIG. 6b, c, f). Stromata and epilithic hyphae apparently attached to substrate by melanin and easily detached when wet. Fertile stromata 1 to several locules (FIG. 7d, e), emerging from foundation of sterile tissue or dividing from side of fertile stromata, black, round, flat, more often cupulate, sessile or stipitate (FIG. 6h–l) usually wider than higher (Figs 6k, 10d, 10e), 80–260 µm wide, 50–170 µm high, with stipe narrowing to bottom, in cups occasionally with accretions (FIG. 6l), interconnected with very thin epilithic hyphae (FIG. 6g); outer wall black–brown–blue, smooth to lightly ornamented (FIG. 7b), in section paraplectenchymatic, dark blue–brown, 25–36 µm thick, cells 5–10 µm in diam. (FIG. 7c, d), beneath ascus layer paraplectenchymatous, brown (FIG. 7e), loculi inside with subhyaline moniliform hyphae (FIG. 7f), narrow interascal filaments only around asci, subhyaline to pale bluish–gray, 1.5–2.5 µm wide, of cylindrical cells 4–6 µm long, forked in upper part, upper cells swollen, tips widely clavate to globose, black–brown up to 6–7 µm (FIG. 7g), interascal gel I+ pale blue. Asci arising from bottom of stroma, with thickened tholus and ocular chamber (FIG. 7h, i, k), 8–spored, widely saccate (FIG. 7j), 35–40 × 15–21 µm, ascospores aseptate, hyaline even out of asci (FIG. 7o), finally becoming pale brown (FIG. 7p), widely cylindrical with round ends, (7.4–)8.5–9.7–10.8(–11.8) × (4.2–)5.3–5.8–6.4(–6.8) µm, (n=20; l/b (1.3–)1.5–1.7–1.8(–2.0), ascoplasm and plasm of ascospores I– (dextrinoid), outer wall I+ light blue (FIG. 7m). Conidiomata stromatic, formed on side of sterile or fertile stromata, subglobose, 60–80 µm in diam., wall of conidiomata dark red brown to dark brown blue, conidiogenous cells widely ampulliform, hyaline to subhyaline (FIG. 7p), 2.5–4.5 × 3.5–4.5 µm, conidia hyaline, bacilliform (FIG. 7q), (2.8–)3–3.4–3.8(–4.1) × 1.2–1.3–1.4(–1.5) µm, (n=15).

Cultured strains: No culture isolates have been obtained for this species; however, culture isolates obtained correspond to the *Saxomyces* clade [L2293–L2296 (9*)].

Ecology and distribution: Known only from the type locality on north–facing limestone slopes in Pinyon-juniper woodland from 1849–1865 m. Sources of nutrition unknown.

Notes: *Lichenothelia papilliformis* forms dense colonies of sterile areoles with rare fertile stromata. It produces epilithic and aerial hyphae generating new stromata at the terminus and papillae on sterile stromata. Its morphology suggests it is a species more successfully spread vegetatively than generatively, replicating by forming new stromata at the end of epilithic or aerial hyphae and by papillae breaking off rather than by low number of ascospores produced in rather rare fertile stromata with low number of asci. Aerial hyphae and stromata are broken off in microflooding or by grains of rock in high wind and allow the new stromata to lodge among the limestone crevices, even several centimeters away from originating stroma. Because we did not find aerial hyphae with only stromata broken off, we hypothesize that whole aerial units break away. Henssen (1987) described *Lichenothelia globulifera* Henssen from single specimen on granite from Seychelles. It had similar stroma on aerial hyphae but only the stroma broke off, leaving behind aerial hyphae, and the taxon was also fertile.

Lichenothelia papilliformis is the only known species of *Lichenothelia* with subhyaline and non–septate ascospores but we have been able to observe only few ascospores released from asci and therefore it is possible there is further maturation and septation as well as darkening.

Specimens examined. U.S.A, CALIFORNIA, San Bernardino Co.: San Bernardino Mountains: Cactus Flats, north–facing slope, Pinyon-juniper woodland, 34°18'19.6"N, 116°47'55.5"W, 1865 m, on limestone, 25 Sept. 2015, *K. Knudsen 17935* (GZU, UCR), 17939 (GZU, UCR), 17940 (GZU, UCR). Cactus Flats, north–facing slope, Pinyon-juniper woodland, 34°18'18.6"N, 116°47'54.7"W, 1849 m, on limestone, 25 Sept. 2015, *K. Knudsen 17946* (GZU, Topotype).

The DNA extraction numbers of the analyzed samples correspond to L2312, L2316 and L2317 (FIG. 1, Table 1).

Figure 6. (Following page) *Lichenothelia papilliformis*, habitus of thalli. **a, e, g** sample *K. Knudsen 17943*, Holotype (GZU), **b, f** sample *K. Knudsen 17940* (GZU), **c, i, l** sample *K. Knudsen 17939* (GZU), **d, j** sample *K. Knudsen 17935* (GZU). **a** Areolate thallus with sterile and fertile stromata, **b, c** developing stromata on dendrites, **d, e** papilles, **f** aerial dendrite forming young fertile stroma on tip, **g** fertile stromata connected with very thin epilitic hyphae, **h, i** fertile stromata in thallus, **j** rarely occurring fertile stroma with flat surface, **k** cupulate fertile stromata from side view, **l** accretion in cupulate fertile stroma. Scale bars: **a** = 200 µm; **b–d, f–g** = 50 µm; **e, h–l** = 100 µm.

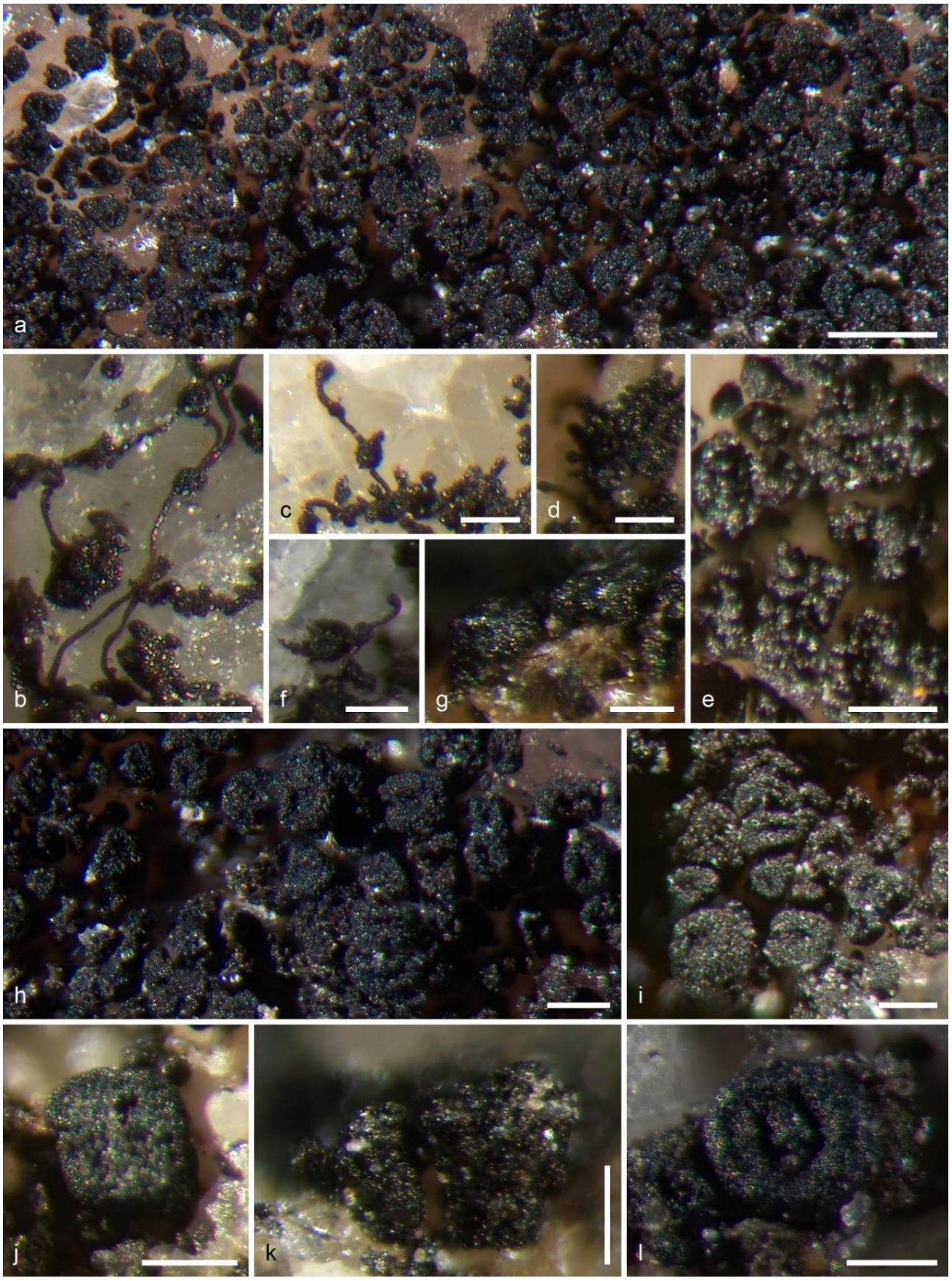
a
b
c
d
e
f
g
h
i
j
k
l

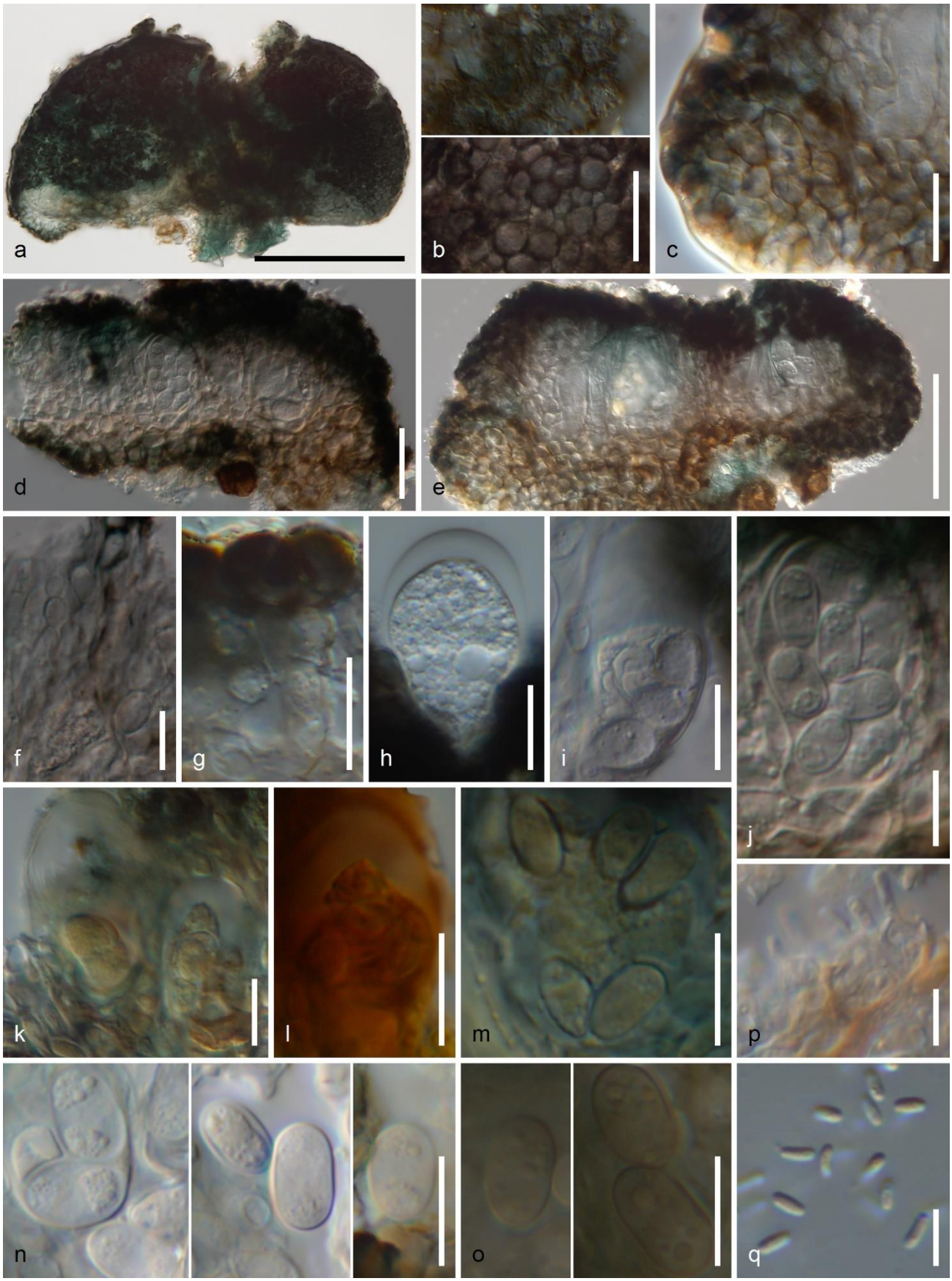
a
b
c
d
e
f
g
h
i
j
k
l
m
p
n
o
q

Figure 7. (Previous page) *Lichenothelia papilliformis*, anatomical structures of fertile stromata. **a, b, e, g, k–m, n, o** (right ascospore)**, q** sample *K. Knudsen 17943* (GZU – Holotype), **f, h, i, n** (two left ascospores) sample *K. Knudsen 17939* (GZU), **d, j** specimen of *L. intermixta K. Knudsen 17947* (hb. K & K). **a** Half sectioned fertile stroma with stipe (from upper view), **b** ornamented upper surface of fertile stroma, **c** vertical section of fertile stroma with dark bluish–brown wall of paraplectenchymatic tissue, **d** one loculate fertile stroma in vertical section, **e** two loculate fertile stroma, **f** internal, subhyaline moniliform filaments, **g** hyaline interascal filaments forked in upper part, with blackish widely clavate end cells, **h, i** young asci with tholus, **j** 8–spored ascus, **k** I+ pale blue (amyloid) reaction of ascus wall, **l** dextrinoid reaction of ascoplasm, **m** perispore of ascospores turning blue in iodine, ascospore plasm dextrinoid, **n** hyaline aseptate ascospores**, o** pale brown ascospores maturing outside of asci, **p** ampulliform conidiogenous cells with conidia, **q** bacilliform conidia. Scale bars: **a** = 100 µm; **b**, **c, d** = 20 µm; **e** = 50 µm; **f–o** = 10 µm; **p, q** = 5 µm.

Saxomyces americanus Ametrano, K. Knudsen, Kocourk., & Muggia, sp. nov. – MycoBank MB 825182; FIG. 8

Type: U.S.A., CALIFORNIA, San Bernardino Co., San Bernardino Mountains, Lightning Gulch, conifer forest, 34°10'29.9"N, 116°44'48.1"W, 2294 m, on granite boulders in open understory, 11 July 2015, *K. Knudsen 17521.1* (GZU, holotype).

Diagnosis: Similar to *Saxomyces penninicus* but differing especially in having a non–areolate dendrite thallus and larger ascospores ((16–)17–19.2–21.3(–23) × (6–)7.5–9–10.5(–12) µm vs. (11–)12.4–14–15.6(–17) × (4.5–)5.3–6.2–7(–8).

Etymology: The name refers to this taxon being the first *Saxomyces* described from North America.

Description: Thallus black, saxicolous, orbicular (FIG. 8a, b) to irregularly dendrite with epilithic branches (FIG. 8b, c), up to 2 cm wide. Branches at outer edge of thallus linear, with multiple side branches, 40–100 µm wide, 30–60 µm thick, up to 6 layers of cells thick, cells round or angular, surface smooth, 5–8 µm, cells on surface with black walls, internal cells hyaline, branches becoming thicker with melanin, eventually forming plates of cells with some cracks but without distinct areoles (FIG. 8c, d) between and beneath abundant emergent stromata at center of the thallus. No hyphae penetrating rock, glued to substrate by melanin, easily removed when wet. Fertile stromata round, stipitate, applanate, ostiolate (FIG. 8e, f), often dividing (FIG. 8f), uniloculate or biloculate (FIG. 8g, h), 150–300 µm wide, up to 200 µm high, base of stromata attached to thallus with short stipe up to 100 µm high (FIG. 8g), outer wall up to 30 µm thick, dark red brown to black, paraplectenchymatous, verruculose (FIG. 8i), internal cells dark–walled to hyaline, angular, 5–13 µm wide, 10–15 µm long (FIG. 8j), filaments abundant filling the whole internal space of loculus, branched, hyaline, irregularly segmented or not, 1.5–4 µm wide (FIG. 8k), cells cylindrical, 7–10 µm long not dissolving, interascal gel I–(dextrinoid). Asci cylindrical or saccate (FIG. 8l–o), with distinct foot (FIG. 8m), 6–8(–12)–spored (FIG. 8n, o), ascospores biseriate or non-seriate in asci, outer wall I+ amyloid, light to dark blue, 40–80 × 18–25 µm, with thick tholus and ocular chamber, ascoplasm I– (dextrinoid). Ascospores 1–3–septate, hyaline in early development (FIG. 8l), becoming dark brown, with hyaline perispore, halonate, with halo 1–2 µm wide (FIG. 8q) soon dissolving after ascospores release from asci, ascospore wall finely verruculose (FIG. 8r), turning blue in I (FIG. 8o, s), ascospore plasm I– dextrinoid (FIG. 8o), (16–)17–19.2–21.3(–23) × (6–)7.5–9–10.5(–12) µm [n=20; l/b (1.8–)1.9–2.2–2.4(–2.8)]. Ascospores in 12–spored asci substantially smaller, only up to 17 µm long. Conidiomata stromatic, uni- to multiloculate, dark red-brown, 100–150 µm in diam., conidiogenous cells ampuliform, hyaline to pale brown, 5–9 µm high and 2.5–4 µm wide, conidia bacilliform, (3–)3.7–4.3–4.8(–5.5) × (0.9–)1–1.1–1.3(–1.4) µm, (n=20); l/b (2.7–)3.3–3.8–4.2(–4.6).

Cultured strains: The analyzed strains L2291 (FIG. 2l–o) and L2293 (FIG. 2p–s) grown on MY medium form hyphae overall highly melanized, (FIG. 2m–o, q–s), branching and composed by both elongated (FIG. 2m–o, r, s) and isodiametric cells, which densely agglomerate (FIG. 2q) in older parts of the colony.

Ecology and distribution: On siliceous rock, only once collected on limestone boulder among metamorphosed shale outcrops on which it was abundant but poorly developed. No populations were collected in association with lichens or detritus under trees, usually found in full sun or under conifers, but not in deep

shade, on boulders free of detritus from trees like pine needles, source of nutrition unknown. It occurs in North America, in California from Tioga Pass in Sierra Nevada Mountains south to San Bernardino Mountains, above 2000 meters. Probably wide-spread in western North America.

Notes: *Saxomyces penninicus* differs from *S. americanus* mainly in having an areolate thallus, much shorter and narrower asci 40–60 × 12–19 µm vs. 40–80 × 18–25 µm and ascospores (11–)12.4–14–15.6(–17) × (4.5–)5.3–6.2–7(–8) µm vs. (16–)17–19.2–21.3(–23) × (6–)7.5–9–10.5(–12) µm which are not halonate, and in having non–amyloid ascus and ascospore walls.

Specimens examined. U.S.A, CALIFORNIA, Inyo Co., Tioga Pass, Sierra Nevada Mountains, 37°56'17.5"N, 119°14'46.2"W, 2893 m, on metamorphosed shale under old pine along stream, 13 July 2012, *K. Knudsen 14765.1 & J. Kocourková* (UCR). White Mountains, pinyon juniper woodland, 37°18'28"N, 118°10'29.23"W, 80 m, on metamorphosed shale beneath pinyon pine, 14 Aug. 2014, *K. Knudsen 16947* (UCR, Hb. K & K), 37°18'46.2"N, 118°10'54.3"W, 2550 m, on hard limestone under pinyon pine, 14 Aug. 2014, *K. Knudsen 16946* (UCR, Hb. K & K); East of White Mountain Road, 37°18'20"N, 118°11'26.4"W, 2391 m, on metamorphosed shale in full sun, 15 Sept. 2015, *K. Knudsen 17855* (GZU, Hb. K&K), below Grandview, 37°21'18"N, 118°10'51"W, 2779 m, on metamorphosed shale beneath and between alpine *Eriogonum* species, 14 Aug. 2014, *K. Knudsen 16936* (B, KRAM PRM, UCR, UPS, Hb. K & K) San Bernardino Co.: San Bernardino Mountains, Onyx Summit. Pinyon-juniper woodland, 34°12'29"N, 116°43'03"W, 2636 m, on granite in sun, 7 Oct. 2008, *K. Knudsen 10406 & J. Lendemer* (UCR, Hb. K & K).

The DNA extraction numbers of the analyzed samples correspond to L1798, L2155, L2156, L2214, L2215, L2218, L2219, L2309 (FIG. 1, Table 1).

Figure 8. (Following page) *Saxomyces americanus,* habitus and anatomical structures, sample *K. Knudsen 17521.1* (GZU – Holotype). **a** Habitus of thalli, **b** orbicular dendrite thallus, **c** bundles of flat branches, **d** detail of branch under light microscope, **e** abundant fertile stromata, **f** dividing fertile stromata, **g** vertical section of uniloculate fertile stroma with excentric stipe, **h** bilocular fertile stroma, **i** verruculose upper surface of fertile stroma, **j** vertical section of fertile stroma wall with dark brown paraplectenchymatous tissue of angular cells, **k** slender branched interascal filaments, **l** young asci in different stages of development with thickened tholus and widened ocular chamber, **m** 8–spored ascus with basal foot, **n** two mature asci, with 1–septate ascospores on left, with 3–septate brown ascospores on right side, respectively, **o** 12–spored ascus in I(Lugol), I+ amyloid ascus and spore wall and I– dextrinoid ascus and ascospore plasm, **p** young 1–septate ascospores with perispore, **q** 3–septate mature ascospores, left one halonate, **r** verruculose ascospore, **s** amyloid ascospore wall, **t** stromatic conidioma from upper view, **u** ampuliform conidiogenous cells producing bacilliform conidia. Scale bars: **a** = 1 mm; **b** = 500 µm; **c, e–f** = 200 µm; **d, g–h, t** = 100 µm; **i, j, p–s** = 10 µm; **k–n** = 20 µm; **u** = 5 µm.

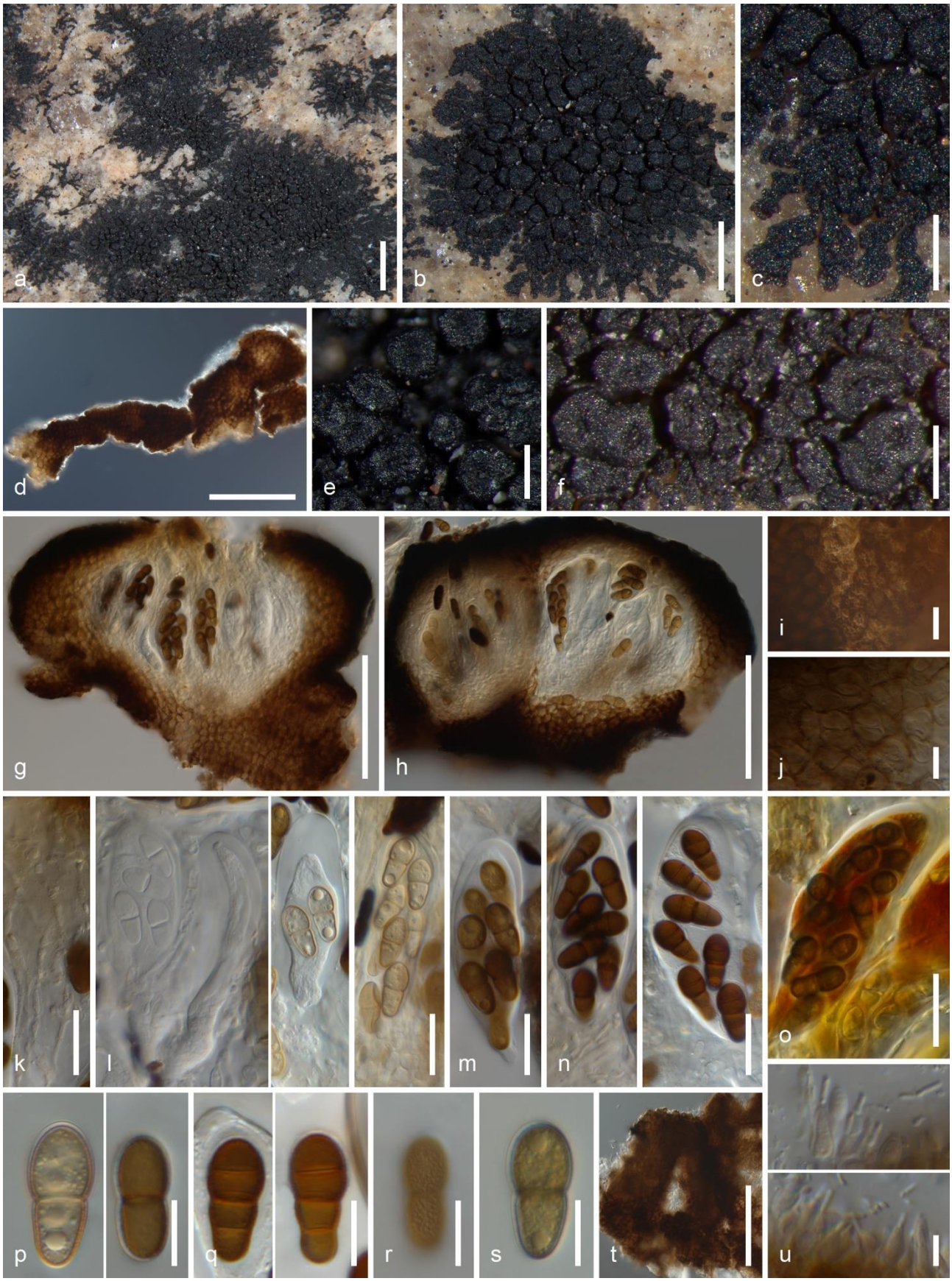
a
b
c
d
e
f
g
h
i
j
k
l
m
n
o
p
q
r
s
t
u

Saxomyces penninicus Zucconi & Onofri, Fungal Diversity 86: 422 (2017) – MycoBank MB802900, MB819852; FIG. 9

Holotype: EUROPE, Italy, Alps, Punta Indren, Monte Rosa, sandstone; CBS H–22053 (exiccatum) = CCFEE 5495. Culture preserved in dried condition (NCBI accession numbers: KC315864 (nucSSU), KC315875 (nucLSU), KC315886 (mtSSU), taxonomic species delimitation supported by molecular data.

Diagnosis: Selbmann et al. (2014), described from cultured anamorph [name not validly published, ICN (Melbourne) Art. 40.6, validated in Wijayawardene et al. (2017)].

Description of teleomorph (based on two collections): Thallus black, saxicolous, irregular in shape, areolate (FIG. 9a) of sterile and fertile stromata, irregularly and locally dendrite (FIG. 9b), 3–4 or more centimeters across. Young thallus with sterile stroma with epilithic hyphae (FIG. 9c), one cell wide, 4–5.5 µm, soon growing into flat bundles of epilithic branches (FIG. 9d), paraplectenchymatic, parallel chains of 3–6 red–brown cells, 15–21 µm wide, 1–2 cells high, smooth or lightly ornamented, bearing new stromata at their terminals, hyphae not penetrating rock, attached to the substrate by melanin and easily detached when wet. Older thalli with coalescing epilithic branches forming net of branches, (FIG. 9d), finally coalescing into continuous thalli with distinct areoles separated by cracks areolate (FIG. 9e). Sterile stromata angular to irregular, sessile to very shortly stipitate areoles (FIG. 9e), 70–200 µm long, 50–160 µm wide, 50–70 up to 100 µm high, mostly flat and smooth, outer wall dark red–brown, smooth to lightly ornamented, paraplectenchymatous throughout, internal cells pale brown to pale red–brown, subglobose to polyhedral, mostly 4–8.5 µm long, 3.5–5.5 µm wide. Some young areoles with rough surface, producing short external outgrowths (FIG. 9f) 1 cell wide, 2– to several cells 3.5–6 µm long, 6–7 µm wide (called macroconidia in Henssen 1987; toruloid hyphae breaking off with rhexolythic secession in Selbmann et al. 2014, FIG. 3h, i), later breaking off and growing new stromata. Fertile stromata (FIG. 9g) black, round, applanate, uniloculate, occasionally dividing by splitting and then biloculate, disc–like depression with 1 central ostiole, usually not wider than higher, 100–180 µm wide, 80–130 µm high, shortly stipitate with stipe up to 140 µm high, 70–110 wide (FIG. 9h) or almost sessile and then attached to substrate by melanin plate, outer wall 25–35 µm thick, dark red–brown to black, paraplectenchymatous, surface lightly verruculose (FIG. 9i), in section cells round to polyedral, 3–5.5 µm in diam. (FIG. 9j), internal layer 2–3 cells wide of hyaline cells, up to 10 µm wide, cells 2.5–5 µm long and 2–.5–4 µm wide, paraplectenchyma beneath of ascus layer inspersed (FIG. 9k), narrow interascal filaments around asci not developed, loculus filled with hyaline, moniliform, branched hyphae (FIG. 9m) consisting of broadly ellipsoidal to cylindrical 0–1 septate cells 3–6.5 µm long, 2.5–4.7 µm wide (FIG. 9n), later dissolving and gelatina with ascospores filling the loculus (FIG. 9l), interascal gel I– (dextrinoid). Asci arising from bottom of stroma, 8–spored, clavate to saccate, with tholus, ocular chamber and basal foot (FIG. 9o–q), 40–60 × 12–19 µm. Ascoplasm and wall of asci I– (dextrinoid) (FIG. 9q). Ascospores 1–3–septate, very rarely submuriform with 1 vertical septum per spore, lightly verruculose, with perispore only 1µm wide (FIG. 9s), initially hyaline, very soon 1–septate (FIG. 9r), later brown to red–brown, usually constricted on central septum, upper cell wider, finally forming secondary horizontal septa and/ or a vertical septum (FIG. 9s), (11–)12.4–14–15.6(–17) × (4.5–)5.3–6.2–7(–8), n=20; l/b (1.9–)2–2.3–2.6(–2.9). Ascospore wall and plasma I– (dextrinoid). Conidiomata not seen.

Notes: Saxomyces penninicus was described from culture isolate CCFEE 5495 as a sterile mycelium. Here we describe the teleomorph of the species based on two collections (and 1 duplicate) from California and Italy. *Saxomyces penninicus* differs from *S. americanus* mainly in having areolate thallus, much shorter and narrower asci 40–60 × 12–19 µm vs. 40–80 × 18–25 µm and ascospores (11–)12.4–14–15.6(–17) × (4.5–)5.3–6.2–7(–8) µm vs. (16–)17–19.2–21.3(–23) × (6–)7.5–9–10.5(–12) µm which are not halonate, and in having non–amyloid ascus and ascospore walls.

Lichenothelia macrocarpa Henssen (Henssen 1987) was described from Mount Rosa in Italy. It also has an areolate thallus, non-amyloid interascal gel, and interascal filaments like *Saxomyces penninicus*, but differs in having larger two-celled ascospores size of 19–24 × 8–15 µm. This may be earliest name of *Saxomyces penninicus* if the ascospores measured from our two specimens for this study represent too narrow

a sampling. It could also be earliest name of the teleomorph of *S. alpina* which was more abundant than *S. penninicus* in environmental samples from Mount Rose (Selbmann et al. 2013).

Cultured strains: We obtained three culture isolates for this species forming well–defined lineage with the cultured type strain *S. penninicus* CCFEE5495; samples L2304, L2305 and L2337, from California and Italy, respectively.

Ecology and distribution: Previously collected in Italy, in Pennine Alps in Monte Rosa and described from sterile culture strain CCFEE 5495. We collected fertile samples on shady mica–schist boulder in edge of gorge in lower alpine elevation (1391 m) in Ötztaler Alps in Italy and on shady granite boulder in forest along the south fork of the Santa Anna River in the San Bernardino Mts. (1913 m) in California.

Specimens examined. EUROPE, ITALY, South Tyrol, Trentino–Alto Adige, Bolzano, Vezzano (Vetzan), NW of the village, 400 m E of cattle farm, 46° 38' 13.14" N, 10° 48' 13.37" E, 1391 m, narrow gorge crossing the contour dirty road, on vertical wall of big boulder fallen of overhang, on mica–schist (Vinschauger schist), 27 May 2016, coll. *J. Kocourková* 8993 & *K. Knudsen* (Hb. K&K). U.S.A., CALIFORNIA, Transverse Range, San Bernardino Co., San Bernardino Mts, south fork of Santa Ana River, edge of burnt area of Lake Fire, 34°10'12.6" N/ 116°49'51.1" W, 1913 m, conifer forest with willows along stream, on shady granite, *K. Knudsen 17509* (H, GZU, UCR, Hb. K&K).

The DNA extraction numbers of the analyzed samples correspond to L2304, L2305 and L2337 (FIG. 1, Table 1).

Figure 9. (Following page) *Saxomyces penninicus,* habitus and anatomical structures. **a–e, g–n, q–s** sample *J. Kocourková et al. 8993* (hb. K & K), **f, o, p** sample *K. Knudsen 17509* (GZU). **a** Areolate dendrite thallus with fertile stromata, **b** marginal bundles of flat branches, **c** young thallus, stromata with 1 cell wide hyphae, **d** net of flat branches, **e** areolate thallus with fertile stromata, **f** one cell wide toruloid hyphae later breaking off with rhexolythic secession, **g** round fertile stromata with ostiolum, some dividing by splitting, **h** vertical section of shortly stipitate fertile stroma, **i** lightly ornamented cells of fertile stroma surface, **j** polyedral cells of fertile stroma wall in vertical section, **k** insperse paraplectenchyma beneath of ascus layer, **l** dissolved interascal filaments forming gelatina and ascospores released from fertile stroma, **m** vertical section of fertile stroma with moniliform interascal filaments, **n** detail of branched moniliform interascal filaments, **o** young ascus with tholus and still hyaline ascospores, **p** ascus with ocular chamber in tholus and overmature collapsing ascospores, **q** I– (dextrinoid) ascoplasma in Lugol, **r** young 1–septate hyaline ascospore, **s** brown mature ascospores with septa in various stage of development, some ascospores with perispore, right spore verruculose. Scale bars: **a, b, e** = 200 µm; **c, d, g** = 100 µm; **h**, **l** = 50 µm; **m** = 20 µm; **n** = 5 µm; **f, i–k, o–s** = 10 µm.

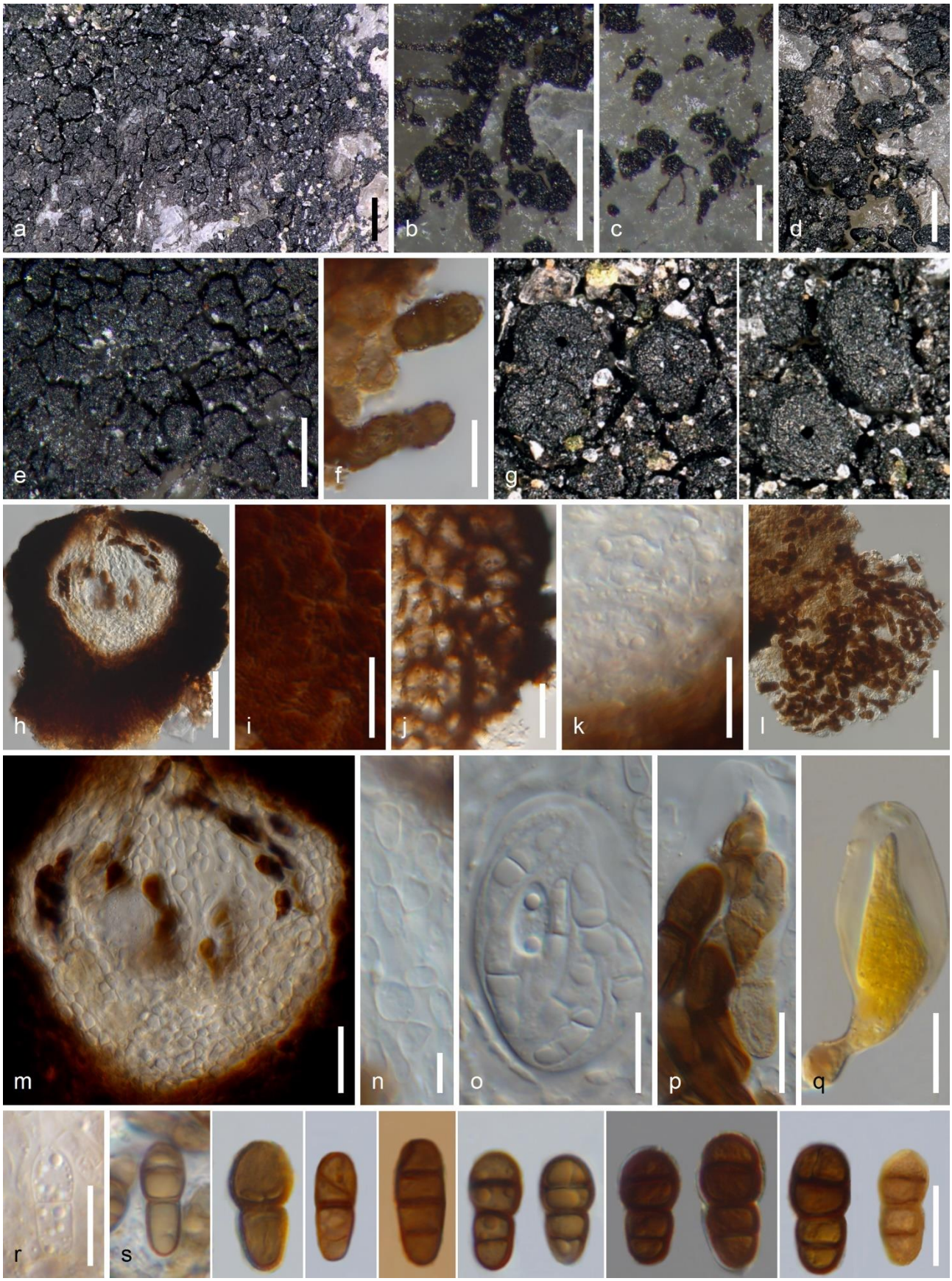
a
b
c
d
e
f
g
h
i
j
k
l
m
n
o
p
q
r
s

Discussion

The relationships of Lichenothelia, Saxomyces and other RIF in Dothideomycetes. — We used an expanded and targeted taxon sampling of dothidealean RIF, and the inclusion of anamorphs and teleomorphs, to shed light on the cryptic diversity of these fungi and to support the process of species delimitation. We also show that combining molecular data from environmental samples with morphological analyses of environmental material and cultured isolates improves the recognition of taxa.

Previous studies have reported incongruence between genetic data gained from environmental samples and their corresponding cultures (Muggia et al. 2013, 2015). The species diversity entangled in both the epilithic and endolithic RIF assemblages can be misestimated by primer biases or by culture conditions which favor the amplification and the growth, respectively, of only certain strains and leave others undetected. So far, we have recovered RIF associated to morphologically identified *Lichenothelia* and *Saxomyces* thalli in four lineages of Dothideomycetes. Interestingly, six isolates form a lineage within Lichenostigmatales, an order sister to Arthoniomycetes established by Ertz et al. (2014) to accommodate the lichen parasitic genera *Etayoa* and *Lichenostigma*. Eight cultured isolates together with two environmental samples are recovered within Capnodiales as close relatives of other RIF isolated from calcareous rocks from the Mediterranean region (Ruibal et al. 2005, 2009), from Antarctica (Egidi et al. 2014), and as plant pathogens. Two environmental samples (L2311 and L2320) constitute a small lineage with a fungus isolated from lichen thalli (Muggia et al. 2016) and the single sample L2307 is basal to all the orders of Dothideomycetes. These results support the idea that certain RIF strains are widely distributed and can be recovered from diverse ecologies.

The present phylogenetic inference resolves *Lichenothelia* and *Saxomyces* into three lineages. The first, Lichenotheliales s.str., represents the core of *Lichenothelia* species, corresponding to Lichenotheliaceae/Lichenotheliales as circumscribed by Hyde et al. (2013) and Muggia et al. (2013, 2015). It now includes seven well recognized species (*L. arida*, *L. convexa*, *L. dimelaenae*, *L. intermixa*, *L. muriformis*, *L. papilliformis* and *L. umbrophila*), two cultured strains representing *Lichenothelia dimelaenae* (L2184 and L2299), and twelve samples for which no name has been assigned yet (FIG. 1). Among these, we find the cultured strain L1851, which was isolated from a thallus of *Lichenostigma epirupestre* infecting the lichen *Pertusaria pertusa* (Perez-Ortega S. 1433). For this unique sample we refrain from proposing here a new combination and wait to gather further molecular and morphological data.

Samples of *L. calcarea* and an additional three samples of *L. arida* group together in the second lineage, named Lichenotheliales (1), basal to Tubeufiales, Patellariales and additional orders. These samples grouped with the core taxa of Lichenotheliaceae/Lichenotheliales in the previous analysis of Muggia et al. (2015). Also, in previous analyses (Muggia et al. 2013, 2015; Liu et al. 2017) the order Lichenotheliales has been poorly supported, consistent with the broken monophyly of Lichenotheliales recovered here. The relationship of the most basal lineages in Dothideomycetes is still not fully settled.

The third lineage groups the type species of *Saxomyces alpinus*, *S. penninicus* and *S. americanus.* Here *S. americanus* is described as a new species based on fertile environmental samples and their cultured isolates. Within this lineage, additional samples, represented by both fertile and sterile thalli and isolates, show a multiplicity of morphologies. Further collections are necessary to corroborate their species description.

Even though both Lichenotheliales s. str. and *Saxomyces*–group are individually monophyletic, their clades do not receive statistical support, and the placement of few samples still impairs an understanding of this relationship. In fact, the environmental samples L2216 and L2217 are recognized in Lichenotheliales s. str. as *L. intermixa* and *L. arida*, respectively. However, their cultured isolates are related to the *Saxomyces* group together with other environmental samples coming from the same locality and their corresponding culture which are here formally described as *S. americanus*. This discrepancy between environmental samples and culture isolates derivated from them recalls biases that may be due either to primer specificity (universal fungal primers were used), or that environmental samples each had material of several fungal species, with other species being amplified or cultured by chance. The risk of culturing or amplifying other species than the target one, however, were drastically reduced for fertile specimens, whose inocula were taken from fruiting

bodies.

Species delimitation within Lichenothelia and Saxomyces. — In view of the difficulty to use morphological characters alone for species recognition in *Lichenothelia* and *Saxomyces*, we were interested to complement morphological information with molecular data. Unfortunately, we could not obtain ITS sequence data for the majority of the samples and therefore could not base our species delimitation analyses on the standard barcode for Fungi (Schoch et al. 2012).

The more conserved nuclear genes, nucLSU and nucSSU rDNA, proved to be not suitable for ESU delimitation at species level. Significantly higher values than the null model likelihood values in the LRT were found indeed only for the mitochondrial SSU marker. Nevertheless, species delimitations performed on BEAST–inferred phylogenies turned out to be the most coherent across different markers (Supplementary material Table S2 and Table S3).

As reported in literature (Fujisawa & Barraclough 2013; Tang et al. 2014; Kapli et al. 2017), mPTP and sGMYC were robust methods, often able to find enough separation between putative speciation events. Alternativley sPTP, and to a lesser extent mGMYG, often over-split the dataset. The ABGD method did not find any valid barcode gaps to split the dataset into different clusters.

For our dataset, species delimitation methods did not always provide number and sample composition of ESU consistent with the species recognized by morphological analyses and phylogenetic inference. However, some main clusters are consistently recovered and correspond to the taxa recognized by classical taxonomy. *Lichenothelia arida*, *L. convexa* and *L. intermixta* are consistently identified by sGMYC, while most of the samples of *S. alpinus* and *S. americanus* are identified by both PTP and GMYC methods (from the mtSSU-based BEAST phylogeny). More samples from different localities, and informative loci at the species level, are needed to consistently delimit species within *Lichenothelia* and *Saxomyces*.

Integrative taxonomy, teleomorphs and anamorphs in RIF. — Comprehensive approaches to delimit and describe species by integrating data from multiple types of analyses are known as integrative taxonomy (Dayrat 2005; Will et al. 2005; Schlick–Steiner et al. 2010). In mycology, integrative taxonomy has been applied widely when the circumscription of many taxa has been hampered by cryptic speciation, inconspicuous taxonomically diagnostic characters or the lack of sexual reproductive forms (anamorph; e.g. Crous et al. 2004; Muggia et al. 2008, 2009; Taylor 2011; Lücking et al. 2014).

More recently, integrated approached including molecular data proved successful for fungi to find correspondences between anamorphs and teleomorphs. *Saxomyces* is here a further example, as the teleomorphic state was unknown at the time of its description (Selbmann et al. 2014). Our first report in this paper of the sexual morph for a pure rock inhabiting fungus in the new species *S. americanus* fills this lack of knowledge. The species forms a conspicuous, non-areolate mycelium on rock surfaces and bears fertile stromata (see species description above) which have allowed detailed analyses of asci and ascospores. *Saxomyces americanus* has been collected primarily on siliceous rocks (only once on limestone), usually in full sun above 2000 m elevation in mountains in California. Due to the presence of fertile stromata, the collections were first determined as *Lichenothelia* sp. according to stromata morphology and spore septation. However, molecular results unequivocally placed the specimens next to the type species of *S. alpinus* and *S. penninicus*. Our molecular data suggest that also *S. penninicus* bears its teleomorphic state, represented by the samples L2304, L2305 and L2337. These are fertile areolate mycelia with fertile stromata collected in California and Italy, respectively, and they form a well-defined lineage with the cultured type strain *S. penninicus* CCFEE5495. It is likely that any future collection of RIF in the same ecological settings of *S. alpinus* might find its corresponding teleomorph, and this could be contemplated for other, remarkable rock inhabiting genera included in the family Teratosphaeriaceae (e.g., *Recurvomyces*, *Elasticomyces*, *Cryomyces* as well as the Antarctic endemic *Friedmanniomyces*) known so far from cultured isolates only.

Our integrative approach demonstrates that in the case of *Lichenothelia* and *Saxomyces,* the use of

genetic data and the application of the phylogenetic species concept proved necessary to better circumscribe taxa. Unfortunately, descriptions of new species based on detailed morphological analyses cannot be always complemented by genetic data (Valadbeigi et al. 2016). However, previous studies (Henssen 1987, Muggia et al. 2013, 2015) and the present one have shown that the subtle continuum of morphological differences may mirror intraspecific variability or a phenotypic plasticity (Handry 2016), necessitating examination of multiple specimens per taxon. Additionally, the lack of genetic data for putatively new taxa with the available frame of Lichenotheliales s.str. (Hyde et al. 2013; Muggia et al. 2013, 2015) may introduce further biases when new species of this group are presented to science. In Henssen (1987), the descriptions in the protologs were based on few or even single samples and did not properly estimate the variation of diagnostic traits.

Acknowledgements

We are thankful to Theodora Kopun and Sigrun Kraker for the help in the lab. Special thanks belong to the management of the Olympus Czech Group, s.r.o., namely Petr Patera and Václav Krejzlík for supplying several digital cameras for microphotography to JK. We thank the Italian National Antarctic Museum 'Felice Ippolito' for funding the Mycological Section (University of Tuscia) and its Culture Collection of Fungi from Extreme Environments (CCFEE).

Funding

This work was supported by the Austrian Science Fund (FWF) project P24114-B16 and by the the University of Trieste project FRA-2014 (Finanziamenti di Ateneo per progetti di Ricerca scientifica) assigned to LM. Jana Kocourková and Kerry Knudsen were financially supported by the grant ''Environmental aspects of sustainable development of society″ 42900/1312/3166 from the Faculty of Environmental Sciences, Czech University of Life Sciences Prague.

References

Ahmadjian V (1967) The lichen symbiosis. Massachusetts: Blaisdell Publishing Co.

Akaike H. 1974. A new look at the statistical model identification. IEEE Transactions on Automatic Control 19:716–723.

Ametrano CG, Selbmann L, Muggia L (2017) A standardized approach for co–culturing Dothidealean rock-inhabiting fungi and lichen photobionts in vitro. Symbiosis 73:35-44

Atienza V, Hawksworth DL (2008) Lichenothelia renobalesiana sp. nov. Lichenotheliaceae. for a lichenicolous ascomycete confused with Polycoccum opulentum Dacampiaceae. The Lichenologist 40:87–96.

Bold HC (1949) The morphology of *Chlamydomonas chlamydogama* sp. nov. Bulletin Torrey Botany Club 76:101–108.

Brunauer G, Blaha J, Hager A, Turk R, Stocker-Worgotter E, Grube M (2007) An isolated lichenicolous fungus forms lichenoid structures when co-cultured with various coccoid algae. Symbiosis 44:127–136.

Bubrick P, Galun M (1986) Spore to spore resynthesis of *Xanthoria parietina*. The Lichenologist 18:47–49.

Crous PW, Groenewald JZ, Mansilla JP, Hunter GC, Wingfield MJ (2004) Phylogenetic reassessment of Mycosphaerella spp. and their anamorphs occurring on Eucalyptus. Study in Mycology 50:195–214.

Darriba D, Taboada GL, Doallo R, Posada D (2012) 'jModelTest 2: more models, new heuristics and parallel computing'. Nature Methods 9:772.

Dayrat B. (2005) Towards integrative taxonomy. Biological Journal of the Linnean Society 85:407–415.

Davidson R, MacKinnon JG (2004) Econometric Theory and Methods, New York, Oxford University Press.

Egidi E, de Hoog S, Isola D et al. (10 authors) (2014) Phylogeny and taxonomy of meristematic rock-inhabiting black fungi in the Dothideomycetes based on multi-locus phylogenies. Fungal Diversityity 65:127–165.

Ertz D, Lawrey JD, Common RS, Diederich P (2014) Molecular data resolve a new order of Arthoniomycetes sister to the primarily lichenized Arthoniales and composed of black yeasts, lichenicolous and rock-inhabiting species. Fungal Diversityity 66:113–137.

Etayo J (2010) Líquenes y hongos liquenícolas de Aragón. Guineana 16:1–501.

Friedmann EI (1982) Endolithic microorganisms in the Antarctic cold desert. Science 215:1045e1053.

Fujisawa T, Barraclough TG (2013) Delimiting species using single-locus data and the Generalized Mixed Yule Coalescent approach: a revised method and evaluation on simulated data sets. Systematic Biology62:707–724.
Gardens M, Bruns TD (1993) ITS primers with enhanced specificity for basidiomycetes. Application for the identification of mycorrhizae and rust. Molecular Ecology 2:113–118.
Gargas A, Taylor JW (1992) Polymerase chain reaction PCR. primers for amplifying, sequencing nuclear 18S rDNA from lichenized fungi. Mycologia 84:589–592.
Gorbushina A. (2007) Life on the rocks. Environm Microbiol 9:1613–1631.
Gorbushina A, Beck A, Schulte A (2005) Microcolonial rock inhabiting fungi and lichen photobionts: evidence for mutualistic interactions. Mycological Research 109:1288–1296.
Gorbushina A, Broughton WJ (2009) Microbiology of the atmosphere-rock interface: how biological interactions and physical stresses modulate a sophisticated microbial ecosystem. Annual Review of Microbiology 63:431–450.
Gostincar C, Grube M, Gunde-Cimerman N (2011) Evolution of fungal pathogens in domestic environments? Fungal Biology 115:1008–1018.
Gostincar C, Muggia L, Grube M (2012) Polyextremotolerant black fungi: oligotrophism, adaptive potential and a link to lichen symbioses. Frontiers in Microbiology 3:390.
Gueidan C, Ruibal C, De Hoog GS, Schneider H (2011) Rock-inhabiting fungi originated during periods of dry climate in the late Devonian and middle Triassic. Fungal Biology115:987–996.
Gueidan C, Ruibal C, Villaseñor C, de Hoog GS, Gorbushina AA, Untereiner WA, Lutzoni F (2008) A rock-inhabiting ancestor for mutualistic and pathogen–rich fungal lineages. Studies in Mycology 61:111–119.
Halici M, Akata I, Kocakaya M (2010) New records of lichenicolous and lichenized fungi from Turkey. Mycotaxon 114:311–314.
Hall TA (1999) BioEdit: a user-friendly biological sequence alignment editor and analysis program for Windows 95/98/NT. Nucleic Acids Symposium Series41:95–98.
Handry AP (2016) Key questions on the role of phenotypic plasticity in eco-evolutionary dynamics. J Heredity 107:25–41.
Harutyunyan S, Muggia L, Grube M (2008) Black fungi in lichens from seasonally arid habitats. Studies in Mycology 61:83–90.
Hawksworth DL (1981) *Lichenothelia*, a new genus for the *Microthelia aterrima* group. The Lichenologist 13:141–153.
Hessen H. (1987) *Lichenothelia*, a genus of microfungi on rocks. In: Peveling E ed. Progress and problems in lichenology in the Eighties. Bibliotheca Lichenologica25:257–293.
Hyde K D, Jones EG, Liu JK et al. (68 authors) (2013) Families of Dothideomycetes. Fungal Diversity 63:1–313.
Kapli P, Lutteropp S, Zhang J, Kobert K, Pavlidis P, Stamatakis A, Flouri T (2017) Multi–rate Poisson tree processes for single-locus species delimitation under maximum likelihood and Markov chain Monte Carlo. Bioinformatics 33:1630–1638.
Kocourková J, Knudsen K (2009) Three lichenicolous fungi new for North America. Evansia 26:148–151.
Kocourková, J., & Knudsen, K. (2011). Lichenological notes 2: Lichenothelia convexa, a poorly known rock-inhabiting and lichenicolous fungus. *Mycotaxon*, *115*(1), 345-351.
Kocourková J, Knudsen K (2015) Notes on the California lichen flora 7: more new records. Opuscula Philolichenum 14:118–120.
Liu JK, Hyde KD, Jeewon R, Philips AJL, Maharachchikumbura SSN, Ryberg M, Liu ZY, Zhao Q (2017) Ranking higher taxa using divergence time: a case study in Dothideomycetes. Fungal Diversity 84:75–99.
Lohtander K, Oksanen I, Rikkinen J (2002) A phylogenetic study of *Nephroma* lichen-forming Ascomycota. Molecular Ecology106:777–787.
Lücking R, Dal Forno M, Sikaroodi M et al (2014) A single macrolichen constitutes hundreds of unrecognized species. Proceedings of the National Academy of Sciences 111:11091–11096.
Maniatis T, Fritsch EF, Sambrook J (1982) Molecular cloning: a laboratory manual. Cold spring harbor Laboratory, Cold spring Harbor, N. Y.
Miller M A, Pfeiffer W, Schwartz T (2010) Creating the CIPRES Science Gateway for inference of large phylogenetic trees. In Gateway Computing Environments Workshop GCE., Ieee, pp 1–8
Muggia L, Fleischhacker A, Kopun T, Grube M (2016) Extremotolerant fungi from alpine rock lichens and their phylogenetic relationships. Fungal Diversity 76:119–142.
Muggia L, Gueidan C, Perlmutter G, Eriksson OE, Grube M (2009) Molecular data confirm the position of *Flakea papillata* in the Verrucariaceae. The Bryologist 112:538–543.
Muggia L, Gueidan C, Knudsen K, Perlmutter G, Grube M (2013) The lichen connection of black fungi. Mycopathologia 175:523–535.
Muggia L, Hafellner J, Wirtz N, Hawksworth DL, Grube M (2008) The sterile microfilamentous lichenized fungi *Cystocoleus ebeneus* and *Racodium rupestre* are relatives of plant pathogens and clinically important dothidealean fungi. Molecular Ecology112:50–56.
Muggia L, Kocourková J, Knudsen K (2015) Disentangling the complex of *Lichenothelia* species from rock communities in the desert. Mycologia 107:1233–1253.

Onofri S (1999) Antarctic microfungi. In Enigmatic microorganisms and life in extreme environments, Springer Netherlands 323–336.
Onofri S, Barreca D, Selbmann L et al. (2008) Resistance of Antarctic black fungi and cryptoendolithic communities to simulated space and Martian conditions. Studies in Mycology 61:99–109.
Paradis E, Claude J, Strimmer K (2004) APE: Analyses of Phylogenetics and Evolution in R language. Bioinformatics 20:289–290.
Pons J, Barraclough TG, Gomez-Zurita J, Cardoso A, Duran DP, Hazell S, Vogler AP (2006) Sequence–based species delimitation for the DNA taxonomy of undescribed insects. Systematic Biology 55:595–609
Puillandre N, Lambert A, Brouillet S, Achaz G (2012) ABGD, Automatic Barcode Gap Discovery for primary species delimitation. Molecular Ecology 21:1864–1877.
Rambaut A, Drummond A (2007) Tracer. Available from: beast.bio.ed.ac.uk/Tracer. 2017 May 10
Rittmayer EN, Austin CC (2012) The effects of sampling on delimiting species from multi-locus sequence data. Molecular Phylogenetics and Evolution 65:451–463.
Ruibal C, Gueidan C, Selbmann L, Gorbushina AA, Crous PW, Groenewald JZ, Staley JT (2009) Phylogeny of rock-inhabiting fungi related to Dothideomycetes. Studies in Mycology 64:123–133.
Ruibal C, Platas G, Bills GF (2005) Isolation and characterization of melanized fungi from limestone formations in Mallorca. Mycological Progress 4:23–38.
Schlick–Steiner BC, Steiner FM, Seifert B, Stauffer C, Christian E, Crozier RH (2010) Integrative taxonomy: a multisource approach to exploring biodiversity. Annual Review of Enthomology 55:421–438.
Schoch CL, Crous PW, Groenewald JZ et al. (2009) A class–wide phylogenetic assessment of Dothideomycetes. Studies in Mycology64:1–15.
Schoch CL, Seifert KA, Huhndorf S, Robert V, Spouge JL, Levesque CA, Chen W and the Fungal Barcoding Consortium (2012) Nuclear ribosomal internal transcribed spacer ITS. region as a universal DNA barcode marker for Fungi. Proceedings of the National Academy of Sciences 109:6241–6246.
Selbmann L, de Hoog GS, Gerrits van den Ende AHG, Ruibal C, De Leo F, Zucconi L, Isola D, Ruisi S Onofri S (2008) Drought meets acid: three new genera in a dothidealean clade of extremotolerant fungi. Studies in Mycology 61:1–20.
Selbmann L, de Hoog GS, Mazzaglia A, Friedmann EI, Onofri S (2005) Fungi at the edge of life: cryptoendolithic black fungi from Antarctic Desert. Studies in Mycology 51:1–32.
Selbmann L, Grube M, Onofri S, Isola D, Zucconi L (2013) Antarctic epilithic lichens as niches for meristematic fungi. Biology 2:784–797.
Selbmann L, Isola D, Egidi E, Zucconi L, Gueidan C, de Hoog GS, Onofri S (2014) Mountain tips as reservoirs for new rock-fungal entities: *Saxomyces* gen. Nov. and four new species from the alps. Fungal Diversity 65:167–182.
Selbmann L, Zucconi L, Isola D, Onofri S (2015) Rock black fungi: excellence in the extremes, from the Antarctic to space. Current Genetics 61:335–345.
Simpson GG (1951) The species concept. Evolution 5:285–298.
Staley T, Palmer F, Adams JB (1982) Microcolonial fungi: common inhabitants on desert rocks? Science 215:1093–1095.
Stamatakis A (2006) RAxML-VI-HPC: Maximum Likelihood-based Phylogenetic Analyses with Thousands of Taxa and Mixed Models. Bioinformatics 22:2688–2690.
Stamatakis A, Ludwig T, Meier H (2005) RAxML-iii: a fast program for maximum likelihood–based inference of large phylogenetic trees. Bioinformatics 21:456–463.
Sterflinger K (2006) Black yeasts and meristematic fungi: ecology, diversity and identification. In: Gabor P, Carlos R eds. Biodiversity and Ecophysiology of Yeasts 501–514. Springer, New York.
Tang CQ, Humphreys AM, Fontaneto D, Barraclough TG (2014) Effects of phylogenetic reconstruction method on the robustness of species delimitation using single-locus data. Methods in Ecology and Evolution 5:1086–1094.
Taylor JW (2011) One Fungus = One Name: DNA and fungal nomenclature twenty years after PCR. IMA Fungus 2:113–120.
Valadbeigi T, Schultz M, Von Brackel W (2016) Two new species of *Lichenothelia* Lichenotheliaceae from Iran. The Lichenologist 48:191–199.
Vilgalys R, Hester M (1990) Rapid genetic identification and mapping of enzymatically amplified ribosomal DNA from several *Cryptococcus* species. Journal of Bacteriology 172:4238–4246.
White TJ, Burns TD, Lee S, Taylor J (1990) Amplification and direct sequencing of fungal ribosomal DNA genes for phylogenies. In: Innis MA, Gelfand DH, Snisky JJ, White TJ eds. PCR protocols: a guide to methods and applications. San Diego, California: Academic Press, pp 315–322.
Wijayawardene NN, Crous PW, Kirk PM et al. (52 authors) (2014) Naming and outline of Dothideomycetes–2014 including proposals for the protection or suppression of generic names. Fungal Diversity 69:1–55.
Wijayawardene NN, Hyde KH, Rajeshkumar KC et al. (97 authors) (2017) Notes for genera: Ascomycota. Fungal Diversity 86:1–594.
Will KW, Mishler BD, Wheeler Q (2005) The perils of DNA barcoding and the need for integrative taxonomy. Systematic Biology 54:844–851.

Yazici K, Etayo J (2014) Lichenicolous fungi in Igdir province, Turkey. Acta Bot Brasilica 28:1–7
Zhang J, Kapli P, Pavlidis P, Stamatakis A (2013) A general species delimitation method with application to phylogenetic placements. Bioinformatics 29:2869–2876.
Zhou S, Stanosz GR (2001) Primers for amplification of mt SSU rDNA and a phylogenetic study of Botryosphaeria and associated anamorphic fungi. Molecular Ecology105:1033–1044.
Zhurbenko MP (2008) A new species from the genus *Lichenothelia* Ascomycota. from the northern Ural. Mikologiya i Fitopatologiya 42:240–243.

Chapter 3

A standardized approach for co-culturing Dothidealean rock-inhabiting fungi and lichen photobionts *in vitro*

Claudio G. AMETRANO[1*], Laura SELBMANN[2] & Lucia MUGGIA[1]

[1]University of Trieste, Department of Life Sciences, via Giorgieri 10, 34127 Trieste, Italy
[2]University of Tuscia, Department of Ecological and Biological Sciences, Largo dell'Università snc, 01100 Viterbo, Italy

*Corresponding author: University of Trieste, Department of Life Sciences, via Giorgieri 10, 34127 Trieste, Italy. E-mail: claudiogennaro.ametrano@phd.units.it; Phone: 00390405588825

Keywords: carbon sources, *Coccomyxa*, mixed culture, *Lichenothelia, Saxomyces*, *Trebouxia*.

Abstract

Black, rock inhabiting fungi (RIF) are polyextremotolerant, oligotrophic organisms which colonize bare rocks and are specialized to grow in niches precluded to other microorganisms in the harshest environments. In many cases RIF share this environment with green algae and cyanobacteria forming subaerial biofilms; some of them have also been found to be associated with lichen thalli. The RIF genus *Lichenothelia* is of particular interest because it includes lichen parasites and species which are loosely associated with algae or grow independently on rocks. Here, *in vitro* culture experiments studied the development of three *Lichenothelia* species when co-cultured with two different lichen photobionts on growth media differing in nutrient content. The growth rates of these fungi were statistically evaluated, and the structure of the mixed cultures was analyzed by light and scanning electron microscopy. The results show that the presence of algae neither influence the growth rate of fungi nor the formation of any lichen-like structure; tight contacts between the hyphae and the algal cells were also not detected. Since multiple trials were carried out on well characterized species of microcolonial fungi and the methodological procedures were established and standardized and coupled with morphological analyses, this approach proves suitable for future investigations on fungal-algal interactions in other systems.

Introduction

Rock inhabiting fungi (RIF) and black fungi (BF) belonging to the classes Dothideomycetes and Eurotiomycetes are oligotrophic, micro-colonial, melanized fungi which are among the most stress-tolerant microorganisms on Earth (Sterflinger 1998). Thanks to their polyextremotolerance (Gostincar et al. 2011, 2012) and their oligotrophy, RIF can colonize the harshest environments, such as the Antarctic Dry Valleys, the Atacama Desert or high alpine habitats in the Alps and the Andes (Selbmann et al. 2005, 2008, 2014; Kuhlman et al. 2008; Wierzchos et al. 2011). Rock inhabiting fungi can even cope with the hostile conditions of long-term exposure in outer space, which includes high vacuum, extreme temperature fluctuation and a complete spectrum of solar electromagnetic radiations (Onofri et al. 2012). Some species are able to employ unusual sources of carbon which are usually spurned by other microorganisms, such as volatile organic carbon (Qi et al. 2002) or recalcitrant carbon as monoaromatic compounds (Isola et al. 2013; Nai et al. 2013). It has also been hypothesized that certain taxa can use aerial CO_2 as a carbon source (Palmer and Friedman 1988) and are able to generate a transmembrane proton gradient exploiting solar radiation (Waschuk et al. 2005) or rely on ionizing radiation to generate metabolic energy (Dadachova et al. 2007; Pacelli et al. 2017).

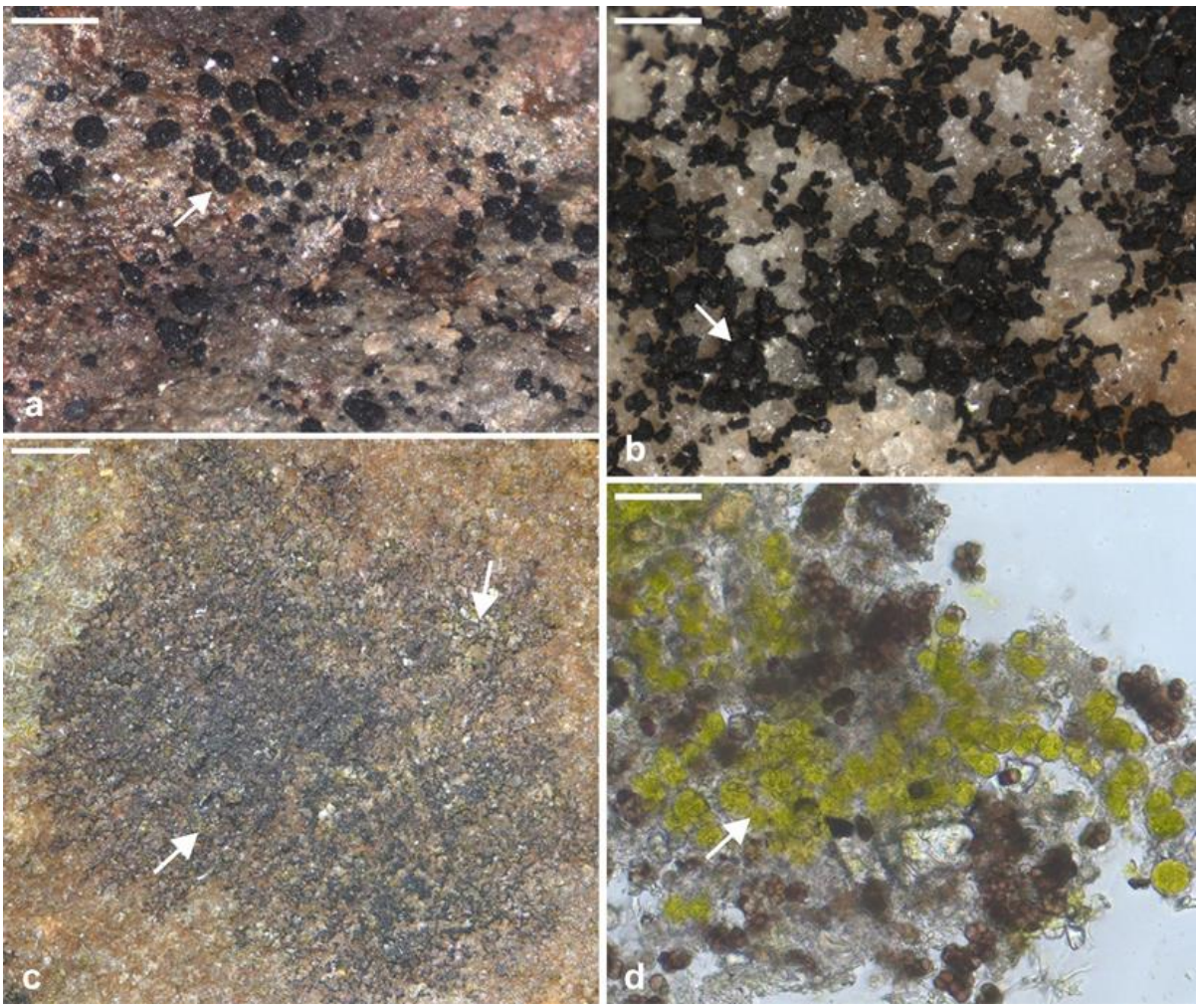

Figure 1 Habit of *Lichenothelia* species in environmental samples: a) *Lichenothelia convexa* (ID: L1608, *K. Knudsen* 12452 - URC1304KK64), b) *L. tenuissima* (ID: L1798, *K. Knudsen* 10406 - UCR197485), c) *Lichenothelia* sp. (ID: L1716, *K. Knudsen* 13057 - UCR1990KK64), d) squash preparation of *Lichenothelia* sp. in (c). a) and b) are the original samples from which the culture isolates were obtained and used in this research. Arrows indicate ascomata (a, b) and algal colonies (c, d) among the melanized fungal hyphae. Scale bars = a, b) 0.4 mm; c) 1 mm; d) 50 µm.

Rock inhabiting fungi often share strongly oligotrophic environments with green algae and cyanobacteria in a form of subaerial biofilms on bare rock surfaces or crevices. They might take advantage from the presence of these primary producers and potentially develop lichen-like association with algae. Recently, multiple symbiotic patterns have been studied *in vitro* by employing culture conditions with a diverse degree of complexity and variability to study the interactions built between fungi and algae. While these experiments have mainly focused on the re-establishment of the lichen symbiosis *in vitro* by co-cultivating previously isolated mycobionts and photobionts and considering evidences of lichenization by observations of morphological and anatomical structures, detection of lichen secondary compounds and analyses of gene expression (Ahmadjian et al. 1978, Culberson & Ahmadjian 1980; Ahmadjian & Jacobs, 1981; Stocker-Wörgötter and Turk 1991; Yoshimura and Kurokawa 1993; Gorbushina et al. 2005; Joneson & Lutzoni 2009; Joneson et al. 2011; Meeßen & Ott 2013), still too few have been done using those not-lichenized fungi found in loose association with algae. Culture experiment considering lichen-like symbioses have been analyzed in model organisms, such as *Saccaromyces cervisiae* and *Chlamydomonas reinhardtii* (Hom and Murray 2014), and in few fungi closely related to true lichen-forming fungi and known to optionally lichenize, such as the system involving *Schizoxylon albescens* and the algae *Coccomyxa* sp. (Muggia et al. 2011, 2016). Hom and Murray (2014), in particular, stressed how the capacity for symbiosis between fungi and algae might be hidden and arise only when the right environmental conditions encourage free living organisms to coexist with mutual benefits derived by the exchange of nutrients.

Microcolonial black fungi have been broadly isolated in culture but only very few have also been tested for their interactions with algae (Turian 1977; Gorbushina et al. 2005; Brunauer et al. 2007). No experiments have been performed on the widespread, black fungal genus *Lichenothelia*, which has arisen particular interest since the time of its description (Hawksworth 1981) when it was suggested to be a possible link between the lecanoralean and the dothidealean lineages, i.e. between the lichenized and the non-lichenized life styles. Currently, the genus includes 29 species (www.mycobank.org; Hessen 1987; Muggia et al. 2015; Valadbeigi et al. 2016) which represent fungi with multiple life styles: on bare rocks they can grow alone (Fig. 1a, b) or in association with green algae (Fig. 1c, d), and other species are known to be parasite on lichens (Kocourková and Knudsen 2008, 2011). The genus *Lichenothelia* is a monophyletic, though it is poorly supported, lineage representing the family Lichenotheliaceae and the order Lichenotheliales, which still has a wobbling phylogenetic placement within Dothideomycetes (Hyde et al. 2013; Muggia et al. 2013, 2015; Wijayawardene et al. 2014). Recently a new genus of RIF, *Saxomyces*, was described by Selbmann et al. (2014) only from pure culture and our preliminary analysis has revealed its close relationships with *Lichenothelia* taxa (Ametrano et al. in prep.)

Here we were interested to test whether the growth rates of selected species of *Lichenothelia* and *Saxomyces* depend on or are influenced by the presence of algae in *in vitro* culture conditions. Four taxa, three *Lichenothelia* and one *Saxomyces* species, already characterized in their morphological traits and phylogenetic relationships, (Muggia et al. 2015; Selbmann et al. 2014) were selected and co-cultured with two different algae (lichen photobionts) on different media. We hypothesize that (a) the presence of primary producers, supplying sugars by photosynthesis, enhances the growth of the black fungi when no organic carbon source is provided in the medium, and (b) the co-growth of the fungus and algae stimulate the formation of lichen-like structures when hyphae come in contact with algal cells. During our experiments we also standardized a methodological approach for inoculum preparation and for measuring fungal growth and these prove suitable to be used in future studies investigating fungal-algal interactions.

Material and Methods

Selection of the material – Four fungal species from the last author's culture collection (LM in GZU), which are also stored in The Mycotheca Universitatis Taurinensis (MUT) and the Culture Collection of Fungi From Extreme Environments (CCFEE), were selected for the experiments: *Lichenothelia calcarea* L1840

(LMCC0065, MUT5685), *L. convexa* L1844 (LMCC0061, MUT5682), *L. tenuissima* L1853 (LMCC0060) and *Saxomyces alpinus* (CBS135222**,** CCFEE5470). *Lichenothelia calcarea* is saxicolous, *L. convexa* is saxicolous and lichenicolous on saxicolous lichens, *L. tenuissima* is saxicolous and lichenicolous and *S. alpinus* is a RIF isolated form rocks from high altitudes. The fungal species have been studied in their morphology and phylogenetic relationships in previous studies (Hessen 1987; Selbmann et al. 2014; Muggia et al. 2015).

The algal species were selected from the most common algae known to lichenize and were also available in the culture collection of LM (LMCC in GZU), namely *Trebouxia* sp.1 (here shortened to '*Trebouxia*') isolated from *Tephromela atra* (Muggia et al. 2008) and *Coccomyxa* sp. PL2-1 (here shortened to '*Coccomyxa*') isolated from *Schizoxylon albescens* MW7645 (Muggia et al. 2011).

Mixed culture experiments – A protocol for carrying out a reproducible method for co-culturing dothidealean rock-inhabiting fungi and algae *in vitro* including measuring their growth was optimized as follows. Suitable inoculum concentrations of algae and fungi for mixed cultures and the procedure to standardize the inocula were established in a preliminary growth experiment using fungal and algal strains grown individually. Each fungal and algal inoculum was standardized according to the following protocol: (1) 200-700 mg of fungal biomass (wet weight) was taken from the axenic culture and put into a 2 ml sterile tube containing steel beads and 1 ml of sterile ddH_20; (2) fungal colonies were grinded in a beads beater for 3 min at 2000 strokes/min; (3) fungal suspensions were put into a 50 ml tube and diluted to 10 ml total volume; (4) 1 ml of each suspension (prepared in triplicates) was filtered on 0.45 µm pre-weighted filter; (5) filters were oven-dried at 80 °C until their weight was stable; (6) by knowing the dry weight, each fungal suspension was then adjusted to a final concentration of 3.0, 0.5 and 0.3 mg/ml, whereas algal suspensions were adjusted to 0.5, 0.25 and 0.05 mg/ml.

One ml of either fungal or algal suspension was plated on *Trebouxia* agar medium (TM, Ahmadjian 1973) in triplicate using 6 cm diameter Petri plates. The cultures were grown in growth chambers under the following conditions: 20 °C, 20 µmol fot*m^{-2}*s^{-1}, with a light/dark cycle of 14/10 hours.

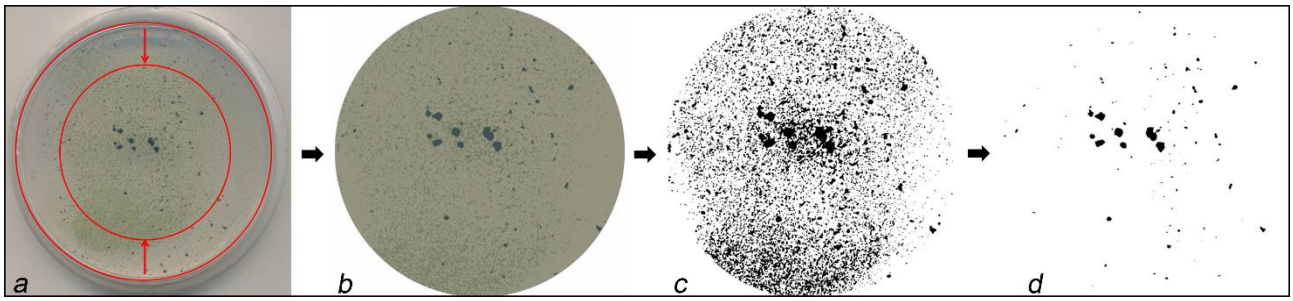

Figure 2. Workflow of the image processing by recording the growth rate of the mixed cultures: the 600 dpi scanning of the plates (a) was re-scaled to 70% of the total area to avoid the marginal parts of the plates which were affected by shadows and imperfections. (b) Color segmentation of images was performed sampling manually at least 20 RGB values each wanted color layer (medium, algae, fungi); (c) fungal layer was detached by threshold color plugin (black and white mode) and (d) measured by analyze particle command.

Fungal growth was evaluated weekly using digital images (RGB 600 dpi TIFF) of the plates acquired by an A4 scanner. Growth indicators such as the total area of colonies, the average size and the Feret average diameter of colonies were measured by the software ImageJ v. 1.50 (National Institute of Health, USA). Initially, three methods were tested to measure the colony growth: particle analysis by thresholding, k-means clustering algorithm, and color segmentation. Due to its suitability and flexibility the color segmentation approach was chosen to evaluate the growth. The k-means clustering algorithm was affected by the choice of the number of pixels layers in which the image is divided, as this might lead to an overestimation or an

underestimation of the fungal surface area, whereas the threshold methods might be affected by scarce sensitivity and repeatability for small growth rates. To set up the final mixed culture experiment 0.5 mg/ml of fungal and 0.05 mg/ml of algal suspensions were selected as the most suitable amounts. It was in fact estimated that 0.5 mg/ml of fungal material would have generated colonies which would have not been overgrown by algal cells (plated as 0.05 mg/ml). One ml of fungal culture suspension and 0.5 ml of algal culture suspension of the same age (grown individually for 4 weeks) were plated in triplicate using the following combinations: (a) fungus alone, (b) fungus together with *Trebouxia*, and (c) fungus together with *Coccomyxa*. Each combination was plated on the TM and Bold Basal Medium (BBM, Bold 1949; Bishoff and Bold 1963) and plates were then sealed with Parafilm® to avoid contamination and desiccation. A total of 18 plates were therefore prepared for each fungus, resulting in an overall total of 72 plates. Fungal growth was assessed weekly using the color segmentation plugin (Sage, 2008) in ImageJ as showed in Fig. 2. An ImageJ macro was used to speed up preliminary operations on plate pictures – essential to carry out surface measurements:
(1) manual selection of the plate was performed by the selection brush tool; (2) the selection was automatically re-scaled and cropped to 70% of the original area to avoid the shadow projected by the edge of the plate; (3) at least 20 point each layer (medium, fungus, algae) and one for the white background (Fig. 2b) were manually selected in color segmentation plugin to set the RGB values used to cluster image pixels; (4) the already clustered image was then analyzed with color threshold plugin (threshold method: default; threshold color: B&W) to select the fungal pixel cluster; (5) after setting the scale, analyze particles ImageJ function was finally used to measure total area covered by fungus as well as single colony size and diameter.

According to the growth rate of the cultures, two main periods, period I and II, were distinguished. The distinction of the two periods is an operative, *a posteriori* definition. In period I we include the weeks during which the growth rate was measurable by the imaging method. In period II, alternatively, the growth rate has decreased to 1/10 of that measured in period I and therefore it was not recordable by the imaging method. Period I includes weeks 3 to 5 and period II includes weeks 6 to 9. The time lap of the first two weeks in which no measures were taken is due to the lag in growth that the fungi have when subcultured. Following a two week lag, growth measurements were reported for all fungal strains up to the ninth week, as no further increase in mycelium are was observed for *L. convexa* and *L. tenuissima* (as reported in the Results).

Statistical analyses – Statistically significant differences in fungal growth co-cultured with the two photobionts were measured on the different media and were assessed using general linear model (GLM) with Statistica 8.0 software (StatSoft. Inc.).

Light microscopy – After 5 months of incubation, one of the three replicates of the mixed cultures was analyzed under a dissecting microscope and sections (lightly squashed) were mounted in water and examined by light microscopy. Digital images of both growth habit and sections were acquired with a ZeissAxioCam MRc5 digital camera fitted to the stereo and light microscopes and were digitally optimized using Combine ZM software (image processing software available at www.hadleyweb.pwp.blueyonder.co.uk/CZM/).

Scanning electron microscopy (SEM) – The replicates analyzed by light microscopy were selected also for SEM observations. About 1 cm^2 of the culture (including fungal mycelium, algal cells and the underneath medium) was excised from the plate and fixed with 2% glutaraldehyde (final concentration) in cacodylate buffer 0.2 M for 45 min at room temperature. Samples were then quickly washed with cacodylate buffer 0.1 M and dehydrated using increasing concentration of ethanol. Three quick washes were used with 30% and 50% ethanol, whereas two 5 min washes, two 12 min washes and two 15 min washes were necessary for 70%, 90% and 100% ethanol, respectively. Samples were then dried at the liquid CO_2 critical point (CPD) to avoid deformation and collapse of colony structures. Samples were gold sputtered with a S150A Sputter Coater (Edwards High Vacuum**,** Crawley, UK). Microscopy observation were performed using a Leica Stereoscan 430i (Leica Cambridge Ltd, Cambridge, UK) with a Si (Li) detector PENTAFET PLUS TM, with window

ATW TM (Oxford Instruments, UK) for microanalyses.

Results

Mixed culture experiments and statistical analyses –The mixed culture experiments with *Saxomyces* have been excluded from the statistical analyses since, although using the same inoculum concentration as the other fungi, the colonies completely covered the surface of the plates within a relatively short time, making therefore the measurements infeasible. Growth measurements were recorded for the other three *Lichenothelia* species from the third week, since a two week lag phase was observed (Fig. 3a) for *L. convexa* and *L. tenuissima*. The growth experiments were stopped at week nine because cultures growing on BBM (Fig. 3e, f) already reached the stationary phase and did not show any increment in mycelial growth. The cultures on BBM showed a significantly slower growth rate than those on TM (GLM; Fisher post-hoc $p < 0.05$; Fig. 3b, c, d). *L. calcarea* had a shorter lag phase than *L. convexa* and *L. tenuissima* and showed already high growth rate during the first weeks (not included). *L. convexa* and *L. tenuissima* when cultured on TM showed a longer lag phase and were still in the exponential growth phase at the end of the experiment. *L. calcarea* reduced its growth rate likely due to a lack of space and nutrient depletion in the culture medium.

Analyses of variance of growth data for period I (Fig. 3e) do not statistically support the difference in growth rate between the fungus alone and the fungus co-cultured with algae (GLM; Fisher post-hoc $p < 0.05$). However, a significant difference is statistically supported for the case of *L. calcarea* co-cultured with *Trebouxia*: here the fungus grew slower when co-cultured with the algae than alone on the same medium. Measurements from period II showed that the growth rates were significantly lower by one order of magnitude than in period I (GLM; Fisher post-hoc $p < 0.05$; Fig. 3f) and it seems that the growth is not enhanced by the presence of the algae at any stage of the co-culture. The growth rate was also checked at the end of the experiment to assess if the presence of dying algal biomass could induce fungal growth, but no evidence was found for this possible interaction.

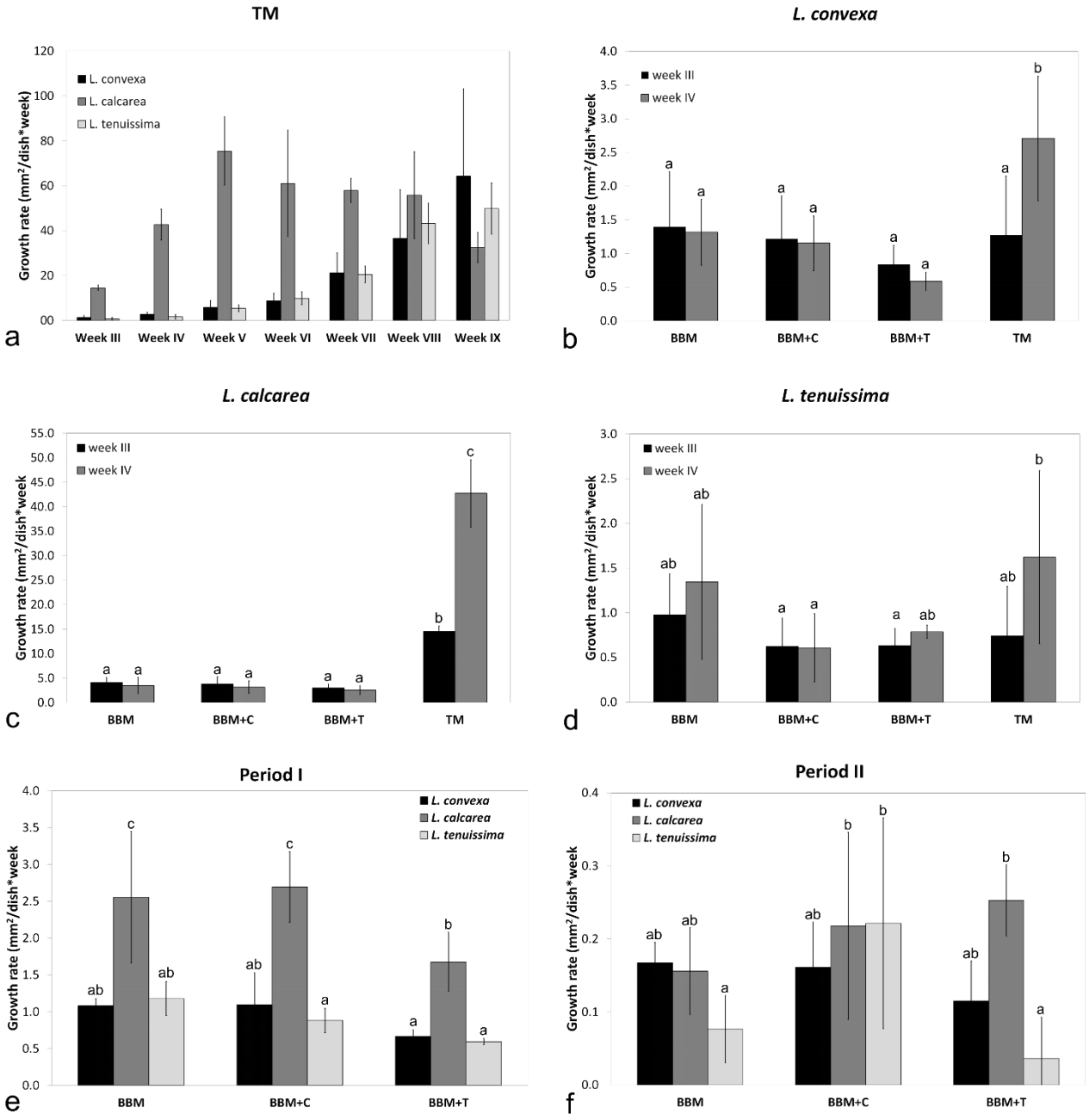

Figure 3. The growth rates of black fungi is expressed as weekly average increase of colony surface area (mm^2/dish*week): a) growth of fungi without any photobiont on TM medium; b-d) growth of the *Lichenothelia* strains under the four experimental conditions tested during week III and IV (mixed culture on TM are missing due to algae overgrowth); e, f) growth period of nine weeks divided into period I (week III to V) and period II (week VI to IX). b-f) BBM+C and BBM+T stand for culture on BBM together with *Coccomyxa* and together with *Trebouxia*, respectively. b-f) Letters (a, b, c) are used to designate statistical significance: bars with different letters are significantly different ($p < 0.05$) and bars with the same letter indicate no statistical difference.

Light and electron scanning microscopy – Light microscopy observations (Fig. 4) do not provide evidence for the formation of any structural interaction between the fungi and the algae. There is no preferential growth of the hyphae toward the algae or hyphae contacting algal cells. When the fungi are cultured with *Coccomyxa* (Fig. 4a, b), the algae remain completely outside the fungal mycelium and easily detach in the preparation when mounted in water. *Trebouxia* cells, which are larger in size (up to 15-20 □m) and remain aggregated after the dissolution of the autospore cell walls due the presence of extracellular polymeric substance (EPS),

are alternatively observed to be located also within the mycelium (Fig. 4c-i). However, no fungal haustoria were identified. In the culture of *Lichenothelia convexa* on BBM (Fig. 4d, e) the *Trebouxia* cells grew as a thick layer within the mycelium. Neither continuous stratification between algae and the fungus was observed, nor we identified any growth pattern of the fungi differing from that observed when they grow alone (not shown).

Scanning electron microscopy analyses also suggest the lack of any structure or tight contact between algal cells and hyphae, particularly for the mixed cultures with *Coccomyxa* (Fig. 5a-c). In this case, the majority of the algal cells were washed out during the sample preparation, and the remaining cells remained only at the base of the fungal colonies, where they were trapped by the coarse surface generated by the presence of hyphae. When the black fungi were co-cultured with *Trebouxia* (Fig. 5d-h) the algae grew between hyphae but the hyphae did not wrap around the algae, which usually remained aggregated into clumps.

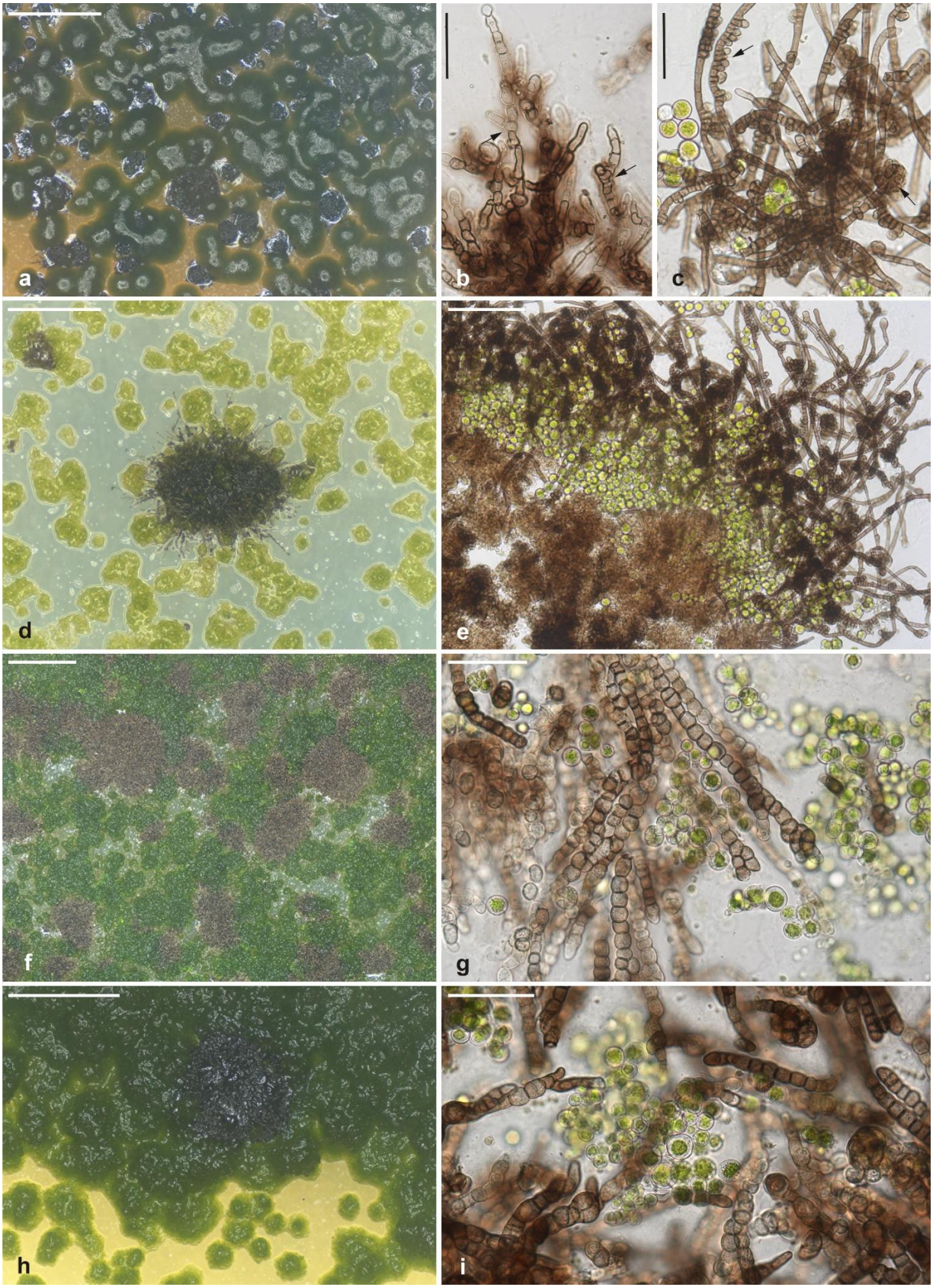

Figure 4 Habit of mixed cultures of fungi and algae observed at stereo (a, d, f, h) and light microscopy (b, c, e, g, i) on different growth media: a, b) *Saxomyces alpinus* co-cultured with *Coccomyxa* on TM; c-e) *Lichenothelia convexa* co-cultured with *Trebouxia* on BBM; f, g) *Lichenothelia calcarea* co-cultured with *Trebouxia* on TM; h, i) *Lichenothelia tenuissima* co-cultured with *Trebouxia* on TM. Scale bars = a, f, h) 1 mm; d) 0,5 mm; e) 100 µm; b, c, g, i) 50 µm.

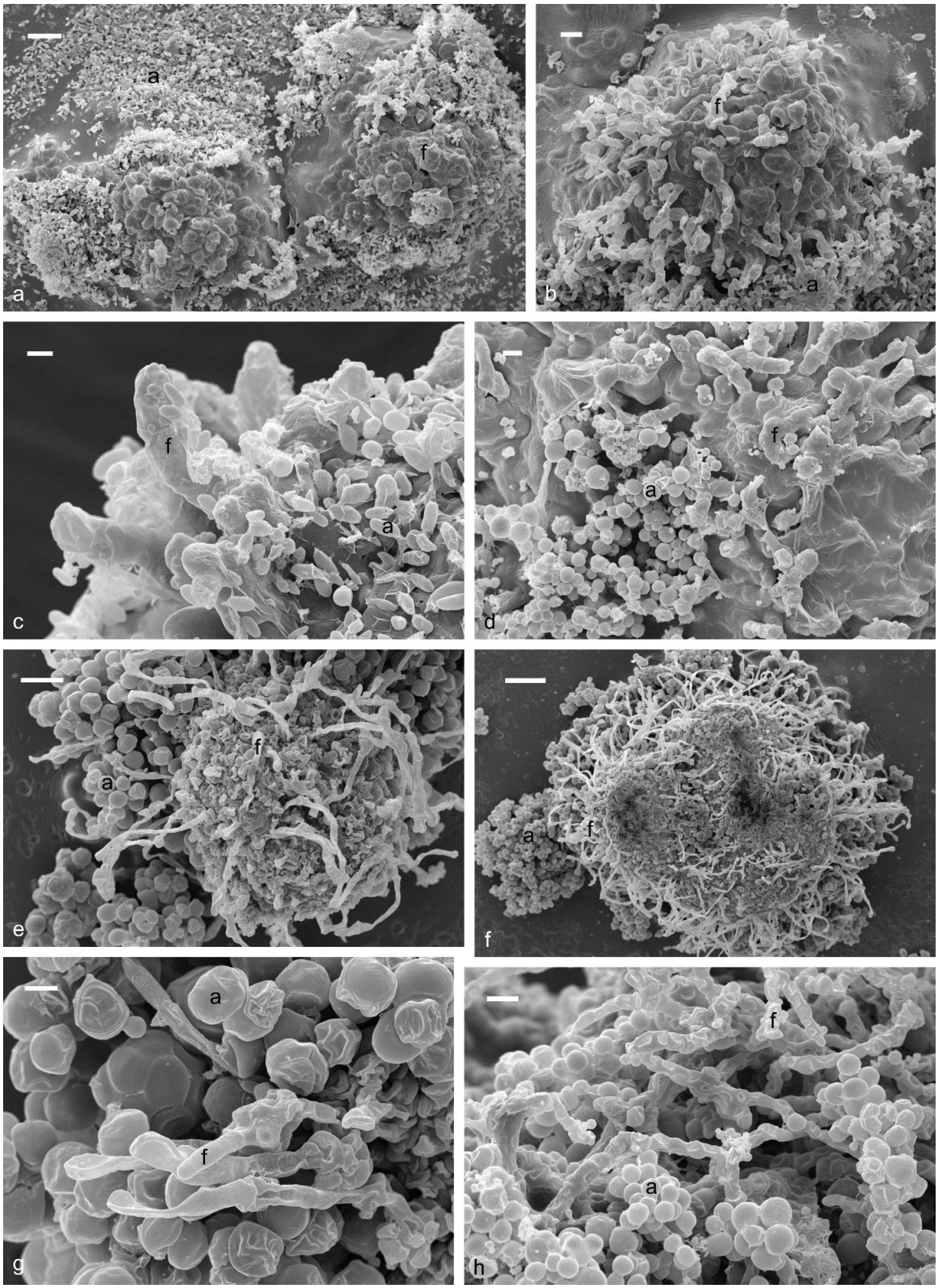

Figure 5 Scanning electron microscopy observation of mixed cultures of fungi and algae on different growth media: a, b) *Saxomyces alpinus* co-cultured with *Coccomyxa* on TM; c) *Lichenothelia tenuissima* co-cultured with *Coccomyxa* on TM; d) *Lichenothelia tenuissima* co-cultured with *Trebouxia* on TM; e-g) *Lichenothelia convexa* co-cultured with *Trebouxia* on BBM; h) *Lichenothelia calcarea* co-cultured with *Trebouxia* on TM. Scale bars = a) 30 µm; b, d, h) 10 µm; c, g) 5 µm; e) 20 µm; f) 50 µm. f = fungus hyphae; a = algal cells.

Discussion

In our study, inoculum standardization, the suitability and the application of digital imaging to evaluate the growth of micro-colonial fungi with photobionts in *in vitro* mixed culture experiments were assessed. Following this approach, it was possible to discriminate different growth rates of the fungi even on inorganic medium, where colonies are predictably characterized by low growth rates. Standardization of the starting inoculum by dry weight assessment proved to be the only applicable method, as the thick, black fungal colonies typical of RIF do not dissolve easily. Further, classical methods to measure cellular density would be ineffective. Optical density, viable cell counts in CFU and counting cells in light microscopy were not taken in account since it is not possible to get single cell suspensions but only hyphae fragments of different size.

Even though it is not easy to correlate the surface area occupied by colonies with biomass or cell number, the surface area serves as an effective indicator of growth for colonial fungi: it provides information on growth rates under different culture conditions and may be correlated with fungal-algal interactions. However, the method does not seem to be sensitive enough for low growth rates, as the rates measured during period II on the inorganic medium, and this might bias the data. The very high standard deviation (SD) recorded was due to high variance among replicates and among measurements on the same plate. These results do not provide evidence for positive trophic effects of the algae on the fungus when cultured together, as fungal growth rates did not increase when fungi were co-grown with the photobionts. However, it seems that there is competition for space and resources between the fungus and the algae when they were co-cultured on the organic medium (TM). In this case the fungus alone grew faster than when co-cultured with algae (data not shown). However, the growth rate on the inorganic medium (BBM) was particularly low and limited in time compared to the one on organic medium (TM).

Furthermore, microscopical observations do not support the formation of any structural interaction between the black fungi and the algae. These results are in contrast to what was reported by Gorbushina et al. (2005) in the only previous study concerning *in vitro* observation of interactions between the algae, *Trebouxia* and *Asterochloris*, and black fungi belonging to Dothidealean and Chaetothyrialean groups. The incubation time and the methodology for observation applied by Gorbushina et al. (2005) are comparable with our set up, but while they highlighted the formation of appressoria-like structures by the fungi enveloping the photobiont cells, we cannot confirm this behaviour for the analysed *Lichenothelia* and *Saxomyces* species. The different growth patterns observed in these RIF can be traced back on their phylogenetic and evolutionary relationships. The used *Lichenothelia* and those RIF strains studied by Gorbushina et al. (2005) belong to the classes Dothideomycetes and Chaetothyriomycetes, respectively. Though their ancestors were suggested to most likely be rock inhabitants (Gueidan et al. 2007), the two classes diverged at different times, Dothideomycetes having more ancient origins than Chaetothyriomycetes (Gueidan et al. 2011). RIF also have a much broader phylogenetic spectrum in Dothideomycetes than in Chaetothyriomycetes, while Chaetothyrialean RIF are closely related to lichen-forming fungi of the family Verrucariaceae (Geiser et al. 2006, Gueidan et al. 2007) with Trebouxiaceae as photobionts (Thüs et al. 2011). On the other hand, those previous studies implementing re-lichenization experiments with lichenized fungi and photobionts did observe fungal-algal interaction (pre-contact, increased fungal branching, enveloping of the algae by fungal hyphae) already in the very first stages of colony development (Joneson & Lutzoni 2009; Joneson et al. 2011). It is, therefore, plausible that Dothidealean fungi, as those investigated here, have evolved to a lesser extent the capacity to develop interaction structures (branching or appressoria-like) when growing with photobionts. Furthermore, the interactions observed by Gorbushina et al. (2005) may have been enhanced by the choice of the most suitable algae. This suggests that further trials should be performed by using different photobionts or those algae microscopically observed on the environmental samples.

Our results pave the way for further targeted analyses to understand the availability of organic carbon sources on inorganic media and nutrient sources available for rock inhabiting black fungi. It remains to be investigated whether the increase of colony surface on inorganic media represents real growth or only a reorganization of the inoculum biomass, as no evident sources of organic carbon were provided.

Since multiple trials were carried out on well characterized species of microcolonial fungi (e.g. *Lichenothelia* and *Saxomyces*) and the methodological procedures were established, standardized and can be coupled with morphological analyses, this approach proves suitable for future investigations on fungal-algal interactions in other systems. Future mixed culture experiments shall consider the co-culture of fungi with different life styles (such as lichen mycobionts, saprotrophs and parasite – e.g. lichenicolous fungi) with algae (either lichen photobionts or free-living algae) to assess carbon exchanges between the symbionts for better understanding the establishment of symbiotic interactions.

Acknowledgments

This research was supported by the project FRA-2014 (Finanziamenti di Ateneo per progetti di Ricerca scientifica) assigned to LM by the University of Trieste. Francesca Vita is thanked for the support in the SEM analyses; Martin Grube and Lorenzo Fortuna are thanked for the constructive discussions. The Italian National Antarctic Museum "Felice Ippolito" is kindly acknowledged for funding CCFEE (Culture Collection of Fungi from Extreme Environments).

References

Ahmadjian V (1973) Methods of isolation and culturing lichen symbiont and thalli. In: Ahmadjian V and Hale M E The Lichens. Academic press, New York pp: 653-660

Ahmadjian V, Jacobs JB (1981) Relationship between fungus and alga in the lichen *Cladonia cristatella* Tuck. Nature 289: 169-172

Ahmadjian V, Jacobs JB, Russell LA (1978) Scanning electron microscope study of early lichen symbiosis. Science 200: 1062-1064

Bischoff H W, Bold H C (1963) Phycological studies IV. Some soil algae from Enchanted Rock and related algal species. Univ Texas Publ 6318: 1-95

Bold HC (1949) The morphology of *Chlamydomonas chlamydogama* sp. nov. Bull Torrey Bot Club 76: 101-108

Brunauer G, Blaha J, Hager A, Turk R, Stocker-Wörgötter E, Grube M (2007) An isolated lichenicolous fungus forms lichenoid structures when co-cultured with various coccoid algae. Symbiosis 44: 127-136

Culberson CF, Ahmadjian V (1980) Artificial reestablishment of lichens. II. Secondary products of resynthesized *Cladonia cristatella* and *Lecanora chrysoleuca*. Mycologia 72: 90-109.

Dadachova E, Bryan RA, Huang X et al. (8authors) (2007) Ionizing radiation changes the electronic properties of melanin and enhances the growth of melanized fungi. PLoS One 2(5): e457

Geiser D M, Gueidan C, Miadlikowska J et al (11authors) (2006) Eurotiomycetes: Eurotiomycetidae and Chaetothyriomycetidae. Mycologia 98: 1053-1064

Gorbushina A A, Beck A, Schulte A (2005) Microcolonial rock inhabiting fungi and lichen photobionts: evidence for mutualistic interactions. Mycol Res 109: 1288–1296

Gostincar C, Grube M, Gunde-Cimerman N (2011) Evolution of fungal pathogens in domestic environments? Fungal Biol 115: 1008-1018

Gostincar C, Muggia L, Grube M (2012) Polyextremotolerant black fungi: oligotrophism, adaptive potential, and a link to lichen symbioses. Front Microbiol 3: 390

Gueidan C, Roux C, Lutzoni F (2007) Using a multigene analysis to assess generic delineation and character evolution in the Verrucariaceae (Eurotiomycetes, Ascomycota). Mycol Res 111: 1147-1170

Gueidan C, Ruibal C, de Hoog G S, Schneider H (2011) Rock-inhabiting fungi originated during periods of dry climate in the late Devonian and middle Triassic. Fungal Biol 115: 987-996

Hawksworth D L (1981) *Lichenothelia*, A New Genus for the *Microthelia aterrima* group. The Lichenologist 13: 141-153

Hessen H (1987) *Lichenothelia*, a genus of microfungi on rocks. In Peveling E, ed. Progress and problems in lichenology in the eighties. Bibl Lichenol 25: 257-293.

Hom E F Y, Murray A W (2014) Plant-fungal ecology. Niche engineering demonstrates a latent capacity for fungal-algal mutualism. Science 345 : 94-98

Hyde K D, Jones E G, Liu, J K et al. (68 authors) (2013) Families of Dothideomycetes. Fungal Diversity 63: 1-313

Isola D, Selbmann L, de Hoog G S, Fenice M, Onofri S, Prenafeta-Boldù F X, Zucconi L (2013) Isolation and screening of black fungi as degraders of volatile aromatic hydrocarbons. Mycopathologia 175: 369-379

Joneson S, Armaleo D, Lutzoni F (2011) Fungal and algal gene expression in early developmental stages of lichen-symbiosis. Mycologia 103: 291-306.

Joneson S, Lutzoni F (2009) Compatibility and thigmotropism in the lichen symbiosis: a reappraisal. *Symbiosis* 47: 109-115
Kocourková J, Knudsen K (2008) Four new lichenicolous fungi from North America. Evansia 25: 62-64
Kocourková J, Knudsen K (2011) Lichenological notes 2: *Lichenothelia convexa*, a poorly known rock-inhabiting and lichenicolous fungus. Mycotaxon 115: 345-351
Kuhlman K R, Venkat P, La Duc M T, Kuhlman G M, McKay C P (2008) Evidence of a microbial community associated with rock varnish at Yungay, Atacama Desert, Chile. J Geophys Res: Biogeosciences 113: G04022
Meeßen J, Ott S (2013) Recognition mechanisms during the pre-contact state of lichens: I. Mycobiont-photobiont interactions of the mycobiont of *Fulgensia bracteata*. Symbiosis 59: 121-130
Muggia L, Baloch E, Stabentheiner E, Grube M, Wedin M (2011) Photobiont association and genetic diversity of the optionally lichenized fungus *Schizoxylon albescens*. FEMS Microbiol Ecol 75: 255-272
Muggia L, Fernàndez-Brime S, Grube M, Wedin M (2016) *Schizoxylon* as an experimental model for studying interkingdom symbiosis. FEMS Microbiol Ecol 92: fiw165
Muggia L, Grube M, Tretiach M (2008) Genetic diversity and photobiont associations in selected taxa of the *Tephromela atra* group (Lecanorales, lichenized Ascomycota). Mycol Prog 7: 147-160
Muggia L, Gueidan C, Knudsen K, Perlmutter G, Grube M (2013) The lichen connection of black fungi. Mycopathologia 175: 523-535
Muggia L, Kocourkova J, Knudsen K (2015) Disentangling the complex of *Lichenothelia* species from rock communities in the desert. Mycologia 107: 1233-1253
Nai C, Wonga H Y, Pannenbecker A et al (8 authors) (2013) Nutritional physiology of a rock-inhabiting, model microcolonial fungus from an ancestral lineage of the Chaetothyriales (Ascomycetes). Fungal Genet Biol 56: 54-66
Onofri S, de la Torre R, de Vera J et al. (11 authors) (2012) Survival of rock-colonizing organisms after 1.5 years in outer space. Astrobiology 12: 508-516
Pacelli C, Bryan R A, Onofri S, Selbmann L, Shuryak I, Dadachova E (2017) Melanin is effective in protecting fast and slow growing fungi from various types of ionizing radiation. Environ Microbiol (in press).
Palmer R J, Friedman E I (1988) Incorporation of inorganic carbon by Antarctic cryptoendolithic fungi. Polarforschung 58: 189-191
Qi B, Moe W M, Kinney K A (2002) Biodegradation of volatile organic compounds by five fungal species. Appl Microbiol Biotechnol 58: 684–689
Sage D (2008) Biomedical Imaging Group (BIG) Ecole Polytechnique Fédérale de Lausanne (EPFL) http:/bigwww.epfl.ch/sage/soft/colorsegmentation/. Accessed October 2016
Selbmann L, de Hoog G S, Mazzaglia A, Friedmann E I, Onofri S (2005) Fungi at the edge of life: cryptoendolithic black fungi from Antarctic desert. Stud Mycol 51: 1-32
Selbmann L, de Hoog G S, Zucconi L et al. (10 authors) (2008) Drought meets acid: three new genera in a dothidealean clade of extremotolerant fungi. Stud Mycol 61: 1-20
Selbmann L, Isola D, Egidi E, Zucconi L, Gueidan C, de Hoog G S, Onofri S (2014) Mountain tips as reservoirs for new rock-fungal entities: *Saxomyces* gen. nov. and four new species from the Alps. Fun Div 65: 167-182
Sterflinger K (1998) Temperature and NaCl tolerance of rock-inhabiting meristematic fungi. Anton Van Lee 74: 271-281
Stocker-Wörgötter E, Türk R (1991) Artificial resynthesis of thalli of the cyanobacterial lichen *Peltigera praetextata* under laboratory conditions. The Lichenologist 23: 127-138
Thüs H, Muggia L, Pérez-Ortega S, et al. (12 authors) (2011) Revisiting photobiont diversity in the lichen family Verrucariaceae (Ascomycota). Eur J Phycol 46: 399-415
Turian G (1977) *Coniosporium aeroalgicolum* sp. nov. – a dematiceous fungus living in balanced parasitism with aerial algae. Bull soc Bot Suisse 87: 19-24
Valadbeigi T, Schultz M, Von Brackel W (2016) Two new species of *Lichenothelia* (Lichenotheliaceae) from Iran. The Lichenologist 48: 191-199
Waschuk S A, Bezerra A G, Shi L Brown L S (2005) *Leptosphaeria* rhodopsin: bacteriorhodopsin-like proton pump from a eukaryote. Proc Natl Acad Sci USA 102: 6879–6883
Wierzchos J, Cámara B, De Los Rios A, Davila A F, Sánchez Almazo I M, Artieda O, Ascaso C (2011) Microbial colonization of Ca-sulfate crusts in the hyperarid core of the Atacama Desert: implications for the search for life on Mars. Geobiology 9: 44-60
Wijayawardene N N, Crous P W, Kirk P M et al. (50 authors) (2014) Naming and outline of *Dothideomycetes*–2014 including proposals for the protection or suppression of generic names. Fun Div 69: 1-55
Yoshimura I, Kurokawa T (1993) Development of lichen thalli in vitro. Bryologist 96: 412-421

Chapter 4

Genome-scale data suggest an ancestral rock-inhabiting life-style of Dothideomycetes (Ascomycota)

Claudio G. Ametrano[a*], Felix Grewe[b], Laura Selbmann[c] H. Thorsten Lumbsch[b], Steven D. Leavitt[d] & Lucia Muggia[a]

[a] University of Trieste, Department of Life Sciences, via Giorgieri 10, 34127 Trieste, Italy
[b] Integrative Research Center, Science and Education, Field Museum of Natural History, 1400 S Lake Shore Drive, Chicago, IL 60605, USA
[c] University of Tuscia, Largo dell' Università, Department of Ecological and Biological Sciences, 01100 Viterbo, Italy
[d] Department of Biology and M.L. Bean Life Science Museum, Brigham Young University, 4102 Life Science Building, Provo, UT 84602, USA

* Corresponding author: Claudio G. Ametrano. Address: University of Trieste, Department of Life Sciences, via Giorgieri 10, 34127 Trieste, Italy. E-mail: claudiogennaro.ametrano@phd.units.it

Keywords: *Lichenothelia*, phylogenomics, *Saxomyces*, species tree, supermatrix, supertree

Abstract

Dothideomycetes, the most diverse fungal class in Ascomycota, includes species with a wide range of lifestyles. Previous multilocus studies have investigated the taxonomic and evolutionary relationships of these taxa but often failed to resolve the early diverging nodes and frequently generated inconsistent placements of some clades. Here, we use a phylogenomic approach to resolve relationships in Dothideomycetes, focusing on two genera of melanized, extremotolerant rock-inhabiting fungi - *Lichenothelia* and *Saxomyces* – that have been suggested to be early diverging lineages. We generated phylogenomic datasets from newly sequenced and previously available genomes comprised of 242 individuals. We explored the influence of tree inference methods, supermatrix vs. coalescent-based species tree, and the impact of varying amounts of genomic data. Overall, our phylogenetic reconstructions provide consistent and well-supported topologies for Dothideomycetes, recovering *Lichenothelia* and *Saxomyces* among the earliest diverging lineages in the class. In addition, many of the major lineages within Dothideomycetes are recovered as monophyletic, and the phylogenomic approach implemented here recovers relationships among these lineages with strong support. Ancestral character reconstructions suggest that the rock-inhabiting life-style is ancestral within the class.

Introduction

Dothideomycetes is the largest and most diverse fungal class of ascomycetes, comprise of c. 20,000 species (Jaklitsch et al. 2016) classified into 105 families (Hyde et al. 2013) and 32 orders (Liu et al. 2017). The class comprehends a great variation of fungal life-styles, including saprotrophs, plant pathogens, endophytes, epiphytes, fungicolous, lichenized, lichenicolous, and free-living rock-inhabiting fungi.

Several phylogenetic inferences have been generated to resolve taxonomic and evolutionary relationships within Dothideomycetes at different systematic levels (e.g. Schoch et al. 2006, 2009; Nelsen et al. 2009; Ruibal et al. 2009; Hyde et al. 2013, Muggia et al. 2015 Liu et al. 2017; Ametrano et al. in press). These analyses usually considered wide taxon samplings and were based on combinations of nuclear and

mitochondrial loci, such as the nuclear and mitochondrial ribosomal DNA regions (rDNA, e.g. nucLSU, nucSSU, mtSSU) and protein-coding genes (e.g., TEF1, RPB1, RPB2). However, these analyses occasionally failed to resolve basal nodes, generating inconsistent placement of some orders or families. In spite of the increased use of genome-scale data to resolve long-standing evolutionary and taxonomic issues (Chan & Ragan, 2013), phylogenomic approaches have not yet been implemented for Dothideomycetes, although about 250 sequenced genomes of its representatives are available. Within this class, genome sequencing effort has been mostly focused on plant and human pathogenic fungi (Hane et al. 2007; Ohm et al. 2012; Raffaele & Kamoun, 2012), and fungi with a certain ecological (e.g., melanized, halotolerant yeast; Gostinčar et al. 2011) or economic interest (e.g. those able to degrade hydrocarbon; Prenafeta-Boldu et al. 2006; Sterflinger 2006; Nai et al. 2013). On the other hand, the most inconspicuous taxa−especially those belonging to the group of melanized, meristematic, rock-inhabiting fungi (RIF)−have been largely neglected in genomic research. This shortcoming is likely due to the difficulty to retrieve them in nature, isolate them axenically in vitro and their extremely slow growth rate in culture.

Two dothidealean genera, *Lichenothelia* and *Saxomyces*, are iconic representatives of RIF (Ametrano et al. 2017). Species of *Lichenothelia* and *Saxomyces* are widespread worldwide, occurring on exposed rocks, often in extreme environments, and having evolved life-styles on nutrient-poor substrates. Because they can survive in harsh environments, characterized by high solar radiation, very high and very low temperatures, and drought stress, they have been recognized within the group of polyextremotolerant fungi (Gostinčar et al. 2012). *Lichenothelia* species are of particular interest because they exhibit a multiplicity of lifestyles, e.g. non-lichenized rock-inhabiting, parasitic on lichens, and loosely associated with green algae on rocks. Due to the affinity towards algae, *Lichenothelia* has been historically considered an evolutionary link between the non-lichenized Dothideomycetes and the lichenized Lecanoromycetes (Hawksworth 1981). However, recent phylogenetic analyses have identified *Lichenothelia* and *Saxomyces* as two individually monophyletic lineages (Ametrano et al. in press), but their phylogenetic placement within Dothideomycetes remained unresolved. There is, therefore, the need to gain more information from *Lichenothelia* and *Saxomyces* genomes to better understand their genetic diversity and evolutionary relationships with other closely related, dothideomycetous taxa with varying lifestyles.

Here, we present a phylogenomic study on the evolutionary relationships of *Lichenothelia* and *Saxomyces* within Dothideomycetes. Genes of *de novo* genome assemblies from two species of *Lichenothelia* and two of *Saxomyces* were added to a supermatrix including genes of most Dothideomycetes taxa for which the whole genome data were available. Our study aimed to (i) generate the first genome-scale phylogeny of Dothideomycetes to resolve the phylogenetic placement of still unsupported lineages and in particular clarify that of *Lichenothelia* and *Saxomyces* and their relationships with other RIF lineages within the class, (ii) assess whether and to which extent the amount of genetic information, the alignment processing and the phylogenomic reconstruction method impact on the final phylogenetic inference, (iii) assess the minimum amount of genomic information for which a significant topology improvement is not met when compared to the phylogeny generated with the entire set of genes.

Materials and methods

Culture isolation, DNA extraction and sequencing — Fungal strains representing *Lichenothelia* and *Saxomyces* species were available from previous culture isolations reported by Muggia et al. (2013, 2015), Ametrano et al. (in press) and Selbmann et al. (2014). The strains which were selected for genome sequencing are: *Lichenothelia convexa* L1844 (LMCC0061, MUT5682), *Lichenothelia intermixta* L2282 (LMCC0543), *Saxomyces alpinus* CCFEE5470 (CBS135222) and *Saxomyces americanus* L1853 (LMCC0060, MUT5853). Isolates were sub-cultured on malt yeast medium (MY, Ahmadjian 1967) at 20 °C, and DNA was extracted as soon as the mycelium grew to a sufficient biomass (about 4 weeks).

Genomic DNA was extracted using the ZR Fungal/Bacterial DNA MicroPrep™ Kit (Zymo Research) according to the manufacturer's protocol after the fungal biomass was grinded in liquid nitrogen. The quality of the genomic DNA was checked by gel electrophoresis on 0.8% agarose gel, and the nucLSU rDNA was sequenced to confirm the identity of the strains. The four genomic DNA extractions were sent to the University of Illinois at Chicago sequencing facility for library preparation (Nextera XT) and sequencing on an Illumina MiSeq platform. The strain of *Lichenothelia convexa* was sequenced with three times deeper coverage than the other three strains to obtain a better assembly.

Bioinformatics — A bioinformatic pipeline consisting of several programs was generated to extract single-copy genes from whole-genome assemblies and create individual gene alignments and phylogenies (Fig. 1). Fastq files containing 2 x 150 bp paired-end (PE) reads were quality filtered with Trimmomatic 0.35 (Bolger et al. 2014) to remove sequencing adapters, low quality nucleotides and short reads. We changed the recommended settings to LEADING:10, TRAILING:10, and MINLEN:25 to cut bases off the reads when the quality was below ten and subsequently remove sequences shorter than 25 bases. The quality check was performed with FastQC 0.11.5 both before and after reads trimming. High quality, paired-end and orphan reads were then assembled with SPAdes 3.5.0 (Bankevich et al. 2012). The assemblies of the multi k-mer SPAdes approach were checked with Quality Assessments Tool for genome assemblies (QUAST 4.5, Gurevich et al. 2013). The best assembly for each taxon was selected and analyzed with Benchmarking Universal Single Copy Orthologs (BUSCO 3.0.1; Waterhouse et al. 2017). In addition, 238 whole-genome assemblies of other Dothideomycetes were downloaded from NCBI GenBank and JGI Genome portal (Table S1) and processed with BUSCO (All the Dothideomycetes assemblies available on June 2017, when the dataset was built, were included, except those which resulted taxonomically misassigned during test runs of the dataset, references in Table S1). Distribution of the BUSCO completeness of the assemblies was assessed for outliers with Thompson Tau test (Thompson, 1935). BUSCO evaluation of the completeness of the genome assemblies is based on a set of orthologous genes (OrthoDB; Zdobnov et al. 2016) present in the members of the taxonomic group of interest. Among the genes predicted by BUSCO, only single copy orthologs, which are suitable for phylogenetic inference, were selected and used for subsequent analyses. Orthologous genes which were present in single copy but predicted in multiple possible versions were also discarded. Selected single-copy genes from each taxon were aligned with MAFFT 7 (Katoh and Standley, 2013) using default parameters. As the alignment filtering method can affect the output of the subsequent phylogenetic inferences (Tan et al. 2015), sometimes worsening phylogenetic inference results, sequence alignments from MAFFT were filtered either with Gblocks (Castresana, 2000) or with GUIDe tree-based AligNment ConfidencE (GUIDANCE 2.02, Penn et al. 2010).

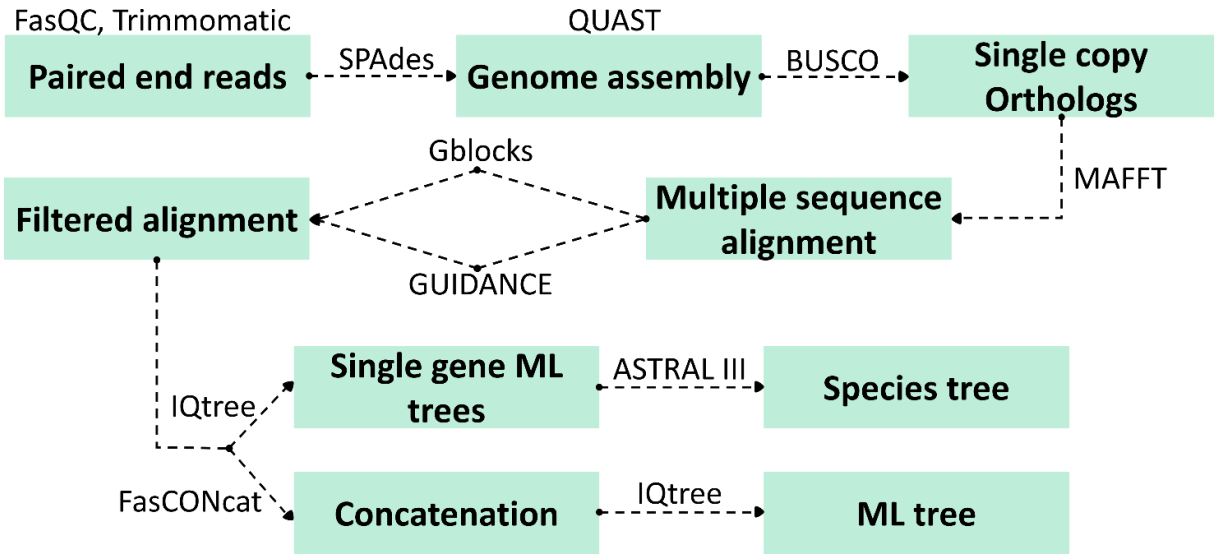

Figure 1. (Previous page) Flow chart reporting the bioinformatic pipeline used for the analyses. The pipeline begins in the upper left corner; input and output of the pipeline are reported inside the boxes, the software used for each pipeline step is reported above or between the boxes.

Phylogenomic analyses — The phylogenetic reliability of the generated data was tested with different number of genes, alignment filtering methods and tree reconstruction methods. Five individual data sets were constructed: (i) A dataset of genes longer than 1000 bp after Gblocks trimming (">1kb Gblocks" dataset) or (ii) GUIDANCE trimming with less than 50% of gaps (">1kb GUIDANCE" dataset), (iii) the complete set of retrieved genes, which includes both genes longer and shorter than 1kb after Gblocks filtering ("Complete Gblocks" dataset) or (iv) GUIDANCE trimming ("Complete GUIDANCE" dataset), and (v) a reduced dataset, both in gene number and samples, without any missing data in order to estimate the impact of missing data on tree ("No missing" dataset). The individual gene alignments of each dataset were either used for individual gene tree calculations or concatenated into a supermatrix with FasCONcat 1.0 (Kück and Meusemann, 2010) (Fig. 1). Maximum likelihood (ML) phylogenetic inferences from the supermatrix, as well as the single locus inferences, were produced with IQTree 1.6.1 (Nguyen et al. 2014) using 1000 replicates of ultra-fast bootstrap (-bb) to get node support values (Hoang et al. 2017) and Model Finder Plus (-MFP) to select the most suitable nucleotide substitution model. Gene trees resulting from single locus inferences were further combined in a supertree with the coalescent-based species tree estimation software ASTRAL III (Zhang et al. 2017). The resulting topologies were compared with normalized Robinson-Foulds distance (RF, Robinson and Foulds, 1981).

As the analyses of a genome-based supermatrix with bootstrap support can be very computationally demanding, an alternative, customized, resampling strategy was tested in the analyses on the ">1kb Gblocks" concatenated alignment. Thirty runs of IQTree were carried out on reduced concatenated matrices made of an increasing, randomly selected, number of columns from this alignment. The phylogeny resulting from the complete supermatrix was taken as the reference and used to compute RF distances in RAxML 8.2 (Stamatakis, 2014) with the phylogenies generated from the re-sampled alignments. Resampling was performed without replacing and the sampling effort was increased until no statistically significant difference among RF distance distributions was detected (one-way ANalysis Of Variance (ANOVA) $p < 0.01$ and *post hoc* pairwise tests: Tukey, Bonferroni and Scheffe, Statistica 6).

Reproducibility — Genome assemblies has been deposited at GenBank under the accession XXXX. Resampling as well as alignment filtering by length or gap percentage, and other tasks which connect the pipeline steps were performed using Python3 scripts (available on GitHub: https://github.com/claudioametrano/Alignment_filtering_and_resampling).

Results

Assembly statistics and completeness of the genomes — After quality filtering a total of 39.4 10^6 PE reads were generated for *Lichenothelia convexa* L1844, 9.7 10^6 PE reads for *Lichenothelia intermixta* L2282, 8.6 10^6 PE reads for *Saxomyces alpinus* CCFEE 5470 and 9.9 10^6 PE reads for *Saxomyces americanus* L1853. Assemblies statistics are reported in Table 1. BUSCO assembly completeness analysis on 3156 orthologous genes for the subphylum Pezizomycotina recovered 93.1% for *L. convexa*, 92.3% for *L. intermixta*, 46.1% for *S. alpinus* and 95.7% for *S. americanus*. The mean and standard deviation for the entire assembly dataset of the 242 Dothideomycetes is 96.3 ± 6 (see Fig. S1 for the complete output of the BUSCO analysis).

Table 1. Total number of reads (mil), number of contigs longer than 500 bp, longest contig dimension (bp), N50 (bp), L50 and assembly size (Mbp) of the four sequenced samples.

Sample	Total reads	Contigs (> 500 bp)	Longest contig	N50	L50	Assembly size
Lichenothelia convexa L1844	39.4	1669	539,045	61,890	165	36.6
Lichenothelia intermixta L2282	9.7	3619	205,447	35,632	233	29.4
Saxomyces alpinus CCFEE 5470	8.6	22,101	67,075	3086	3727	51.4
Saxomyces americanus L1853	9.9	10111	115,917	18,029	561	42.3

Phylogenomic datasets — The ">1Kb Gblocks" dataset comprises 242 samples (including the four newly sequenced species of *Lichenothelia* and *Saxomyces*) and 664 genes longer than 1000 bp after Gblocks trimming. The total alignment length is 1.1 Mb. "Complete Gblocks" dataset comprises the same samples, but it includes all the 2998 genes which are in single copy, not predicted in multiple version and not empty after Gblocks trimming. As Gblocks does not allow gaps and it selects only perfectly aligned regions, many genes were drastically shortened, the final length of the alignment is indeed only double (2.2 Mb) than the ">1Kb Gblocks" dataset, which is a subset of this. The presence of samples characterized by relevant events of genes duplication or low-quality assemblies (Fig. S1) hampered to find genes, among BUSCO orthologs, which were in common to all samples. The number of the samples was therefore reduced to 229 taxa in the "No missing" dataset, retaining, however, all *Lichenothelia* and *Saxomyces* assemblies. A total of 63 genes and 31 Kb alignment were used to run the phylogenetic inference. ">1Kb GUIDANCE dataset" comprises the complete 242 samples and, as GUIDANCE tends to be less strict than Gblocks, 1260 genes longer than 1 Kb have been included in the final alignment with a length of 7.4 Mb.

Comparison of the phylogenies produced — Phylogenies inferred from the same dataset but applying different reconstruction methods produced highly similar topologies. Only three incongruences were detected when comparing the two phylogenies obtained from the concatenation ML inference and the coalescent-based species tree inference of "1Kb Gblocks" dataset. These concern the placement of *Eremomyces bilateralis*, *Lineolata rhizophorae* and *Patellaria atrata* (Fig. 2). The RF distance between these two phylogenies is indeed only 0.109 and it is similar to the one obtained from the comparison of the two inferences on "1Kb GUIDANCE" dataset (0.100) (Table S2). Unsurprisingly, varying both the starting dataset, ("Complete Gblocks" or "1Kb Gblocks") and the reconstruction method (concatenation or coalescent-based) generated the most diverse topologies (RF distance value of 0.117), though even in this case, they are still highly congruent (Table S2). The most similar topologies were produced by coalescent-based approach on "1Kb Gblocks" and "1Kb GUIDANCE" (Fig. S5). Though, these inferences based on a rather different gene dataset produced almost the same topology with a RF distance of 0.025 (Table S2). This is remarkable, because the datasets are of 664 and 1260 genes, respectively, and even if the same markers are considered, the retained parts of the alignment are not the same, as have been obtained using two different filtering methods. Only *Eremomyces bilateralis* presents here a slightly different placement, although this is not supported (ultrafast bootstrap value lower than 95). Three runs of "1Kb Gblocks" dataset with the concatenation approach produced perfectly congruent topologies which only differs in few support values of the less supported lineages, as shown by weighed RF distance values, which are anyway very close to zero. Few other samples show an unstable position within the phylogeny. *Neofusicoccum parvum*, for instance, is basal to *Botryosphaeria-Macrophomina* clade using "1Kb Gblocks" dataset, while it is basal to the *Lasidiplodia-Diplodia-Bptryosphaeria-Macrophomina* clade considering the "Complete Gblocks" dataset run as a concatenated supermatrix (Fig. S2). However, these phylogenetic positions are not fully supported by ultrafast bootstrap

value. The “No missing” dataset, although built on both a reduced number of samples (229) and markers (63), produced highly similar results when considering the phylogeny obtained from the concatenation (Fig. S3a). However, when the same dataset is used to apply the coalescent-based approach (Fig. S3b) the resulting RF distance between the two phylogenies is the highest recovered (0.181), though still rather low.

Figure 2. (Following page) Phylogenomic inferences based on a concatenated supermatrix (left) and multispecies coalescent (right) approaches. The dataset was composed by 664 single-copy gene regions longer than 1 Kb (after alignment trimming with Gblocks). Topology mismatches between the trees are highlighted by red dashed branch lines. Bootstrap support values lower than 100% are shown. *Lichenothelia* and *Saxomyces* clades are highlighted by orange boxes. Pink and green boxes alternatively delimitate the other lineages, wither represented by a single genus or by multiple genera.

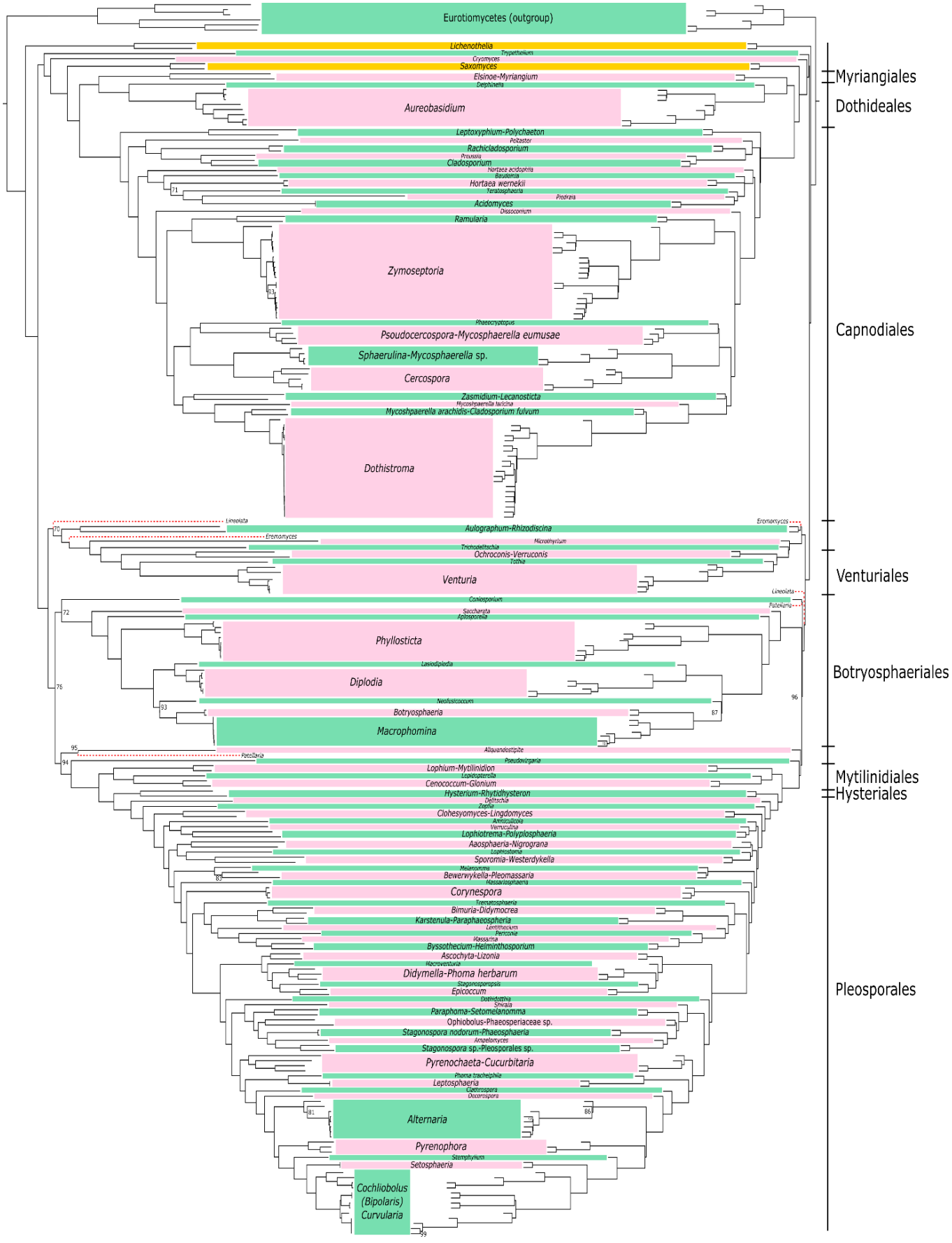
Eurotiomycetes (outgroup)
Lichenothelia
Trypethelium
Cryomyces
Saxomyces
Elsinoe-Myriangium
Delphinella
Aureobasidium
Leptoxyphium-Polychaeton
Pelazter
Rachicladosporium
Prousdia
Cladosporium
Hortaea acidophila
Baudoinia
Hortaea werneckii
Teratosphaeria
Phedraia
Acidomyces
Dissoconium
Ramularia
Zymoseptoria
Phaeocryptopus
Psoudocercospora-Mycosphaerella eumusae
Sphaerulina-Mycosphaerella sp.
Cercospora
Zasmidium-Lecanosticta
Mycosphaerella tassiana
Mycoshpaerella arachidis-Cladosporium fulvum
Dothistroma
Myriangiales
Dothideales
Capnodiales
Lineolata
Eremomyces
Aulographum-Rhizodiscina
Microthyrium
Trichodelitschia
Ochroconis-Verruconis
Tothia
Venturia
Venturiales
Coniosporium
Saccharata
Aplosporella
Phyllosticta
Lasiodiplodia
Diplodia
Neofusicoccum
Botryosphaeria
Macrophomina
Botryosphaeriales
Patellaria
Aliquandostipite
Pseudomirgania
Lophium-Mytilinidion
Loculoascoma
Cenococcum-Glonium
Hysterium-Rhytidhysteron
Delitschia
Zeplea
Clohesyomyces-Lindgomyces
Aniptodera
Vermiculina
Lophiotrema-Polyplosphaeria
Aaosphaeria-Nigrograna
Loptosstoma
Sporomia-Westerdykella
Melanomma
Bewerwykella-Pleomassaria
Massarinaphaeria
Corynespora
Trematosphaeria
Bimuria-Didymocrea
Karstenula-Paraphaeospheria
Lentithecium
Periconia
Massarina
Byssothecium-Helminthosporium
Ascochyta-Lizonia
Macroventuria
Didymella-Phoma herbarum
Stagonosporopsis
Epicoccum
Didymosphaeria
Shiraia
Paraphoma-Setomelanomma
Ophiobolus-Phaeospheriaceae sp.
Stagonospora nodorum-Phaeosphaeria
Amplelomyces
Stagonospora sp.-Pleosporales sp.
Pyrenochaeta-Cucurbitaria
Phoma trachelphila
Leptosphaeria
Clathrospora
Occosinspora
Alternaria
Pyrenophora
Stemphylium
Setosphaeria
Cochliobolus (Bipolaris) Curvularia
Mytilinidiales
Hysteriales
Pleosporales

Supermatrix resampling — Phylogenetic analyses based on the randomly resampled, increasingly bigger alignment from "1Kb Gblocks" produced, as expected, topologies which progressively approach the reference (Fig. 3). The results show both an increase of precision and accuracy when the sampling effort is increased. The increase in precision is highlighted by the RF distance among the same dimension resampled matrix topologies, becoming smaller as the amount of resampled column is increased (Table S4). The increase of accuracy is shown by the RF distance from the reference topology becoming progressively smaller (concatenation of "1Kb Gblocks" dataset; Fig. 3). The standard deviation (SD) also decreases from 0.026 (0.1% resampling effort) to 0.011 (30% resampling effort), highlighting a smaller distribution variance when the sampling effort is increased. ANOVA and post hoc tests show significant differences among increasing resampling effort up to 20% (ANOVA $p < 0.01$; post hoc tests $p < 0.01$), conversely, increasing the resampling effort from 20 to 30% did not produce a significant shift of the distances from the reference topology.

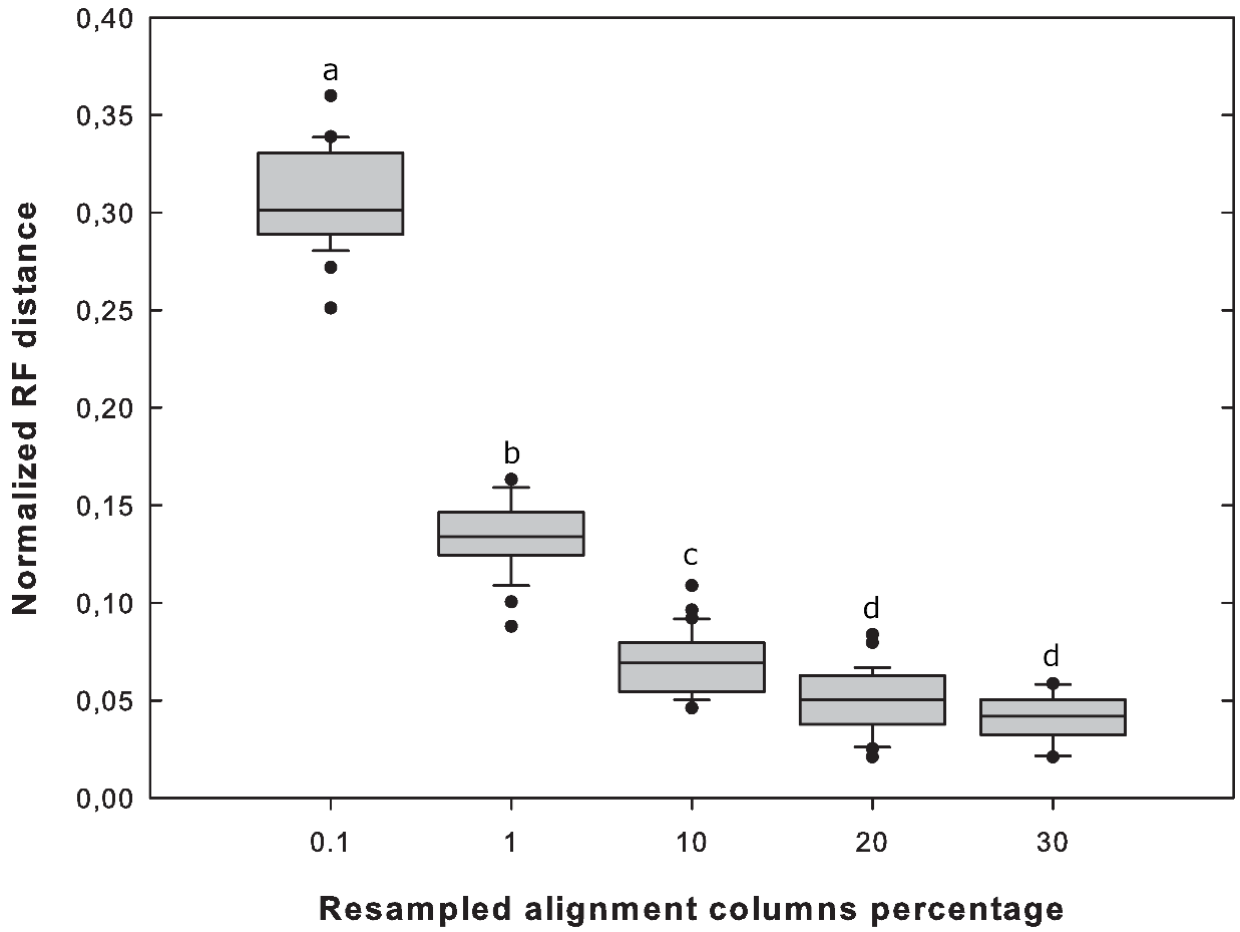

Figure 3. Distribution of the 30 normalized RF distances from the reference topology for each of the five resampling efforts. Boxes are delimited by the distance between 25th and 75th percentile; lines inside the boxes show the median value of the distribution; whiskers refer to 10th and 90th percentiles; outliers are marked with black dots. Letters (a, b, c, d) are used to label statistical significance: boxes with different letters are significantly different ($p < 0.01$) while the same letter indicates no statistical difference.

Comparison to published Dothideomycetes phylogenies and the phylogenetic placement of RIF —Subclasses Dothideomycetidae, which includes the orders Capnodiales, Myriangiales and Dothideales, and Pleosporomycetidae, which includes the orders Pleosporales, Mytilinidiales, and Hysteriales, which are well supported in classical, multilocus approaches (Ruibal et al. 2009; Schoch et al. 2009; Muggia et al. 2015; Liu et al. 2017), were also recovered in our genome-based inference. Most inferences, and this study too, identify Hysteriales and Pleosporales as sister clades within Pleosporomycetidae, and the lineage Mytilinidiales basal

to them; on the contrary, Hyde et al. (2013) reported Hysteriales as sister to Mytilinidiales. The relationships of taxa within the subclass Dothideomycetidae is instead congruent among all the other previous phylogenies and in the present one, confirming Myriangiales and Dothideales as sister groups and Capnodiales basal to them. Among the other orders, the placement of Bothryosphaeriales agrees with the previous phylogenies, being basal to the orders belonging to the subclass Pleosporomycetidae in our phylogeny and being related to them also in literature. On the other hand, the phylogenetic position of Venturiales substantially differs in the present phylogeny from other most recent multilocus phylogenies produced by Hyde et al. (2013) and Liu et al. (2017). These inferences, indeed, place Venturiales as related to the subclass Dothideomycetidae (e.g. orders Dothideales, Myriangiales and Capnodiales), while our analyses recover it at the base of the subclass Pleosporomycetidae and order Botryosphaeriales, whereas its relationship with Microthyriales is maintained.

Lichenothelia and *Saxomyces* are confirmed as distinct, independent lineages, as recently reported by Ametrano et al. (in press). However, their placement within Dothideomycetes differs when the inference is based on genomic data. Here, indeed, *Lichenothelia* samples are recovered as basal to the Dothideomycetes, while *Saxomyces* is early diverging in Dothideomycetidae, diverging from the rest of the clade after *Trypethelium* and *Cryomyces*. Other few extremotolerant black fungi have been included in the phylogeny, such as the genera *Rachicladosporium* and *Hortaea*, which both here belong to the order Capnodiales, as in previous multilocus phylogenies.

Discussion

Supermatrix resampling and phylogenomic inference — The phylogenomic analyses presented here provide a robust inference of evolutionary relationships in the Dothideomycetes, including the RIF genera *Lichenothelia* and *Saxomyces*. Assessing many combinations of markers, different alignment filtering and phylogenetic reconstruction methods supported the overarching phylogenetic relationships in this diverse clade of fungi.

Strict alignment filtering criteria have been shown to worsen single locus inference (Tan et al. 2015). However, in our analyses, strict filtering criteria did not significantly affect the resulting topologies when the length of each locus in the alignment was > 1 kb. We adopted this threshold, e.g., alignments > 1 kb arbitrarily, without testing the effect of a progressively reduced length of each single marker on the resulting phylogenies. Though the effect of the alignment filtering was tested using only two approaches, i.e. a strict filtering strategy (Gblocks) and a relaxed strategy (GUIDANCE), we noticed that RF distances between phylogenies, whose pipelines only differ by the filtering step, are among the smallest registered (0.063 and 0.025; Table S2). This highlights the stability of the phylogenetic signal in our genome-scale data in spite of differences in filtering strategies. Similarly, while diverse phylogenetic reconstruction methods implemented here, they produced consistent phylogenies with low RF values, thus suggesting that concatenation is a valid method, particularly for that concerns the sampling and lineage sorting condition of our dataset.

Concatenation approaches have been shown to produce highly supported but wrong topologies in some cases, particularly when sufficiently short branch lengths are generated in relation to effective population size (Kubatko et al. 2007). In this study, coalescent-based approaches were not applied on the whole set of markers because single locus inferences were heavily affected either by difficult-to-align regions or by strict filtering criteria. The latter would highly reduce the markers length and, consequently, their phylogenetic signal, leading to single locus phylogenies dominated by stochastic error (Jeffroy et al. 2006). In this study, the coalescent-based method ASTRAL III was applied using 664 individual BUSCO gene topologies (Fig. 2b), resulting in relationships that were largely consistent with the concatenated supermatrix approaches (Fig. 2a). Future, coalescent-based inferences in Dothideomycetes would benefit of a more extensive taxon sampling – a condition not met for many of the species represented by genomic data in this study.

Large-scale sequencing projects, such as "One thousand fungal genomes" (http://1000.fungalgenomes.org) and other laboratories which investigate hidden fungal biodiversity, are filling this gap, sequencing fungal genomes from the least known families. This effort, from a phylogenetic

point of view, will make the taxon sampling more comprehensive and, therefore, the phylogenetic inference in Dothideomycetes more accurate.

As we did not find significant topological discrepancies between methods with different sensitiveness to the noise of phylogenetic signal caused by sequence substitution saturation and/or compositional bias, we refrained to test targeted filtering approaches (e.g. the exclusion of variable third codon positions from the alignment) or the use of amino acid alignments instead of nucleotide sequences. The latter would exploit the redundancy of the genetic code to better "preserve" phylogenetic signal (Jeffroy et al. 2006). However, these possible sources of noise should be considered when the most ancient phylogenetic relationships of the tree of life are investigated.

Phylogenies are increasingly inferred from datasets comprising unprecedented numbers of samples and genetic markers. However, the number of samples and genetic loci, which both drive the accuracy of phylogenetic inferences, are always far from being complete. Further, which of the two contributes more than the other in the phylogenetic accuracy remains hotly debated, although recent empirical evidences tend to support the importance of extensive species sampling (Delsuc et al. 2005 and references therein).

As our taxon sampling was determined by the availability of genomes, we focused our attention on how the differences in the amount of information used for phylogenomic reconstructions may affect the topology and nodal support. While the results of the resampling experiment should not be generalized, they provide insight into the robustness of phylogenomic inference. Even if samples with a high amount of missing data (up to 90%) were included, we showed that a subset of the whole supermatrix, corresponding to about 20% of our dataset, provides a phylogenetic accuracy which did not improve significantly further increasing the amount of data (Fig. 3). Moreover, the range of the RF distance of the 20% resampling effort distribution is even smaller than that registered when only the phylogenetic reconstruction method is changed on the complete supermatrix. A dataset without any missing data was also tested. In this case, the phylogenetic inferences were reconstructed only based on 63 markers common to all the samples and when certain samples containing high amount of missing data were excluded (e.g. *Rachicladosporium* due to massive gene duplication). We anticipated that this drastic reduction of genetic markers would likely have a greater effect on the resulting phylogeny than the missing data. However, we recovered largely the same topology with the dataset of 664 concatenated genes. Only minor differences concerning the placement of single samples were noted, but these did not involve the most basal nodes. In accordance with other studies which tested real and simulated data (Driskell et al. 2004; Philippe et al. 2004), phylogenomic dataset assembled here is not negatively affected by missing data, as the incomplete sequences are still represented by enough informative characters.

Comparison to published Dothideomycetes phylogenies and the phylogenetic placement of RIF — Phylogenomic data have contributed to shift in our view of evolution, reshuffling many deep evolutionary relationships along the tree of life (Rokas et al. 2003; Fizpatrick et al. 2006; Wang et al. 2009). In addition, the increasing availability of fungal genomes allows us to investigate evolutionary histories at a finer taxonomic rank. A consistent comparison of tree topologies among previously published phylogenies and the genome-based phylogeny inferred in this study is still not straightforward. This is mostly because many orders reported in other studies are missing in our phylogenomic inference. Nevertheless, it was possible to detect main clades which are present in literature and whose phylogenetic position is confirmed by our inference. Dothideomycetes phylogenies published to date identified well-defined lineages at both order and family levels; however, some relationships have remained unsettled. Genome-based inference, as inferred here, helped to strengthen these relationships but cannot be considered the final step to explain all the evolutionary relationships, as limitations concerning the phylogenetic signal of the data and limits of the reconstruction methods can still affect the results. Moreover, sequences availability is still the most relevant bottleneck in phylogenomics, but the scenario is changing quickly.

Though some deep phylogenetic relationship might be hard to resolve, the phylogenomic approach here applied contributes indeed to confirm and strengthen many order level relationships within Dothideomycetes, whereas few others were reshuffled.

As highlighted in results, the phylogenetic placement of the two focus genera *Lichenothelia* and *Saxomyces* were found to be basal to the whole class, in contrast to the previous results of Muggia et al. (2013, 2015) and Ametrano et al. (in press). In particular, *Saxomyces* is closely related to the lichenized genus *Trypethelium* and the extremophilic RIF genus *Cryomyces*; and together they are the most basal lineages of the subclass Dothideomycetidae, whereas the *Lichenothelia* lineage was recovered as basal to the whole class. This is particularly interesting because it highlights once more the connection between the lichenized and the not-lichenized lifestyles intrinsic of the two genera (Hawksworth 1981; Muggia et al. 2013, 2015; Ametrano et al. 2017). It also further strengthens the argument that the earliest diverging taxa of the subclass Dothideomycetidae were rock inhabitants that might have been able to form a lichen-like association with algae. This is in accordance with previous studies where the rock-inhabiting lifestyle was suggested as ancestral for both Dothideomycetes and Chaetothyriomycetes (Gueidan et al 2007). The rock-inhabiting lifestyle was kept, therefore, by several groups of fungi during their evolution. In the superclass Dothideomyceta, rock inhabitants are known from Capnodiales (Egidi et al. 2014), of which *Rachicladosporium* is a representative in this study, and Lichenostigmatales (Ertz et al. 2014). Future studies investigating character evolution in Dothideomycetes will further elucidate the evolution of distinct lifestyle in this dynamic lineage.

Funding

This work was supported by: Robert A. Pritzker Center for Meteoritics and Polar Studies and the Tawani Foundation; University of Trieste project FRA-2014 (Finanziamenti di Ateneo per progetti di Ricerca scientifica) assigned to LM.

References

Ahmadjian V (1967) The lichen symbiosis. Massachusetts: Blaisdell Publishing Co.

Ametrano C G, Selbmann L & Muggia L (2017) A standardized approach for co-culturing dothidealean rock-inhabiting fungi and lichen photobionts in vitro Symbiosis, 73(1), 35-44

Aragona M, Minio A, Ferrarini A et al. (12 authors) (2014) De novo genome assembly of the soil-borne fungus and tomato pathogen Pyrenochaeta lycopersici. BMC Genomics, 15(1), 313

Bankevich A, Nurk S, Antipov D et al. (16 authors) (2012) SPAdes: a new genome assembly algorithm and its applications to single-cell sequencing. Journal of Computational Biology, 19(5), 455-477

Bihon W, Wingfield M J, Slippers B, Duong T A, & Wingfield B D (2014) MAT gene idiomorphs suggest a heterothallic sexual cycle in a predominantly asexual and important pine pathogen. Fungal Genetics and Biology, 62, 55-61

Blanco-Ulate B, Rolshausen P, & Cantu D (2013) Draft genome sequence of *Neofusicoccum parvum* isolate UCR-NP2, a fungal vascular pathogen associated with grapevine cankers. Genome Announcements, 1(3), e00339-13

Bock C H, Chen C Y F, Stevenson K L, & Wood B W (2016) Draft genome sequence of *Fusicladium effusum*, cause of pecan scab. Standards in Genomic Sciences, 11(1), 36

Bolger A M, Lohse M, & Usadel B (2014) Trimmomatic: a flexible trimmer for Illumina sequence data. Bioinformatics, *30*(15), 2114-2120

Castresana, J (2000) Selection of conserved blocks from multiple alignments for their use in phylogenetic analysis. Molecular Biology and Evolution, *17*(4), 540-552

Chan C L, Yew S M, Na S L et al. (8 authors) (2014) Draft genome sequence of Ochroconis constricta UM 578, isolated from human skin scraping. Genome Announcements, 2(2), e00074-14

Chan C X, & Ragan M A (2013) Next-generation phylogenomics. Biology Direct, 8(1), 3

Chan G F, Bamadhaj H M, Gan H M, & Rashid N A A (2012) Genome sequence of *Aureobasidium pullulans* AY4, an emerging opportunistic fungal pathogen with diverse biotechnological potential. Eukaryotic Cell, 11(11), 1419-1420

Chang T C, Salvucci A, Crous P W, & Stergiopoulos I (2016) Comparative genomics of the Sigatoka disease complex on banana suggests a link between parallel evolutionary changes in *Pseudocercospora fijiensis* and *Pseudocercospora eumusae* and increased virulence on the banana host. PLoS Genetics, 12(8), e1005904

Coleine C, Masonjones S, Selbmann L, Zucconi L, Onofri S, Pacelli C, & Stajich J E (2017) Draft genome sequences of the Antarctic endolithic fungi *Rachicladosporium antarcticum* CCFEE 5527 and *Rachicladosporium* sp. CCFEE 5018. Genome Announcements, 5(27), e00397-17

Condon B J, Leng Y, Wu D et al. (30 authors) (2013) Comparative genome structure, secondary metabolite, and effector coding capacity across Cochliobolus pathogens. PLoS Genetics, 9(1), e1003233

Cooke I R, Jones D, Bowen J K et al. (11 authors) (2014) Proteogenomic analysis of the *Venturia pirina* (Pear Scab Fungus) secretome reveals potential effectors. Journal of Proteome Research, 13(8), 3635-3644

Cruz F, Julca I, Gómez-Garrido J et al. (17 authors) (2016) Genome sequence of the olive tree, *Olea europaea*, Gigascience, 5(1), 29

Delsuc F, Brinkmann H, & Philippe H (2005) Phylogenomics and the reconstruction of the tree of life. Nature Reviews Genetics, 6(5), 361

Desjardins C A, Champion M D, Holder J W et al. (42 authors) (2011) Comparative genomic analysis of human fungal pathogens causing paracoccidioidomycosis PLoS Genetics, 7(10), e1002345

Driskell A C, Ané C, Burleigh J G, McMahon M M, O'Meara B C, & Sanderson M J (2004) Prospects for building the tree of life from large sequence databases. Science, 306(5699), 1172-1174

Egidi E, De Hoog G S, Isola D et al. (10 authors) (2014) Phylogeny and taxonomy of meristematic rock-inhabiting black fungi in the Dothideomycetes based on multi-locus phylogenies. Fungal Diversity, 65(1), 127-165

Ellwood S R, Liu Z, Syme R A et al. (9 authors) (2010) A first genome assembly of the barley fungal pathogen *Pyrenophora teres f teres*. Genome Biology, 11(11), R109

Ertz D, Lawrey J D, Common R S, & Diederich P (2014) Molecular data resolve a new order of Arthoniomycetes sister to the primarily lichenized Arthoniales and composed of black yeasts, lichenicolous and rock-inhabiting species. Fungal Diversity, 66(1), 113-137

Fedorova N D, Khaldi N, Joardar V S et al. (39 authors) (2008) Genomic islands in the pathogenic filamentous fungus *Aspergillus fumigatus* PLoS Genetics, 4(4), e1000046

Fitzpatrick D A, Logue M E, Stajich J E, & Butler G (2006) A fungal phylogeny based on 42 complete genomes derived from supertree and combined gene analysis. BMC Evolutionary Biology, 6(1), 99

Franco M E, López S, Medina R, Saparrat M C, & Balatti P (2015) Draft genome sequence and gene annotation of Stemphylium lycopersici strain CIDEFI-216. Genome announcements, 3(5), e01069-15

Galagan, J E, Calvo, S E, Cuomo, C et al. (50 authors) (2005) Sequencing of Aspergillus nidulans and comparative analysis with *A. fumigatus* and *A. oryzae*. Nature, 438(7071), 1105

Gao S, Li, Y, Gao J, Suo Y, Fu K, Li Y, & Chen J (2014) Genome sequence and virulence variation-related transcriptome profiles of *Curvularia lunata*, an important maize pathogenic fungus. BMC Genomics, 15(1), 627

Goodwin S B, M'barek S B, Dhillon B et al. (58 authors) (2011) Finished genome of the fungal wheat pathogen *Mycosphaerella graminicola* reveals dispensome structure, chromosome plasticity, and stealth pathogenesis. PLoS Genetics, 7(6), e1002070

Gostinčar C, Lenassi M, Gunde-Cimerman N, & Plemenitaš A (2011) Fungal adaptation to extremely high salt concentrations. Advances in Applied Microbiology (Vol 77, pp 71-96) Academic Press

Gostinčar C, Muggia L, & Grube M (2012) Polyextremotolerant black fungi: oligotrophism, adaptive potential, and a link to lichen symbioses. Frontiers in Microbiology, 3, 390

Gostinčar C, Ohm R A, Kogej T et al. (17 authors) (2014) Genome sequencing of four *Aureobasidium pullulans* varieties: biotechnological potential, stress tolerance, and description of new species. BMC Genomics, 15(1), 549

Grandaubert J, Bhattacharyya A, & Stukenbrock E H (2015) RNA-seq based gene annotation and comparative genomics of four fungal grass pathogens in the genus *Zymoseptoria* identify novel orphan genes and species-specific invasions of transposable elements. G3: Genes, Genomes, Genetics, g3-115

Gueidan C, Roux C, & Lutzoni F (2007) Using a multigene phylogenetic analysis to assess generic delineation and character evolution in Verrucariaceae (Verrucariales, Ascomycota). Mycological research, 111(10), 1145-1168

Gurevich A, Saveliev V, Vyahhi N, & Tesler G (2013) QUAST: quality assessment tool for genome assemblies. Bioinformatics, *29*(8), 1072-1075

Han W B, Lu Y H, Zhang A H et al. (11 authors) (2014) Curvulamine, a new antibacterial alkaloid incorporating two undescribed units from a *Curvularia* species. Organic Letters, 16(20), 5366-5369

Hane J K, Lowe R G, Solomon P S et al. (2007) Dothideomycete–plant interactions illuminated by genome sequencing and EST analysis of the wheat pathogen *Stagonospora nodorum*. The Plant Cell, 19(11), 3347-3368

Hawksworth D L (1981*) Lichenothelia*, a new genus for the Microthelia aterrima group. The Lichenologist, 13(2), 141-153

Hoang D T, Chernomor O, von Haeseler A, Minh B Q, & Vinh L S (2017) UFBoot2: improving the ultrafast bootstrap approximation. Molecular Biology and Evolution, *35*(2), 518-522

Hu J, Chen C, Peever T, Dang H, Lawrence C, & Mitchell T (2012) Genomic characterization of the conditionally dispensable chromosome in Alternaria arborescens provides evidence for horizontal gene transfer. BMC Genomics, 13(1), 171

Hyde K D, Jones E G, Liu J K et al. (68) (2013) Families of dothideomycetes. Fungal Diversity, *63*(1), 1-313

Islam M S, Haque M S, Islam M M et al. (15 authors) (2012) Tools to kill: genome of one of the most destructive plant pathogenic fungi *Macrophomina phaseolina*. Bmc Genomics, 13(1), 493

Jaklitsch W, Baral H O, Lücking R, Lumbsch H T, & Frey W (2016) Syllabus of plant families-A Engler's. Syllabus der Pflanzenfamilien Part 1/2

Jeffroy O, Brinkmann H, Delsuc F, & Philippe H (2006) Phylogenomics: the beginning of incongruence? TRENDS in Genetics, 22(4), 225-231

Joardar V, Abrams N F, Hostetler J et al. (12 authors) (2012) Sequencing of mitochondrial genomes of nine *Aspergillus* and *Penicillium* species identifies mobile introns and accessory genes as main sources of genome size variability. BMC Genomics, 13(1), 698

Katoh K, & Standley D M (2013) MAFFT multiple sequence alignment software version 7: improvements in performance and usability. Molecular Biology and Evolution, 30(4), 772-780

Knapp D G, Németh J B, Barry K et al. (16 authors) (2018) Comparative genomics provides insights into the lifestyle and reveals functional heterogeneity of dark septate endophytic fungi. Scientific Reports, 8(1), 6321

Kuan C S, Yew S M, Toh Y F et al. (10 authors) (2015) Dissecting the fungal biology of *Bipolaris papendorfii*: from phylogenetic to comparative genomic analysis. DNA Research, 22(3), 219-232

Kubatko L S, & Degnan J H (2007) Inconsistency of phylogenetic estimates from concatenated data under coalescence. Systematic Biology, 56(1), 17-24

Kück P, & Meusemann K (2010) FASconCAT: Convenient handling of data matrices. Molecular Phylogenetics and Evolution, 56(3), 1115-1118

Lenassi M, Gostinčar C, Jackman S et al. (10 authors) (2013) Whole genome duplication and enrichment of metal cation transporters revealed by de novo genome sequencing of extremely halotolerant black yeast Hortaea werneckii. PLoS One, 8(8), e71328

Liu J K, Hyde K D, Jeewon R, et al. (8 authors) (2017) Ranking higher taxa using divergence times: a case study in Dothideomycetes. Fungal Diversity, *84*(1), 75-99

Lopez D, Ribeiro S, Label P et al. (17 authors) (2018) Genome-Wide Analysis of *Corynespora cassiicola* Leaf Fall Disease Putative Effectors. Frontiers in Microbiology, 9, 276

Marsberg A, Kemler M, Jami F et al. (12 authors) (2017) *Botryosphaeria dothidea*: a latent pathogen of global importance to woody plant health. Molecular Plant Pathology, 18(4), 477-488

Mondo S J, Dannebaum R O, Kuo R C et al. (30 authors) (2017) Widespread adenine N6-methylation of active genes in fungi. Nature genetics, 49(6), 964

Morales-Cruz A, Amrine K C, Blanco-Ulate B et al. (8 authors) (2015) Distinctive expansion of gene families associated with plant cell wall degradation, secondary metabolism, and nutrient uptake in the genomes of grapevine trunk pathogens. BMC Genomics, 16(1), 469

Mosier A C, Miller C S, Frischkorn K R et al. (16 authors) (2016) Fungi contribute critical but spatially varying roles in nitrogen and carbon cycling in acid mine drainage. Frontiers in Microbiology, 7, 238

Muggia L, Gueidan C, Knudsen K, Perlmutter G, Grube M (2013) The lichen connections of black fungi. *Mycopathol.* 175: 523–535.

Muggia L, Kocourková J, Knudsen K (2015) Disentangling the complex of *Lichenothelia* species from rock communities in the desert. *Mycologia* 107: 1233–1253.

Nai C, Wong HY, Pannenbecker A, Broughton WJ et al. (8 authors) (2013) Nutritional physiology of a rock-inhabiting, model microcolonial fungus from an ancestral lineage of the Chaetothyriales (Ascomycetes). Fung Gen Biol 56: 54–66

Nelsen M P, Lücking R, Grube M, Mbatchou J S, Muggia L, Plata E R, & Lumbsch H T (2009) Unravelling the phylogenetic relationships of lichenised fungi in Dothideomyceta. Studies in Mycology, 64, 135-144

Ng K P, Yew S M, Chan C L et al. (10 authors) (2012) Sequencing of *Cladosporium sphaerospermum*, a Dematiaceous fungus isolated from blood culture. Eukaryotic Cell, 11(5), 705-706

Nguyen H D, Lewis C T, Lévesque C A, & Gräfenhan T (2016) Draft genome sequence of *Alternaria alternata* ATCC 34957. Genome Announcements, 4(1), e01554-15

Nguyen L T, Schmidt H A, von Haeseler A, & Minh B Q (2014) IQ-TREE: a fast and effective stochastic algorithm for estimating maximum-likelihood phylogenies. Molecular Biology and Evolution, 32(1), 268-274

Ohm R A, Feau N, Henrissat B et al. (28 authors) (2012) Diverse lifestyles and strategies of plant pathogenesis encoded in the genomes of eighteen Dothideomycetes fungi. PLoS Pathogens, 8(12), e1003037

Orner V A, Cantonwine E G, Wang X M et al. (9 authors) (2015) Draft genome sequence of *Cercospora arachidicola*, causal agent of early leaf spot in peanuts. Genome Announcements, 3(6), e01281-15

Penn O, Privman E, Landan G, Graur D and Pupko T (2010) An alignment confidence score capturing robustness to guide-tree uncertainty. Molecular Biology and Evolution, 27(8):1759-67

Peter M, Kohler A, Ohm R A, Kuo A, Krützmann J, Morin E, & Clum A (2016) Ectomycorrhizal ecology is imprinted in the genome of the dominant symbiotic fungus *Cenococcum geophilum*. Nature Communications, 7, 12662

Philippe H, Snell E A, Bapteste E, Lopez P, Holland P W, & Casane D (2004) Phylogenomics of eukaryotes: impact of missing data on large alignments. Molecular Biology and Evolution, 21(9), 1740-1752

Prenafeta-Boldu FX, Summerbell R, de Hoog SG (2006) Fungi growing on aromatic hydrocarbons: biotechnology's unexpected encounter with biohazard? FEMS Microbiol Rev 30: 109–130
Raffaele S, & Kamoun S (2012) Genome evolution in filamentous plant pathogens: why bigger can be better. Nature Reviews Microbiology, 10(6), 417–430
Robinson D F, & Foulds L R (1981) Comparison of phylogenetic trees. Mathematical Biosciences, 53(1-2), 131-147
Rokas A, Williams B L, King N, & Carroll S B (2003) Genome-scale approaches to resolving incongruence in molecular phylogenies. Nature, 425(6960), 798
Rouxel T, Grandaubert J, Hane J K et al. (42 authors) (2011) Effector diversification within compartments of the *Leptosphaeria maculans* genome affected by Repeat-Induced Point mutations. Nature Communications, 2, 202
Ruibal C, Gueidan C, Selbmann L et al. (13 authors) (2009) Phylogeny of rock-inhabiting fungi related to Dothideomycetes. Studies in Mycology, 64, 123-133
Schoch C L, Crous P W, Groenewald J Z et al. (54 authors) (2009) A class-wide phylogenetic assessment of Dothideomycetes. Studies in Mycology, 64, 1-15
Schoch C L, Shoemaker R A, Seifert K A, Hambleton S, Spatafora J W & Crous P W (2006) A multigene phylogeny of the Dothideomycetes using four nuclear loci. Mycologia, 98(6), 1041-1052
Selbmann L, Isola D, Egidi E, Zucconi L, Gueidan C, de Hoog G S, Onofri S (2014) Mountain tips as reservoirs for new rock-fungal entities: *Saxomyces* gen. nov. and four new species from the Alps. Fun Div 65: 167-182
Sharpton T J, Stajich J E, Rounsley S D et al. (24 authors) (2009) Comparative genomic analyses of the human fungal pathogens *Coccidioides* and their relatives. Genome Research
Shaw J J, Spakowicz D J, Dalal R S et al. (9 authors) (2015) Biosynthesis and genomic analysis of medium-chain hydrocarbon production by the endophytic fungal isolate *Nigrograna mackinnonii* E5202H. Applied Microbiology and Biotechnology, 99(8), 3715-3728
Shiller J, Van de Wouw A P, Taranto A P et al. (8 authors) (2015) A large family of AvrLm6-like genes in the apple and pear scab pathogens, *Venturia inaequalis* and *Venturia pirina*. Frontiers in Plant Science, 6, 980
Shrestha S K, Cochran A, Mengistu A, Lamour K, Castro-Rocha A, & Young-Kelly H (2017) Genetic diversity, QoI fungicide resistance, and mating type distribution of *Cercospora sojina*—Implications for the disease dynamics of frogeye leaf spot on soybean. PLoS One, 12(5), e0177220
Soliai M M, Meyer S E, Udall J A, et al. (8 authors) (2014) De novo genome assembly of the fungal plant pathogen *Pyrenophora semeniperda*. PLoS One, 9(1), e87045
Spatafora J W, Owensby C A, Douhan G W, Boehm E W, & Schoch C L (2012) Phylogenetic placement of the ectomycorrhizal genus *Cenococcum* in Gloniaceae (Dothideomycetes). Mycologia, 104(3), 758-765
Stamatakis, A (2014) RAxML version 8: a tool for phylogenetic analysis and post-analysis of large phylogenies. Bioinformatics, 30(9), 1312-1313
Sterflinger K (2006) Black yeasts and meristematic fungi: ecology, diversity and identification. In Rosa CA, Peter G (eds) Biodiversity and ecophysiology of yeasts. Springer Berlin Heidelberg, pp 501–514
Sterflinger K, Lopandic K, Pandey R V, Blasi B, & Kriegner A (2014) Nothing special in the specialist? Draft genome sequence of *Cryomyces antarcticus*, the most extremophilic fungus from Antarctica. PLoS One, 9(10), e109908
Stukenbrock E H, Bataillon T, Dutheil J Y et al. (9 authors) (2011) The making of a new pathogen: insights from comparative population genomics of the domesticated wheat pathogen *Mycosphaerella graminicola* and its wild sister species. Genome research
Tan G, Muffato M, Ledergerber C, Herrero J, Goldman N, Gil M, & Dessimoz C (2015) Current methods for automated filtering of multiple sequence alignments frequently worsen single-gene phylogenetic inference. Systematic Biology, *64*(5), 778-791
Teixeira M D M, Moreno L F, Stielow B J et al. (28 authors) (2017) Exploring the genomic diversity of black yeasts and relatives (Chaetothyriales, Ascomycota). Studies in Mycology, 86, 1-28
Thompson WR, (1935) On the criterion for the rejection of observations and the distribution of the ratio of deviation to sample standard deviation. Annals of Mathematical Statistics, Vol 6, No 4, pp 214-219
Vaghefi N, Ades P K, Hay F S, Pethybridge S J, Ford R, & Taylor P W (2015) Identification of the MAT1 locus in *Stagonosporopsis tanaceti* and exploring its potential for sexual reproduction in Australian pyrethrum fields. Fungal biology, 119(5), 408-419
Van der Nest M A, Bihon W, De Vos L et al. (12 authors) (2014) Draft genome sequences of *Diplodia sapinea*, *Ceratocystis manginecans*, and *Ceratocystis moniliformis*. IMA Fungus, 5(1), 135-140
Verma S, Gazara R K, Nizam S, Parween S, Chattopadhyay D, & Verma P K (2016) Draft genome sequencing and secretome analysis of fungal phytopathogen *Ascochyta rabiei* provides insight into the necrotrophic effector repertoire. Scientific Reports, 6, 24638
Wang H, Xu Z, Gao L, & Hao B (2009) A fungal phylogeny based on 82 complete genomes using the composition vector method. BMC Evolutionary Biology, 9(1), 195
Wang M, Sun X, Yu D, Xu J, Chung K, & Li H (2016) Genomic and transcriptomic analyses of the tangerine pathotype of *Alternaria alternata* in response to oxidative stress. Scientific Reports, 6, 32437
Waterhouse R M, Seppey M, Simão F A, Manni M, Ioannidis P, Klioutchnikov G, & Zdobnov E M (2017) BUSCO applications from quality assessments to gene prediction and phylogenomics. Molecular Biology and Evolution

Wingfield B D, Ades P K, Al-Naemi F A et al. (24 authors) (2015) IMA Genome-F 4: Draft genome sequences of *Chrysoporthe austroafricana*, *Diplodia scrobiculata*, *Fusarium nygamai*, *Leptographium lundbergii*, *Limonomyces culmigenus*, *Stagonosporopsis tanaceti*, and *Thielaviopsis punctulate*. IMA Fungus, 6(1), 233-248

Xu C, Chen H, Gleason M L, Xu J R, Liu H, Zhang R, & Sun G (2016) *Peltaster fructicola* genome reveals evolution from an invasive phytopathogen to an ectophytic parasite. Scientific Reports, 6, 22926

Yang H, Wang Y, Zhang Z, Yan R, & Zhu D (2014) Whole-genome shotgun assembly and analysis of the genome of *Shiraia* sp. strain Slf14, a novel endophytic fungus producing huperzine A and hypocrellin A. Genome Announcements, 2(1), e00011-14

Yew S M, Chan C L, Soo-Hoo T S et al. (11 authors) (2013) Draft genome sequence of dematiaceous coelomycete *Pyrenochaeta* sp. strain UM 256, isolated from skin scraping. Genome Announcements, 1(3), e00158-13

Zdobnov E M, Tegenfeldt F, Kuznetsov D et al. (9authors) (2016) OrthoDB v9 1: cataloging evolutionary and functional annotations for animal, fungal, plant, archaeal, bacterial and viral orthologs. Nucleic Acids Research, 45(D1), D744-D749

Zeiner C A, Purvine S O, Zink E M et al. (12 authors) (2016) Comparative analysis of secretome profiles of manganese (II)-oxidizing Ascomycete fungi. PLoS One, 11(7), e0157844

Zeng F, Wang C, Zhang G, Wei J, Bradley C A, & Ming R (2017) Draft genome sequence of *Cercospora sojina* isolate S9, a fungus causing frogeye leaf spot (FLS) disease of soybean. Genomics Data, 12, 79-80

Zhang C, Sayyari E, & Mirarab S (2017, October) ASTRAL-III: increased scalability and impacts of contracting low support branches In RECOMB International Workshop on Comparative Genomics (pp 53-75) Springer, Cham

Appendix

DNA metabarcoding uncovers fungal diversity of mixed airborne samples in Italy; *PLoS One*, *13*(3), e0194489.

Elisa Banchi[1], Claudio Gennaro Ametrano[1], David Stanković[1,2], Pierluigi Verardo[3], Olga Moretti[4], Francesca Gabrielli[5], Stefania Lazzarin[6], Maria Francesca Borney[7], Francesca Tassan[8], Mauro Tretiach[1], Alberto Pallavicini[1], Lucia Muggia[1]

[1] Department of Life Sciences, University of Trieste, Trieste, Italy; [2] Marine Biology Station, National Institute of Biology, Piran, Slovenia; [3] Regional Agency for Environmental Protection Friuli Venezia Giulia, Department of Pordenone, Pordenone, Italy; [4] Regional Agency for Environmental Protection Umbria, Terni, Italy; [5] Regional Agency for Environmental Protection Marche, Ascoli Piceno, Italy; [6] Regional Agency for Environmental Protection Veneto, Vicenza, Italy; [7] Regional Agency for Environmental Protection Valle d'Aosta, Saint-Christophe, Italy; [8] Regional Agency for Environmental Protection Friuli Venezia Giulia, Department of Trieste, Trieste, Italy.

Abstract

Fungal spores and mycelium fragments are particles which become and remain airborne and have been subjects of aerobiological studies. The presence and the abundance of taxa in aerobiological samples can be very variable and impaired by changeable climatic conditions. Because many fungi produce mycotoxins and both their mycelium fragments and spores are potential allergens, monitoring the presence of these taxa is of key importance. So far data on exposure and sensitization to fungal allergens are mainly based on the assessment of few, easily identifiable taxa and focused only on certain environments. The microscopic method used to analyze aerobiological samples and the inconspicuous fungal characters do not allow a in depth taxonomical identification. Here, we present a first assessment of fungal diversity from airborne samples using a DNA metabarcoding analysis. The nuclear ITS2 region was selected as barcode to catch fungal diversity in mixed airborne samples gathered during two weeks in four sites of North-Eastern and Central Italy. We assessed the taxonomic composition and diversity within and among the sampled sites and compared the molecular data with those obtained by traditional microscopy. The molecular analyses provide a tenfold more comprehensive determination of the taxa than the traditional morphological inspections. Our results prove that the metabarcoding analysis is a promising approach to increases quality and sensitivity of the aerobiological monitoring. The laboratory and bioinformatic workflow implemented here is now suitable for routine, highthroughput, regional analyses of airborne fungi.

Ongoing project - preliminary title: "Trends in diversity and dispersal of airborne spores and pollens are highlighted by one-year survey and DNA metabarcoding"

Diversity of airborne particles (e.g. fungal spores, pollens, mycelium fragments, subaerial algae) was assessed in uncountable studies in the past years, but only few still implemented DNA metabarcoding. Alternatively, DNA metabarcoding has now become the standard technique to investigate whole community divesity in a wide range of environment and on matrices and it proved to be indeed a solid approach to increase sensitivity in environmental monitoring. "Air" samples are no exception and can be sampled both in outdoor and indoor environments with various research aims. Here we set up a comprehensive study to assess both fungi and plant

diversity in airborne sample during one year in five localities in Italy. Our aim is to 1) compare the diversity estimated by microscopy and molecular data, 2) identify major trends in pollen and spore dispersion and 3) relate them to environmental parameter (e.g. average wind speed, rainfall, humidity) and land use. The internal transcribed spacer 2 (ITS2) was confirmed to be a suitable barcode for its sensitivity in the identification of fungi and plants; it also has a fragment length compatibile with the sequencing platform. The sampling was carried out from March to November 2017 (nine months) every second week. A total of 540 DNA extractions (six days/week) were performed and the DNA extractions of the same week were pooled into one single sample. DNA library preparation consisted in applying barcodes, cleaning, quantifying and pooling the PCR products. Libraries composed by 58 multiplexed samples were sequenced on two 316 chips on an Ion Torrent PGM platform (hosted in house). Bioinformatic analyses are now in progress and follow these main steps: demultiplexing, quality filtering of raw sequences and ITS2 extraction with ITSx. This latter step is performed to delete primers and irrelevant regions both on samples and reference databases built from sequences retrieved from NCBI. QIIME2 environment will be used for sequences clustering, taxonomic assignment and calculation of α and β diversity indexes, while multivariate analyses testing both environmental parameters and land use (Corine land cover) correlation to diversity measures will be performed in R.

General conclusions and future perspectives

The ability of rock inhabiting black fungi to cope with many kinds of stressful abiotic conditions has been tested during last years using multiple experimental settings and has suggested these organisms to serve as suitable models or references for more detailed physiological and molecular investigations. The results of the experiments conducted so far highlighted more their poikilohydric traits than their ability to grow under condition which would be lethal for other microorganisms. However, these organisms indubitably share adaptations which make them either extremotolerants or extremophiles. Although extremophyly seems to be always ready as these fungi only live in environment with fairly invariable, extreme conditions, this is not necessarily true for the extremotolerant black fungi, which experience both harsh and mild abiotic conditions. Within this frame, the genera *Lichenothelia* and *Saxomyces* are good example which better define their extremotolerace rather than extremophyly. Furthermore, *Lichenothelia* presents phenotypic and life style plasticity which make it worthy to be investigated in future experiments.

In this study I have investigated rock-inhabiting black fungi mainly from a phylogenetic point of view, which serves as a necessary premise both to understand their cryptic diversity and to frame these morphologically inconspicuous fungi in an evolutionary perspective.

The comparison between the multi-locus and the genome-based inferences, though biased by the largely different taxon sampling, highlighted many similarities but also relevant topological differences, especially for the taxa of interest. The genome-based inference, indeed, showed the early event which characterized the speciation of *Lichenothelia* genus providing a further reason of interest towards this group of fungi and their lifestyle. The results I obtained, in the phylogenomic analysis pave the way for a more targeted comparative genomic effort which could reveal peculiar traits related to the latent capacity of establishing symbiotic interaction or to the extremophily of this group of fungi. *Lichenothelia*, indeed, and secondly *Saxomyces*, early diverged from the rest of Dothideomycetes together with other taxa which are either extremophilic, such as the black fungus *Cryomyces*, or lichenized, such as *Trypethelium*. Thought, recent analyses of genomes of some black fungi did not highlight new peculiar traits related to extremophily. In the same way, the establishment of fungal-algal interactions would be probably difficult to investigate using genomic data only, whereas a transcriptomic approach could be more effective. Also, it might be speculated that any genomic prints of the capacity of black fungi to interact and establish lichen-like symbioses with algae might be found only in those lineages closer related to lichenized lineages in Dothideomycetes.

The co-culture experiment that I set using *Lichenothelia* did not show fungal-algal interaction. Future experiments, aiming at understanding the potential of rock inhabiting fungi of establishing symbiotic structure or demonstrating metabolite exchange between the partners, could be set up using different fungi and algae combinations, as well as different growth media, culture conditions and a combination of both. Lichen mycobiont phylogenetically related to *Lichenothelia* and their algal partner could be considered in future experiments of lichen resynthesis to investigate which are the molecular bases of symbiosis within Dothideomycetes. As genomic approach could hardly address this research question by itself, further *in vitro* co-culture experiments could be effectively coupled with transcriptomics, and possibly metabolomics analyses, aiming at comparing the responses of lichenized and not lichenized fungi. In this context it would be worthy to compare the behaviour of these fungi when they grow alone and when they are co-cultured with algal and cyanobacterial photobiont as well as with other subaerial, not-lichenized algae and may establish various degrees of interaction. A successful experimentation would be useful (i) to identify which conditions can trigger the establishment of a primitive or more complex structural and/or trophic interaction and (ii) to obtain a kind of "positive control" for possible up/downregulated genes related to the establishment of symbiosis and its regulation. *In vitro* culture experiments, coupled with -omic techniques would also be useful to understand if specific mechanisms are present in the response of *Lichenothelia* and *Saxomyces* to the most common abiotic stresses they are used to withstand, in the same way it has been performed, for instance, with *Knufia* and *Cryomyces*.

As the final goal of these research developments would be a better understanding of fungal-algal interaction also in fungi which usually do not exhibit a symbiotic lifestyle, the assessment of nutrient exchange would be another key point. Co-culture experiments could also be set up using culture media provided with isotopically labelled inorganic nutrients in order to assess the presence of nutrient exchange between algae and fungi in the absence of any other source of, for instance, C, N and P.

The extreme oligotrophy and the high stress resistance make the research on these fungi an important field in a perspective of global changes driven by climate change. Global changes will both put at risk the biodiversity in extreme environments, including the obligate extremophile fungi, and will increase the need to understanding the molecular bases of oligotrophy and extremotolerance for potential biotechnological application and exploitation.

Supplementary materials of the manuscript

Phylogenetic relationships of rock-inhabiting black fungi belonging to the widespread genera *Lichenothelia* and *Saxomyces*

Claudio G. AMETRANO, Kerry KNUDSEN, Jana KOCOURKOVÁ, Martin GRUBE, Laura SELBMANN, Lucia MUGGIA

Table S1. Sequences retrieved from NCBI database and used in the Dothideomycetes phylogeny of Fig. 1; "*" highlights the taxa used as outgroup.

DOTHIDEOMYCETES

Taxon	**Sample ID**	**nucLSU**	**nucSSU**	**mtSSU**
Abrothallus acetabuli	SPO308	KF816232	KF816215	KF816205
Abrothallus parmeliarum	AB57	KF816227	KF816221	-
Abrothallus parmotrematis	AB1	KF816231	KF816225	-
Abrothallus secedens	SPO305	KF816236	KF816216	KF816206
Abrothallus sp.	SP-2014	KF816230	KF816224	KF816213
Acrospermium adeanum	M133	EU940104	EU940031	EU940256
Acrospermium compressum	M151	EU940084	EU940012	EU940237
Acrospermium gramineum	M152	EU940085	EU940013	EU940238
Anisomeridium phaeospermum	MPN539	JN887394	JN887374	-
Anisomeridium polypori	AFTOL 101	-	DQ782877	-
Anisomeridium sp.	MPN534	JN887396	JN887376	JN887408
Anisomeridium sp.	MPN542	JN887398	JN887378	JN887410
Anisomeridium ubianum	-	GU327709	JN887379	GU327682
*Arthonia caesia**	AFTOL 775	FJ469668	-	FJ469671
Arthopyrenia salicis	CBS 368.94	AY538339	AY538333	AY779288
Asterina fuchsiae	TH590	GU586216	GU586210	-
Asterina phenacis	TH589	GU586217	GU586211	-
Bimuria novae-zelandae	CBS 107.79/ AFTOL 931	AY016356	AY016338	FJ190605
Botryosphaeria dothidea	CBS 115.476/ AFTOL 946	DQ678051	DQ677998	FJ190612
Botryosphaeria ribis	AFTOL-ID 1232	DQ678053	DQ678000	-
Capnobotryella renispora	CBS 214.90	EU019248	Y18698	-
Capnodium coffeae	CBS 147.52/ AFTOL 939	DQ247808	DQ247801	FJ190609
Capnodiales sp.	A557	KT263447	KT263481	KT263516
Capnodiales sp.	A863	KT263451	KT263485	KT263520
Capnodiales sp.	A886	KT263453	KT263488	KT263523
Capnodiales sp.	A923	KT263456	KT263491	KT263526
Capnodiales sp.	A997	KT263449	KT263483	KT263518
Capnodiales sp.	L1704	-	KR045787	KR045760
Capnodiales sp.	L1285	-	KC015090	KR045763
Capnodiales sp.	L1286	-	KC015091	KR045764
Capnodiales sp.	L1287	-	KC015092	KR045765
Capnodiales sp.	L1288	-	KC015093	KR045766

Capnodiales sp.	L2186	KR045756	KR045789	KR045761
Catenulostoma abietis	CBS 459.93/ AFTOL 2210	DQ678092	DQ678040	-
Cladosporium allicinum	CBS 115683	GU214408	AY251096	-
Cladosporium cladosporioides	CBS 170.54/ AFTOL 1289	DQ678057	DQ678004	FJ190628
Coniosporium apollinis	CBS 352.97	GU250895	GU250916	GU250906
Coniosporium apollinis	CBS 100.213	GU250896	GU250917	GU250907
Coniosporium apollinis	CBS 100.214	GU250897	GU250918	GU250908
Coniosporium apollinis	CBS 100.218	GU250898	GU250919	GU250909
Coniosporium apollinis	CBS 109.860	GU250899	GU250920	GU250910
Coniosporium apollinis	CBS 109.867	GU250901	-	GU250912
Cryomyces antarcticus	CCFEE 536	GU250365	GU250321	GU250411
Cryomyces antarcticus	CCFEE 456	-	GU250316	GU250405
Cryomyces minteri	CBS 116302/ CCFEE 5187	GU250369	DQ066714	GU250417
Cryomyces sp. '*montanus*'	CCFEE 5476	GU250394	GU250352	GU250434
Cystocoleus ebeneus	L348 (GZU, Hafellner 41566)	EU048580	EU048573	-
Davidiella tassiana	CBS 399.80/AFTOL 1591 (CPC11600 for mtSSU)	DQ678074	DQ678022	EU514455
Delphiniella strobiligena	CBS 735.71/ AFTOL 1257	DQ470977	DQ471029	-
Dendrographa leucophaea f. *minor**	AFTOL 355	AF279382	AF279381	GU561843
*Dendrographa leucophaea**	AFTOL 308	AY548810	AY548803	AY571385
Dendryphiella arenaria	CBS 181.58/ AFTOL 995	DQ470971	DQ471022	FJ190617
Devriesia streliziae	CBS 122379	GU296146	GU301810	GU561845
Didymocyrtis consimilis	CBS 129.338	JQ238643	-	JQ238642
Didymocyrtis consimilis	CBS 129.140	JQ238637	-	JQ238636
Didymocyrtis cladoniicola	CBS 128.027	JQ238631	-	JQ238630
Didymocyrtis cladoniicola	CBS 128.026	JQ238628	-	JQ238627
Didymocyrtis cladoniicola	CBS 128.025	JQ238625	-	JQ238624
Didymocyrtis cladoniicola	CBS 128.023	JQ238622	-	JQ238621
Didymocyrtis cladoniicola	FL14	JQ318028	-	JQ318027
Didymocyrtis cladoniicola	FL11	JQ318022	-	JQ318021
Discosphaerina fagi	CBS 171.93	AY016359	-	AY016342
Dothidea insculpta	CBS 189.58/ AFTOL 921	DQ247802	DQ247810	FJ190602
Dothideomycetes sp.	A583	KT263438	KT263472	KT263508
Dothideomycetes sp.	A931	KT263435	KT263449	KT263505
Dothideomycetes sp.	L1854	KR04575	KR045791	KR045767
Dothideomycetes sp.	L1855	KR045758	KR045792	KR045768
Dothiora cannabinae	CBS 737.71/ AFTOL 1359	DQ470984	DQ479933	FJ190636
Elasticomyces elasticus	CCFEE 5319	GU250375	GU250332	-
Elasticomyces elasticus	CBS 122540/ CCFEE 5320	GU250376	GU250333	GU250420
Elsinoe centrolobi	CBS 222.50/ AFTOL 1854	DQ678094	DQ678041	FJ190651
Elsinoe phaseoli	CBS 165.31/ AFTOL 1855	DQ678095	DQ678042	-

Elsinoe veneta	AFTOL1360	DQ678060	DQ678007	-
Elsinoe veneta	AFTOL1853	DQ767658	DQ767651	FJ190650
Etayoa trypethelii	Common 9200G	KF176940	-	KF176967
Etayoa trypethelii	Common 9215P	KF176941	-	KF176968
Etayoa trypethelii	Mukherjee	KF176943	-	KF176970
Flavobathelium epiphyllum	-	GU327717	JN887382	-
Friedmanniomyces endolithicus	CCFEE 522	-	DQ066715	-
Friedmanniomyces endolithicus	CCFEE 524	GU250364	DQ066715	GU250409
Friedmanniomyces endolithicus	CCFEE670	GU250366	GU250322	GU250412
Friedmanniomyces endolithicus	CCFEE5283	KF310006	-	-
Friedmanniomyces endolithicus	CCFEE5199	KF310007	-	-
Friedmanniomyces endolithicus	CCFEE5180	GU250367	-	-
Gibbera conferta	CBS 191.53	GU301814	GU296150	-
Gloniopsis praelonga	CBS 112.415	FJ161173	FJ161134	-
Guignardia bidwellii	CBS 237.48/ AFTOL 1618	DQ678085	DQ678034	AF271135
Helicomyces roseus	CBS 283.51/ AFTOL 1613	DQ678083	DQ678032	-
Hysteropatella clavispora	CBS 247.34/ AFTOL 1305	AY541493	DQ678006	AY571388
Hysteropatella elliptica	CBS 935.97/ AFTOL 1790	DQ767657	EF495114	FJ190649
Karschia cezanneii	Ertz 19186 (BR)	KP456154	-	KP456180.1
Kirschsteiniothelia aethiops	CBS 109.53/ AFTOL 925	AY016361	AY016344	FJ190604
Labrocarpon canariense	Ertz 16907 (BR)	KP456158	-	KP456184
Laurera megasperma	AFTOL 2094	FJ267702	GU561841	GU561847
*Lecanactis abietina**	AFTOL 305	AY548812	AY548805	AY548813
Leptosphaeria maculans	DAOM 229267/ AFTOL 277	DQ4709646	DQ470993	-
Lichenoconium aeruginosum	JL359-09	HQ174269	-	HQ174268
Lichenoconium erodens	JL363-09	HQ174267	-	HQ174266
Lichenoconium lecanorae	JL382-10	HQ174263	-	HQ174262
Lichenoconium usneae	JL352-09	HQ174265	-	HQ174264
Lichenoconiales sp.	L2023	KR045759	-	-
Lichenostigma alpinum	Ertz 17522	KF176945	-	KF176972
Lichenostigma alpinum	Ertz 17519	KF176946	-	KF176973
Lichenostigma chlaroterae	Diederich 17329	KF176947	-	KF176974
Lichenostigma chlaroterae	Neuberg	KF176948	-	KF176975
Lichenostigma maureri	Diederich 17306	KF176951	-	KF176978
Lichenostigma maureri	Diederich 17337	KF176952	-	KF176980
Lichenostigma sp.	Diederich 17240	KF176955	-	KF176981
Lichenostigmatales sp.	A930	KT263424	KT263461	KT263495
Lophium mytilinum	CBS 269.34/ AFTOL 1609	DQ678081	DQ678030	-
Macrophomina phaseolina	CBS 227.33/ AFTOL 1783	DQ678088	DQ678037	-
Megalotremis verrucosa	Lucking 26316 (F)	GU327718	JN887383	-
Melaspileopsis diplasiospora	Ertz 16247 (BR)	KP456164	-	KP456189

Microxyphium citri	CBS 451.66	GU301848	GU296177	AF346421
Mycosphaerella euripotami	JK 5586J	GU301852	GZ479761	GU566746
Mycosphaerella fijiensis	OSC 100622/ AFTOL 2021	DQ678098	DQ767652	FJ190656
Myriangium duriaei	CBS 260.36/ AFTOL 1304	DQ678059	AY016347	AY350575
Myriangiales sp.	A554	KT263442	KT263475	KT263511
Myriangiales sp.	A578	KT263443	KT263476	KT263513
Mytilinidion resinicola	CBS 304.34	FJ161185	FJ161145	-
Patellaria atrata	CBS 958.97	GU301855	GU296181	-
Petrophila incerta (ex TRN138)	CBS 118.301	GU323974	GU324003	GU324035
Petrophila incerta (ex TRN62)	CBS 118.305	GU323961	GU323991	GU324022
Petrophila incerta (ex TRN77)	CBS 118.287	GU323963	GU323993	GU324024
Phaeosclera dematioides	CBS 157.81	GU301858	GU296184	-
Phaeotrichum benjaminii	CBS 541.72/ AFTOL 1184	AY004340	AY016348	AY538349
Phyllobathelium anomalum	-	GU327722	JN887386	GU327698
Phyllobathelium firmum	MPN 545	JN887401	JN887387	JN887413
Pleospora herbarum	CBS 541.72/ AFTOL 940	DQ247804	DQ247812	FJ190610
Pleosporales sp.	A537	KT263430	KT263465	KT263499
Pleosporales sp.	A542	KT263432	KT263467	KT263501
Pleosporales sp.	A1028	KT263427	KT263463	KT263498
Pleosporales sp.	A1039	KT263425	KT263462	KT263496
Preussia terricola	DAOM 230091/ AFTOL 282	AY544686	AY544726	AY544754
Rachicladosporium alpinum	CCFEE 5395	KF310035	-	-
Rachicladosporium antarcticum	CCFEE 5527	KF309990	-	-
Rachicladosporium eucalypti	CBS 138900	KP004476	-	-
Rachicladosporium mcmurdoii	CCFEE 5211	GU250371	-	GU250419
Rachicladosporium monteroseus	CCFEE 5458	KF309988	-	-
Racodium rupestre	L424 (TSB 37932)	EU048582	EU048577	EU048589
Ramularia graminicola	CBS 292.38/ AFTOL 1615	DQ678084	DQ678033	-
Ramularia punctiformis	CBS 113265/ AFTOL 942	DQ470968	DQ471017	FJ190611
Recurvomyces mirabilis	CCFEE 5475	KC315876	KC315865	KC315887
Recurvomyces mirabilis	CCFEE 5264	GU250372	GU250329	-
Rhytidhysteron rufulum	CBS 306.38	FJ469672	AF164375	-
*Roccella fuciformis**	AFTOL 126 (Diederich 15572 for mtSSU)	AY584654	AY584678	EU704082
rock isolate TRN11 (Dothideomycetes sp.)	CBS 118.281	GU323957	-	GU324018
rock isolate TRN123 (Dothideomycetes sp.)	CBS 117.932	GU323970	GU323999	GU324031
rock isolate TRN137 (Dothideomycetes sp.)	CBS 118.300	GU323973	GU324002	GU324034
rock isolate TRN142 (Dothideomycetes sp.)	CBS 118.302	GU323975	GU324004	GU324036
rock isolate TRN153 (Dothideomycetes sp.)	CBS 118.330	GU323977	GU324006	GU324038

rock isolate TRN235 (Dothideomycetes sp.)	CBS 118.605	GU323979	-	GU324041
rock isolate TRN267 (Dothideomycetes sp.)	CBS 118.769	-	GU324043	GU324043
rock isolate TRN268 (Dothideomycetes sp.)	CBS 119.305	GU323981	-	GU324044
rock isolate TRN42 (Dothideomycetes sp.)	CBS 117958	GU323958	-	GU324019
rock isolate TRN456 (Dothideomycetes sp.)	-	GU323986	GU324015	GU324049
rock isolate TRN5 (Dothideomycetes sp.)	CBS 118.762	GU323956	GU323988	GU324017
rock isolate TRN529 (Dothideomycetes sp.)	-	GU323987	GU324016	GU32405
rock isolate TRN66 (Dothideomycetes sp.)	CBS 118.306	GU323962	GU323992	GU324023
rock isolate TRN87 (Dothideomycetes sp.)	CBS 118.290	GU323966	GU323996	GU324027
*Schismatomma decolorans**	AFTOL 307	AY548815	AY548809	AY548816
Scorias spongiosa	CBS 325.33/ AFTOL 1594	DQ678075	DQ678024	FJ190643
Sirodesmium olivaceum	CBS 395.59	GU250915	GU250904	GU250904
Stictographa lentiginosa	Ertz 17447 (BR)	KP456169	-	KP456195
Strigula jamesii	MPN548	JN887404	JN887388	JN887416
Strigula nemathora	MPN72	JN887405	JN887389	GU327701
Stylodothis puccinioides	CBS 193.58	AY004342	AY016353	AF346428
Sydowia polyspora	CBS 116.29/ AFTOL 1300	DQ678058	DQ678005	FJ190631
Teratosphaeria jonkershoekensis	CBS 112224	GU301874.1	GU296200.1	-
Tripospermum myrti	CBS 437.68	GU323216	-	-
Trypethelium nitidiusculum	AFTOL 2099	FJ267701	GU561842	GU561848
Trypethelium sp.	AFTOL 110	AY584652	AY584676	AY584632
Tubeufia cerea	CBS 254.75/ AFTOL 1316	DQ470982	DQ471034	FJ190634
Tubeufia paludosa	CBS 245.49/ AFTOL 1589	DQ767654	DQ767649	GU566745
Tyrannosorus pinicola	CBS 124.88/ AFTOL 1235	DQ470974	DQ471025	FJ190620
Venturia inaequalis	CBS 594-70	GU301879	NG016539	-
Venturia inaequalis	ATCC60070	EF114712	EF114737	-
Vermiconia flagrans (ex TRN124)	CBS 118.283	GU323971	GU324000	GU324032
Westerdykella cylindrica	CBS 454.72/ AFTOL 1037	AY004343	AY016355	AF346430
-	-	-	-	-

Table S2. Number of delimited ESUs for the clade Lichenotheliales (Fig. 2). Mean and SD values of all the analyses which were carried out on this clade and below just considering one phylogenetic hypothesis at a time (MrBayes, MrBayes choronos smoothed and BEAST, respectively). Far and near outgroup (OG), refers to the two different tested outgroups. Far: Arthoniomycetes, Near: *Cryomyces* and Myrinagiales for Lichenotheliales and *Saxomyces*, respectively.

Lichenotheliales	No. of ESUs				
Input data	ABGD	sPTP	mPTP	sGMYC	mGMYC
3genes_Distance_matrix_farOG	-	-	-	-	-
3genes_Distance_matrix_nearOG	-	-	-	-	-
3genes_MrBayes_farOG	-	-	-	-	-
3genes_MrBayes_nearOG	-	-	-	-	-
3genes_MrBayes_chronos_farOG	-	-	-	-	-
3genes_MrBayes_chronos_nearOG	-	-	-	-	-
3genes_BEAST_farOG	-	-	-	-	-
3genes_BEAST_nearOG	-	-	-	-	-
mtSSU_Distance_matrix_farOG	1	-	-	-	-
mtSSU_Distance_matrix_nearOG	1	-	-	-	-
mtSSU_MrBayes_farOG	-	5	2	-	-
mtSSU_MrBayes_nearOG	-	32	1	-	-
mtSSU_MrBayes_chronos_farOG	-	11	1	18	19
mtSSU_MrBayes_chronos_nearOG	-	19	8	1	19
mtSSU_BEAST_farOG	-	34	1	2	10
mtSSU_BEAST_nearOG	-	26	1	4	3
nucLSU_Distance_matrix_farOG	1	-	-	-	-
nucLSU_Distance_matrix_nearOG	1	-	-	-	-
nucLSU_MrBayes_farOG	-	20	1	-	-
nucLSU_MrBayes_nearOG	-	28	1	-	-
nucLSU_MrBayes_chronos_farOG	-	6	5	15	17
nucLSU_MrBayes_chronos_nearOG	-	15	10	1	20
nucLSU_BEAST_farOG	-	23	2	2	12
nucLSU_BEAST_nearOG	-	24	1	1	14
nucSSU_Distance_matrix_farOG	1	-	-	-	-
nucSSU_Distance_matrix_nearOG	1	-	-	-	-
nucSSU_MrBayes_farOG	-	11	1	-	-
nucSSU_MrBayes_nearOG	-	26	1	-	-
nucSSU_MrBayes_chronos_farOG	-	25	3	1	18
nucSSU_MrBayes_chronos_nearOG	-	17	1	1	7
nucSSU_BEAST_farOG	-	14	6	3	12
nucSSU_BEAST_nearOG	-	27	5	7	13
mean	1.0	20.2	2.8	4.7	13.7
SD	0.0	8.3	2.7	5.6	5.0
MrBayes					
mean	-	20.3	1.2	-	-
SD	-	10.5	0.4	-	-
Mr Bayes (chronos)					
mean	-	15.5	4.7	6.2	16.7

SD	-	6.6	3.7	8.1	4.8
BEAST					
mean	-	24.7	2.7	3.2	10.7
SD	-	6.5	2.3	2.1	4.0
mtSSU					
mean	1.0	21.2	2.3	6.3	12.8
SD	0.0	11.6	2.8	7.9	7.8
nucLSU					
mean	1.0	19.3	3.3	4.8	15.8
SD	0.0	7.8	3.6	6.8	3.5
nucSSU					
mean	1.0	20.0	2.8	3.0	12.5
SD	0.0	6.9	2.2	2.8	4.5

Table S3. Number of delimited ESUs for the clade *Saxomyces*-group (Fig. 2). Mean and SD values of all the analyses which were carried out on this clade and below just considering one phylogenetic hypothesis at a time (MrBayes, MrBayes *choronos* smoothed and BEAST, respectively). Far and near outgroup (OG), refers to the two different tested outgroups. Far: Arthoniomycetes, Near: *Cryomyces* and Myrinagiales for Lichenotheliales and *Saxomyces*, respectively.

Saxomyces	No. of ESUs				
Input data	ABGD	sPTP	mPTP	sGMYC	mGMYC
3genes_Distance_matrix_farOG	-	-	-	-	-
3genes_Distance_matrix_nearOG	-	-	-	-	-
3genes_MrBayes_farOG	-	-	-	-	-
3genes_MrBayes_nearOG	-	-	-	-	-
3genes_MrBayes_chronos_farOG	-	-	-	-	-
3genes_MrBayes_chronos_nearOG	-	-	-	-	-
3genes_BEAST_farOG	-	-	-	-	-
3genes_BEAST_nearOG	-	-	-	-	-
mtSSU_Distance_matrix_farOG	4	-	-	-	-
mtSSU_Distance_matrix_nearOG	4	-	-	-	-
mtSSU_MrBayes_farOG	-	9	5	-	-
mtSSU_MrBayes_nearOG	-	6	4	-	-
mtSSU_MrBayes_chronos_farOG	-	28	1	1	8
mtSSU_MrBayes_chronos_nearOG	-	13	1	4	8
mtSSU_BEAST_farOG	-	6	6	9	19
mtSSU_BEAST_nearOG	-	6	6	10	9
nucLSU_Distance_matrix_farOG	1	-	-	-	-
nucLSU_Distance_matrix_nearOG	1	-	-	-	-
nucLSU_MrBayes_farOG	-	12	4	-	-
nucLSU_MrBayes_nearOG	-	24	1	-	-
nucLSU_MrBayes_chronos_farOG	-	9	5	13	15
nucLSU_MrBayes_chronos_nearOG	-	30	1	1	12
nucLSU_BEAST_farOG	-	25	1	2	3
nucLSU_BEAST_nearOG	-	27	1	3	4
nucSSU_Distance_matrix_farOG	1	-	-	-	-
nucSSU_Distance_matrix_nearOG	1	-	-	-	-
nucSSU_MrBayes_farOG	-	4	2	-	-
nucSSU_MrBayes_nearOG	-	8	7	-	-
nucSSU_MrBayes_chronos_farOG	-	38	4	1	12
nucSSU_MrBayes_chronos_nearOG	-	9	5	1	13
nucSSU_BEAST_farOG	-	4	4	7	11
nucSSU_BEAST_nearOG	-	24	2	2	6
mean	2.0	15.7	3.3	4.5	10.0
SD	1.4	10.5	2.0	4.0	4.4
MrBayes					
average	-	10.5	3.8	-	-
SD	-	7.1	2.1	-	-
Mr Bayes (chronos)					
average	-	21.2	2.8	3.5	11.3

SD	-	12.4	2	4.8	2.8
BEAST					
average	-	15.3	3.3	5.5	8.7
SD	-	11.0	2.3	3.6	5.9
mtSSU					
mean	4.0	11.3	3.8	6.0	11.0
SD	0.0	8.6	2.3	4.2	5.4
nucLSU					
mean	1.0	21.2	2.2	4.8	8.5
SD	0.0	8.6	1.8	5.6	5.9
nucSSU					
mean	1.0	14.5	4.0	2.8	10.5
SD	0.0	13.7	1.9	2.9	3.1

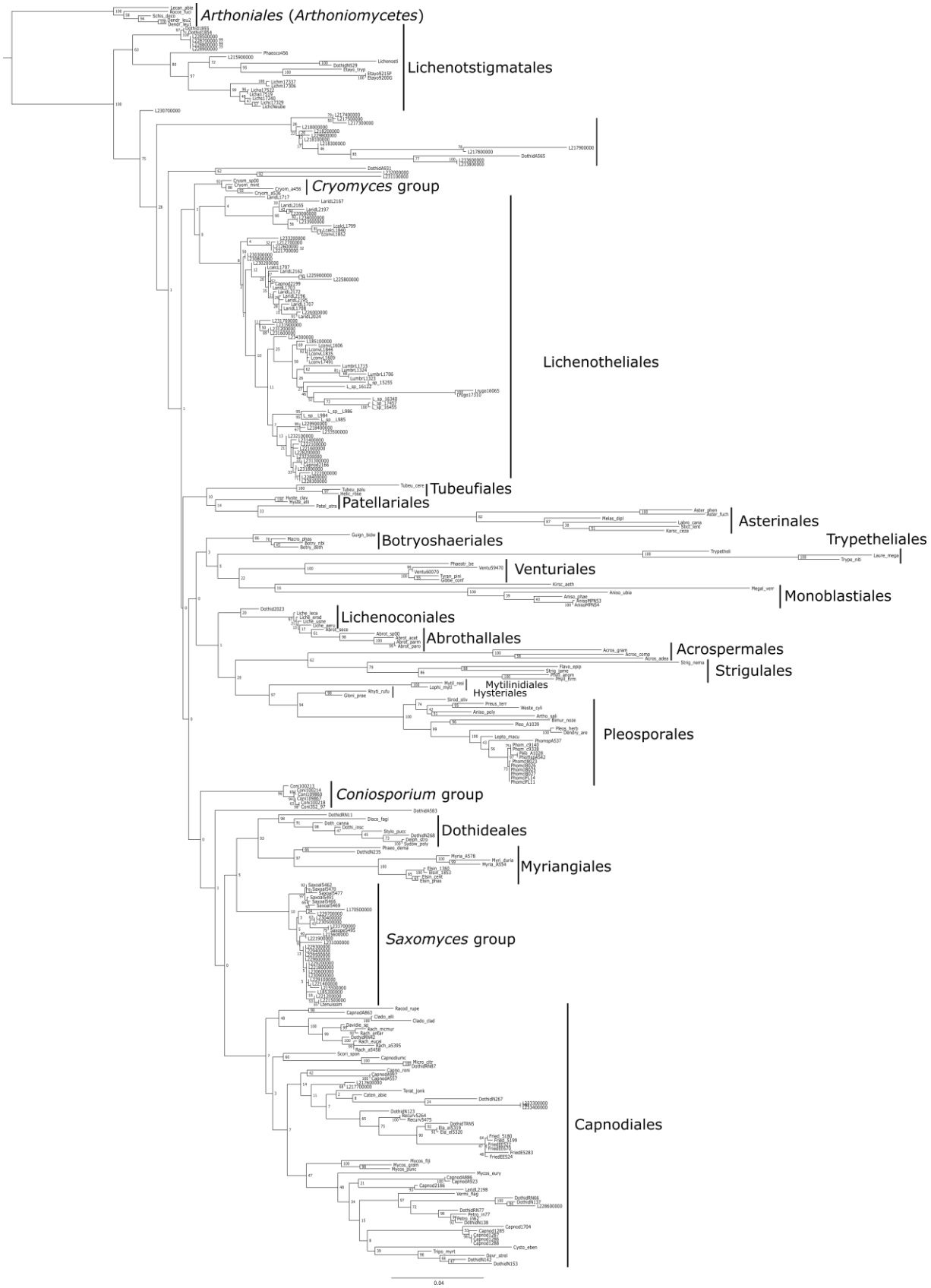

Figure S1. Multilocus ML phylogenetic inference of class Dothideomycetes, starting alignment were the same used for bayesian phylogeny. The phylogenetic hypotheses were inferred from the combined dataset of 28S (nucLSU), 18S (nucSSU) and12S (mtSSU). Bootstrap values were obtained from 1000 bootstrap replicates. Samples names were shortened according to RAxML requirement (ten characters).

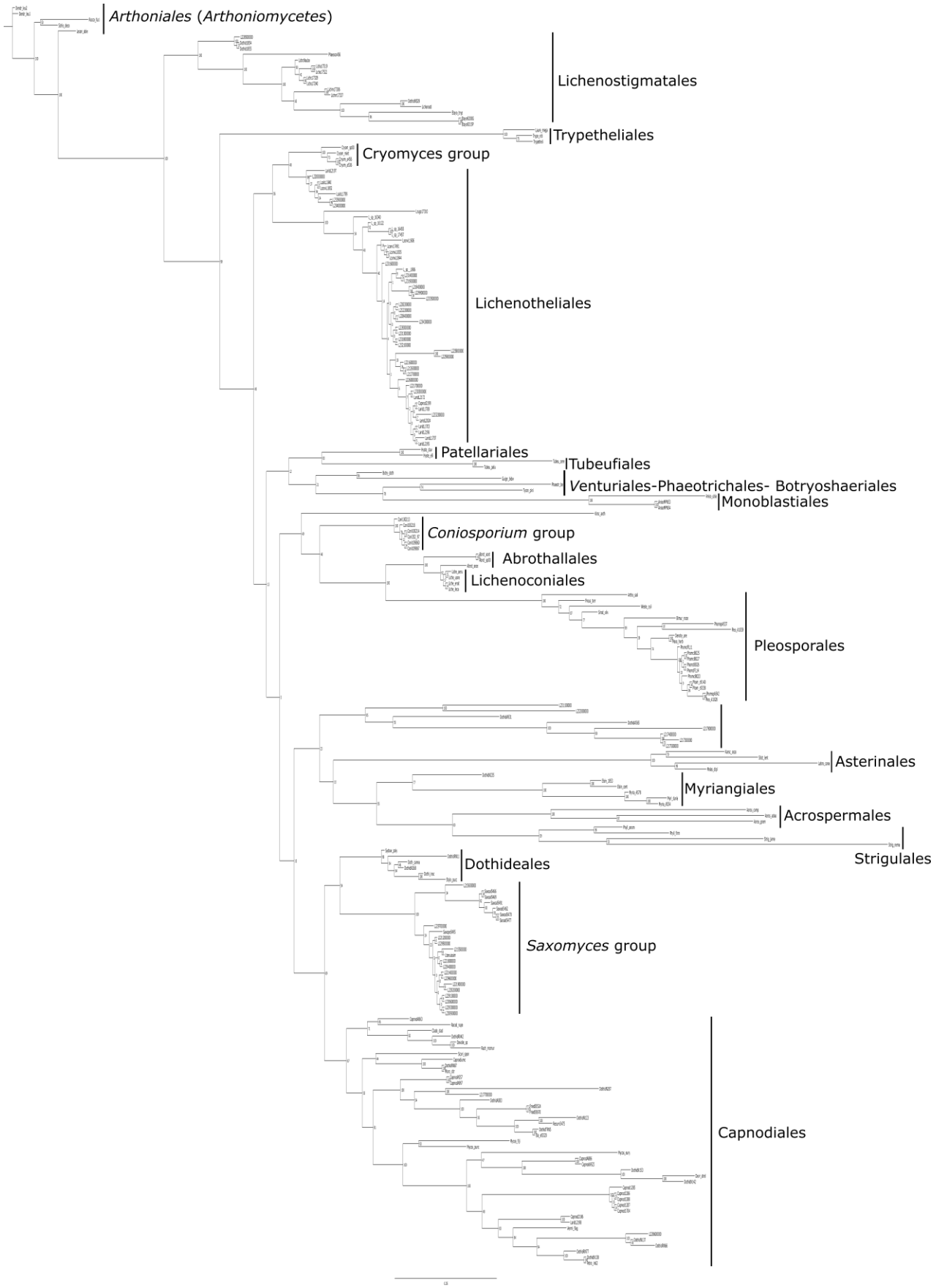

Figure S2a. Bayesian mtSSU single locus phylogenetic inference of the class Dothideomycetes. Bayesian posterior probabilities are shown next to the branches.

Figure S2b. Bayesian nucLSU single locus phylogenetic inference of the class Dothideomycetes. Bayesian posterior probabilities are shown next to the branches.

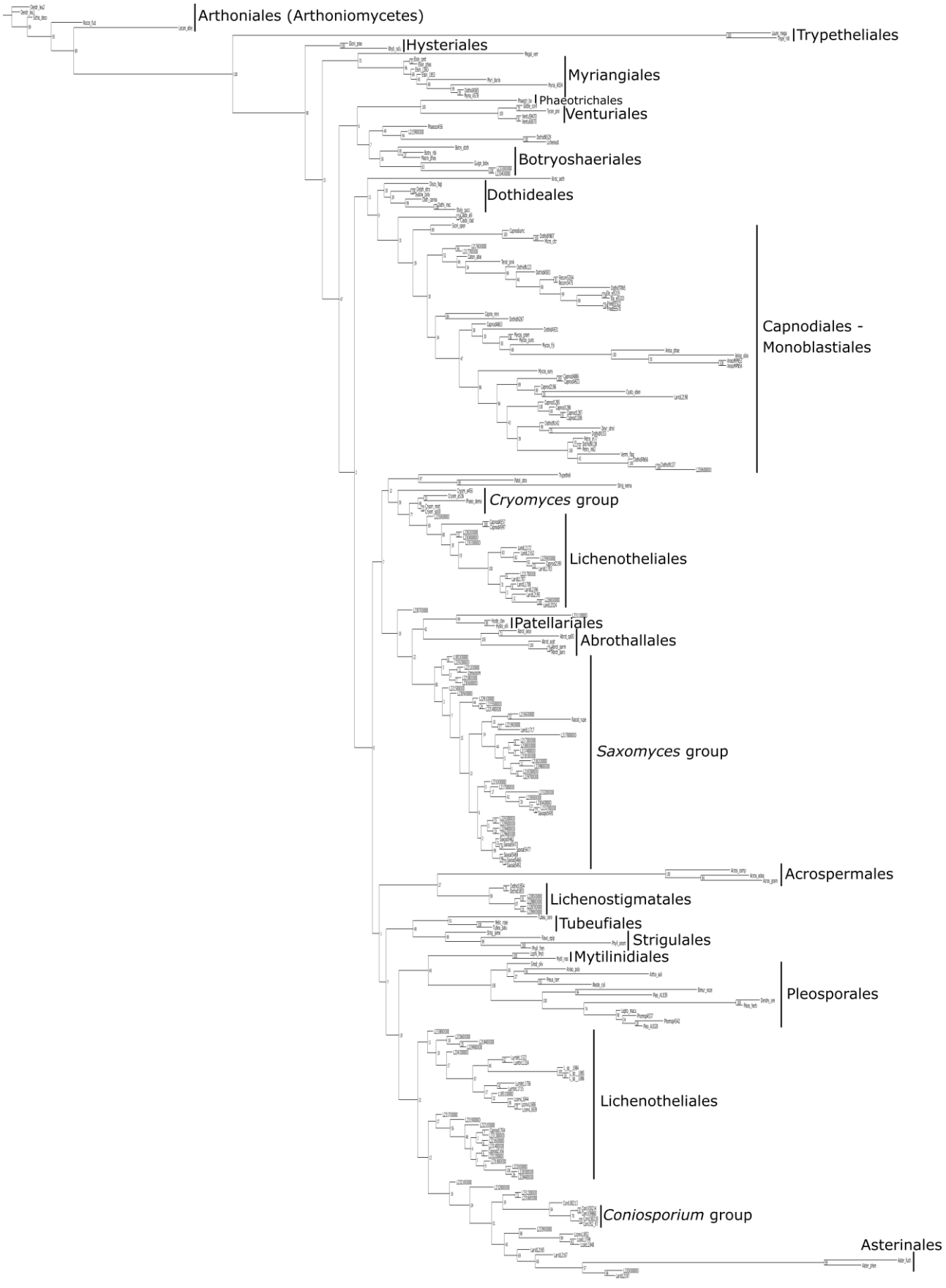

Figure S2c. Bayesian nucSSU single locus phylogenetic inference of the class Dothideomycetes. Bayesian posterior probabilities are shown next to the branches.

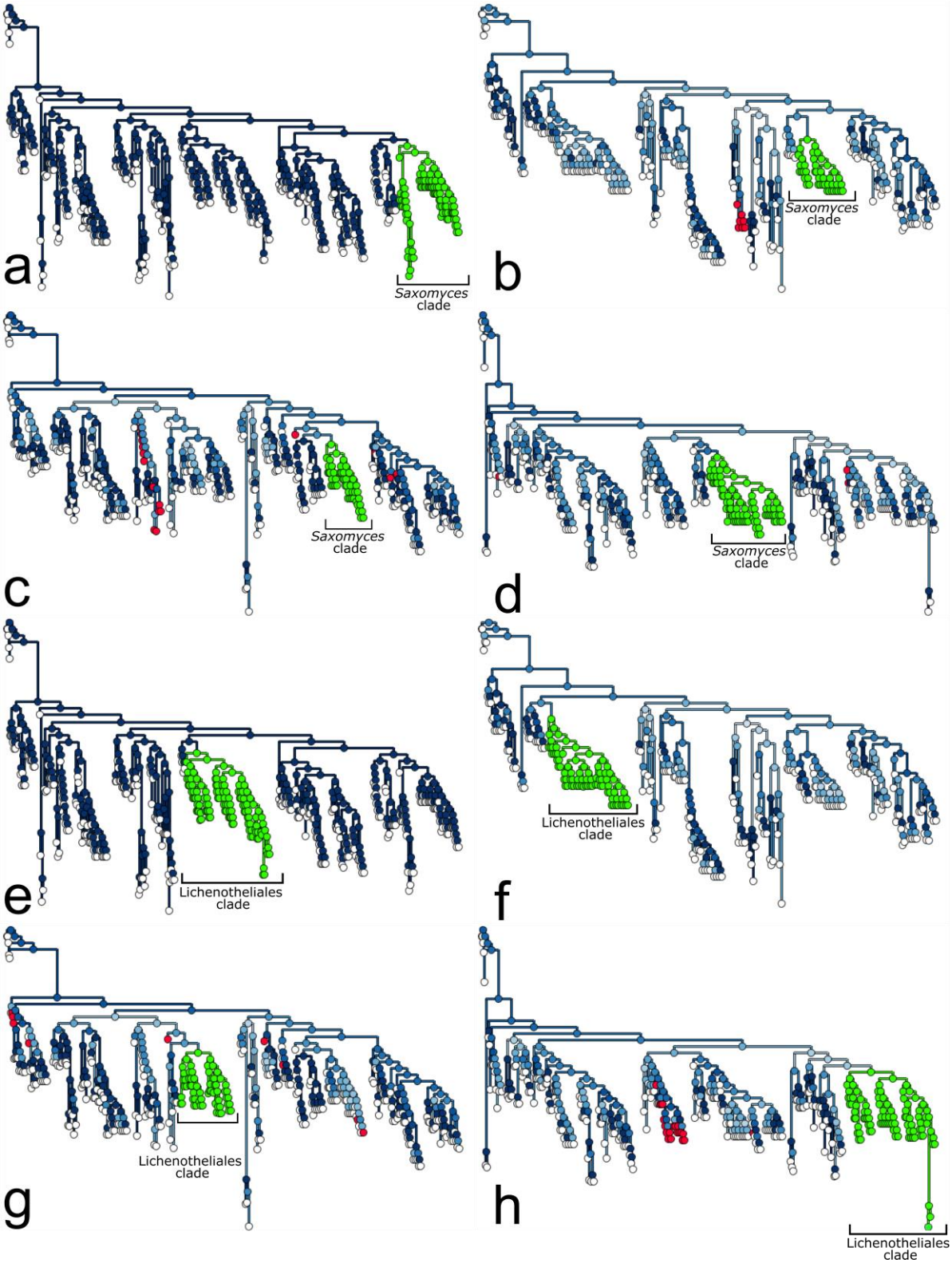

Figure S3. Tree comparison among multi-locus and single locus Bayesian phylogenies. **a, e** multilocus phylogeny highlighting the **a** *Saxomyces* and the **e** Lichenotheliales clade, respectively. **b–d** and **f–h** single locus topologies (b, f mtSSU; c, g nucLSU; d, h nucSSU). Color gradient from dark to light blue refers to leaf–based similarity score calculated by ViPhy. The darker the blue the more consistent are the phylogenetic placements in the single locus topologies (b–d and f–h) with those in the multilocus phylogeny (a and e as in Fig.1) used as reference. *Saxomyces* (a–d) and Lichenotheliales (e–h) lineages are highlighted with the following color code: green, samples which are always present within the same lineage; red, samples with a changeable position in the individual single locus phylogenies.

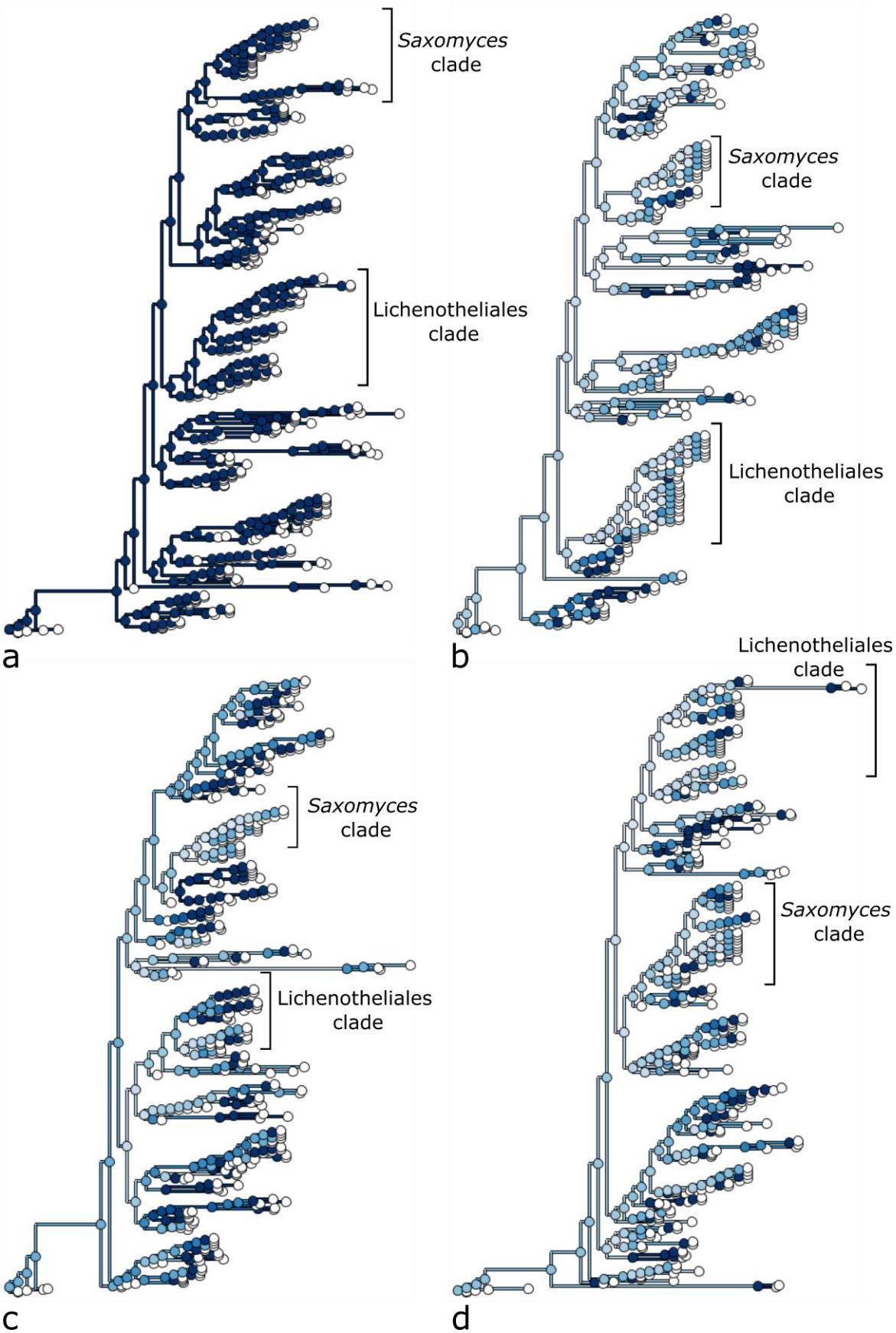

Figure S4. Tree comparison among multi-locus (a as in FIG.1) and single locus Bayesian phylogenies (b mtSSU; c nucLSU; d nucSSU). Color gradient from dark to light blue refers to element–based similarity score calculated by ViPhy. The darker the blue the more consistent are the phylogenetic placements in the single locus topologies with those in the multilocus phylogeny used as reference.

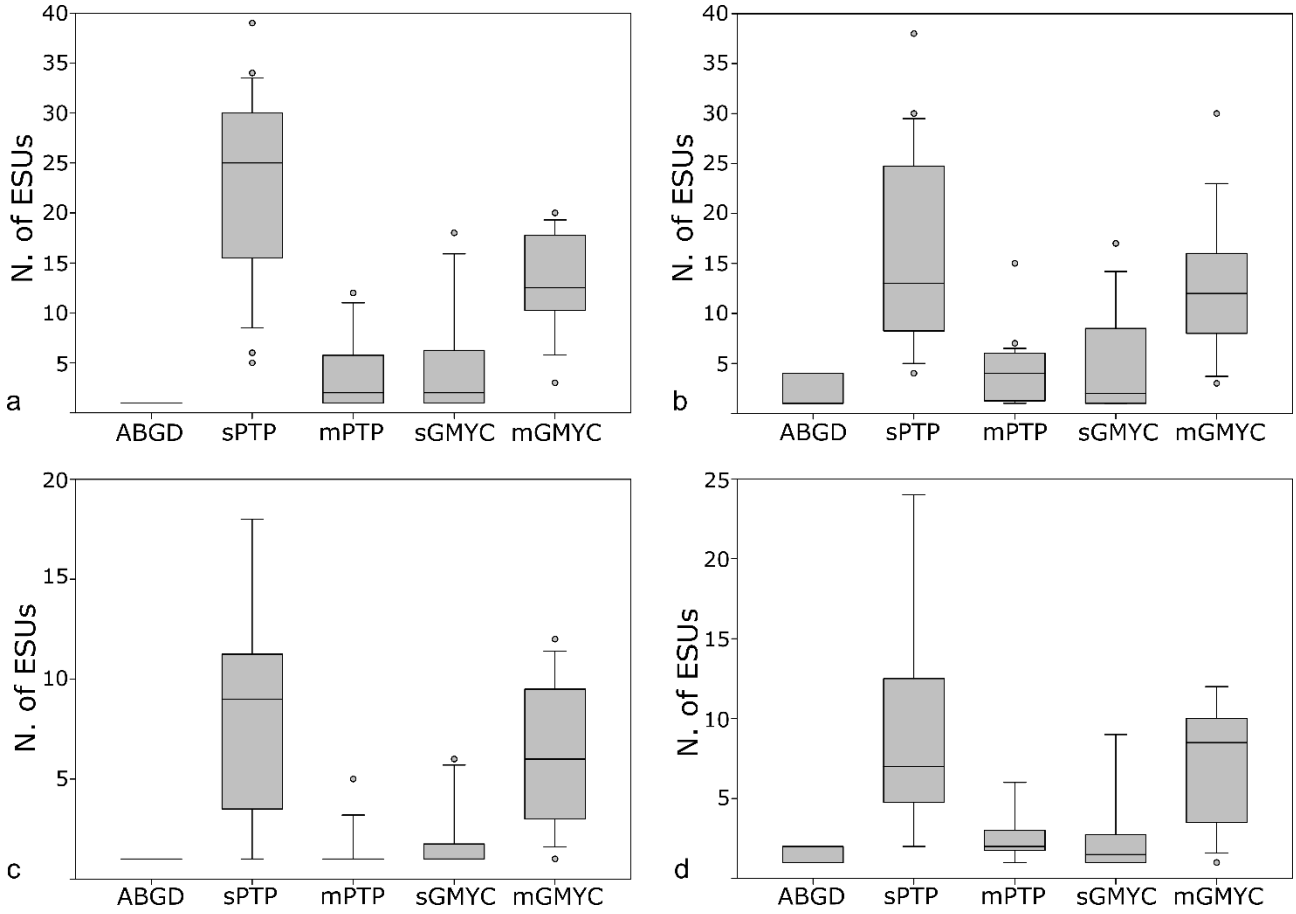

Fig. S5. Distribution of ESU estimates delimited by the methods ABGD, sPTP, mPTP, sGMYC and mGMYC based on all single locus datasets (distance matrix for ABGD, and phylogenetic inferences for PTP and GMYC; original data in Supplementary Material Tables S2 and Table S3). **a, b** Datasets including samples with missing data (for which one or two genes were not sequenced) for **a** Lichenotheliales and **b** *Saxomyces* clades; **c, d** dataset without missing data (including only samples with all three loci sequenced) for **c** Lichenotheliales and **d** *Saxomyces* clades. Boxes are delimited by the distance between 25th and 75th percentile; lines inside the boxes show the median value of the distribution; whiskers refer to 10th and 90th percentiles; outliers are marked with grey dots. Multiple analyses performed with PTP and GMYC are identified as s = single and m = multi.

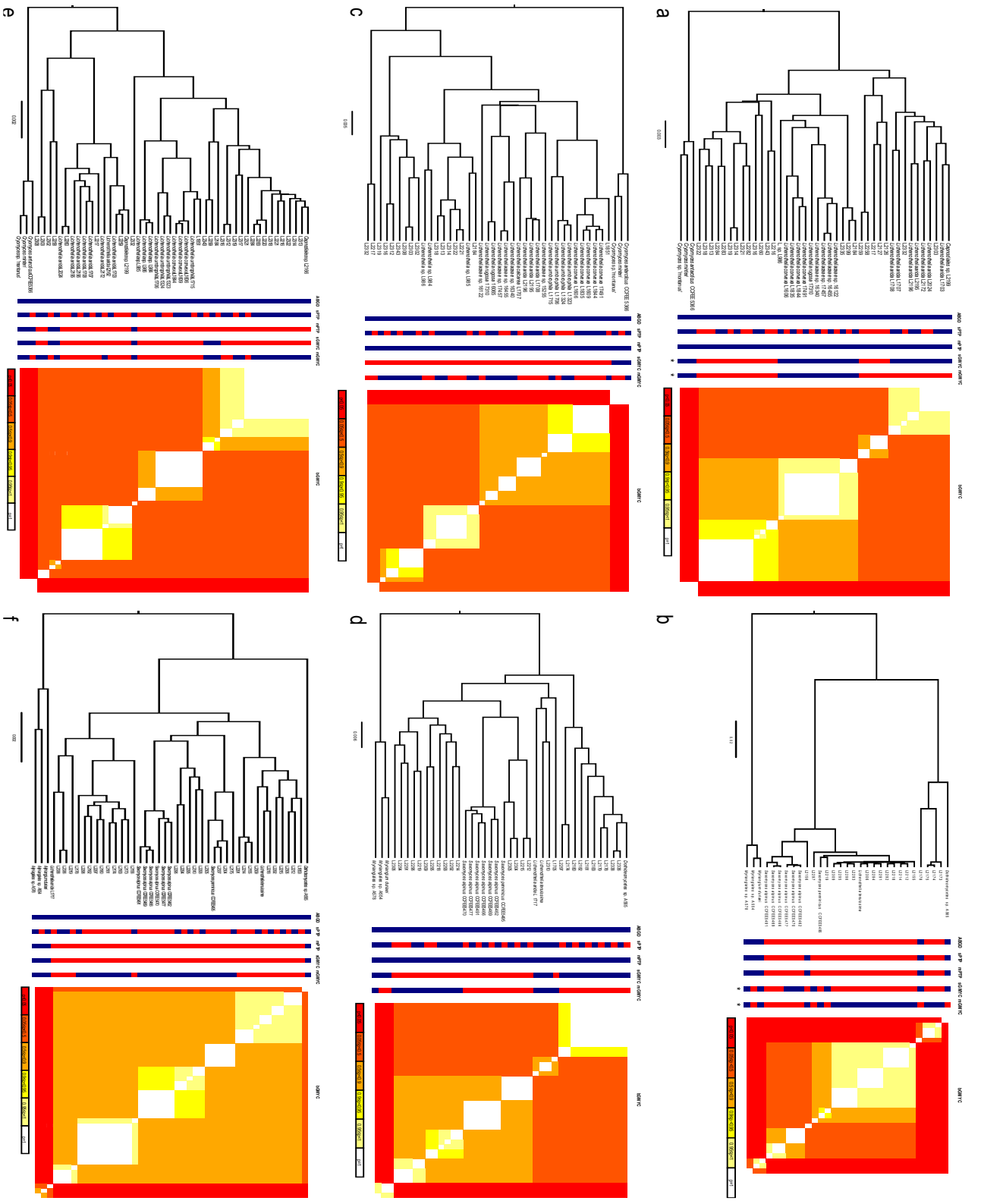

Fig. S6. Species delimitation results are based on BEAST ultrametric trees calculate for **a, b** mtSSU, **c**, **d** nucLSU and **e, f** nucSSU and are reported for the **a**, **c**, **e** Lichenotheliales and **b**, **d**, **f** *Saxomyces* clades. Species delimitation methods are reported above the bar chart. Evolutionarily Significant Units (ESU) are identified by either red or blue segments on the bars. bGMYC results are shown by heat maps which express the posterior probability values (PP values of the square matrix) of samples belonging to the same cluster by color gradient. Multiple analyses performed with PTP and GMYC are identified as s = single, m = multi and b = Bayesian. Asterisks below GMYC bars (a and b) show a significantly higher likelihood of GMYC model compared to the null model (all samples in the same cluster) applying the Likelihood Ratio Test (LRT). No significance tests were applied on ABGD and PTP.

Supplementary materials for the manuscript

Genome-scale data suggest an ancestral rock-inhabiting life-style of Dothideomycetes (Ascomycota)

Claudio G. Ametrano[a*], Felix Grewe[b], H. Thorsten Lumbsch[b], Steven D. Leavitt[c] & Lucia Muggia[a]

Table S1. Assemblies retrieved from NCBI and JGI genome portals and included in the phylogenomic analyses.

Species	Strain	NCBI Accession number, JGI project number	Source	Submitters/Reference
Aspergillus fischeri	NRRL 181	GCA_000149645.2	NCBI	Fedorova et al. 2008
Aspergillus fumigatus	A1163	GCA_000150145.1	NCBI	Joardar et al. 2012
Aspergillus nidulans	FGSC A4	GCA_000149205.2	NCBI	Galagan et al. 2005
Coccidioides immitis	RS	GCA_000149335.2	NCBI	Sharpton et al. 2009
Histoplasma capsulatum	var. capsulatum Tmu	GCA_000313325.1	NCBI	Taipei Medical University, Urology
Paracoccidioides lutzii	Pb01	GCA_000150705.2	NCBI	Desjardins et al. 2011
Aaosphaeria arxii	CBS 175.79	1019657	JGI	Joseph Spatafora, Pedro Crous, Janneke Bloem
Acidomyces richmondensis	BFW	GCA_001592465.1	NCBI	Mosier et al. 2016
Acidomyces richmondensis	meta	GCA_001572075.1	NCBI	Mosier et al. 2016
Aliquandostipite khaoyaiensis	CBS 118232	1019641	JGI	Joseph Spatafora, Jon Karl Magnuson, David E Culley
Alternaria alternata	133aPRJ	1103683	JGI	Francis Michel Martin, Stéphane Hacquard
Alternaria alternata	ATCC 34957	GCA_001443195.1	NCBI	Nguyen et al. 2016
Alternaria alternata	B2a	GCA_001696825.1	NCBI	Wubetu Bihon, Agricultural Research Organization
Alternaria alternata	SRC1lrK2f	GCA_001642055.1, 1029430	NCBI	Zeiner et al. 2016
Alternaria alternata	Z7	GCA_001572055.1	NCBI	Wang et al. 2016
Alternaria arborescens	EGS 39-128	GCA_000256225.1	NCBI	Hu et al. 2012
Alternaria brassicicola	ATCC 96836	GCA_000174375.1	NCBI	Washington University Genome Center (WUGC), Virginia Bioinformatics Institute
Alternaria consortialis	JCM 1940	GCA_001950455.1	NCBI	RIKEN Center for Life Science Technologies, Division of Genomic Technologies
Amniculicola lignicola	CBS 123094	1011329	JGI	Joseph Spatafora, Pedro Crous, Janneke Bloem
Ampelomyces quisqualis	HMLAC05119	1051023	JGI	Joseph Spatafora, Chen Liang
Aplosporella prunicola	CBS 121.167	1006427	JGI	Joseph Spatafora, Pedro Crous, Charles Cannon
Ascochyta rabiei	ArDII	GCA_001630375.1	NCBI	Verma et al. 2016
Aulographum hederae	1006065	1006065	JGI	Joseph Spatafora, Pedro Crous, Lute-Harm Zwiers
Aureobasidium melanogenum	HN6.2	GCA_002156615.1	NCBI	Ocean University of China, Yi Lu
Aureobasidium pullulans	AY4	GCA_000294735.1	NCBI	Chen et al. 2012

Aureobasidium pullulans	IMV 00882	GCA_001931805.1	NCBI	Jet Propulsion Laboratory, California Institute of Technology, Kasthuri Venkateswaran
Aureobasidium pullulans	SAMN04565625	GCA_001678115.1	NCBI	Cruz et al. 2016
Aureobasidium pullulans var. *melanogenum*	CBS 110374	GCA_000721775.1, 403630	JGI	Gosticar et al. 2014
Aureobasidium pullulans var. *namibiae*	CBS 147.97	GCA_000721765.1, 403632	JGI	Gosticar et al. 2014
Aureobasidium pullulans var. *pullulans*	EXF-150	GCA_000721785.1, 403628	JGI	Gosticar et al. 2014
Aureobasidium pullulans var. *subglaciale*	EXF-2481	GCA_000721755.1, 403631	JGI	Gosticar et al. 2014
Aureobasidium sp.	FSWF8-4	GCA_001914275.1	NCBI	Uppsala University, Sarahi Garcia
Baudoinia panamericana	UAMH 10762	GCA_000338955.1	NCBI	Ohm et al. 2012
Beverwykella pulmonaria	JCM 9230	GCA_001599595.1	NCBI	RIKEN Center for Life Science Technologies, Division of Genomic Technologies
Bimuria novae-zelandiae	CBS 107.79	1019717	JGI	Joseph Spatafora, Pedro Crous, Janneke Bloem
Bipolaris maydis	ATCC 48331	GCA_000354255.1	NCBI	Ohm et al. 2012
Bipolaris maydis	C5	GCA_000338975.1	NCBI	Ohm et al. 2012
Bipolaris oryzae	ATCC 44560	GCA_000523455.1	NCBI	Condon et al 2013
Bipolaris oryzae	TG12bL2	GCA_001675385.1	NCBI	University of Minnesota, Juan Gutierrez-Gonzale
Bipolaris sorokiniana	ND90Pr	GCA_000338995.1	NCBI	Ohm et al. 2012
Bipolaris victoriae	FI3	GCA_000527765.1	NCBI	Condon et al 2013
Bipolaris zeicola	26-R-13	GCA_000523435.1	NCBI	Condon et al 2013
Botryosphaeria dothidea Botdo1 1	Botdo1 1	-	JGI	Marsberg et al. 2017
Botryosphaeria dothidea	LW030101	GCA_001717445.1	NCBI	Qingdao Agricultural University, Sen Lian
Byssothecium circinans	CBS 675.92	1019709	JGI	Joseph Spatafora, Pedro Crous, Manfred JK Binder
Cenococcum geophilum	1.58	GCA_001692895.1	NCBI	Peter et al. 2016
Cercospora canescens	BHU	GCA_000347735.1	NCBI	Institute of Agriculture Sciences, Department of Mycology and Plant Pathology
Cercospora cf. *sigesbeckiae*	PP 2012 071	GCA_002217505.1	NCBI	Louisiana State University, Sebastian Albu
Cercospora sojina	FLS21	GCA_002150695.1	NCBI	Shrestha et al. 2017
Cercospora sojina	S9	GCA_002084285.1	NCBI	Zeng et al. 2017
Cercospora zeae-maydis	-	401984	JGI	Stephen B. Goodwin
Cladosporium fulvum	CBS 131901	GCA_000301015.1	NCBI	Ohm et al. 2012

Cladosporium sphaerospermum	IMV 00045	GCA_001931905.2	NCBI	Jet Propulsion Laboratory, California Institute of Technology, Kasthuri Venkateswaran
Cladosporium sphaerospermum	UM 843	GCA_000261425.2	NCBI	Ng et al. 2012
Clathrospora elynae	CBS 161.51	1019661	JGI	Joseph Spatafora, Pedro Crous, Manfred JK Binder
Clohesyomyces aquaticus	CBS 115471	GCA_002105025.1, 1054410	NCBI	Mondo et al. 2017
Cochliobolus heterostrophus	C5 1	52344	JGI	Ohm et al. 2012
Cochliobolus lunatus	m118	403758	JGI	Ohm et al. 2012
Coniosporium apollinis	CBS 100218	GCA_000281105.1	NCBI	Teixeira et al. 2017
Corynespora cassiicola	CCP	1019537	JGI	Lopez et al. 2018
Corynespora cassiicola	SAMEA103891068	GCA_900169545.1	NCBI	University of Bristol
Corynespora cassiicola	UM 591	GCA_000603925.1	NCBI	University of Malaya
Cryomyces antarcticus	CCFEE 534	GCA_000504465.1	NCBI	Sterflinger et al. 2014
Cucurbitaria berberidis	CBS 394.84	1006069	JGI	Joseph Spatafora, Pedro Crous, Janneke Bloem
Curvularia lunata	CX-3	GCA_000743335.1	NCBI	Gao et al. 2014
Curvularia papendorfii	UM 226	GCA_000817285.1	NCBI	Kuan et al. 2015
Curvularia sp.	IFB-Z10	GCA_002161795.1	NCBI	Han et al. 2014
Decorospora gaudefroyi	P77 CBS 332.63	1032355	JGI	Joseph Spatafora, Patrik Inderbitzin
Delitschia confertaspora	ATCC 74209	1020481	JGI	Joseph Spatafora, Gerald Bills
Delphinella strobiligena	CBS 735.71	1019673	JGI	Joseph Spatafora, Jon Karl Magnuson, David E Culley
Didymella exigua	CBS 183.55	407831	JGI	Joseph Spatafora
Didymella zeae-maydis	3018	-	JGI	Gillian Turgeon
Didymocrea sadasivanii	CBS 438.65	1054428	JGI	Joseph Spatafora, Jon Karl Magnuson, David E Culley
Diplodia corticola	CBS 112549	GCA_001883845.1	NCBI	University of Aveiro
Diplodia sapinea	CMW 190	GCA_000671355.1	NCBI	Bihon et al. 2014
Diplodia sapinea	CMW39103	GCA_000729945.1	NCBI	van der Nest et al. 2014
Diplodia scrobiculata	CMW30223	GCA_001455585.1	NCBI	Wingfield et al. 2015
Diplodia seriata	DS831	GCA_001006355.1	NCBI	Morales-Cruz et al. 2015
Diplodia seriata	F98.1	GCA_001975905.1	NCBI	INRA, Guillaume Robert
Dissoconium aciculare	CBS 342.82	1011337	JGI	Joseph Spatafora, Pedro Crous, Manfred JK Binder
Dothidotthia symphoricarpi	CBS 119.687	1011345	JGI	Joseph Spatafora, Pedro Crous, Janneke Bloem
Dothistroma pini	CBS 116.487	GCA_002116355.1	NCBI	Canada's Michael Smith Genome Sciences Centre

Dothistroma septosporum	CMW 10211	GCA_002236575.1	NCBI	Massey University
Dothistroma septosporum	CMW 10798	GCA_002236655.1	NCBI	Massey University
Dothistroma septosporum	CMW 11305	GCA_002236515.1	NCBI	Massey University
Dothistroma septosporum	CMW 13121	GCA_002236675.1	NCBI	Massey University
Dothistroma septosporum	CMW 13123	GCA_002236485.1	NCBI	Massey University
Dothistroma septosporum	CMW 14822	GCA_002236475.1	NCBI	Massey University
Dothistroma septosporum	CMW 14823	GCA_002236775.1	NCBI	Massey University
Dothistroma septosporum	CMW 15843	GCA_002236615.1	NCBI	Massey University
Dothistroma septosporum	CMW 23429	GCA_002236725.1	NCBI	Massey University
Dothistroma septosporum	CMW 37193	GCA_002236645.1	NCBI	Massey University
Dothistroma septosporum	CMW 37194	GCA_002236545.1	NCBI	Massey University
Dothistroma septosporum	CMW 37965	GCA_002236745.1	NCBI	Massey University
Dothistroma septosporum	CMW 38941	GCA_002236925.1	NCBI	Massey University
Dothistroma septosporum	CMW 40004	GCA_002236585.1	NCBI	Massey University
Dothistroma septosporum	CMW 44207	GCA_002236565.1	NCBI	Massey University
Dothistroma septosporum	CMW 44656	GCA_002236685.1	NCBI	Massey University
Dothistroma septosporum	MU NZE8	GCA_002236465.1	NCBI	Massey University
Dothistroma septosporum	NZE10 v1.0	GCA_000340195.1	NCBI	Ohm et al. 2012
Dothistroma septosporum	NZFS4520	GCA_002236755.1	NCBI	Massey University
Elsinoe ampelina CECT 20119	CECT 20119	1064684	JGI	Joseph Spatafora, Manuel Alfaro Sánchez
Epicoccum nigrum	ICMP 19927	GCA_002116315.1	NCBI	The University of Auckland
Epicoccum sorghinum	USPMTOX48	GCA_001879705.1	NCBI	University of Sao Paulo
Eremomyces bilateralis	CBS 781.70	1011349	JGI	Joseph Spatafora, Pedro Crous, Manfred JK Binder
Glonium stellatum	CBS 207.34	GCA_001692915.1	NCBI	Spatafora et al. 2012
Helminthosporium solani	B-AC-16A	GCA_000498615.1	NCBI	University of Wisconsin-Madison
Hortaea acidophila	CBS 113389	1040524	JGI	Joseph Spatafora, Jon Karl Magnuson
Hortaea werneckii	EXF-2000	GCA_002127715.1	NCBI	University of California, Riverside
Hortaea werneckii	EXF-2000M0 scaffolds	GCA_000410955.1	NCBI	Lenassi et al. 2013
Hysterium pulicare	CBS 123377	GCA_000467715.1	NCBI	Ohm et al. 2012
Karstenula rhodostoma	CBS 690.94	1019721	JGI	Joseph Spatafora, Pedro Crous, Janneke Bloem
Lasiodiplodia theobromae	CSS-01s	GCA_002111425.1	NCBI	Beijing Academy of Agriculture and Forestry Sciences

Lecanosticta acicola	CBS 871.95	GCA_000504345.2	NCBI	Canada's Michael Smith Genome Sciences Centre
Lentithecium fluviatile	CBS 122.367	1006093	JGI	Joseph Spatafora, Pedro Crous, Janneke Bloem
Lepidopterella palustris	CBS 459.81	GCA_001692735.1	NCBI	Peter et al.2016
Leptosphaeria maculans	JN3	GCA_000230375.1	NCBI	Rouxel et al. 2011
Leptosphaeria maculans	NZT4	GCA_900465115.1	NCBI	Genomic Standards Consortium
Leptoxyphium fumago	SC3815	GCA_001660795.1	NCBI	International Institute Zittau - TU Dresden, Harald Kellner
Lindgomyces ingoldianus	ATCC 200398	1042879	JGI	Joseph Spatafora, Jon Karl Magnuson, David E Culley
Lineolata rhizophorae	ATCC16933	1051209	JGI	Joseph Spatafora, Jon Karl Magnuson, David E Culley
Lizonia empirigonia	CBS 542.76	1019757	JGI	Joseph Spatafora, Pedro Crous, Manfred JK Binder
Lophiostoma macrostomum	CBS 122.681	1011357	JGI	Joseph Spatafora, Pedro Crous, Manfred JK Binder
Lophiotrema nucula	CBS 627.86	1019701	JGI	Joseph Spatafora, Jon Karl Magnuson, David E Culley
Lophium mytilinum	CBS 269.34	1019725	JGI	Joseph Spatafora, Pedro Crous, Janneke Bloem
Macrophomina phaseolina	MO00014	GCA_001307885.1	NCBI	University of Illinois, Gloria Rendon
Macrophomina phaseolina	MP00003	GCA_001307925.1	NCBI	University of Illinois, Gloria Rendon
Macrophomina phaseolina	MP00065	GCA_001307945.1	NCBI	University of Illinois, Gloria Rendon
Macrophomina phaseolina	MP00325	GCA_001307935.1	NCBI	University of Illinois, Gloria Rendon
Macrophomina phaseolina	MP00327	GCA_001307955.1	NCBI	University of Illinois, Gloria Rendon
Macrophomina phaseolina	MRf1	GCA_001051165.1	NCBI	Junagadh Agricultural University, Manoj Parakhia
Macrophomina phaseolina	MS6	GCA_000302655.1	NCBI	Islam et al. 2012
Macroventuria anomochaeta	CBS 525.71	1019665	JGI	Joseph Spatafora, Pedro Crous, Janneke Bloem
Massarina eburnea	CBS 473.64	1011361	JGI	Joseph Spatafora, Pedro Crous, Manfred JK Binder
Massariosphaeria phaeospora	CBS 611.86	1019705	JGI	Joseph Spatafora, Jon Karl Magnuson, David E Culley
Melanomma pulvis-pyrius	1011365	1011365	JGI	Joseph Spatafora, Pedro Crous, Manfred JK Binder
Microthyrium microscopicum	CBS 115976	1011369	JGI	Joseph Spatafora, Pedro Crous, Manfred JK Binder
Mycosphaerella arachidis	CALF-13A	GCA_001297265.1	NCBI	Orner et al. 2015
Mycosphaerella eumusae	CBS 114824	GCA_001578235.1	NCBI	Chang et al. 2016
Mycosphaerella graminicola	-	16205	JGI	Goodwin et al. 2011
Mycosphaerella laricina	CBS 326.52	GCA_000504385.2	NCBI	Canada's Michael Smith Genome Sciences Centre
Mycosphaerella sp.	PB-2012b Mex 2-1-2	GCA_002116345.1	NCBI	Canada's Michael Smith Genome Sciences Centre
Mycosphaerella sp.	Ston1	GCA_000504405.2	NCBI	Canada's Michael Smith Genome Sciences Centre
Myriangium duriaei	CBS 260.36	1006105	JGI	Joseph Spatafora, Pedro Crous, Janneke Bloem

Mytilinidion resinicola	CBS 304.34	1040537	JGI	Joseph Spatafora, Jon Karl Magnuson, David E Culley
Neofusicoccum parvum	UCRNP2	GCA_000385595.1	NCBI	Blanco-Ulate et al. 2013
Nigrograna mackinnonii	E5202H	GCA_001007845.1	NCBI	Shaw et al. 2015
Ochroconis constricta	UM 578	GCA_000611715.1	NCBI	Chan et al. 2014
Ophiobolus disseminans	CBS 113818	1019733	JGI	Joseph Spatafora, Pedro Crous, Manfred JK Binder
Paraphaeosphaeria sporulosa	AP3s5-JAC2a	1029422	JGI	Zeinier at al. 2016
Paraphoma sp.	B47-9	GCA_001748405.1	NCBI	National Institute for Agro-Environmental Sciences (NIAES)
Parastagonospora nodorum	SN15	GCA_000146915.2	NCBI	National Institute for Agro-Environmental Sciences (NIAES)
Patellaria atrata	CBS 101060	1006113	JGI	Joseph Spatafora, Pedro Crous, Janneke Bloem
Peltaster fructicola	LNHT1506	GCA_001592805.1	NCBI	Xu et al. 2016
Periconia macrospinosa	DSE2036	1025594	JGI	Knapp et al. 2018
Phaeocryptopus gaeumannii	CBS 267.37	GCA_002116385.1	NCBI	Canada's Michael Smith Genome Sciences Centre
Phaeosphaeria nodorum	Sn79 1.0	GCA_002216185.1	NCBI	Canada's Michael Smith Genome Sciences Centre
Phaeosphaeriaceae sp.	PMI 808	1021562	JGI	Joseph Spatafora, Gregory Bonito, Hui-Ling Liao
Phoma herbarum	JCM 15942	GCA_001599375.1	NCBI	RIKEN Center for Life Science Technologies, Division of Genomic Technologies
Phoma tracheiphila	IPT5	1021241	JGI	Joseph Spatafora, David Ezra
Phyllosticta capitalensis	CBS 128.856	1109085	JGI	Francis Michel Martin, Vladimiro Guarnaccia
Phyllosticta capitalensis	Gm33	GCA_001604925.1	NCBI	RIKEN Center for Life Science Technologies, Division of Genomic Technologies
Phyllosticta citriasiana	CBS 120486	1011301	JGI	Joseph Spatafora, Pedro Crous, Manfred JK Binder
Phyllosticta citribraziliensis	CBS 100098	1109089	JGI	Francis Michel Martin, Vladimiro Guarnaccia
Phyllosticta citricarpa	CGMCC3.14348	GCA_000382785.1	NCBI	Zhejiang university
Phyllosticta citricarpa	Gc12	GCA_001604955.1	NCBI	Citrus Research and Education Center, University of Florida
Phyllosticta citrichinaensis	CBS 130529	1109091	JGI	Francis Michel Martin, Vladimiro Guarnaccia
Phyllosticta sp.	CPC 27169	1109095	JGI	Francis Michel Martin, Vladimiro Guarnaccia
Phyllosticta sp.	CPC 27913	1109093	JGI	Francis Michel Martin, Vladimiro Guarnaccia
Piedraia hortae	CBS 480.64	1011305	JGI	Joseph Spatafora, Pedro Crous, Janneke Bloem
Pleomassaria siparia	CBS279.74	1011309	JGI	Joseph Spatafora, Pedro Crous, Manfred JK Binder
Pleosporales sp.	UM 1110	GCA_000263175.2	NCBI	Ng et al. 2012
Polychaeton citri	-	1011313	JGI	Joseph Spatafora, Pedro Crous, Manfred JK Binder
Polyplosphaeria fusca	CBS 125425	1019777	JGI	Joseph Spatafora, Pedro Crous, Manfred JK Binder

Preussia sp.	BSL10	GCA_001553865.1	NCBI	University of Nizwa, Abdul Khan
Pseudocercospora fijiensis	CIRAD86	GCA_000340215.1	NCBI	Ohm et al. 2012
Pseudocercospora musae	CBS 116634	GCA_001578225.1	NCBI	Chang et al. 2016
Pseudocercospora pini-densiflorae	CBS 125139	GCA_000504365.2	NCBI	Canada's Michael Smith Genome Sciences Centre
Pseudovirgaria hyperparasitica	CBS 121739	1032442	JGI	Joseph Spatafora, Pedro Crous, Manfred JK Binder
Pyrenochaeta lycopersici	CRA-PAV ER 1211	GCA_000601435.1	NCBI	Aragona et al. 2014
Pyrenochaeta sp.	DS3sAY3a	GCA_001644535.1	NCBI	Zeiner et al. 2016
Pyrenochaeta sp.	UM 256	GCA_000359685.1	NCBI	Yew et al. 2013
Pyrenophora seminiperda	CCB06	GCA_000465215.1	NCBI	Soliai et al. 2014
Pyrenophora teres	f. teres 0-1	GCA_000166005.1	NCBI	Ellwood et al. 2010
Pyrenophora tritici-repentis	Pt-1C-BFP	GCA_000149985.1	NCBI	Broad Institute of MIT and Harvard
Rachicladosporium antarcticum	CCFEE 5527	GCA_002077065.1	NCBI	Coleine et al. 2017
Rachicladosporium sp.	CCFEE 5018	GCA_002077045.2	NCBI	Coleine et al. 2017
Ramularia collo-cygni	DK05	GCA_001510955.1	NCBI	European Bioinformatics Institute (EBI)
Ramularia endophylla	CBS 113265	GCA_002116395.1	NCBI	Canada's Michael Smith Genome Sciences Centre
Rhizodiscina lignyota	CBS 133067	1019729	JGI	Joseph Spatafora, Pedro Crous, Janneke Bloem
Rhytidhysteron rufulum	CBS 306.38	GCA_000467735.1, 1019729	NCBI	Ohm et al. 2012
Saccharata proteae	CBS 121410	1011317	JGI	Joseph Spatafora, Pedro Crous, Manfred JK Binder
Setomelanomma holmii	CBS 110217	1019737	JGI	Joseph Spatafora, Pedro Crous, Manfred JK Binder
Setosphaeria turcica	Et28A	GCA_000359705.1	NCBI	Ohm et al. 2012
Setosphaeria turcica	NY001	1036047	JGI	Gerrit HJ Kema, Gillian Turgeon
Shiraia sp.	slf14	GCA_000498155.1	NCBI	Yang et al. 2014
Sphaerulina musiva	SO2202	GCA_000320565.2	NCBI	Ohm et al. 2012
Sphaerulina populicola	P02.02b	GCA_000291705.1	NCBI	University of British Columbia, Forest Sciences
Sporormia fimetaria	CBS 119.925	1011321	JGI	Joseph Spatafora, Pedro Crous, Manfred JK Binder
Stagonospora sp.	SRC1lsM3a	GCA_001644525.1	NCBI	Zeiner et al. 2016
Stagonosporopsis tanaceti	CBS 131484	GCA_000812845.1	NCBI	Vaghefi et al. 2015
Stemphylium lycopersici	CIDEFI 216	GCA_001191545.1	NCBI	Franco et al. 2015
Teratosphaeria nubilosa	CBS 116005	1019765	JGI	Joseph Spatafora, Pedro Crous, Manfred JK Binder
Tothia fuscella	CBS 130266	1019713	JGI	Joseph Spatafora, Pedro Crous, Manfred JK Binder
Trematosphaeria pertusa	CBS 122368	1019781	JGI	Joseph Spatafora, Pedro Crous, Manfred JK Binder

Trichodelitschia bisporula	CBS 262.69	1019741	JGI	Joseph Spatafora, Pedro Crous, Manfred JK Binder
Trypethelium eluteriae	-	1006394	JGI	Stephen Goodwin, Daniele Armaleo
Venturia carpophila	JP3-5	GCA_001990985.1	NCBI	USDA-ARS, Chunxian Chen
Venturia effusa	3Des10b	GCA_001901625.1	NCBI	Bock et al. 2016
Venturia inaequalis	1389	GCA_002148275.1	NCBI	Shiller et al. 2015
Venturia inaequalis	1639	GCA_002148295.1	NCBI	Shiller et al. 2015
Venturia inaequalis	EU-B04	GCA_002148305.1	NCBI	Shiller et al. 2015
Venturia inaequalis	ICMP 13258	GCA_001857725.1	NCBI	Shiller et al. 2015
Venturia pyrina	ICMP 11032	GCA_000738655.1	NCBI	Cooke et al. 2014
Verruconis gallopava	CBS 43764	GCA_000836295.1	NCBI	Broad Institute, Sinead Chapman
Verruculina enalia	CBS 304.66	1019669	JGI	Joseph Spatafora, Pedro Crous, Janneke Bloem
Westerdykella ornata	CBS 379.55	1019761	JGI	Joseph Spatafora, Pedro Crous, Manfred JK Binder
Zasmidium cellare	ATCC 36951	402903	JGI	Stephen B. Goodwin
Zopfia rhizophila	-	1011325	JGI	Joseph Spatafora, Pedro Crous, Janneke Bloem
Zymoseptoria ardabiliae	ST11IR 6.1.1	GCA_000983525.1	NCBI	Grandaubert et al. 2015
Zymoseptoria ardabiliae	STIR04 1.1.1	GCA_000223745.2	NCBI	Stukenbrock et al. 2011
Zymoseptoria ardabiliae	STIR04 1.1.2	GCA_000223765.2	NCBI	Stukenbrock et al. 2011
Zymoseptoria ardabiliae	STIR04 3.13.1	GCA_000223785.2	NCBI	Stukenbrock et al. 2011
Zymoseptoria ardabiliae	STIR04 3.3.2	GCA_000223805.2	NCBI	Stukenbrock et al. 2011
Zymoseptoria brevis	ZB163	GCA_000983655.1	NCBI	Grandaubert et al. 2015
Zymoseptoria brevis	Zb18110	GCA_000966595.1	NCBI	Grandaubert et al. 2015
Zymoseptoria passerinii	SP63	GCA_000223825.2	NCBI	Stukenbrock et al. 2011
Zymoseptoria pseudotritici	ST04IR 5.5	GCA_000983605.1	NCBI	Grandaubert et al. 2015
Zymoseptoria pseudotritici	STIR04 2.2.1	GCA_000223665.2	NCBI	Stukenbrock et al. 2011
Zymoseptoria pseudotritici	STIR04 3.11.1	GCA_000226675.2	NCBI	Stukenbrock et al. 2011
Zymoseptoria pseudotritici	STIR04 4.3.1	GCA_000223685.2	NCBI	Stukenbrock et al. 2011
Zymoseptoria pseudotritici	STIR04 5.3	GCA_000223705.2	NCBI	Stukenbrock et al. 2011
Zymoseptoria pseudotritici	STIR04 5.9.1	GCA_000223725.2	NCBI	Stukenbrock et al. 2011
Zymoseptoria tritici	ST99CH 1A5	GCA_900099495.1	NCBI	European Bioinformatics Institute (EBI)
Zymoseptoria tritici	ST99CH 3D7	GCA_900091695.1	NCBI	European Bioinformatics Institute (EBI)
Zymoseptoria tritici	STIR04 A26b	GCA_000223645.2	NCBI	Stukenbrock et al. 2011
Zymoseptoria tritici	STIR04 A48b	GCA_000223625.2	NCBI	Stukenbrock et al. 2011

Table S2. RF distances and normalized RF distance among the main phylogenies generated from the datasets containing the complete set of samples. Three distances are reported: a regular RF distance and two flavours of weighted RF distance as reported in RAxML 8.2 manual. Numbers in the first two columns refer to the following starting datasets and reconstruction methods: (0) ">1kb Gblocks" IQTree run 1, (1) ">1kb Gblocks" IQTree run 2, (2) ">1kb Gblocks" IQTree run 3, (3) ">1kb Gblocks" ASTRAL, (4) "Complete Gblocks" IQTree, (5) ">1Kb GUIDANCE" IQTree, (6) ">1Kb GUIDANCE" ASTRAL.

Phylogenies		**RF**		**WRF1**		**WRF2**	
0	1	0	0,000	0,000	0,000	2,700	0,006
0	2	0	0,000	0,000	0,000	1,300	0,003
0	3	52	0,109	24,620	0,052	444,500	0,930
0	4	30	0,063	27,060	0,057	28,320	0,059
0	5	30	0,063	27,720	0,058	29,880	0,063
0	6	52	0,109	24,450	0,051	444,610	0,930
1	2	0	0,000	0,000	0,000	2,040	0,004
1	3	52	0,109	24,160	0,051	443,900	0,929
1	4	30	0,063	26,800	0,056	29,280	0,061
1	5	30	0,063	27,410	0,057	30,330	0,063
1	6	52	0,109	24,010	0,050	443,990	0,929
2	3	52	0,109	24,510	0,051	444,190	0,929
2	4	30	0,063	26,780	0,056	28,260	0,059
2	5	30	0,063	27,610	0,058	29,930	0,063
2	6	52	0,109	24,270	0,051	444,370	0,930
3	4	56	0,117	26,130	0,055	443,450	0,928
3	5	48	0,100	23,000	0,048	447,200	0,936
3	6	12	0,025	0,020	0,000	0,160	0,000
4	5	28	0,059	25,380	0,053	27,720	0,058
4	6	52	0,109	24,220	0,051	445,340	0,932
5	6	48	0,100	22,860	0,048	447,280	0,936

Table S3. RF distances and normalized RF distances from the reference topology of the 30 resampled matrices for each resampling effort value (0.1-30 %).

0,1%		1%		10%		20%		30%	
120	0,251	52	0,109	22	0,046	10	0,021	22	0,046
144	0,301	66	0,138	44	0,092	20	0,042	18	0,038
160	0,335	74	0,155	26	0,054	22	0,046	20	0,042
148	0,310	70	0,146	34	0,071	12	0,025	28	0,059
162	0,339	58	0,121	32	0,067	24	0,050	18	0,038
172	0,360	66	0,138	34	0,071	24	0,050	12	0,025
146	0,305	62	0,130	36	0,075	30	0,063	18	0,038
138	0,289	66	0,138	32	0,067	28	0,059	20	0,042
146	0,305	52	0,109	24	0,050	24	0,050	22	0,046
160	0,335	70	0,146	32	0,067	32	0,067	14	0,029
148	0,310	60	0,126	34	0,071	18	0,038	24	0,050
142	0,297	70	0,146	38	0,079	38	0,079	10	0,021
140	0,293	64	0,134	26	0,054	32	0,067	20	0,042
138	0,289	60	0,126	52	0,109	18	0,038	22	0,046
138	0,289	64	0,134	40	0,084	26	0,054	24	0,050
134	0,280	76	0,159	22	0,046	28	0,059	10	0,021
158	0,331	74	0,155	26	0,054	16	0,033	26	0,054
158	0,331	42	0,088	38	0,079	18	0,038	16	0,033
160	0,335	76	0,159	42	0,088	40	0,084	14	0,029
134	0,280	70	0,146	28	0,059	22	0,046	20	0,042
146	0,305	66	0,138	24	0,050	32	0,067	22	0,046
142	0,297	78	0,163	36	0,075	20	0,042	12	0,025
158	0,331	60	0,126	30	0,063	28	0,059	28	0,059
172	0,360	60	0,126	46	0,096	20	0,042	20	0,042
142	0,297	78	0,163	34	0,071	12	0,025	10	0,021
144	0,301	48	0,100	40	0,084	32	0,067	18	0,038
130	0,272	54	0,113	26	0,054	30	0,063	26	0,054
138	0,289	62	0,130	38	0,079	20	0,042	22	0,046
136	0,285	58	0,121	26	0,054	16	0,033	28	0,059
142	0,297	62	0,130	26	0,054	26	0,054	24	0,050

Average	147	0,307	64	0,134	33	0,069	24	0,050	20	0,041
SD	12	0,026	9	0,019	8	0,016	7	0,016	5	0,011

Table S4. Average values and standard deviation (SD) of RF distances and normalized RF distances among the 30 phylogenies generated from the randomly resampled matrix with the same resampling effort.

	0,1%		**1%**		**10%**		**20%**		**30%**	
	RF	**nRF**	**RF**	**nRF**	**RF**	**nRF**	**RF**	**nRF**	**RF**	**nRF**
Average	183	0,384	75	0,158	41	0,086	32	0,067	26	0,055
SD	19	0,036	10	0,019	8	0,016	8	0,016	7	0,014

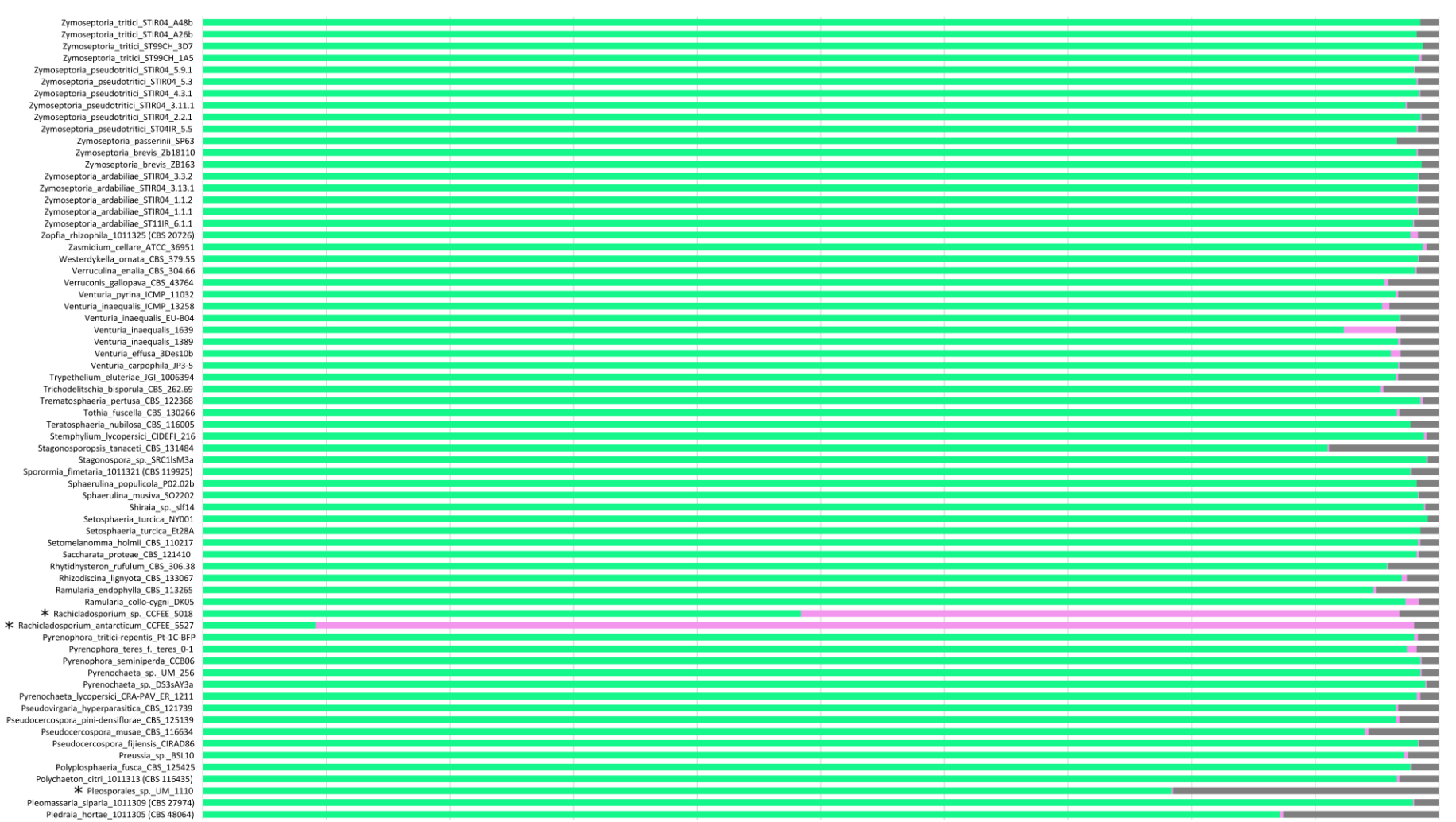
Zymoseptoria_tritici_STIR04_A48b
Zymoseptoria_tritici_STIR04_A26b
Zymoseptoria_tritici_ST99CH_3D7
Zymoseptoria_tritici_ST99CH_1A5
Zymoseptoria_pseudotritici_STIR04_5.9.1
Zymoseptoria_pseudotritici_STIR04_5.3
Zymoseptoria_pseudotritici_STIR04_4.3.1
Zymoseptoria_pseudotritici_STIR04_3.11.1
Zymoseptoria_pseudotritici_STIR04_2.2.1
Zymoseptoria_pseudotritici_ST04IR_5.5
Zymoseptoria_passerinii_SP63
Zymoseptoria_brevis_Zb18110
Zymoseptoria_brevis_ZB163
Zymoseptoria_ardabiliae_STIR04_3.3.2
Zymoseptoria_ardabiliae_STIR04_3.13.1
Zymoseptoria_ardabiliae_STIR04_1.1.2
Zymoseptoria_ardabiliae_STIR04_1.1.1
Zymoseptoria_ardabiliae_ST11IR_6.1.1
Zopfia_rhizophila_1011325 (CBS 20726)
Zasmidium_cellare_ATCC_36951
Westerdykella_ornata_CBS_379.55
Verruculina_enalia_CBS_304.66
Verruconis_gallopava_CBS_43764
Venturia_pyrina_ICMP_11032
Venturia_inaequalis_ICMP_13258
Venturia_inaequalis_EU-B04
Venturia_inaequalis_1639
Venturia_inaequalis_1389
Venturia_effusa_3Des10b
Venturia_carpophila_JP3-5
Trypethelium_eluteriae_JGI_1006394
Trichodelitschia_bisporula_CBS_262.69
Trematosphaeria_pertusa_CBS_122368
Tothia_fuscella_CBS_130266
Teratosphaeria_nubilosa_CBS_116005
Stemphylium_lycopersici_CIDEFI_216
Stagonosporopsis_tanaceti_CBS_131484
Stagonospora_sp._SRC1lsM3a
Sporormia_fimetaria_1011321 (CBS 119925)
Sphaerulina_populicola_P02.02b
Sphaerulina_musiva_SO2202
Shiraia_sp._slf14
Setosphaeria_turcica_NY001
Setosphaeria_turcica_Et28A
Setomelanomma_holmii_CBS_110217
Saccharata_proteae_CBS_121410
Rhytidhysteron_rufulum_CBS_306.38
Rhizodiscina_lignyota_CBS_133067
Ramularia_endophylla_CBS_113265
Ramularia_collo-cygni_DK05
* Rachicladosporium_sp._CCFEE_5018
* Rachicladosporium_antarcticum_CCFEE_5527
Pyrenophora_tritici-repentis_Pt-1C-BFP
Pyrenophora_teres_f._teres_0-1
Pyrenophora_seminiperda_CCB06
Pyrenochaeta_sp._UM_256
Pyrenochaeta_sp._DS3sAY3a
Pyrenochaeta_lycopersici_CRA-PAV_ER_1211
Pseudovirgaria_hyperparasitica_CBS_121739
Pseudocercospora_pini-densiflorae_CBS_125139
Pseudocercospora_musae_CBS_116634
Pseudocercospora_fijiensis_CIRAD86
Preussia_sp._BSL10
Polyplosphaeria_fusca_CBS_125425
Polychaeton_citri_1011313 (CBS 116435)
* Pleosporales_sp._UM_1110
Pleomassaria_siparia_1011309 (CBS 27974)
Piedraia_hortae_1011305 (CBS 48064)

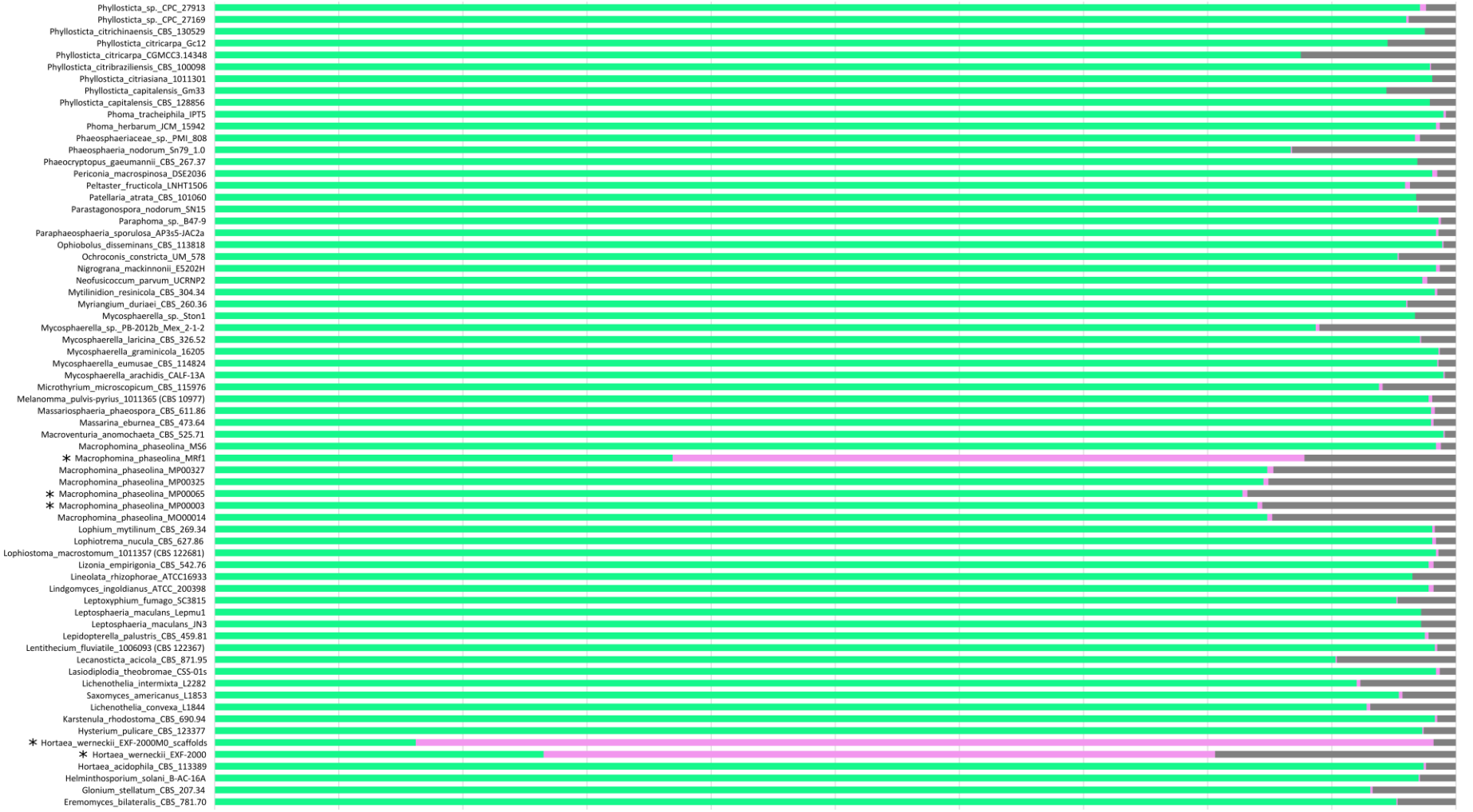
Phyllosticta_sp._CPC_27913
Phyllosticta_sp._CPC_27169
Phyllosticta_citrichinaensis_CBS_130529
Phyllosticta_citricarpa_Gc12
Phyllosticta_citricarpa_CGMCC3.14348
Phyllosticta_citribraziliensis_CBS_100098
Phyllosticta_citriasiana_1011301
Phyllosticta_capitalensis_Gm33
Phyllosticta_capitalensis_CBS_128856
Phoma_tracheiphila_IPT5
Phoma_herbarum_JCM_15942
Phaeosphaeriaceae_sp._PMI_808
Phaeosphaeria_nodorum_Sn79_1.0
Phaeocryptopus_gaeumannii_CBS_267.37
Periconia_macrospinosa_DSE2036
Peltaster_fructicola_LNHT1506
Patellaria_atrata_CBS_101060
Parastagonospora_nodorum_SN15
Paraphoma_sp._B47-9
Paraphaeosphaeria_sporulosa_AP3s5-JAC2a
Ophiobolus_disseminans_CBS_113818
Ochroconis_constricta_UM_578
Nigrograna_mackinnonii_E5202H
Neofusicoccum_parvum_UCRNP2
Mytilinidion_resinicola_CBS_304.34
Myriangium_duriaei_CBS_260.36
Mycosphaerella_sp._Ston1
Mycosphaerella_sp._PB-2012b_Mex_2-1-2
Mycosphaerella_laricina_CBS_326.52
Mycosphaerella_graminicola_16205
Mycosphaerella_eumusae_CBS_114824
Mycosphaerella_arachidis_CALF-13A
Microthyrium_microscopicum_CBS_115976
Melanomma_pulvis-pyrius_1011365 (CBS 10977)
Massariosphaeria_phaeospora_CBS_611.86
Massarina_eburnea_CBS_473.64
Macroventuria_anomochaeta_CBS_525.71
Macrophomina_phaseolina_MS6
* Macrophomina_phaseolina_MRf1
Macrophomina_phaseolina_MP00327
Macrophomina_phaseolina_MP00325
* Macrophomina_phaseolina_MP00065
* Macrophomina_phaseolina_MP00003
Macrophomina_phaseolina_MO00014
Lophium_mytilinum_CBS_269.34
Lophiotrema_nucula_CBS_627.86
Lophiostoma_macrostomum_1011357 (CBS 122681)
Lizonia_empirigonia_CBS_542.76
Lineolata_rhizophorae_ATCC16933
Lindgomyces_ingoldianus_ATCC_200398
Leptoxyphium_fumago_SC3815
Leptosphaeria_maculans_Lepmu1
Leptosphaeria_maculans_JN3
Lepidopterella_palustris_CBS_459.81
Lentithecium_fluviatile_1006093 (CBS 122367)
Lecanosticta_acicola_CBS_871.95
Lasiodiplodia_theobromae_CSS-01s
Lichenothelia_intermixta_L2282
Saxomyces_americanus_L1853
Lichenothelia_convexa_L1844
Karstenula_rhodostoma_CBS_690.94
Hysterium_pulicare_CBS_123377
* Hortaea_werneckii_EXF-2000M0_scaffolds
* Hortaea_werneckii_EXF-2000
Hortaea_acidophila_CBS_113389
Helminthosporium_solani_B-AC-16A
Glonium_stellatum_CBS_207.34
Eremomyces_bilateralis_CBS_781.70

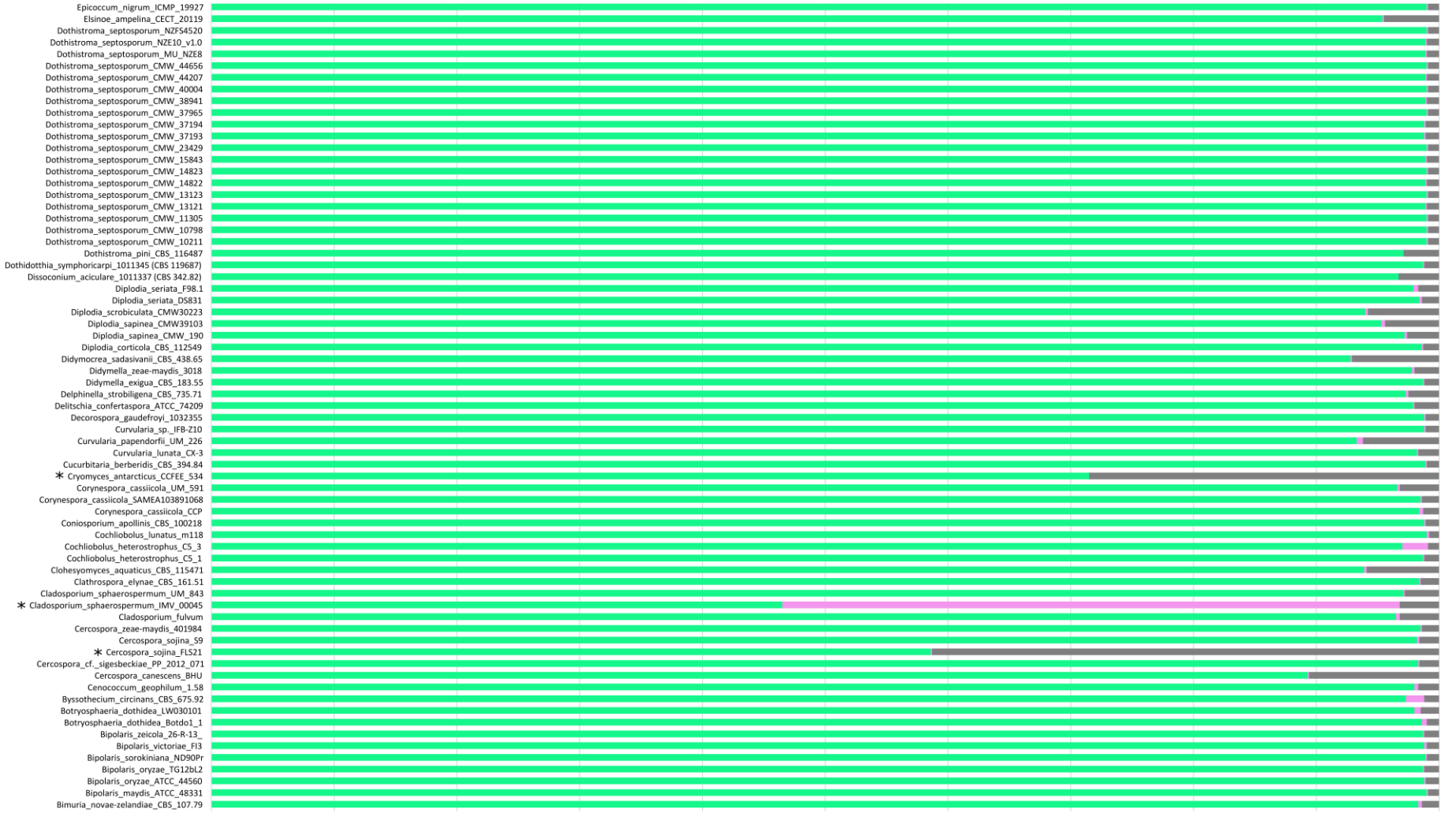
Epicoccum_nigrum_ICMP_19927
Elsinoe_ampelina_CECT_20119
Dothistroma_septosporum_NZFS4520
Dothistroma_septosporum_NZE10_v1.0
Dothistroma_septosporum_MU_NZE8
Dothistroma_septosporum_CMW_44656
Dothistroma_septosporum_CMW_44207
Dothistroma_septosporum_CMW_40004
Dothistroma_septosporum_CMW_38941
Dothistroma_septosporum_CMW_37965
Dothistroma_septosporum_CMW_37194
Dothistroma_septosporum_CMW_37193
Dothistroma_septosporum_CMW_23429
Dothistroma_septosporum_CMW_15843
Dothistroma_septosporum_CMW_14823
Dothistroma_septosporum_CMW_14822
Dothistroma_septosporum_CMW_13123
Dothistroma_septosporum_CMW_13121
Dothistroma_septosporum_CMW_11305
Dothistroma_septosporum_CMW_10798
Dothistroma_septosporum_CMW_10211
Dothistroma_pini_CBS_116487
Dothidotthia_symphoricarpi_1011345 (CBS 119687)
Dissoconium_aciculare_1011337 (CBS 342.82)
Diplodia_seriata_F98.1
Diplodia_seriata_DS831
Diplodia_scrobiculata_CMW30223
Diplodia_sapinea_CMW39103
Diplodia_sapinea_CMW_190
Diplodia_corticola_CBS_112549
Didymocrea_sadasivanii_CBS_438.65
Didymella_zeae-maydis_3018
Didymella_exigua_CBS_183.55
Delphinella_strobiligena_CBS_735.71
Delitschia_confertaspora_ATCC_74209
Decorospora_gaudefroyi_1032355
Curvularia_sp._IFB-Z10
Curvularia_papendorfii_UM_226
Curvularia_lunata_CX-3
Cucurbitaria_berberidis_CBS_394.84
Cryomyces_antarcticus_CCFEE_534
Corynespora_cassiicola_UM_591
Corynespora_cassiicola_SAMEA103891068
Corynespora_cassiicola_CCP
Coniosporium_apollinis_CBS_100218
Cochliobolus_lunatus_m118
Cochliobolus_heterostrophus_C5_3
Cochliobolus_heterostrophus_C5_1
Clohesyomyces_aquaticus_CBS_115471
Clathrospora_elynae_CBS_161.51
Cladosporium_sphaerospermum_UM_843
Cladosporium_sphaerospermum_IMV_00045
Cladosporium_fulvum
Cercospora_zeae-maydis_401984
Cercospora_sojina_S9
Cercospora_sojina_FLS21
Cercospora_cf._sigesbeckiae_PP_2012_071
Cercospora_canescens_BHU
Cenococcum_geophilum_1.58
Byssothecium_circinans_CBS_675.92
Botryosphaeria_dothidea_LW030101
Botryosphaeria_dothidea_Botdo1_1
Bipolaris_zeicola_26-R-13_
Bipolaris_victoriae_FI3
Bipolaris_sorokiniana_ND90Pr
Bipolaris_oryzae_TG12bL2
Bipolaris_oryzae_ATCC_44560
Bipolaris_maydis_ATCC_48331
Bimuria_novae-zelandiae_CBS_107.79

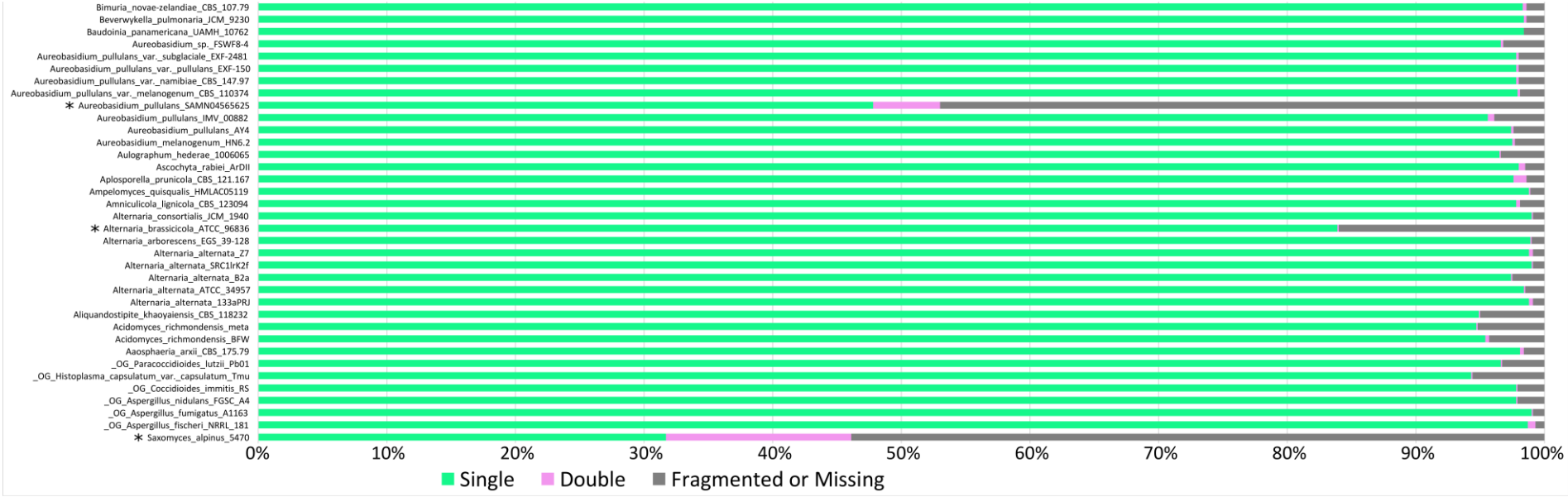

Figure S1. Assembly completeness on the base of 3156 Pezizomycotina orthologs evaluated by BUSCO and expressed as the percentage of complete (green), duplicated (pink) and fragmented or missing (grey) genes. Distribution outliers are highlighted with "*".

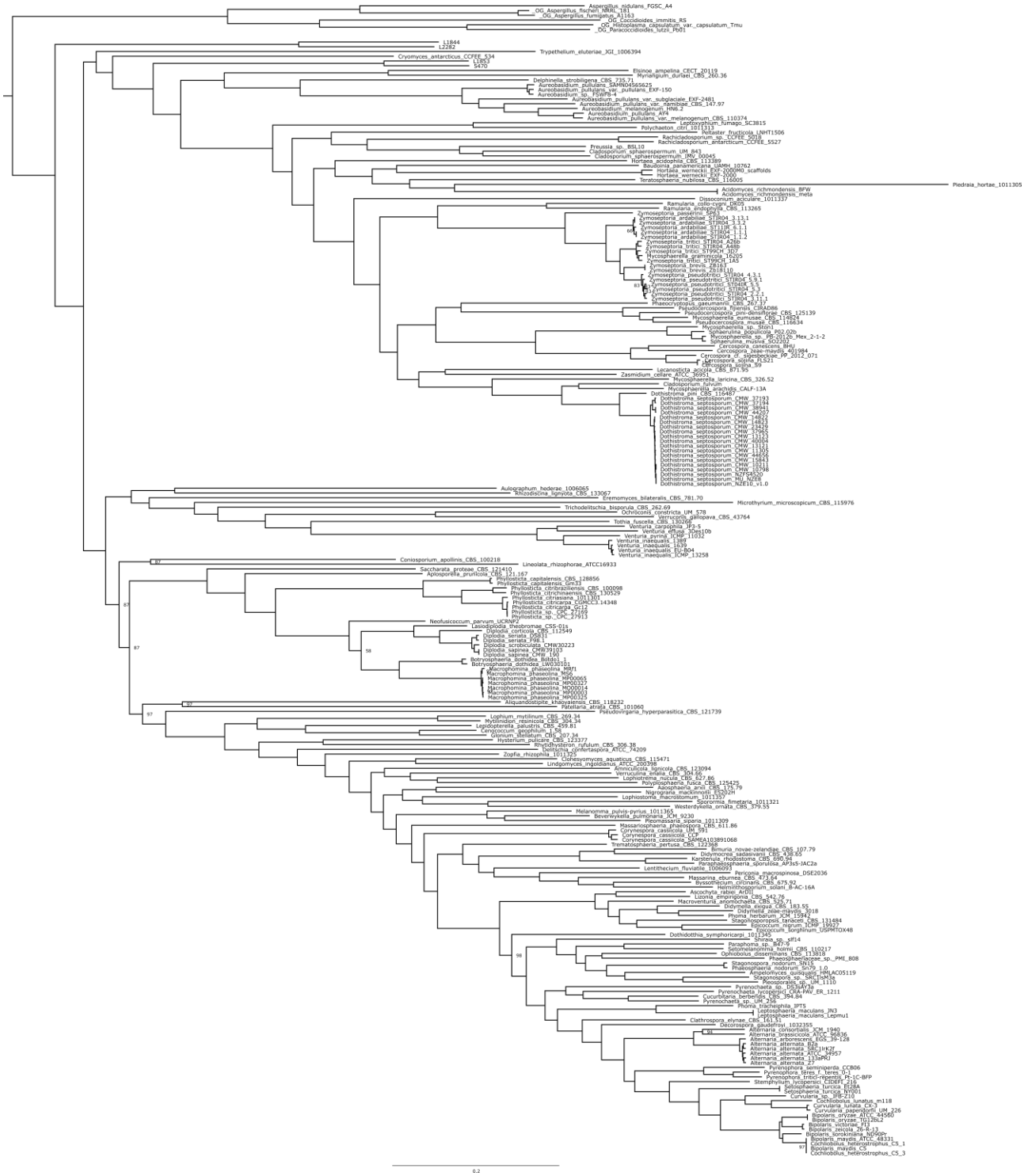

Figure S2. 2998 concatenated genes phylogeny generated from "Complete Gblocks" dataset with IQTree. Support values different from 100 are shown.

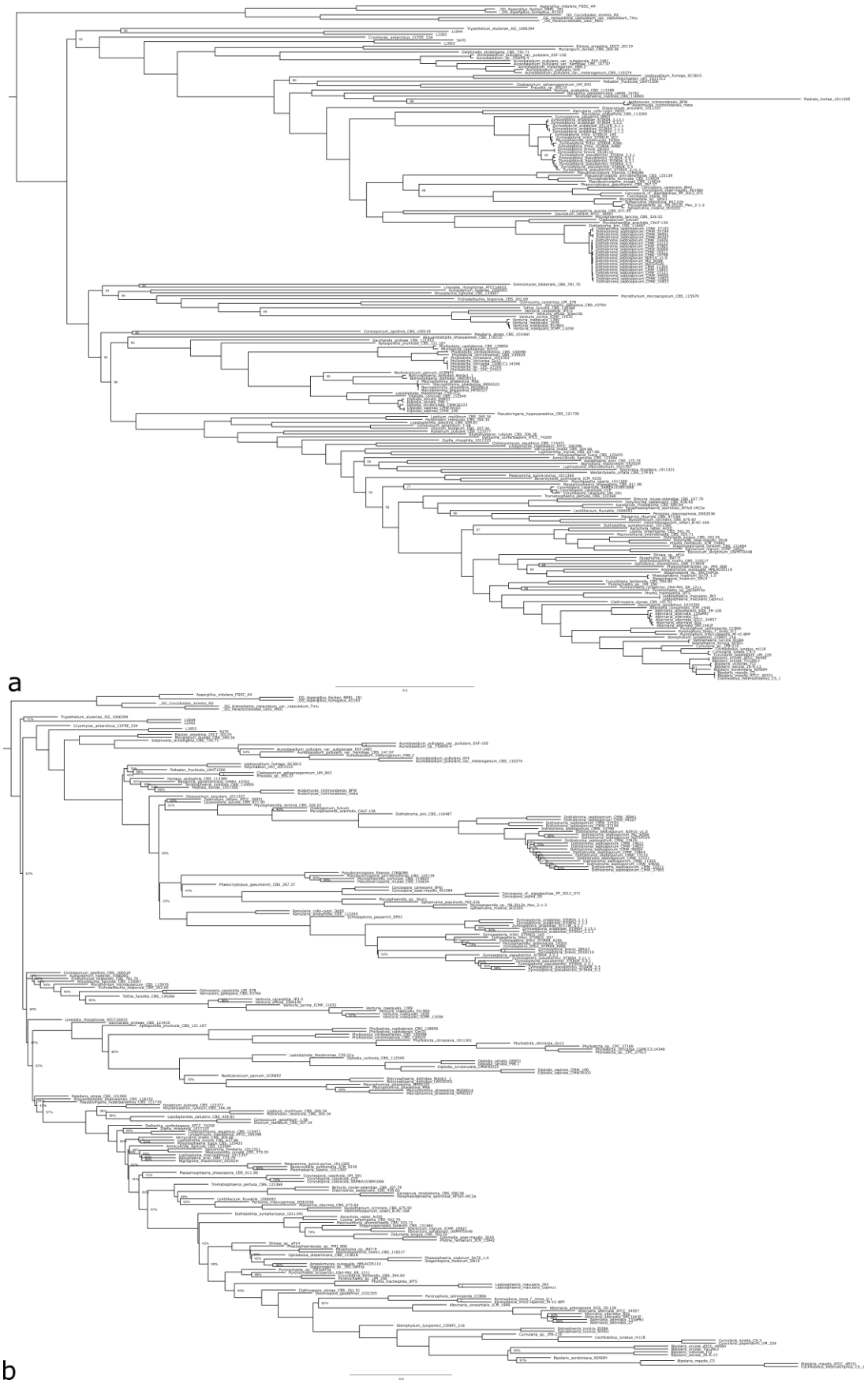

Figure S3. 63 gene phylogeny generated from "No missing" dataset; (a) ML tree generated with IQTree on concatenated genes, (b) ASTRAL III species tree. Support values different from 100 are shown.

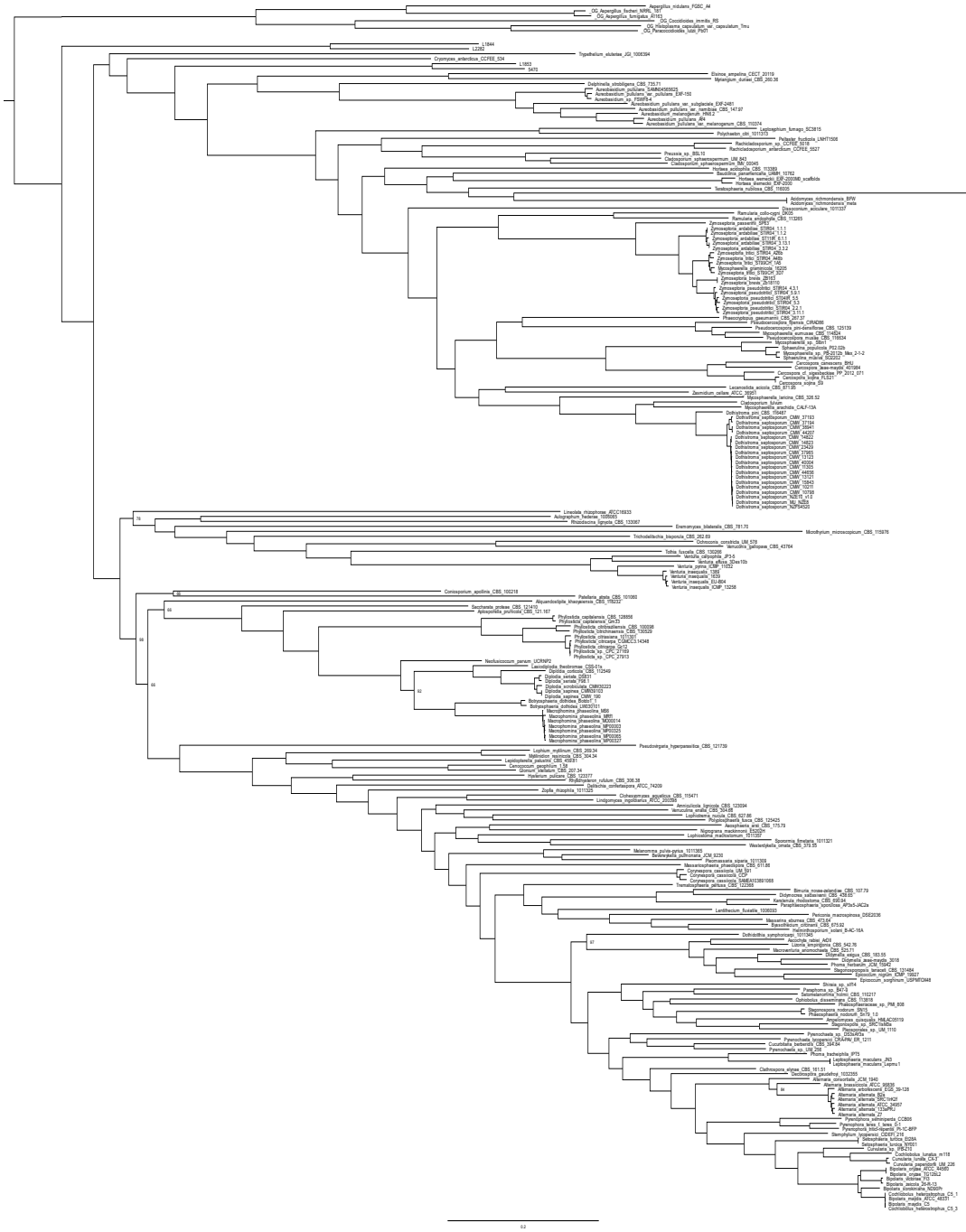

Figure S4. 1260 concatenated genes phylogeny generated from ">1Kb GUIDANCE" dataset with IQTree. Support values different from 100 are shown.

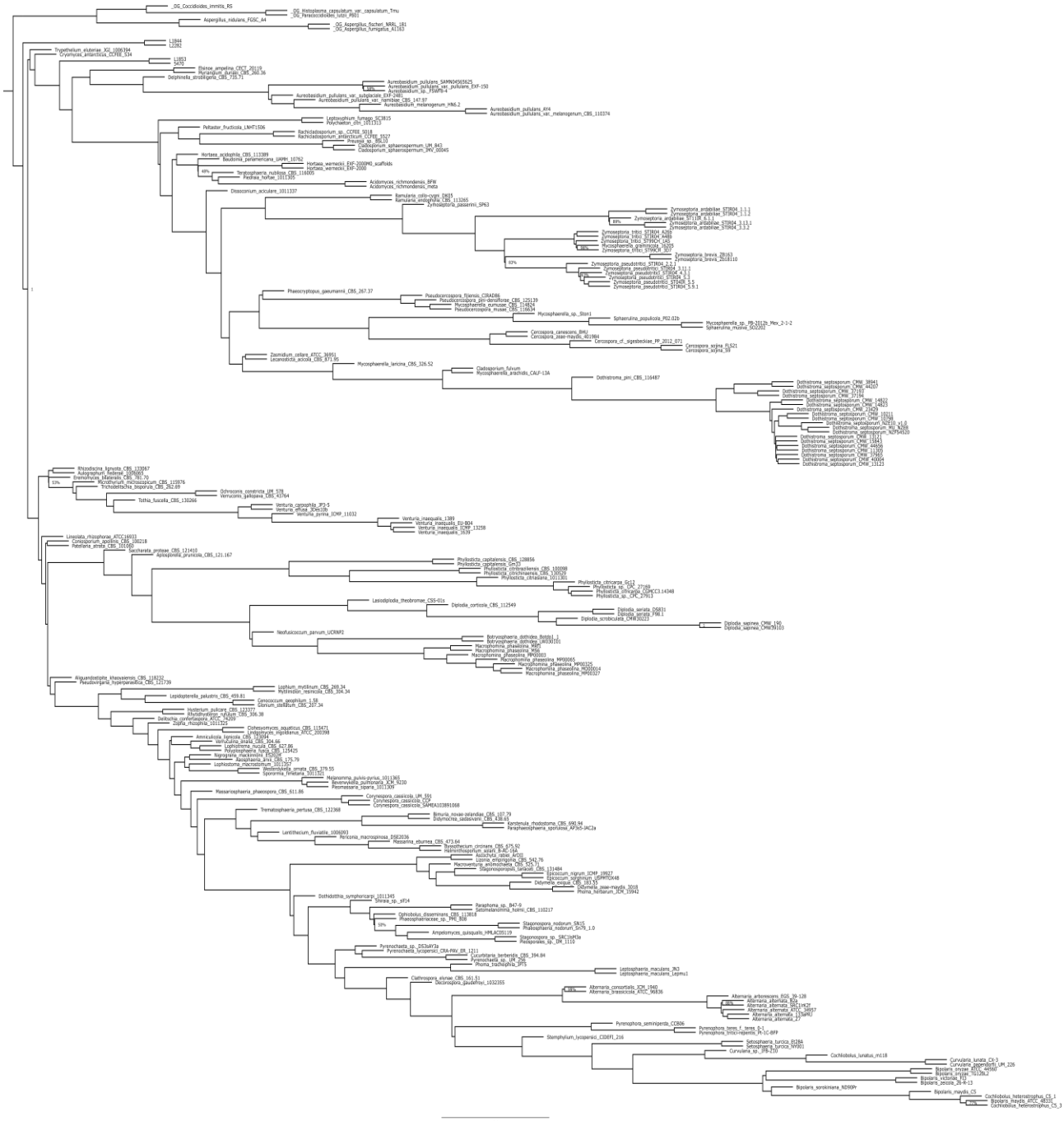

Figure S5. 1260 concatenated genes phylogeny generated from ">1Kb GUIDANCE" dataset with ASTRAL. Support values different from 100 are shown.